Reverse Genetic Analysis of Pericentrin Functions

Yifan Wang

Centre for Chromosome Biology,

School of Natural Sciences,

National University of Ireland, Galway

A thesis submitted to the National University of Ireland, Galway

for the degree of Doctor of Philosophy

June 2012

Supervisor: Prof. Ciaran Morrison

Table of contents

List of figures

List of tables

Acknowledgements

First, I would like to thank my supervisor Prof. Ciaran Morrison for giving me the opportunity to come to Ireland and work in his group. It will be an amazing and unforgettable experience during my lifetime. Many thanks for his constant guidance, encouragement and patience when I worked on my project and wrote the thesis. He is a very good supervisor.

I am very grateful to all the members of the Chromosome Biology Laboratory: Dr. Helen Dodson, Dr. Anna Stephan, Dr. Emer Bourke, Dr. Maciej Kliszczak, Dr. Chiara Saladino, Dr. David Gaboriau, Dr. Burcu Inanç, Pauline Conroy and Sinead King, for all their helpful advice on science and on life. Special thanks to Loretta Breslin for her assistance with correction of my writings. In particular many thanks to Dr. Tiago Dantas for his constant guidance and advice during my experimental work and our long time collaboration.

I would also like to thank our collaborators: Prof. Peter Dockery, Pierce Lalor and Dr. Catherine Liptrot for training me the electron microscopy techniques and allowing me to use their equipment in Department of Anatomy, NUIG.

Many thanks to all the colleagues from the Centre for Chromosome Biology at NUIG for all their help and advice.

Finally, I deeply appreciate my mother's unconditional support and understanding for accepting my decision to move so far away from home. Last but not least, I would like to thank my lovely wife Zheng Lai. Thank you, Zheng, for giving up your job and sharing this adventure with me. Thank you for all your endless love and constant support. Thank you!

Yifan

Abbreviations

53BP1	p53 binding protein 1
AID	auxin-inducible degron
AKAP	A-kinase anchor proteins
APC/C	anaphase-promoting complex/cyclosome
ATM	ataxia telangiectasia, mutated
ATR	ataxia telangiectasia and Rad3 related
BER	base excision repair
BRCA1	breast cancer type susceptibility protein 1
BRCT	BRCA1 carboxy-terminal
BrdU	bromodeoxyuridine
BRIT1	BRCT-repeat inhibitor of hTERT expression 1
BSA	bovine serum albumin
BUBR1	BUB-related 1
CAK	CDK activating kinase
CDK	cyclin-dependent kinases
CDK5RAP2	cyclin-dependent kinase 5 regulatory associated protein 2
CHD	chromodomain helicase DNA-binding protein
CML	chronic myeloid leukemia
CRM	chromosome region maintenance
DDR	DNA damage response
DISC1	disrupted in Schizophrenia 1
DMSO	dimethyl sulfoxide
D-PLP	*Drosophila* pericentrin like protein
DSB	double strand break
EB1	microtubule end-binding protein 1
FACS	fluorescence-activated cell sorting
FBS	fetal bovine serum
GCP	γ-tubulin complex protein
GFP	green fluorescent protein
γ-TuRC	γ-tubulin ring complex
γ-TuSC	γ-tubulin small complex
HR	homologous recombination
hTERT	human telomere reverse transcriptase
HU	hydroxyurea
IAA	indole-3-acetic acid
IR	ionizing radiation
IRIF	irradiation-induced foci
LB	Luria-Bertani medium
LCL	lymphoblastoid cell line
MAD1	mitotic arrest deficient 1
MCC	mitotic checkpoint complex

MDC1	mediator of DNA checkpoint 1
MIM	Mendelian Inheritance in Man
MMR	mismatch repair
MOPD II	Majewski osteodysplastic primordial dwarfism type II
MRN	MRE11-RAD50-NBS1
MTOC	microtubule organising center
NBS	Nijmegen breakage syndrome
NER	nucleotide excision repair
NES	nuclear export signal
NHEJ	non-homologous end joining
NLS	nuclear localisation signal
NuMA	nuclear mitotic apparatus
NuRD	nucleosome remodeling deacetylase
ORC	origin recognition complexes
PACT	pericentrin-AKAP450 centrosomal targeting
PARP	poly (ADP-ribose) polymerase
PCC	premature chromosome condensation
PCM	pericentriolar material
PKA	protein kinase A
PLK	polo-like kinase
RB	retinoblastoma
RPA	replication protein A
SAC	spindle assembly checkpoint
SCC1	sister chromatid cohesion 1
SMC1	structural maintenance of chromosome 1
SNP	single-nucleotide polymorphism
SPB	spindle pole bodies
TAM	4-hydroxytamoxifen
TS	temperature-sensitive
tTA	tetracycline-controlled transactivator
UV	ultraviolet
WT	wild-type

Abstract

The centrosome is a subcellular organelle that organises the mitotic spindle microtubules to ensure accurate segregation of chromosomes during cell division. Most animal centrosomes comprise a pair of centrioles which are encircled with an electron-dense substance termed the pericentriolar material (PCM). Pericentrin is a large, coiled-coil protein that acts as a scaffold to recruit proteins to the centrosome for PCM assembly. Mutations in the human pericentrin gene which lead to the expression of non-functional protein result in dysfunctional microtubule nucleation and cell cycle checkpoints. To better understand the function of pericentrin, we used reverse genetics to study the roles of pericentrin in centrosome organisation, cell cycle progression and the responses to DNA damage.

We successfully generated *Pericentrin* (*Pcnt*) knockouts in hyper-recombinogenic chicken DT40 cells, using a strategy designed to target the promoter region of *Pcnt*. Targeting of the *Pcnt* promoter caused *Pcnt* mRNA levels to decline to 2% of wild-type levels, as determined by quantitative RT-PCR. However, no protein was detectable by immunofluorescence microscopy in the knockout cells. Unexpectedly, *Pcnt*-deficient cells were viable, but grew slower than controls. Cell cycle analysis and live cell imaging suggest that *Pcnt*-deficiency leads to a delay in the cell cycle at mitosis. Light and electron microscopy analyses revealed no detectable defects in centrosome composition or ultrastructure in *Pcnt*-deficient cells. Although centrosomal γ-tubulin was not recruited efficiently, *Pcnt*-deficient centrosomes were able to nucleate microtubules as rapidly as wild-type cells. Consistent with the finding of abnormal elongated mitotic spindles, *Pcnt*-deficient cells had a defect in the satisfaction of the spindle assembly checkpoint after spindle poison treatment. Cell cycle arrest, centrosome amplification and survival rates after ionising radiation treatment were normal in *Pcnt*-deficient cells. However, it is interesting that pericentrin deficiency abrogated the centrosome hyperamplification noted in

Mcph1$^{-/-}$ cells. We found a reduced nuclear CHK1 activation after damage in *Pcnt*-deficient cells. These data suggest a genetic interaction between *Pcnt* and *Mcph1* in the control of genomic stability through CHK1.

Chapter 1. Introduction

1.1 The cell cycle

The cell cycle is an ordered series of events which lead to the duplication and transmission of genetic information from one mother cell to two identical daughter cells. The cell cycle contains four consecutive phases whose transitions are strictly regulated (Figure 1.1). RNAs and proteins are synthesised in G (gap) 1 and G2 phases. DNA synthesis and chromosome replication occur in S (synthesis) phase. In M (mitosis) phase, the duplicated DNA is equally segregated with the help of the microtubule spindle and daughter cells each inherit one copy of the parental chromosomes. The period between mitosis (i.e. G1, S and G2) is termed interphase.

According to changes observed in dividing cells under the light microscope, mitosis is mainly subdivided into five detailed phases: prophase, prometaphase, metaphase, anaphase, and telophase. Chromosomes begin to condense and resolve in prophase. The nuclear envelope breaks down and microtubules enter the nucleus in prometaphase. Microtubules connect to the chromosomes at the kinetochore and the bipolar spindle forms in metaphase. After all the chromosomes are aligned at the plane equidistant from the two poles of the mitotic spindle, the sister chromatids are separated and migrate to the opposite poles during anaphase. In telophase, the nuclear envelope re-forms around the decondensing chromosomes which are released from the depolymerised microtubules. The cells are physically cleaved at the end of the cell cycle during cytokinesis (Lodish et al., 2003).

1.1.1 Regulation of the cell cycle

Transitions from one stage to the next must be precisely controlled throughout the cell cycle to ensure one stage is completed before entry into the next stage. Central players are cyclins and the cyclin-dependent kinases (CDKs) which drive processes including the initiation, progression and completion of cell cycle events (Gitig and

Koff, 2000; Morgan, 1997). The catalytic subunits, CDKs, must be associated with their respective cyclins for activation as monomeric CDKs are inactive. The CDK activating kinase (CAK) may also be required for full activation of the complexes (Kaldis, 1999; Morgan, 1997). CDK inhibitors (CDKIs) block CDKs' function and stop the cells entering the next stage (Besson et al., 2008; Gitig and Koff, 2000). The kinase activity of specific cyclin-CDK complexes in distinct stages of the cell cycle is regulated by the accumulation and degradation or phosphorylation and dephosphorylation of the proteins (Figure 1.1) (Gitig and Koff, 2000; Morgan, 1997).

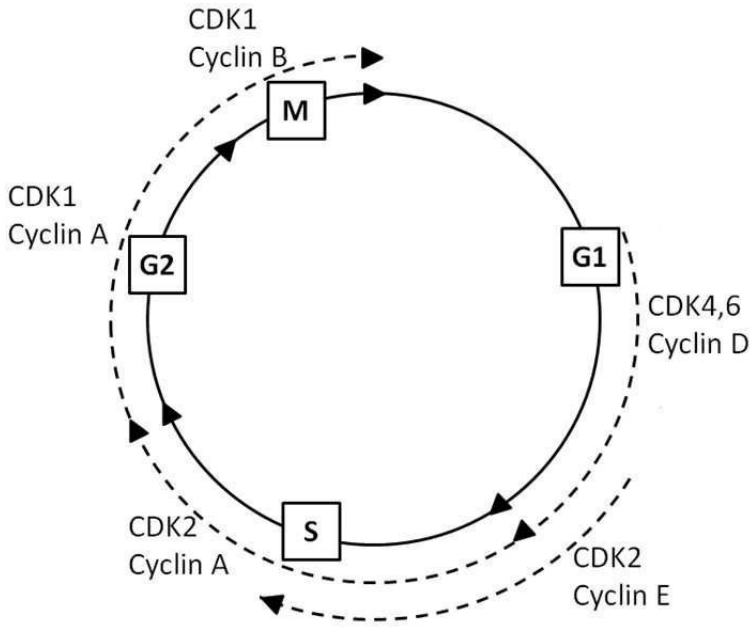

Figure 1.1 Schematic representation of cyclin-CDK protein complexes and the cell cycle.

The cell cycle is divided into four phases (G1, S, G2, and M). Progression through the different phases of the cell cycle is driven by specific cyclin-CDK complexes. The cyclin D-CDK4/6 complex is responsible for cell cycle progression in the G1 phase. The cyclin E-CDK2 complex comes up and initiates S phase. The cyclin A-CDK2 complex furthers the progression of S phase. The cyclin A/B-CDK1 complexes then cause the entry from G2 phase into mitosis and finally cells divide into two identical daughters.

1.1.2 The G1/S transition

Cells commit to division when cyclin D is induced in response to extracellular mitogens and growth factors in early G1 phase (Sewing et al., 1993). Cyclin D preferentially binds and activates CDK4 and CDK6 (Matsushime et al., 1992;

Meyerson and Harlow, 1994). These complexes subsequently phosphorylate retinoblastoma (RB) protein, the product of the retinoblastoma susceptibility gene. RB works as an antiproliferative protein by blocking transcriptional activity of the transcription factor E2F, and recruiting histone deacetylases and chromosome remodeling complexes to the promoters of E2F-activated genes (Herwig and Strauss, 1997). Phosphorylated RB dissociates from E2F so that E2F promotes transcription of genes required for DNA synthesis including *cyclins E*, *A*, and *B*, and *E2F* itself (Herwig and Strauss, 1997; Morgan, 1997). Cyclin E, whose expression increases in late G1 phase, binds and activates CDK2 (Harbour et al., 1999). The cyclin E-CDK2 complex further phosphorylates and inactivates RB because hypophosphorylated RB tightly binds E2F again (Harbour et al., 1999; Lundberg and Weinberg, 1998). Cyclin E-CDK2 also phosphorylates and degrades the CDK2 inhibitor p27 (Bartek and Lukas, 2001). Thus cyclin E-CDK2 activity reaches its peak and initiates S phase.

1.1.3 Intra S phase

Cyclins D and E are degraded by ubiquitination after entry to S phase (Elledge and Harper, 1998). CDK2 is subsequently bound and activated by cyclin A throughout S phase (Pines and Hunter, 1991). Cyclin A protein levels are low in G1 phase but increase from S phase through G2 phase and degrade during mitosis. Cyclin A-CDK2 binds and phosphorylates E2F resulting in E2F release from DNA to terminate DNA synthesis. Constitutive activation of E2F leads to S phase arrest or delay followed by apoptosis (Krek et al., 1995). Cyclin A then binds and activates CDK1 in late S and throughout G2 phases.

1.1.4 The G2/M transition

The expression of *Cyclin B* starts in S phase, increases through G2 phase, peaks at the G2/M border and remains until it suddenly is degraded at anaphase (Fung and Poon, 2005). At the G2/M transition, cyclin A is degraded and the nuclear envelope

breaks down. The cytoplasmic cyclin B binds CDK1 which is phosphorylated on Thr14 and Tyr15 by WEE1 and MYT1 (Gitig and Koff, 2000; Morgan, 1997). These phosphorylations negatively regulate the activity of cyclin B-CDK1 complex. After the complex shuttles into the nucleus, the inhibitory phosphorylation on CDK1 is removed by the dual-specificity phosphatase CDC25C (Gitig and Koff, 2000; Morgan, 1997). Activated cyclin B-CDK1 in turn phosphorylates CDC25C, which activates it. The autocatalytic positive feedback loop results in an extremely rapid activation of cyclin B-CDK1 at the G2/M border (Hoffmann et al., 1993). Becoming further activated by phosphorylation on Tyr161 by its CAK, cyclin B-CDK1 initiates mitotic entry (Fung and Poon, 2005; Morgan, 1997).

1.2 DNA damage response

Organisms are constantly exposed to both endogenous and exogenous DNA damage sources (Friedberg, 2003). Endogenous DNA damage sources include reactive oxygen species generated by normal metabolic processes, nitrogen species arising from metabolism and inflammatory responses, alkylating agents, and replication errors, such as stalled and collapsed replication forks (Lindahl and Barnes, 2000). Exogenous DNA damage sources include ultraviolet (UV) radiation, ionizing radiation (IR), thermal factors, and various chemicals agents (Harper and Elledge, 2007). Both endogenous and exogenous DNA damage induce modifications in the DNA, including base modifications (deaminations, alkylations, oxidations), sugar modifications, DNA-protein adducts, base-free sites, strand alterations, single and double strand breaks, intra- and interstrand cross-links (Ciccia and Elledge, 2010).

To transmit accurate genomic information to the next generation, cells have evolved DNA damage response (DDR) and repair pathways. Three major groups of proteins are engaged in DDR pathways (Zhou and Elledge, 2000). Sensor proteins detect DNA lesions directly or indirectly to initiate a signal transduction cascade. The damage signal is then transmitted and amplified by transducer proteins, which are

mainly protein kinases. At the end, effector proteins regulated by transducer proteins slow down or arrest cell cycle progression at different stages, termed checkpoints, to allow repair of DNA lesions before DNA replication or mitosis. Effector proteins also trigger the apoptosis or senescence of cells carrying damaged DNA (Campisi and d'Adda di Fagagna, 2007; Halazonetis et al., 2008).

1.2.1 DNA damage response proteins

The central sensor proteins of the DDR are proteins of the phosphatidylinositol 3-kinase like protein kinase (PIKK) family, which includes the ATM (ataxia telangiectasia, mutated), ATR (ataxia telangiectasia and Rad3 related) and DNA-PK (DNA dependent protein kinase) kinases (Harper and Elledge, 2007; Meek et al., 2008). Members of the poly (ADP-ribose) polymerase (PARP) family also help to recruit DDR factors to chromatin breaks (Schreiber et al., 2006). ATR is activated primarily in the response to UV damage and replication stress while ATM and DNA-PK are more involved in the response to double strand breaks (DSBs) (Harper and Elledge, 2007; Meek et al., 2008). However, it has also been reported that ATR is activated by DSBs created by IR (Jazayeri et al., 2006). ATR is activated by TopBP1 (DNA topoisomerase 2-binding protein 1) after it is recruited to replication protein A (RPA)-coated ssDNA ends of stalled replication forks by ATM or to damage sites via the interaction of its heterodimeric partner, ATR interacting protein, with the RAD17/9-1-1 complex (Choi et al., 2010a; Jazayeri et al., 2006; Kumagai et al., 2006). The RAD17/9-1-1 complex may also recruit ATR substrates for phosphorylation. ATM is present as a homodimer and inactive in unstressed cells because the kinase domain is physically blocked in the homodimer. ATM is recruited to DSBs and activated by dissociation into monomers following autophosphorylation and acetylation (Bakkenist and Kastan, 2003; Kozlov et al., 2006). ATM substrates for phosphorylation may be recruited by the MRE11-RAD50-NBS1 (MRN) complex. Mutations in either ATM or ATR are associated with two autosomal recessive disorders, ataxia-telangiectasia (AT) and Seckel syndrome, respectively. Cells

derived from patients with either disease show defects in cell cycle checkpoints and increased genomic instability after IR exposure (O'Driscoll and Jeggo, 2006).

Mediator proteins such as Nijmegen breakage syndrome 1 (NBS1), mediator of DNA checkpoint 1 (MDC1), breast cancer type susceptibility protein 1 (BRCA1) and p53 binding protein 1 (53BP1) are required for amplification of the DNA damage signal before transducer proteins CHK1 and CHK2 are activated (Zhou and Elledge, 2000). These mediator proteins, which are phosphorylated by ATM/ATR, quickly accumulate at DNA damage sites and form discrete foci. Mammalian cells that lack any of these mediators show enhanced sensitivity to DNA-damaging agents and impaired cell cycle checkpoints. Another mediator protein, claspin, specifically contributes to the phosphorylation and activation of CHK1 by ATR (Lee et al., 2003).

Subsequently, CHK2 is phosphorylated and activated by ATM while CHK1 is phosphorylated and activated predominantly by ATR (Schwarz et al., 2003; Zhao and Piwnica-Worms, 2001). CHK1 and CHK2 share many overlapping substrates among effector proteins (Bartek and Lukas, 2003). The most important effector proteins are the CDC25 phosphatase family, whose members are phosphorylated and inactivated by CHK1/2 (Bartek and Lukas, 2003). CDC25 in turn regulates the activation of CDKs, which control cell cycle events (see Section 1.1.4).

1.2.2 The G1/S checkpoint

If DNA damage occurs in G1 phase, most eukaryotic cells are blocked prior to S phase in order to prevent the replication of a damaged template. Activated ATM/ATR phosphorylates CHK1/2, which phosphorylates and degrades CDC25A (Figure 1.2) (Mailand et al., 2000). Loss of CDC25A results in the accumulation of phosphorylated CDK2 and its dissociation from cyclin E. Therefore, the localisation of CDC45 mediated polymerase to origin recognition complexes (ORCs) for the

initiation of new origin firing is abolished and DNA replication pauses (Falck et al., 2001; Jin et al., 2003). It has also been reported that destruction of CDC25A maintains the inhibitory phosphorylation on CDK4 to ensure G1 arrest (Terada et al., 1995).

1.2.3 The S phase checkpoint

Stalling of replication forks is induced by the S phase checkpoint in cases of DNA structural abnormalities. These can be caused by either normal DNA replication or environmental insults during S phase. The checkpoint ensures that correct replication is completed before the cell cycle progresses (Bartek et al., 2004; Sancar et al., 2004). CDC25A is degraded following ATM/ATR and CHK1/CHK2 activation (Sancar et al., 2004). DNA polymerase is not loaded to ORCs due to mislocation of CDC45 caused by inactivation of the S phase cyclin E-CDK2 complex. The S phase checkpoint is also imposed by phosphorylation of BRCA1, NBS1 and SMC1 (structural maintenance of chromosome 1) via ATM/ATR, through an undefined mechanism (Kitagawa et al., 2004; Osborn et al., 2002).

1.2.4 The G2/M checkpoint

The G2/M checkpoint is the last opportunity for repair before cell division for G2 cells that have been exposed to DNA damage and for un-repaired damage that arose in G1 and S phases (Nyberg et al., 2002). Following DNA damage, activated ATM/ATR phosphorylate CHK1/2 which in turn phosphorylate CDC25C (Figure 1.2). Phosphorylated CDC25C, which is in a complex with the 14-3-3 proteins, is secluded in the cytoplasm away from its substrate CDK1 (Kramer et al., 2004; Peng et al., 1997). CHK1/CHK2 phosphorylate and upregulate the inhibitory kinase of CDK1, WEE1 (Lee et al, 2001). CHK1/CHK2 also phosphorylate polo-like kinase 1 (PLK1) and inhibit PLK1's activating phosphorylation of CDC25C, which in turn decreases CDC25C activity (van Vugt et al., 2010). In response to UV damage, CDC25B, not CDC25C, is phosphorylated by the mitogen-activated protein kinase

p38 and bound to the 14-3-3 proteins, leading to loss of CDC25B activity (Bulavin et al., 2001). Eventually, decreased cyclin B-CDK1 kinase activity effectively blocks cells from entering mitosis.

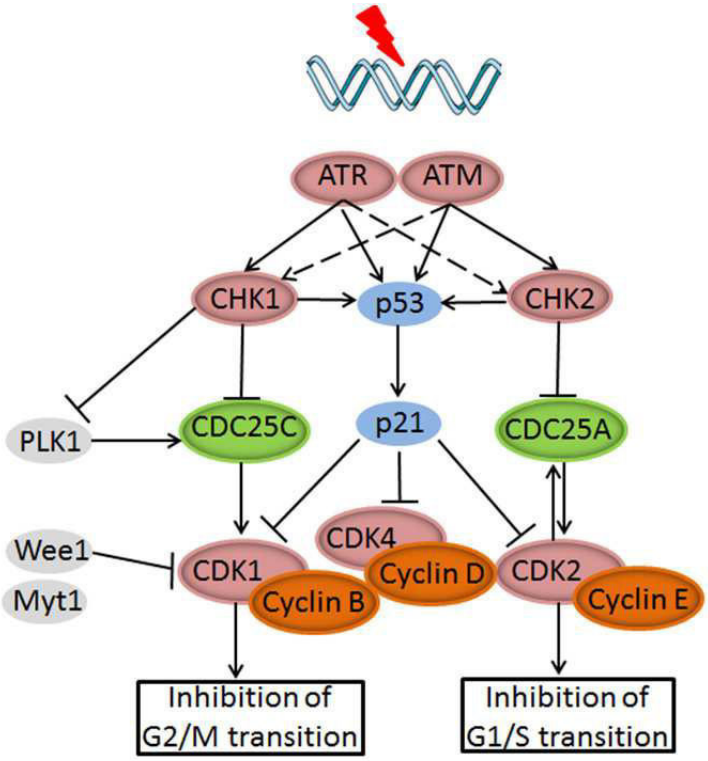

Figure 1.2 Schematic representation of cell cycle checkpoint activation following DNA damage.

There are two parallel but overlapping pathways in the DNA damage response network. ATM/ATR and CHK1/CHK2 are the core kinases of the network. The upstream proteins sense the damage and downstream proteins effect the response. The ATM pathway mainly responds to DNA double-strand breaks and activates CHK2. It can also activate, but more slowly, many of the downstream components of the ATR pathway including CHK1 and ATR itself. The ATR pathway responds to diverse stimuli such as stalled replication forks, ultraviolet light and hydroxyurea and primarily activates CHK1. Activated CHK1/CHK2 inhibit CDC25 family proteins which control cell cycle progression via activation of cyclin-CDK complexes. The cell cycle progression is blocked before either completion of S phase or onset of mitosis. After DNA damage, p53 can also be activated and subsequently elevate the expression of the CDK inhibitor p21, which in turn binds to cyclin-CDK complexes and leads to cell cycle arrest.

1.2.5 The p53-dependent checkpoints

In mammalian cells, p53 is phosphorylated by ATM/ATR and CHK1/CHK2 after DNA damage. The phosphorylation activates and stabilises p53 (Sancar et al., 2004).

Activated p53 functions as a regulatory transcription factor and transactivates p21 and 14-3-3. p21 is an inhibitor of CDKs, including CDK1, CDK2 and CDK4 (Figure 1.2) (Bartek and Lukas, 2001; Ekholm and Reed, 2000). The cell cycle is then arrested in G1 or G2 phase for the repair of damaged DNA. Cells exit the checkpoints and re-enter normal cell cycle progression with completed repair, while p53-dependent apoptosis and senescence are triggered by unsuccessful repair (Chipuk and Green, 2006; Collado et al., 2007).

1.3 DNA repair

Improper repair of damaged DNA results in genomic instability, apoptosis and senescence (Kastan and Bartek, 2004). It has also been demonstrated that people with defective DNA repair capacity are susceptible to immunodeficiency, neurological disorders, and cancer (Subba Rao, 2007; Thoms et al., 2007). There are various DNA repair pathways corresponding to numerous distinct types of DNA lesions. These conserved pathways include the mismatch repair (MMR) pathway, the nucleotide excision repair (NER) pathway, the base excision repair (BER) pathway, the homologous recombination (HR) pathway, and the non-homologous end joining (NHEJ) pathway (Hakem, 2008).

1.4 The microtubule cytoskeleton

As the key cytoskeletal components of eukaryotic cells, microtubules play important roles in composing of the spindle apparatus during cell division, in directed intracellular transport and division and in ciliary and flagellar motility (Raynaud-Messina and Merdes, 2007). They are hollow cylinders (approx 25 nm in diameter) assembled by heterodimers of α-and β-tubulin. The walls of the microtubule are made up of 9-16 protofilaments which are formed by a head-to-tail arrangement of tubulin heterodimers (Figure 1.3) (Nogales et al., 1999; Nogales et al., 1998). Therefore, microtubules have an intrinsic polarity of α-tubulin at the slower-growing minus end and β-tubulin at the faster-growing plus end (Chretien et

al., 1995).

1.4.1 Microtubule nucleation

The formation of new microtubule polymers is termed microtubule nucleation, after which microtubules can rapidly elongate. Microtubules can polymerise spontaneously *in vitro* by self-assembly with the presence of GTP, Mg^{2+} and a high concentration of tubulin heterodimers, forming structures with dynamic instability (Somers and Engelborghs, 1990). However, *in vivo* microtubule nucleation requires a microtubule organising centre (MTOC) for initiation because of the low concentration of tubulin heterodimers. An MTOC is a small structure that controls the assembly, orientation and organisation of microtubules within cells (Mitchison and Kirschner, 1984). According to morphology, several distinct MTOCs are described in different species, including fungal spindle pole bodies (SPBs), protozoan basal bodies, and the higher eukaryotic centrosome (Cuschieri et al., 2007). However, all these structures have the conserved function of providing nucleation sites.

In most animal somatic cells, microtubules are organised with the minus end localised at the centrosome and plus end radiating into the cytoplasm. The ring-shaped γ-tubulin ring complex (γ-TuRC) is essential for the stabilisation and anchoring of the minus ends at the centrosome (Zheng et al., 1995). The γ-TuRC contains γ-tubulin, γ-tubulin complex protein (GCP)-2, -3, -4, -5 and -6, NEDD1, and other components among which γ-tubulin is thought to directly interact with the tubulin heterodimers and other proteins to have supporting roles (Pereira and Schiebel, 1997; Zheng et al., 1995). Two molecules of γ-tubulin and one each of GCP-2 and GCP-3 form the γ-tubulin small complex (γ-TuSC), which is essential for microtubule-nucleating activity but whose activity is much lower than γ-TuRC (Oegema et al., 1999). Recently, two small non-GCP family proteins, MOZART (mitotic-spindle organizing protein associated with a ring of γ-tubulin) 1 and 2 were

described as γ-TuRC components in human cell lines. They are involved in γ-TuRC recruitment to centrosomes (Hutchins et al., 2010). It is believed that additional integral γ-TuRC components yet to be discovered.

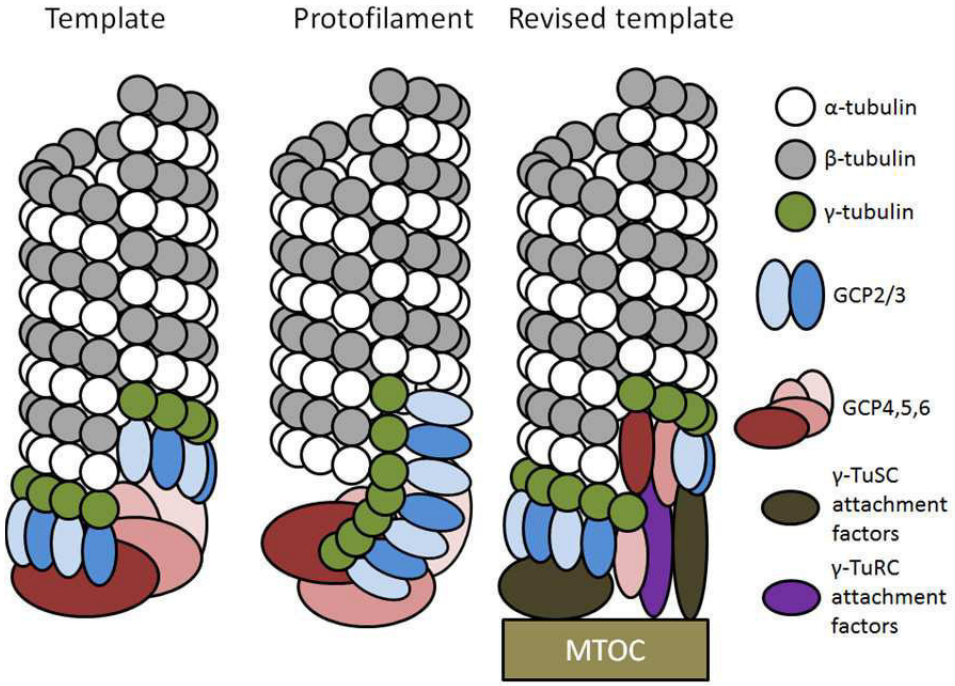

Figure 1.3 Schematic drawings of potential models of microtubule nucleation.
Microtubules are hollow tubes comprised of α-tubulin and β-tubulin heterodimers. Microtubule nucleation requires γ-TuRCs. The γ-TuSC contains two copies of γ-tubulin, each of which is associated with one molecule of GCP-2 and GCP-3. The γ-TuRC contans multiple copies of γ-TuSC and several additional proteins, including GCP-4, -5 and -6.
Template model: γ-tubulin molecules interact with each other laterally to form a ring-shaped complex. α- and β-tubulin heterodimers associate with γ-tubulin longitudinally for the elongation of microtubules. γ-tubulin only contacts α-tubulin and determines the number of protofilaments in this model.
Protofilament model: γ-tubulin molecules interact with each other longitudinally to form a γ-tubulin protofilament. α- and β-tubulin heterodimers associate with γ-tubulin laterally and longitudinally and form protofilaments that close into a microtubule. γ-tubulin contacts both α- and β-tubulin in this model.
In both models, GCP-4, -5 and -6 work as a cap-like scaffold for γ-TuSCs assembly. They do not interact with γ-tubulin directly.
Revised template model: all GCP family proteins act as γ-TuSC-like components. GCP-4, -5 and -6 bind γ-tubulin directly and form a ring structure together with γ-TuSCs. They associate with each other and GCP-2 and -3 laterally and localise at the ends of the ring structure. γ-TuSC and γ-TuRC are attached to MTOCs with the help of attachment factors such as pericentrin, AKAP450 and ninein.

Two models were proposed for microtubule polymerisation (Figure 1.3). In the 'template model', adjacent γ-tubulins in the γ-TuRC interact laterally with each other and each of them links one α-tubulin longitudinally at the minus end of a protofilament. In the 'protofilament model', γ-tubulins in the γ-TuRC interact with each other perpendicularly and are elongated by addition of α- and β-tubulin dimers at the plus end direction to form a protofilament. The protofilament then interacts laterally with α- and β-tubulin and nucleates them for further growth of other protofilaments. An asymmetric cap composed of GCP-4, -5 and -6 acts as a scaffold for arranging γ-TuSCs assembly into ring shape in both models (Kollman et al., 2011; Moritz and Agard, 2001; Wiese and Zheng, 2006). A recent study has demonstrated that there are more γ-tubulins than GCP-2 and -3 in the γ-TuRC (Choi et al., 2010b). Together with the progress in crystal structural studies of GCP-4 (Guillet et al., 2011), template model has been confirmed and revised. In this new model, GCP-4, -5 and -6 directly bind to γ-tubulin as γ-TuSC and contribute to the ring structure. GCP-4, -5 and -6 interact with each other, and also interact with GCP-2 and -3 laterally. GCP-4, -5 and -6 localise at opposite ends of the ring, where they overlap with the half γ-TuSC (Kollman et al., 2011).

1.4.2 Spindle assembly

Chromosome separation in mitosis requires the mitotic spindle, which consists of centrosomes, chromosomes and microtubules in animal somatic cells. At metaphase, microtubule bundles are linked to the kinetochores on individual sister chromosomes, with both centrosomes localised at the opposite poles of the bipolar spindle. Prior to metaphase, microtubules nucleated from each centrosome extend radially, forming microtubule asters. The plus ends of the microtubules rapidly and repeatedly interconvert from growth to shrinkage, in a process termed 'dynamic instability' (Mitchison and Kirschner, 1984). When the nuclear envelope breaks down, the microtubule asters grow asymmetrically with more dynamic microtubules toward the chromosomes to 'search and capture' kinetochores (Kirschner and Mitchison, 1986).

Once the kinetochores contact the plus ends of the microtubules (i.e. kinetochore fibres), the dynamic instability of microtubules is suppressed. Some microtubules which do not capture kinetochores (i.e. interpolar microtubules) extend and overlap at the spindle equator to form an antiparallel array. Other microtubules (i.e. astral microtubules) reach the cell cortex and interact with cortical factors. They all contribute to the maintenance of spindle length and inward tension (Wollman et al., 2008).

However, bipolar spindles are also observed in cells of higher plants and many meiotic eggs in which centrosomes are absent (Bannigan et al., 2008; Doubilet and McKim, 2007). Therefore, there must be an alternative mechanism for spindle assembly. One possibility is that microtubule nucleation and stabilisation are driven by chromosomes with the help of RanGTP (Heald et al., 1996; Kalab et al., 1999). After nuclear envelope breakdown, the nucleation is triggered by a local high concentration of RanGTP in the vicinity of the chromosomes. Microtubules elongate around the chromosomes and are randomly oriented. They can then be sorted into symmetric, bipolar arrays by a structural protein, NuMA (nuclear mitotic apparatus) and microtubule minus-end-directed motors, such as dynein through the coalescence of microtubule minus ends at spindle poles (Gadde and Heald, 2004; Haren and Merdes, 2002; Heald et al., 1997). Chromosome-mediated spindle assembly is not exclusive to classical 'search and capture' mechanisms. Indeed, the two pathways work synergistically and both contribute to the incorporation of chromosomes and microtubules into the spindle (Wadsworth and Khodjakov, 2004). Microtubules nucleated at kinetochores ultimately interact with those emanating from centrosomes, which facilitate the capture of astral microtubules by kinetochores.

1.4.3 The spindle assembly checkpoint

During metaphase, the kinetochore of each paired sister chromatid is attached to microtubules from the opposite poles of the bipolar spindle. This guarantees that

each daughter cell inherits one complete set of parental genetic material after the sister chromatids are pulled towards opposite poles in anaphase. The spindle assembly checkpoint (SAC) ensures that all chromosomes are aligned on the cell equator and achieve bipolar attachment to the mitotic spindle before the onset of segregation (Musacchio and Hardwick, 2002; Taylor et al., 2004). The SAC is not inactivated unless all kinetochores are properly attached to microtubules.

Chromosome segregation requires inactivation of the SAC and activation of the anaphase-promoting complex/cyclosome (APC/C), an E3 ubiquitin ligase responsible for targeting many cell cycle proteins for degradation by the 26S proteasome (Peters, 2002). The specific target selection of the complex is mediated by its cofactors, CDC20 or CDH1 (Kramer et al., 2000). Once all kinetochores are correctly aligned, two main substrates, securin and cyclin B, are targeted for degradation (Hagting et al., 2002). Securin is a stoichiometric inhibitor of the protease separase, which degrades the SCC1 (sister chromatid cohesion 1) subunit of cohesin and allows chromosome separation (Hornig et al., 2002). The principal function of the cohesin complex is to keep sister chromatids together (Alexandru et al., 2001). Degradation of securin activates separase, which in turn cleaves cohesin and lets sister chromatids separate in anaphase. On the other hand, the proteolysis of cyclin B causes the inactivation of cyclin B-CDK1, which is essential for keeping the cells in mitosis (see Section 1.1) (Brito and Rieder, 2006). Thereafter, cells carry out cytokinesis and exit mitosis. A schematic representation of the SAC signaling pathway is shown in Figure 1.4.

1.4.4 Components of the SAC

Components of the SAC were first identified and characterised in yeast (Hoyt et al., 1991; Li and Murray, 1991). The conserved orthologs in higher eukaryotes were then identified, including MAD1 (mitotic arrest deficient 1), MAD2, BUB1 (budding uninhibited by benzamidazoles 1), BUB3, MAD3/BUBR1 (BUB-related 1), MPS1

(monopolar spindle 1) and Aurora B which all accumulate on unattached kinetochores (Lew and Burke, 2003). In higher eukaryotes, loss of SAC function was observed after depletion of these SAC proteins. This resulted in chromosome mis-segregation, aneuploidy and a failure to arrest in mitosis in the presence of microtubule poisons (Bharadwaj and Yu, 2004).

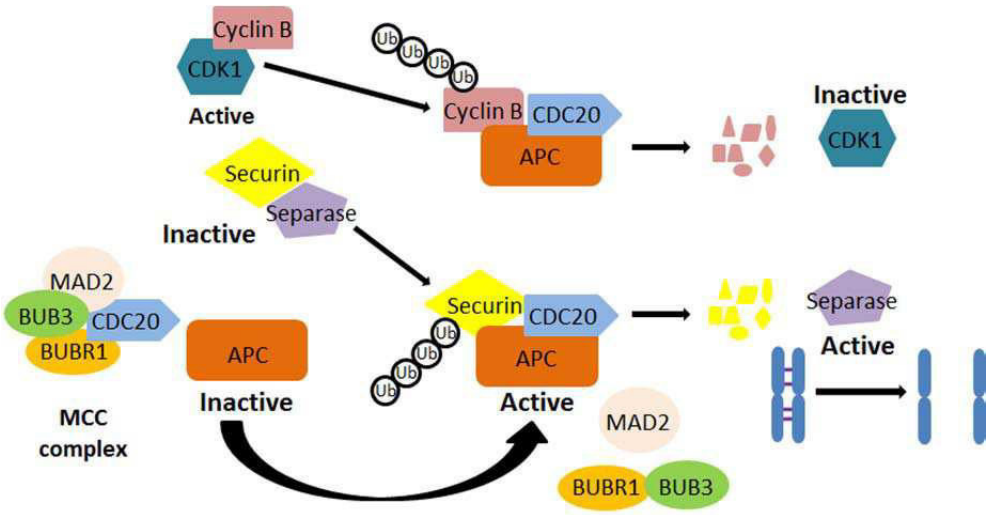

Figure 1.4 The spindle assembly checkpoint signaling.
The APC/C-CDC20 complex targets securin and cyclin B for ubiquitin-mediated degradation in a SAC-independent manner. During prometaphase, the SAC is activated as a result of unattached or improperly attached kinetochores. MAD2, BUBR1, BUB3 and CDC20 then form a single quaternary complex, MCC which prevents APC/C-CDC20 mediated ubiquitination. Once the bipolar attachment of all sister-kinetochore pairs to kinetochore microtubules is completed, the SAC is switched off. The disruption of MCC results in the release of CDC20 and the activation of APC/C which in turn leads to the ubiquitination and subsequent proteolytic destruction of securin. Degradation of securin activates separase which is kept inactive by direct association with securin. Separase then cleaves the SCC1 subunit of the sister-chromatid cohesion complex, cohesin and triggers the separation of sister chromatids. In addition, cyclin B is ubiquitylated and degraded. Therefore, the master mitotic kinase cyclin B-CDK1 is inactivated and the mitotic exit programme is initiated.

During SAC activation, a mitotic checkpoint complex (MCC), which consists of MAD2, BUBR1, BUB3 and CDC20, localises to the unattached kinetochores (Sudakin et al., 2001). An unattached kinetochore is thought to function as the catalytic platform for activation of the MCC, as all components of the MCC

concentrate and turn over at unattached kinetochores (Ciliberto and Shah, 2009). The conformational conversion activates MAD2, which binds to CDC20 to form a MAD2-CDC20 subcomplex. MAD2-CDC20 then promotes the formation of a BUBR1-CDC20 complex which can inhibit the APC/C independently of MAD2. However, MAD2 functions synergistically with BUBR1 to fully inhibit APC/C activity (Musacchio and Salmon, 2007; Peters, 2002). Sequestration of CDC20 by the MCC in turn inactivates APC/C and inhibits the onset of anaphase.

When all kinetochores are attached to microtubules, the SAC must be switched off for chromosome separation to begin. The central step is to inactivate the MAD2-CDC20 complex and remove it from kinetochores. Cytoplasmic dynein motility along the microtubules may contribute to MAD2 depletion from kinetochores. When dynein is inhibited, MAD2 is re-localised to attached kinetochores (Howell et al., 2001; Wojcik et al., 2001). MAD2-CDC20 can be inactivated by the re-activation of the inhibitor $p31^{comet}$ (Mapelli et al., 2006; Xia et al., 2004). The phosphorylated MAD2 dissociates from the MCC and liberates CDC20.

1.4.5 Tension or attachment?

The exact nature of what triggers the activation of the SAC remains under debate (Figure 1.5). One model is that the SAC monitors microtubule attachment to the kinetochores (Howell et al., 2001). The SAC proteins, MAD1 and MAD2, concentrate at unattached kinetochores and disappear at attached kinetochores (Skoufias et al., 2001; Waters et al., 1998). It has also been shown that even a single unattached kinetochore is sufficient to activate the SAC and cause a delay in chromosome segregation. The cell cycle proceeded to anaphase after laser ablation of the unattached kinetochore on the last mono-oriented chromosome (Rieder et al., 1995). In addition, cells arrest at mitosis after treatment with microtubule-depolymerising drugs such as colcemid and nocodazole, confirming that the SAC is

activated by unattached kinetochores and prevents anaphase initiation (Waters et al., 1998). However, treatment of mammalian cells with a microtubule-stabilising drug, such as taxol, also activates the SAC and induces mitotic arrest. The microtubules remain attached to kinetochores, whereas tension across the paired kinetochores decreases in these cells (Waters et al., 1998). Tension is usually generated between sister kinetochores when they are attached to microtubules and pulled toward two opposite spindle poles (Zhou et al., 2002). Therefore, the second model proposed is that the SAC monitors tension (Nicklas et al., 1995). Sister kinetochores attached to microtubules from the same pole, in what is termed syntelic attachment, lack tension and activate the SAC, also implying that lack of tension is sufficient for checkpoint activation (Kapoor et al., 2000).

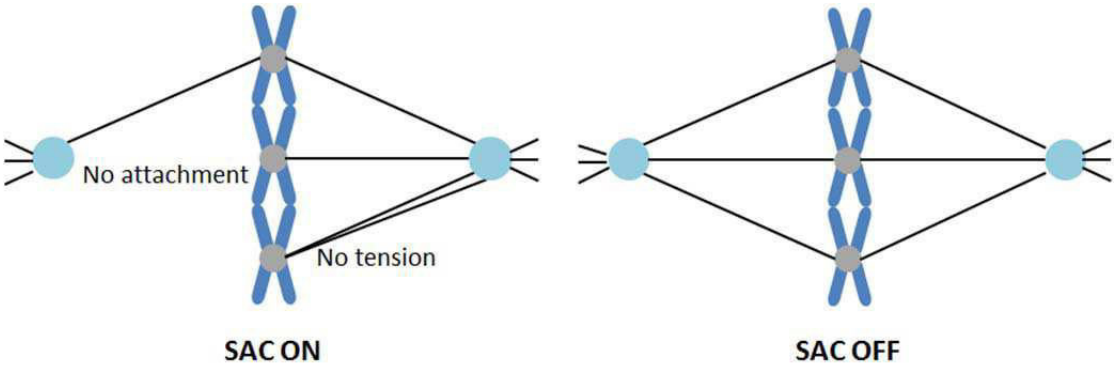

Figure 1.5 Two models of spindle assembly checkpoint activation/silencing.
Defects in tension and attachment are separate signals which activate the SAC. In the 'attachment model', the full attachment of all sister kinetochores to microtubules from two opposite spindle poles (amphitelic attachment) switches off the checkpoint. In the 'tension model', tension generated by the bipolar microtubule attachment to paired kinetochores controls the activation of the checkpoint. The sister kinetochores are not under tension if only one kinetochore binds microtubules and one is unattached (monotelic attachment). There is no enough tension if one or both sister kinetochores are bound by microtubules from the same pole (syntelic attachment).

It should be noted that it is technically impossible to distinguish lack of tension from unattachment of microtubules to kinetochores because they occur at the same time. Tension can only be generated when both sister kinetochores are attached to microtubule and tension itself stabilises kinetochore microtubule attachment. On the

other hand, tension is apparently absent on unattached kinetochores (Kapoor et al., 2000; Nezi and Musacchio, 2009). It is likely that kinetochores transiently and undetectably dissociate from microtubules in the case of tension loss but without unattached kinetochores (Lew and Burke, 2003). Further work in this area may help elucidate whether attachment or tension, or both, is monitored by the SAC.

1.5 The centrosome

As the main microtubule organising centres, centrosomes are small (1-2μm^3) subcellular, non-membrane-enclosed organelles localised at the centre of the cells, usually close to the nucleus. A typical centrosome of vertebrate cells consists of two centrioles and pericentriolar material (PCM) (Fig 1.6). Centrioles comprise nine radially symmetrical sets of triplet microtubules which form barrel-shaped arrays together with other components. The microtubules of each triplet are normally referred to as the A-, B- and C-tubules. The two centrioles of the same centrosome are connected perpendicularly by a proteinaceous fibre linker at the proximal ends. One of the centrioles possesses two sets of appendages at the distal end furthest from the other centriole, termed the mother or maternal centriole. The immature daughter centriole is about 20% shorter than the mother centriole (Chretien et al., 1997). Microtubules are anchored to the subdistal appendage of the maternal centriole (Paintrand et al., 1992; Semmler et al., 2000). The PCM is a lattice-like structure around the centrioles which contains all the elements for anchoring the proteins involved in microtubule nucleation and other activities (Doxsey, 2001). According to mass spectroscopy results of purified centrosomes, about 500 proteins are thought to be related with the centrosome (Andersen et al., 2003; Jakobsen et al., 2011). Many are not structural centrosome proteins but employ centrosomes as a docking station for their cell cycle-specific functions. Some centrosome proteins are permanently connected with the centrosome, including γ-tubulin and centrin, whereas other proteins are temporarily connected with the centrosome at specific cell cycle stages.

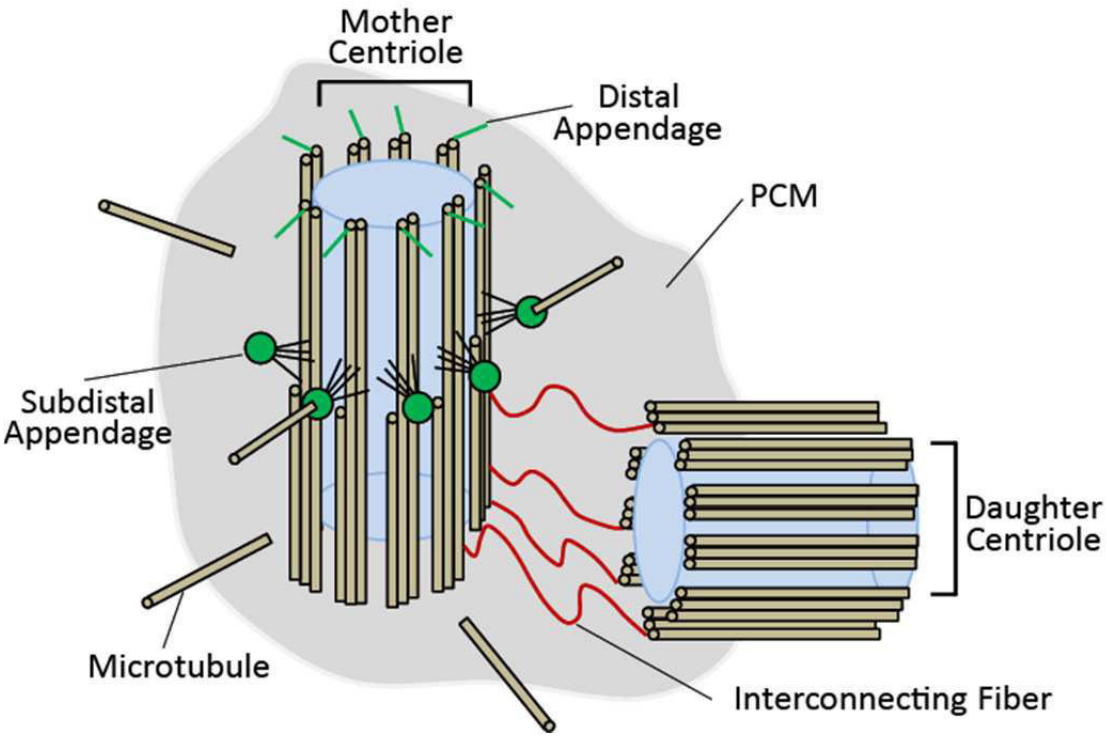

Figure 1.6 Centrosome structure.
There is one centrosome during G1 phase in vertebrate cells. The centrosome contains two centrioles which are composed of nine triplet microtubules. The daughter centriole is shorter and lacks the maturity markers of the mother centriole, the distal and subdistal appendages. The two centrioles are connected by flexible fibres and embedded in PCM.

1.5.1 Centrosome functions

Given its microtubule organising functions, the centrosome governs most microtubule-related functions (see Section 1.4). In addition, the centrosome also plays important roles in cell cycle progression and the DNA damage response (Kramer et al., 2004).

1.5.1.1 Microtubule organisation

As described in Section 1.4.1, the centrosome is the major MTOC in animal cells. Its main function is microtubule nucleation and anchoring. Following nucleation, microtubules are either released into the cytoplasm or anchored on the subdistal appendages of the mother centriole (Belmont et al., 1990). During interphase, microtubules nucleated by the centrosome extend into the cytoplasm near the cell cortex. The dynamically instable microtubules let cells quickly sense and respond to

changes of the cell boundary (Komarova et al., 2002). In mitosis, an increased number of microtubules (up to five times more than during interphase) are nucleated by the centrosome (Piehl et al., 2004). In addition, the dynamicity of the microtubules increases (Belmont et al., 1990). The increased number and dynamicity of microtubules allow the bipolar spindle to form efficiently.

1.5.1.2 The centrosome and the cell cycle

The centrosome also plays a role in cell cycle progression. Cyclin E-CDK2 complex is essential for entry into S phase (see Section 1.1.2). It has been reported that cyclin E-CDK2 has to localise to the centrosome prior to DNA synthesis (Matsumoto and Maller, 2004). RNAi depletion of centrosome proteins, including PCM-1 and pericentrin caused a reduction in the activity of cyclin A/E-CDK2 which resulted in G1 arrest (Mikule et al., 2007; Srsen et al., 2006). Similarly, cytokinesis defects and G1 phase arrest occurred when pericentrin, AKAP (A-kinase anchor proteins) 450 or PKA (protein kinase A) were mislocalised from centrosomes (Gillingham and Munro, 2000; Keryer et al., 2003b). More direct evidence comes from experiments that removed the centrosomes/centrioles by microsurgery or laser ablation. Although acentriolar MTOCs and functional mitotic spindles formed in the cells after the centrioles and associated PCM were removed, half of the cells could not undergo cytokinesis (Hinchcliffe et al., 2001; Khodjakov and Rieder, 2001). Cytokinesis delay usually leads to G1 arrest (Gromley et al., 2003). In addition, if only one of the centrosomes was excised in prometaphase cells, the daughter cells which had an acentriolar MTOC, failed to enter S phase (Uetake and Sluder, 2004; Wong and Stearns, 2003). These data suggest that disruption of core centrosome structures or components induces cytokinesis defects followed by G1 phase arrest.

Mitotic kinases and cyclins are found at centrosomes, suggesting that the centrosome also plays a role in mitosis. Overexpression of the centrosome binding domain of polo kinase, a centrosome-associated mitotic regulator, induced cell cycle arrest just

before mitosis (Hirota et al., 2003). Cyclin B-CDK1 activation is a key event in initiating mitosis (see Section 1.1.3). It has been shown recently that centrosomal localisation of CDK1 is required for the G2/M transition (Kramer et al., 2004). Although cyclin B is found in the cytoplasm of interphase cells, the activated cyclin B-CDK1 is first detected at the centrosome before histone H3 is phosphorylated (Jackman et al., 2003). As a direct activator of cyclin B-CDK1, CDC25B was observed to be phosphorylated by Aurora A at centrosomes (Dutertre et al., 2004). Aurora A may also contribute to the centrosomal recruitment of cyclin B-CDK1 (Hirota et al., 2003).

Although the mechanism for the role of the centrosome in cytokinesis has not been well clarified, time-lapse microscopy of cells expressing centrin-GFP has suggested that the temporal and spatial interaction between the centrosome and the midbody is important for completion of cytokinesis (Piel et al., 2001). The mother centriole was observed to translocate transiently and rapidly to the intracellular bridge near the midbody before abscission. Once the mother centriole relocated from the bridge to the centre of the cell, abscission continued and cytokinesis finished (Piel et al., 2001). Similarly, centrosomes associated with the Golgi complex moved from the poles to the intracellular bridge and back prior to cytokinesis (Mack and Rattner, 1993; Moskalewski and Thyberg, 1992). In addition, centrosome proteins, such as centriolin and pericentrin, are found at the midbody, indicating that the centrosome docks regulatory proteins required for cytokinesis (Gromley et al., 2003).

1.5.1.3 The centrosome and the DNA damage response

Given its roles in unperturbed cell cycle progression, it is plausible that the centrosome is also involved in the DNA damage response. More and more components of the DDR pathway are found to be associated with centrosomes but the mechanism remains unclear. Both ATM and ATR localise at the centrosome in addition to the nucleus (Oricchio et al., 2006; Zhang et al., 2007). Loss of ATM leads

to defects in p53 centrosomal localisation and phosphorylation which in turn inhibit the G1/S transition (Ciciarello et al., 2001; Tritarelli et al., 2004). Moreover, the proper centrosomal localisation of CHK1, another central protein in the DDR pathway, is involved in regulating its function. It has been shown that CHK1 localises at the centrosome during interphase but disappears at the onset of prophase. Centrosomal immobilisation of CHK1 by fusing it with the PACT (pericentrin-AKAP450 centrosomal targeting) domain inhibited CDK1 activation at centrosomes and subsequent mitosis (Kramer et al., 2004). It has been suggested that CHK1 inhibits CDK1 activation at the centrosomes via the phosphorylation of CDC25B. Therefore, inhibition of CHK1 causes the activation of centrosomal CDK1, which in turn leads to premature mitotic entry characterised by increased microtubule nucleation, recruitment of mitosis-specific motor proteins to spindles, premature separation of centrosomes and an increased amount of mitotic cells (Kramer et al., 2004). However, it should be noted that a recent study demonstrated that CHK1 did not localise at centrosomes, challenging this model. The centrosomal reactivity of the anti-CHK1 antibody (DCS-310) used in previous studies is due to its cross reactivity with another protein, Ccdc151 (Matsuyama et al., 2011). CHK1-PACT was also detected in nucleus and mitotic entry was delayed by forced nuclear localisation of the CHK1 mutant (Matsuyama et al., 2011).

DNA repair proteins are also present at the centrosome. NBS1, one of the components of the MRN complex, localises at the centrosome throughout the cell cycle. NBS1 knockdown impairs centrosome separation but elevates centriole overduplication, leading to centrosome amplification (Shimada et al., 2009). In addition, several components of the PARP system, which is involved in BER, localise to the centrosome. PARP-1 localises to both centrioles, whereas PARP-3 predominantly to the daughter throughout the cell cycle (Augustin et al., 2003; Kanai et al., 2000). Moreover, centrosome amplification is observed in PARP-$1^{-/-}$ cells and cells treated with PARP inhibitor, indicating that PARP-1-mediated poly (ADP-

ribosyl)ation of centrosomal proteins is a potential regulatory mechanism for centrosome function (Kanai et al., 2003). Recently, we have shown that centrin, a widely accepted centriole marker, are required for efficient NER. Centrin-null DT40 cells are hypersensitive to UV in clonogenic survival assays, but DNA damage checkpoint responses in the cells are normal (Dantas et al., 2011). Taken together, these findings suggest that the centrosome co-ordinates the checkpoints at cell cycle transitions after DNA damage.

1.5.2 The centrosome cycle

As a bipolar mitotic spindle is essential for faithful chromosome segregation, centrosome duplication must be tightly coordinated with the cell cycle. Like the genetic material, centrosomes duplicate exactly once within each cell cycle in a semi-conservative manner (Nigg and Stearns, 2011). The canonical centrosome duplication cycle involves five consecutive steps: centriole disengagement, procentriole biogenesis, procentriole elongation, centrosome maturation and centrosome separation (Figure 1.7).

During G1 phase, the tightly-associated centrioles disengage from each other, losing their strict orthogonal configuration but remaining connected via cohesion fibres. Centriole disengagement is crucial for the licensing of the subsequent new round of centrosome duplication in S phase (Tsou and Stearns, 2006). It has been shown that activated PLK1 and separase are the major forces which drive centriole disengagement (Tsou and Stearns, 2006; Tsou et al., 2009; Wang et al., 2008). Separase cleaves cohesin which may link the centrioles together (Nakamura et al., 2009). PLK1 phosphorylates sSgo1 which works as a protector of centriolar cohesion from separase activity (Wang et al., 2008).

At the G1/S transition, procentrioles form at the proximal end of the pre-existing centrioles in a perpendicular arrangement. The protein kinase, PLK4, and the

coiled-coil protein, SAS-6, are believed to control centriole biogenesis (Kleylein-Sohn et al., 2007; Puklowski et al., 2011). Overexpression of PLK4 or SAS-6 causes the generation of supernumerary centrioles, whereas depletion of PLK4 leads to a reduction in centriole number (Guderian et al., 2010; Holland et al., 2010; Strnad et al., 2007). PLK4 induces the activation of SCF-FBXW5 E3-ubiquitin ligase, which in turn stabilises SAS-6 (Puklowski et al., 2011). Oligomerisation of SAS-6 forms a cartwheel-like structure, which serves as the basis of the centriolar nine-fold symmetry (Nakazawa et al., 2007; Strnad et al., 2007).

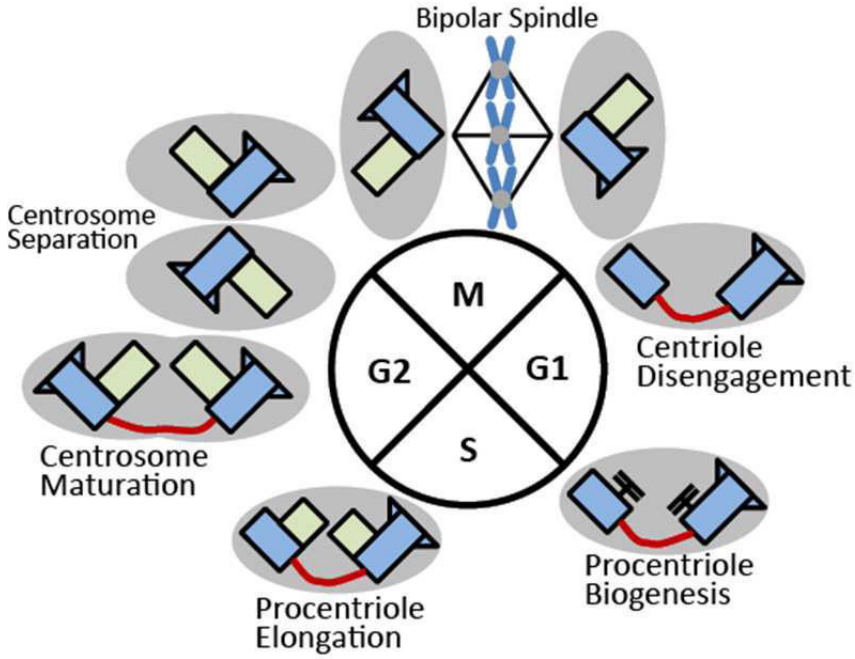

Figure 1.7 The canonical centrosome duplication cycle.
At the end of mitosis/the beginning of G1 phase, the mature centrioles (blue bar) of the centrosome lose the tight link (centriole disengagement), but remain connected by a loose fibrous structure (red line). The mother centriole (blue bar with two triangles) is assembled at least two cell cycles previously, whereas the daughter centriole is generated in the previous cell cycle. In S phase, two new centrioles (green bar) form at the proximal end of the mature centrioles in a perpendicular arrangement and elongate throughout S and G2 phases. At the end of G2 phase, the daughter centriole acquires the same structures as the mother centriole. The two centrosomes undergo maturation by recruiting additional PCM (grey oval). Then the fibrous tether between the mature centrioles is degraded and the two centrosomes separate and move to the opposite sides of the nucleus. The two centrosomes finally form the poles of the bipolar spindle.

Procentrioles elongate throughout S and G2 phases. Several proteins, such as SAS-4

(also known as CPAP or CENPJ) and CP110, are involved in this elongation process (Nigg and Stearns, 2011). SAS-4 promotes the deposition of centriolar microtubules, thereby facilitating procentriole elongation (Kleylein-Sohn et al., 2007; Tang et al., 2009). CP110 localises the growing end of the daughter centriole, possibly forming a cap to limit microtubule extension (Kleylein-Sohn et al., 2007; Schmidt et al., 2009).

The centrosomes then undergo maturation by accumulation of additional PCM proteins. This results in an increase in centrosome size and microtubule nucleation activity. The procentrioles only completely mature as mother centrioles in the following cycle when they acquire distal and subdistal appendages (Azimzadeh and Bornens, 2007). PLK1 and Aurora A have been directly implicated in the control of centrosome maturation (Lukasiewicz and Lingle, 2009).

In interphase cells, the two new centrosomes are connected via another type of proteinaceous linker between the proximal end of the two mother centrioles until mitotic entry (O'Regan et al., 2007). Several proteins such as C-NAP1, rootletin, as well as CEP68 and CDK5RAP2 are the known components of the linker (Bahe et al., 2005; Graser et al., 2007b; Mayor et al., 2000). At the G2/M transition, these linker proteins are phosphorylated by the kinase NEK2 and become susceptible to ubiquitination and proteolysis (Fry, 2002). Therefore, the cohesion between the two mature centrosomes, each containing a pair of engaged centrioles, disappears. The separated centrosomes participate in mitotic spindle pole formation. At the end of mitosis, centrioles disengage again and the new centrosome cycle begins.

To ensure that centrosomes duplicate only once in each cell cycle, there must be an intrinsic block to the re-duplication. Cyclin E-CDK2 was proposed to be a licensing factor for centrosome duplication (Hinchcliffe et al., 1999). However, it was demonstrated that centrosomes duplicated normally in *Cdk2*$^{-/-}$ cells (Duensing et al., 2006). In addition, a second round of centrosome duplicate is still absent during S

phase arrest where CDK2 is highly activated (Wong and Stearns, 2003). Therefore, it has been suggested that centriole disengagement licenses centrosome duplication and that the engaged state of centrioles at S, G2 and mitosis blocks re-duplication. This hypothesis was confirmed by cell fusion experiment of G1 phase cells and G2 phase cells. Only the G1 centrosome duplicated whereas the already-duplicated G2 centrosomes did not re-duplicate in the fused cells (Wong and Stearns, 2003). Furthermore, the mother centriole of S phase cells re-duplicated after the daughter centriole was removed by laser ablation (Loncarek et al., 2008).

1.5.3 Centrosome amplification

The formation of bipolar mitotic spindles is essential for accurate chromosome segregation. Abnormal amplification of centrosomes can cause multiple spindle poles which in turn results in asymmetrical chromosome segregation and genomic instability. Centrosome amplification is prevalent in almost all types of solid tumours, implying aneuploidy in cancers (Fukasawa, 2005). Coincidently, supernumerary centrosomes have been described in cells carrying mutations in checkpoint or DNA repair genes (Dodson et al., 2004; Fukasawa et al., 1996; Griffin et al., 2000; Matsuura et al., 1998). Centrosome amplification also frequently occurs in response to DNA damage (Sato et al., 2000). Usually, most cells with tripolar spindles can undergo cytokinesis. Some of the daughter cells are still viable but aneuploid. Cells with more than 3 centrosomes can cluster on a bipolar axis and form pseudo-bipolar spindles which structurally resemble normal bipolar spindles. Thus, cells can undergo normal chromosome segregation (Quintyne et al., 2005). However, it is likely that aneuploidy develops in some daughter cells because several amplified centrosomes are not clustered but still nucleate spindle microtubules (Shimada and Komatsu, 2009).

Several mechanisms of centrosome amplification have been proposed. The centrosome cycle can be dissociated from normal cell cycle control under certain

circumstances. It was first reported that supernumerary centrosomes were produced when the centrosome cycle continues during an S phase arrest induced in CHO cells by hydroxyurea or aphidicolin treatment (Balczon et al., 1995). In addition, centrosome amplification happens during an extended G2 arrest after DNA damage (Dodson et al., 2004; Steere et al., 2011). Centriole disengagement observed in G2 phase centrosomes after irradiation may license centrosome reduplication (Inanc et al., 2010). The cell cycle arrest offers cells time for centrosome reduplication and cells re-enter the cell cycle with an excess number of centrosomes. More evidence comes from the analysis of CDK1 and CDK2's roles in centrosome amplification. Multiple centrosomes formed in the cells where CDK1 was suppressed by either a chemical inhibitor or chemical genetics (Bourke et al., 2010; Hochegger et al., 2007; Loncarek et al., 2010). Overexpression of cyclin E upregulated CDK2 activity, which in turn induced centrosome amplification in *p53*-deficient cells (Kawamura et al., 2004; Mussman et al., 2000). Overexpression of cyclin E also restored DNA damage-induced centrosome amplification which was inhibited by loss of CHK1 (Bourke et al., 2010). However, defects in exiting mitosis after the radiation-induced G2 arrest results in cells containing not only supernumerary centrosomes but also multiple nuclei (Fletcher et al., 2004; Meraldi et al., 2002). The centrosome amplification which occurs in these circumstances is likely to have been caused by cytokinesis failure and subsequent tetraploidization.

It is also possible that untimely splitting of paired centrioles can cause each centriole to form supernumerary centrosomes (Hut et al., 2003; Saladino et al., 2009). Interphase overduplication of centrioles arises from the overexpression of key centriole duplication proteins. It has been shown that overexpression of PLK4, SAS-6 or SIL causes the formation of multiple procentrioles around pre-existing centrioles (Arquint et al., 2012; Habedanck et al., 2005; Leidel et al., 2005). Furthermore, overexpression of the same proteins can lead to *de novo* centriole assembly (Peel et al., 2007). These different mechanisms may not be mutually

exclusive during the generation of supernumerary centrosomes.

1.6 Pericentrin

The human *PCNT* gene, located at 21q22.3, spans 121.6 kb of genomic sequence and contains 47 exons. Pericentrin, which is encoded by *PCNT*, is a very large coiled-coil protein that serves as an integral component of the PCM (Li et al., 2001). Pericentrin specifically localises to centrosomes throughout the cell cycle (Flory and Davis, 2003). Pericentrin is highly conserved throughout evolution (Doxsey et al., 1994) and two isoforms have been described in humans. The full-length protein, pericentrin B (~380kDa), also referred to as kendrin or PCNT2, contains two long central regions predicted to form coiled-coils flanked by noncoiled regions (Flory et al., 2000). Pericentrin A (250 kDa), originally cloned in mouse, shares strong overall homology with the noncoiled N-terminal domain and the first coiled-coil region of pericentrin B but lacks the second coiled-coil region and the unique C-terminal calmodulin-binding site (Flory and Davis, 2003). Pericentrin B is found in most tissues in human and mouse while pericentrin A is detected in a subset of tissues. Pericentrin A and pericentrin B are now regarded as the alternatively spliced variants of one gene (Flory and Davis, 2003). Another N-terminally truncated isoform, pericentrin S (250 kDa) has been found in mouse (Miyoshi et al., 2006a). The N-terminal region of pericentrin B and Spc110p (the homologue in budding yeast) binds directly to the γ-tubulin complex (Dictenberg et al., 1998; Knop and Schiebel, 1997; Nguyen et al., 1998), whereas the C-terminal region binds to the centrosome and core of the spindle pole body (the analogous structure in budding yeast) (Dictenberg et al., 1998; Kilmartin and Goh, 1996; Stirling et al., 1996; Sundberg et al., 1996). Pericentrin is localised to the centrosome by its C-terminal PACT domain (Gillingham and Munro, 2000). The conserved PACT domain is also present in *Drosophila* and *Schizosaccharomyces pombe*, and the *Drosophila* PACT domain is sufficient for localisation to the centrosome in mammalian cells (Gillingham and Munro, 2000).

Pericentrin serves as a multifunctional scaffold for anchoring numerous proteins and protein complexes. Through these interactions, pericentrin plays a role in diverse cellular processes (Delaval and Doxsey, 2009), including microtubule nucleation and spindle organisation (Doxsey et al., 1994; Takahashi et al., 2002), cilia formation (Jurczyk et al., 2004; Martinez-Campos et al., 2004; Miyoshi et al., 2006b), and the centrosomal recruitment of signaling proteins, such as CHK1, MCPH1, PKA, PKCβII and disrupted in Schizophrenia 1 (DISC1) (Chen et al., 2004; Diviani et al., 2000; Matsuzaki and Tohyama, 2007; Miyoshi et al., 2004; Tibelius et al., 2009). Recent studies have revealed that pericentrin might have a nuclear function. Pericentrin can interact with chromodomain helicase DNA-binding protein 3/4 (CHD3/4), components of the multiprotein nucleosome remodeling deacetylase (NuRD) complex (Sillibourne et al., 2007) and pericentrin accumulates into the nucleus after inhibiting of CRM1 (chromosome region maintenance 1)-mediated nuclear export (Keryer et al., 2003a; Liu et al., 2009). The unusual tripartite nuclear localisation signal (NLS) and five classical nuclear export signals (NESs) of pericentrin may be responsible for its nuclear localisation and nucleo-cytoplasmic shuttling during the cell cycle (Liu et al., 2010), because the interaction of NLSs and NESs domains with their respective transport proteins determines the nuclear entry and exit of the protein (Gorlich and Kutay, 1999; Sorokin et al., 2007).

Given its interaction with abundant proteins, pericentrin functions both at structural and regulatory levels. On one hand, pericentrin controls several structural centrosomal proteins, particularly those participating in microtubule nucleation and spindle organisation (Dictenberg et al., 1998; Doxsey et al., 1994; Miyoshi et al., 2004; Zimmerman et al., 2004). On the other hand, it is involved in cell cycle regulation by its interaction with the ATR pathway components (Griffith et al., 2008; Tibelius et al., 2009).

1.6.1 Pericentrin, microtubules and the mitotic spindle

Several studies have demonstrated that pericentrin works as a multifunctional scaffold protein for anchoring proteins to centrosomes for spindle organisation and microtubule nucleation (Doxsey et al., 1994; Takahashi et al., 2002; Kawaguchi and Zheng, 2003; Keryer et al., 2003a). Pericentrin and its orthologues are found at centrosomes (Miyoshi et al., 2006b; Zimmerman et al., 2004) or the equivalent structure in the budding yeast *Saccharomyces cerevisiae* (spc110p/Nuf1p) (Knop and Schiebel, 1997), the fission yeast *S. pombe* (Pcp1p2) (Flory et al., 2002), the filamentous fungus *Aspergillus nidulans* (Flory et al., 2002), and *Drosophila* (Martinez-Campos et al., 2004).

γ-TuRC is the best studied component that is anchored to the centrosome by pericentrin to participate in microtubule nucleation (Dictenberg et al., 1998; Zheng et al., 1995). Pericentrin anchors γ-TuRCs via binding with GCP-2 and -3 (Takahashi et al., 2002; Zimmerman et al., 2004). Silencing of pericentrin induces reduction of centrosomal γ-tubulin, inhibition of astral microtubules, formation of monopolar spindles and chromosome mis-segregation. These phenotypes seem to be mitosis-specific as there is no difference in interphase cells (Dictenberg et al., 1998; Doxsey et al., 1994; Griffith et al., 2008; Stirling et al., 1996; Zimmerman et al., 2004). A similar phenotype is observed in the case of functional abrogation of γ-tubulin or overexpression of the GCP-2 and -3 binding domain of pericentrin. It is noteworthy that some studies observed that depletion of pericentrin did not affect centrosomal γ-tubulin recruitment, aster formation, microtubule organisation or cell division (Griffith et al., 2008; Li et al., 2001; Martinez-Campos et al., 2004; Takahashi et al., 2002).

Pericentrin and γ-TuRC complex also require a microtubule-based transport mechanism to achieve spindle microtubule nucleation. Dynein is a good candidate for centrosome-dependent microtubule nucleation (Young et al., 2000). The complex

is recruited to the centrosome through the interaction between pericentrin and dynein light intermediate chain 1 (Purohit *et al.*, 1999), followed by the release of dynein from the complex to the cytoplasm. Immunodepletion of dynein leads to a significant decrease of centrosomal pericentrin and the γ-tubulin (Young et al., 2000). A recent study proposed that pericentrin and the γ-TuRC complex were also recruited to the mitotic centrosome in a PLK1 dependent pathway (Haren et al., 2009). Both centrosomal pericentrin and γ-tubulin were reduced after either treatment with a PLK1 inhibitor or PLK1 depletion by RNAi. Monopolar spindles and prometaphase arrest were observed as a result of impaired microtubule nucleation (Haren et al., 2009; Lee and Rhee, 2011).

Several other proteins, such as CRM1 and CHD3, may also be involved in centrosomal recruitment of pericentrin and the γ-TuRC complex. The main function of CRM1 is exporting RNA and NES-containing proteins from the nucleus to the cytoplasm (Fornerod et al., 1997). However, recent studies demonstrate that CRM1 can regulate centrosome duplication and microtubule nucleation by targeting the proteins involved to centrosomes (Budhu and Wang, 2005; Neuber et al., 2008; Wang et al., 2005). It has been revealed that there are five NESs and one NLS in pericentrin (Liu et al., 2010), suggesting that pericentrin can interact with CRM1. Both overexpression of the N-terminal CRIME domain of CRM1, which is responsible for centrosomal targeting, and depletion of CRM1 by RNAi cause loss of pericentrin and γ-tubulin from centrosomes and defects in microtubule nucleation (Liu et al., 2009). Pericentrin has also been found interacting with CHD3/4 at the centrosome (Dictenberg et al., 1998). CHD3 is a component of the NuRD complex. It is involved in regulating the deacetylation and inactivation of p53, loading cohesin onto chromatin, the DNA damage response and silencing cell cycle regulating genes (Dictenberg et al., 1998). Depletion of CHD3 by RNAi causes reduced recruitment of pericentrin at centrosomes and subsequent disturbance of centrosome and microtubule organisation (Sillibourne et al., 2007).

In general, a large number of proteins participate in microtubule nucleation and spindle organisation. But pericentrin may be more important, as it works as a scaffold. Pericentrin directly anchors the γ-TuRC to the centrosome for microtubule nucleation. Other proteins indirectly influence γ-TuRC via their interaction with pericentrin. Abnormal microtubule nucleation leads to a disorganised mitotic spindle (Purohit et al., 1999; Rauch et al., 2008; Zimmerman et al., 2004).

1.6.2 Pericentrin and cell cycle progression

Considering the microtubule nucleation and spindle organisation functions of pericentrin, it is not surprising that pericentrin is also involved in cell cycle progression. Several studies show cell cycle defects in pericentrin deficient cells. An increased G1 population, along with decreased S and G2 cell number were observed in pericentrin-depleted cells and in cells expressing a dominant-negative pericentrin domain (Matsuo et al., 2010; Mikule et al., 2007; Srsen et al., 2006). Both the p53 upstream regulator, activated p38, and phosphorylated p53 itself accumulated at centrosomes, whereas cyclin A-CDK2 activity declined in pericentrin-depleted cells (Mikule et al., 2007). However, depletion of pericentrin in *p53*-deficient cell lines does not cause G1 arrest. These data suggest that the G1/S arrest caused by depletion of pericentrin is *p53*-dependent (Mikule et al., 2007).

Centosome separation, which normally occurs in late G2 phase, is also found in pericentrin-depleted cells arrested at G1 phase (Graser et al., 2007b; Matsuo et al., 2010; Mikule et al., 2007). This may be due to the loss of centrosomal NEK2A and CDK5RAP2 in pericentrin-depleted cells (Buchman et al., 2010; Matsuo et al., 2010). NEK2A, a cell cycle-regulated serine/threonine protein kinase, can localise at the centrosome and promote the splitting of the centrosome and centrioles (Faragher and Fry, 2003; Fry, 2002; Fry et al., 1998). NEK2A kinase activity is inhibited after it associates with pericentrin at centrosomes via the C-terminal regions of both proteins

(Matsuo et al., 2010). Pericentrin-depleted cells fail to suppress NEK2A activity and thus show increased premature centrosome splitting in G1 phase. CDK5RAP2 is another protein involved in centriole cohesion until centrosome separation in late G2 phase (Barrera et al., 2010; Graser et al., 2007b). CDK5RAP2 localises at the centrosome through its interaction with pericentrin and at the Golgi apparatus by additional binding with AKAP450 (Wang et al., 2010). Reduced centrosomal CDK5RAP2 expression in pericentrin-depleted cells causes strong centrosome splitting in G1 phase (Buchman et al., 2010; Graser et al., 2007b).

A yeast two-hybrid screen indicated that pericentrin also interacted with PKC (Chen et al., 2004). PKC proteins are evolutionarily conserved serine/threonine kinases involved in cell cycle progression by regulating microtubules (Jaken and Parker, 2000; Kiley and Parker, 1995; Takahashi et al., 2000). PKCβII colocalises with pericentrin at centrosomes. Loss of the interaction between PKCβII and pericentrin by disruption of either protein leads to microtubule disorganisation and subsequent cytokinesis failure (Chen et al., 2004). The impaired pericentrin-γ-TuRC interaction ultimately induces G2/antephase (the cell cycle period between late G2 and mitosis) delay and apoptosis (Zimmerman et al., 2004).

In conclusion, pericentrin plays an important role in cell cycle progression. It ensures precise centriole duplication, mitotic spindle formation and cytokinesis, which all contribute to normal cell cycle progression.

1.6.3 Pericentrin and cell cycle checkpoint control

Recent studies have demonstrated that pericentrin functions in the maintenance of cell cycle integrity and regulates DNA damage checkpoints. *PCNT* mutant lymphoblastoid cell lines (LCLs) have a defect in the G2/M checkpoint response induced by UV, but not in the IR-induced G2/M checkpoint arrest (Griffith et al., 2008; Tibelius et al., 2009). The same results are also observed in pericentrin-

depleted HeLa cells (Griffith et al., 2008). These data suggest that *PCNT* plays a role in ATR-dependent, but not ATM-dependent DDR signaling pathways. However, γH2AX foci formation is normal in *PCNT* mutant LCLs after UV damage, suggesting that *PCNT* may be involved downstream of ATR-pathway signaling (Griffith et al., 2008).

Components of the DDR pathways, including ATM, BRCA1, CHK1, NBS1 and MCPH1 have been observed to localise to the centrosome (Jeffers et al., 2008; Kramer et al., 2004; Zhang et al., 2007). Cyclin B-CDK1 is activated in the cytoplasm and localises to the centrosome before it moves to the nucleus to carry out its functions (Jackman et al., 2003). However, there is no direct evidence to show whether pericentrin recruits these checkpoint proteins to the centrosome, except CHK1. Forced immobilisation of CHK1 to centrosomes by fusion of CHK1 with the PACT domain prevents the transition from G2 to M (Kramer et al., 2004). Furthermore, overexpression of *PCNT* in COS cells induces G2/antephase arrest followed by apoptosis (Zimmerman et al., 2004). Another study has demonstrated that pericentrin directly mediates the centrosomal recruitment of CHK1. Pericentrin deficiency caused by mutation or RNAi induced the specific loss of CHK1 from centrosomes whereas the total cellular CHK1 levels remained almost the same as controls (Tibelius et al., 2009). Insufficient CHK1 anchored at centrosomes subsequently led to reduced inhibitory phosphorylation of centrosomal cyclin B-CDK1, resulting in premature mitotic entry, mitotic delay, and cell death (Tibelius et al., 2009). However, a very recent paper has reported contradictory results. In this study, it was shown that nuclear CHK1 controlled mitotic entry and overexpressed CHK1-PACT was also found in the nucleus (see Section 1.5.1.3) (Matsuyama et al., 2011).

1.6.4 Pericentrin and human disorders

Recent studies link pericentrin dysfunction to four human disorders: primordial

dwarfism, human cancer, mental disorders and ciliopathies.

1.6.4.1 Pericentrin and primordial dwarfism

Given the roles of pericentrin in spindle assembly and cell cycle progression, impairment of pericentrin may result in global reduction of cell number, thus eventually causing reduced body and brain size. Recent studies show that *PCNT* mutations are associated with two rare autosomal recessive genetic disorders, Majewski/microcephalic osteodysplastic primordial dwarfism type II (MOPD II, Mendelian Inheritance in Man (MIM) 210720) and Seckel syndrome (SCKL, MIM 210600) (Griffith et al., 2008; Rauch et al., 2008). MOPD II and SCKL are two kinds of primordial dwarfism whose clinical features include intrauterine and postnatal growth retardation, proportionate short stature and a pronounced reduction in brain size relative to body size (microcephaly) (Majewski et al., 1982). MOPD II is distinct from SCKL because individuals with MOPD II show skeletal dysplasia and mild/absent mental retardation (Hall et al., 2004). SCKL cell lines show defects in ATR-dependent DNA damage signaling, including impaired phosphorylation of ATR-dependent substrates, impaired G2/M checkpoint arrest, and elevated micronucleus formation following exposure to UV agents that cause replication stalling (Alderton et al., 2004). Recent studies demonstrate that the clinical features of SCKL individuals with *PCNT* mutations (PCNT-SCKL) are comparable with MOPD II, suggesting that PCNT-SCKL should be diagnosed as MOPD II (Piane et al., 2009; Willems et al., 2009).

To date, all studies have reported that all MOPD II patients examined show homozygous or compound heterozygous missense *PCNT* mutations (splice site, stop, or frameshift mutations). Western blots have confirmed that the pericentrin protein is absent or truncated in LCLs generated from patients with MOPD II. *Pcnt* knockout mice also displayed features of microcephalic primordial dwarfism (Miyoshi et al., 2009). Cells of MOPD II individuals possess disorganised mitotic spindles,

misaligned chromosomes, premature sister chromatid separation and aneuploidy, which result in apoptosis and growth defects (Rauch et al., 2008). Therefore, MOPD II is a distinct clinical entity caused by biallelic loss-of-function mutations in *PCNT*.

1.6.4.2 Pericentrin and mental disorders

The *PCNT* locus is localised in a mood disorder susceptibility region of chromosome (Baron, 2002; Lin et al., 2005a). *DISC1* is an important genetic risk factor for mental disorders such as schizophrenia (Cannon et al., 2005), bipolar disorder (Thomson et al., 2005) and major depressive disorder (Hashimoto and Egly, 2009). DISC1 is anchored to the centrosome by its interaction with the N-terminal region of pericentrin (Miyoshi et al., 2004). Overexpression of the DISC1-binding regions of pericentrin or lack of the pericentrin-binding region of DISC1 impaired the microtubule organisation (Shimizu et al., 2008). Thus, the DISC1-pericentrin interaction might contribute to the pathophysiology of mental disorders due to pericentrin function in microtubule organisation. DISC1 also associates with a number of proteins involved in essential processes of neuronal function, including neuronal migration, neurite outgrowth, cytoskeletal modulation, and signal transduction (Hennah et al., 2006). It is reasonable that a change in pericentrin would influence any of these processes and possibly cause psychiatric illnesses.

Recent studies confirm the role of pericentrin in mental disorders. Single-nucleotide polymorphisms (SNPs) in *PCNT* associate significantly with schizophrenia and major depressive disorders (Anitha et al., 2009; Numata et al., 2009). Furthermore, the mRNA levels of *PCNT* are significantly higher in the postmortem brain and peripheral blood lymphocytes of bipolar disorder patients and the dorsolateral prefrontal cortex of patients with schizophrenia than in control subjects (Anitha et al., 2008; Lipska et al., 2006). It is possible that abnormalities of *PCNT* can lead to defects in microtubule integrity, resulting in alterations in neuronal migration, axonal extension, and neurite outgrowth, subsequently leading to impaired neuro-

development (Anitha et al., 2008).

1.6.4.3 Pericentrin in human cancer

High levels of pericentrin were observed in primary and metastatic tumours of breast, prostate, lung, colon and brain by immunoperoxidase labeling of these tissues (Katsetos et al., 2006; Kim et al., 2008; Piel et al., 2001; Pihan et al., 1998; Schneeweiss et al., 2003). Immunofluorescence microscopy showed the tumour-derived cell lines had one significantly larger pericentrin spot or multiple pericentrin spots (Pihan et al., 1998). Pericentrin levels are also greatly elevated in hematological malignancies, including acute myeloid leukemia (Graser et al.; Kramer et al., 2005; Neben et al., 2004), chronic myeloid leukemia (CML) (Patel and Gordon, 2009) and mantle cell lymphoma (Neben et al., 2007), in which centrosomal abnormalities and genetic instability have been described. In addition, *Pcnt* transgenic mice show a syndrome resembling human myelodysplasia, carcinoma and sarcoma. Fibroblasts and bone marrow cells from these mice are aneuploid and have supernumerary centrosomes, multipolar spindles and bipolar spindles with clustered centrosomes, confirming the potential role of pericentrin in cancer (Delaval and Doxsey, 2009).

Two proteins have been suggested to contribute to the relationship between overexpression of pericentrin and cancer. PKCβII is a PKC family member which mediates cytokinesis and cell proliferation by regulation of microtubule organisation (Mochly-Rosen, 1995; Newton, 1997). PKCβII colocalises with pericentrin at centrosomes in wild-type cells (Chen et al., 2004; Kim et al., 2008). Overexpression of the PKCβII-binding regions of pericentrin leads to mislocalisation of PKCβII away from the centrosome and a loss of microtubule anchoring at the centrosome, resulting in cytokinesis failure and aneuploidy (Chen et al., 2004). Cancer cells with multiple centrosomes may undergo relatively normal cell divisions because of centrosome clustering (Kwon et al., 2008; Quintyne et al., 2005). However,

overexpression of pericentrin would finally cause genetic instability via atypical and supernumerary centrosomes, multiple spindle poles for sister chromatid attachment and higher potential for unequal chromosome segregation (Chen et al., 2004; Kim et al., 2008).

The $p210^{BCR-ABL1}$ fusion protein produced by the BCR-ABL1 translocation is another candidate anchored to the centrosomes by pericentrin in CML (Patel and Gordon, 2009). It is a constitutively active tyrosine kinase which activates multiple signaling cascades and dysregulates many cellular behaviours, including cell proliferation and maintenance of genomic stability. Pericentrin may anchor $p210^{BCR-ABL1}$ at the centrosome, where it could alter centrosome function and cause numerical and structural centrosomal abnormalities (Patel and Gordon, 2009).

1.6.4.4 Pericentrin in ciliopathies

Cilia are microtubule-based cell surface organelles which assemble from basal bodies (derivatives of the mother centrioles) in quiescent cells and perceive a diverse variety of extracellular signals. In vertebrates, cilia are important in many environment-responsive processes, including sperm motility, sensory neuron function, phototransduction and the generation of left/right asymmetry during development. Cilia-related diseases, termed 'ciliopathies', are caused by dysfunction of centrosomes and cilia (Hildebrandt and Otto, 2005; Hurd and Hildebrandt, 2011). Dysfunction of the motile cilia of the ependymal cells and the bronchiolar epithelial cells, as well as primary cilia of the renal tubular epithelial cells, is linked to the pathogenesis of hydrocephalus, respiratory tract infections, and polycystic kidney disease (Pan et al., 2005). Abnomalies of sperm flagella, which are ultrastructurally identical with motile cilia, cause male infertility (Pan et al., 2005).

Given the intimate relationship between the centrosome and the primary cilium and *PCNT*'s pivotal role in centrosome organisation, *PCNT* may contribute to defects in

cilia and flagella. Although no direct evidence shows that pericentrin is linked to human ciliopathies, recent studies have demonstrated that disruption of pericentrin leads to ciliopathy-associated phenotypes in *Drosophila* and mice (Martinez-Campos et al., 2004; Miyoshi et al., 2009), suggesting that pericentrin dysfunction might contribute to ciliopathies. In *Drosophila*, the *Drosophila* pericentrin like protein (D-PLP) is the only recognisable PACT domain-containing protein. The centrosomes in *d-plp* mutants are disorganised whereas the arrangement of microtubules and cell division are not dramatically defective (Martinez-Campos et al., 2004). *d-plp* mutant flies are severely uncoordinated, a phenotype associated with defects in disturbed neuron function. Malformed sensory cilia are displayed in chemosensory and mechanosensory neurons and sensory transduction of external stimuli is affected in *d-plp* mutants. Moreover, the flagella in *d-plp* mutant sperm cells, the only other ciliated cells in flies (Han et al., 2003), are nonmotile (Martinez-Campos et al., 2004). On the other hand, pericentrin localises to the base of primary cilia in multiple mouse embryonic tissues, which suggests pericentrin is involved in ciliogenesis in mammals (Miyoshi et al., 2006b). However, only the olfactory cilia of chemosensory neurons in the nasal olfactory epithelium were malformed in the mice harboring a hypomorphic mutation of mouse *Pcnt* (Miyoshi et al., 2009).

Studies in cultured mammal cells propose and confirm a model for the involvement of *PCNT* in cilia assembly and function. Primary cilium formation and function require intraflagellar transport (IFT) proteins and the cation channel polycystin-2 (PC2), which form a complex with pericentrin at basal bodies in vertebrate cells (Pazour et al., 2000; Pazour et al., 2002). Pericentrin depletion by RNA interference disrupts basal body localisation of IFTs and PC2, and inhibits primary cilia assembly (Jurczyk et al., 2004).

1.7 Microcephalin

Autosomal recessive primary microcephaly (MIM, 251200) is a rare, congenital,

neurodevelopmental disorder. It is characterized by severely reduced brain size at birth which is defined as at least three standard deviations below the mean. Microcephaly is one of the clinical features of other genetic diseases such as Seckel syndrome (O'Driscoll et al., 2003) and Nijmegen breakage syndrome (Varon et al., 1998). Currently seven autosomal loci (MCPH1-7) which are named according to their order of discovery, have been mapped to be responsible for primary microcephaly. Mutations in the seven corresponding genes including *MCPH1* (encoding Microcephalin; locus *MCPH1*), *WDR62* (WD repeat domain 62; *MCPH2*), *CDK5RAP2* (cyclin-dependent kinase 5 regulatory associated protein 2; *MCPH3*), *CEP152* (centrosomal protein 152 kDa; *MCPH4*), *ASPM* (abnormal spindle-like microcephaly-associated protein; *MCPH5*), *CENPJ* (centromeric protein J; *MCPH6*), and *STIL/SIL* (SCL/TAL1 interrupting locus; *MCPH7*) have also been shown to cause primary microcephaly (Jackson et al., 1998; Jamieson et al., 1999; Kumar et al., 2009; Leal et al., 2003; Moynihan et al., 2000; Pattison et al., 2000; Roberts et al., 1999).

Microcephalin (*MCPH1*), also known as *BRIT1* (BRCT-repeat inhibitor of hTERT expression) was the first identified causative gene of primary microcephaly (Jackson et al., 2002; Woods et al., 2005). BRIT1 was initially described as a transcriptional repressor of human telomere reverse transcriptase (hTERT), which is the catalytic subunit of human telomerase (Lin and Elledge, 2003). Primary microcephaly caused by biallelic mutations in *MCPH1* presents as mental retardation and short stature. MCPH1 contains three BRCA1 carboxy-terminal (BRCT) domains (one N-terminal and two C-terminal) and a nuclear localisation signal motif (Jackson et al., 2002; Woods et al., 2005). MCPH1 has been reported to localise at the nucleus and the centrosome and plays roles in chromosome condensation, the DNA damage response, DNA repair and regulating mitotic entry (Brunk et al., 2007; Jeffers et al., 2008; Tibelius et al., 2009; Zhong et al., 2006).

1.7.1 MCPH1 and DNA damage

Evolutionarily conserved BRCT domains are found in many DNA damage-responsive proteins, including cell cycle checkpoint proteins, such as 53BP1, MDC1 and BRCA1 (Manke et al., 2003; Yu et al., 2003). This suggests that *MCPH1* is involved in the DNA damage response and/or repair pathways.

After IR or UV damage, MCPH1 forms foci in the nucleus, similarly to the other DNA damage sensors and mediators (Alderton et al., 2006; Lin et al., 2005b; Xu et al., 2004). MCPH1 localises to break sites via the interaction of its C-terminal tandem BRCT domains with phosphorylated H2AX (Jeffers et al., 2008; Wood et al., 2007). MCPH1 foci colocalise with γ-H2AX, MDC1, 53BP1, NBS1, p-ATM, ATR, p-RAD17 and RPA foci at the damaged loci, suggesting that *MCPH1* is associated with early DNA damage responses in both ATM and ATR signaling pathways (Lin et al., 2005b; Xu et al., 2004). RNAi against MCPH1 blocked the irradiation-induced foci (IRIF) formation of all of these molecules but not γ-H2AX (Rai et al., 2006). However, MCPH1 IRIF did not form in H2AX-deficient cells (Jeffers et al., 2008; Wood et al., 2007). These data indicate that MCPH1 is an upstream component of the effectors of H2AX in the DNA damage response.

Knockdown of *MCPH1* in U2OS cells caused escape from cell cycle arrest and radioresistant DNA synthesis after IR damage, indicating that both the G2/M and intra S checkpoints were defective (Alderton et al., 2006; Lin et al., 2005b; Xu et al., 2004). These defects may be the results of the downregulated mRNA and protein levels of two key checkpoint regulators, BRCA1 and CHK1, in *MCPH1* knockdown cells (Lin et al., 2005b; Xu et al., 2004). It has been reported that MCPH1 is also localised at the centrosome throughout the cell cycle via its N-terminal BRCT domain (Jeffers et al., 2008; Rai et al., 2008; Zhong et al., 2006). MCPH1 targets CHK1 to the centrosome and centrosomal CHK1 is lost in *MCPH1*-deficient cells (Tibelius et al., 2009). Diminished CDC25A degradation and reduced levels of

phospho-CDK1 (Tyr15) were also observed in late S and G2 phase in *MCPH1*-deficient cells (Alderton et al., 2006; Brunk et al., 2007). Thus, in the absence of MCPH1, CHK1 does not localise at the centrosome and cannot degrade CDC25A, which regulates cyclin B-CDK1 activity by reversing inhibitory CDK1 phosphorylation. The active CDK1 allows the cells to enter mitosis with damaged DNA (Le Breton et al., 2005). In addition, phosphorylated BRCA1 is required for transient S-phase arrest (Xu et al., 2002) and CDC25A also inhibits the activation of the CDK2-cyclin complex which controls DNA synthesis (see Section 1.1). So the impaired intra S checkpoints in MCPH1-depleted cells may be correlated with reduced CHK1 and BRCA1.

MCPH1 is also reported to be involved in DSB repair pathways, in both HR and NHEJ (Liang et al., 2010; Peng et al., 2009; Wood et al., 2007; Wu et al., 2009). *Mcph1* knockout mice and derived cells were hypersensitive to IR (Liang et al., 2010). Elevated chromatid breaks were observed in embryonic fibroblasts or T lymphocytes of *Mcph1* knockout mice after IR damage (Liang et al., 2010) and MCPH1-depleted human cells (Rai et al., 2006). The interaction of MCPH1 with the DNA repair complex, BRCA2-RAD51, may contribute to MCPH1's function in HR as the BRCA2-RAD51 complex formed but mislocalised from DSB sites in *MCPH1*-deficent cells (Liang et al., 2010; Wu et al., 2009). A recent study reports that the N-terminal BRCT domain of MCPH1 interacts with SWI/SNF, an evolutionarily conserved ATP-dependent chromatin remodeling complex in DNA repair (Peng et al., 2009). The increased interaction after DNA damage allows chromatin relaxation and recruits DNA repair proteins including RAD51 to the DNA damage sites to execute efficient repair (Peng et al., 2009).

It should be noted that the CHK1 and BRCA1 protein levels are normal in cells derived from patients with *MCPH1* mutations (Alderton et al., 2006). After IR damage, the G2/M checkpoint was intact and chromosomal breakage rates were not

increased in patient-derived cells and cells derived from another *Mcph1* knockout mice (Gavvovidis et al., 2010; Trimborn et al., 2010). Moreover, IRIF of DNA damage proteins formed at DSB sites in these cells (Gavvovidis et al., 2010; Trimborn et al., 2010). These conflicting observations may be due to the incomplete loss of function of the mutants or off-target effects of siRNA. It is also possible that some compensating pathways were established in mutant cells, whereas the observed phenotypes arose immediately after siRNA treatment.

1.7.2 MCPH1 and chromosome condensation

Premature chromosome condensation (PCC, MIM 606858) syndrome is another clinical feature arising from *MCPH1* deficiency (Trimborn et al., 2004). An elevated percentage of prophase-like cells caused by PCC in early G2 phase and delayed decondensation in early G1 phase, appeared uniquely in *MCPH1* mutant cells and MCPH1-depleted cells (Brunk et al., 2007; Trimborn et al., 2004; Trimborn et al., 2010; Trimborn et al., 2006). The N-terminal BRCT domain of MCPH1 is essential to rescue these condensation defects (Wood et al., 2007).

Chromosome condensation is an important cellular process for entry into mitosis and faithful segregation of the genome (Swedlow and Hirano, 2003). The protein complexes regulating chromosome condensation, including condensin, share many similarities. The core domains of these complexes comprise SMC proteins (Hirano, 2006). There are two condensin complexes (condensin I and II) in mammalian cells. Condensin I mainly localises in the cytoplasm and condensin II localises in the nucleus throughout the cell cycle (Ono et al., 2004). Knockdown of condensin II but not condensin I relieved the premature chromosome condensation phenotype and delayed the post-mitotic decondensation phenotype (Trimborn et al., 2006). This suggests that chromosome condensation defects in *MCPH1* deficiency are mediated by the premature binding of condensin II to chromatin. In addition, it was shown that intact MCPH1 and nuclear condensin II are required for homologous repair of DNA

damage (Wood et al., 2007).

Given the multi-functionality of MCPH1 on regulating the cell cycle, chromosome functions, DNA damage response and repair, it is reasonable to suggest that MCPH1 plays a role in genomic instability. In fact, recent studies show that expression of MCPH1 is reduced in breast, ovarian and prostate tumours (Rai et al., 2006) and that IR-induced hyperamplification of centrosomes occurred in *Mcph1* knockout DT40 cells and MCPH1-depleted cells (Alderton et al., 2006; Brown et al., 2010).

1.8 The chicken DT40 cell line

DT40 cell line is a chicken B lymphocyte line transformed with an avian leukosis virus (Baba et al., 1985). DT40 cells, which are approximately 10 μm in diameter, have a high nucleus to cytoplasm ratio and show the characteristics of lymphocytes (Winding and Berchtold, 2001). DT40 cells are suspension cells and grow very rapidly. The doubling time is 8-18 h, depending on the incubation temperature (37-39.5 °C) (Winding and Berchtold, 2001).

The DT40 karyotype is relatively invariant and comprises a modal chromosome number of 80, which contains 11 autosomal macrochromosomes, 67 micro-chromosomes, and the ZW sex chromosomes (Sonoda et al., 1998). Most chromosomes are diploid with the exception of chromosome 2 and one additional microchromosome which are trisomic (Sonoda et al., 1998). The stable karyotype and phenotype allow the targeting of multiple genes to investigate genetic interactions on a cellular level (Yamazoe et al., 2004). The DT40 knockout system has been used to illuminate various processes including B cell antigen receptor signaling, histone gene function, RNA processing, DNA damage response and repair, cell cycle, centrosome gene function and calcium signaling (Winding and Berchtold, 2001).

1.8.1 DT40 cells lack functional p53

It should be noted that DT40 cells are functionally p53 null. This important difference may lead to inconsistent results between DT40 and p53-competent mammalian cells. Wild-type DT40 cells arrest at the G2/M border after IR damage, lacking a G1/S phase checkpoint which is due to loss of p53 (Takao et al., 1999). So the apoptosis pathway is not activated during interphase and the cells can enter M phase with spontaneous chromosomal breaks. This allows comprehensive reverse genetic studies of genome instability (Sonoda et al., 1998). However, Sui et al. found expression of *p53* in DT40 cells at both mRNA and protein levels. DT40 cells undergo apoptosis in the absence of Yin Yang1, which regulates p53 ubiquitination and degradation (Sui et al., 2004). In the later study, the authors did not address p53's role in DNA damage response. Therefore, it is likely that *p53* is expressed in DT40 cells but has no or minor function in G1/S checkpoint pathway.

1.8.2 High targeting efficiency in DT40

After whole genome sequencing, reverse genetics (protein→gene→function) is used to study the function of a gene by analysing the effects of specific gene disruption. The disruption is achieved by HR of DNA constructs to directly modify the genetic loci which are known as gene targeting. In HR of DSBs, the damaged DNA is elongated by using the complementary sequences in the intact homologous DNA segment as templates. However, in HR involving a targeting vector, the targeting construct takes the place of the undamaged sister chromatid as template DNA. Thus the targeting efficiency significantly increases after induction of DSBs in rodent cells (Richardson et al. 1998). Gene targeting has been successfully conducted in several models: in the budding yeast *S. cerevisiae*, in murine embryonic stem cells and subsequently in mouse, in cultured human cells and in chicken DT40 cells (Hudson et al., 2002).

Most transfected DNA integrates randomly into the chromosome in higher

eukaryotic cells including mammalian cells, insect and plant cells. The frequency of homologous integration of exogenous DNA into genomes is 10^{-5} to 10^{-2} in mammalian cells (Hudson et al., 2002). However, the targeting efficiencies are notably higher (up to 90%) in DT40 cells compared with mammalian cells, even though the molecular mechanism is not yet clear (Buerstedde and Takeda, 1991). Recently, it has been shown that the targeting frequency can be remarkably elevated in human T cells by using the combination of zinc-finger nucleases and HR repair of DSBs (Urnov et al., 2005). The ability to perform continuous rearrangement of immunoglobulin (Ig) genes via gene conversion may contribute to the high frequency of homologous integration (Buerstedde et al., 1990). Chicken B precursors, which develop in the bursa of Fabricius (Reynaud et al., 1994), diversify their variable functional IgV segments by intragenic HR, called Ig gene conversion (Reynaud et al., 1985; Reynaud et al., 1987). There are 25 pseudo-V segments followed by a single V and J (V(D)J) segment at the downstream area in the chicken Ig light chain locus (Reynaud et al., 1985; Reynaud et al., 1987). When Ig gene conversion occurs, nucleotide fragments in the pseudo-V region are transferred into the functional rearranged V gene to formation of a large IgV repertoire in preimmune B lymphocytes. Chicken B cells which cannot carry out gene conversion are still able to undergo HR but with frequencies about one order of magnitude lower than those seen in DT40 (Buerstedde and Takeda, 1991).

1.8.3 Gene targeting constructs

The design of gene targeting vectors requires information about the target gene locus. Fortunately, the chicken genomic sequence extends to ~ 90% coverage and large chicken EST and full length cDNA sequence data have been released to the public databases (International Chicken Genome Sequencing Consortium, 2004) (Abdrakhmanov et al., 2000; Boardman et al., 2002). Targeting vectors are comprised of a selection cassette flanked by homologous genomic sequences at both sides. So far, five different drug resistant cassettes have been used in the DT40

system, including neomycin (neo), hygromycin (hygro), histidinol (his), puromycin (puro), and blasticidin S (bsr) (Yamazoe et al., 2004). Recyclable selection markers flanked by loxP can be excised by the transient expression of Cre recombinase (Arakawa et al., 2001). In this way, several genes can be modified by repeat transfections of targeting vectors containing the same drug resistance.

Ideally, it is preferred to delete the entire genomic locus if it is not beyond 5 kb, although more than 20 kb of the immunoglobulin light chain locus could be deleted using a conventionally designed targeting construct (Arakawa and Buerstedde, 2006; Arakawa et al., 2004). If the target gene is big, as many of the exons as possible or a region encoding important domain of the protein can be deleted to disable the protein function. Introduction of point mutations is also used for gene disruption (Hudson et al., 2002). Recently, a strategy which disrupts the promoter region has been applied to shut down the expression of the gene of interest in a case where the exons are far away from each other and the functional domains are not clear (Samejima et al., 2008). Theoretically, longer homologous fragments (target arms) increase targeting efficiency, but larger plasmids are technically difficult to handle (Arakawa and Buerstedde, 2006).

1.8.4 Targeting essential genes

The standard strategy is cannot be applied if the gene is essential for cell survival or proliferation. Alternatively, several methods have been used to disrupt essential genes conditionally in DT40 cells.

1.8.4.1 Conditional expression of targeting genes

First, a rescue construct which can express the deleted gene product is introduced into heterozygote cells by random integration. After all the alleles of the gene of interest are disrupted, the expression of the transgene controlled by a specific promoter can be repressed with an additional effector molecule (Yamazoe et al.,

2004). An *E. coli* tetracycline-off system is most commonly used (Baron and Bujard, 2000; Gossen and Bujard, 1992). The basic principle is that the dissociation of tet repressor (tetR) from the tet operator (tetO) blocks the transcription of the transgene when tetracycline or its more potent analogue doxycycline is added. In the tet-off system, the regulatory protein which is a fusion of tetR and the transcriptional activation domain of the herpes simplex virus VP16 protein, is co-transfected with the rescue construct. The fused protein called tetracycline-controlled transactivator (tTA) binds to the tetO and promotes the expression of the transgene. The binding of doxycycline or tetracycline with tTA changes the conformation of tTA which causes tTA dissociation from tetO and prevents the expression of the transgene (Baron and Bujard, 2000; Gossen and Bujard, 1992). Recently, Samejima et al. replaced the endogenous promoter of the gene of interest with tetO to abolish its expression. A transgene which expresses tTA driven by a rescue promoter was employed to restore the expression of the targeting gene (Samejima et al., 2008).

In some situations, overexpression of the transgene could be toxic. We can modify the VP16 activation domain fused to the tTA (ptTA 2/3/4), change the number of tetO sequences and vary the concentration of the drug to get normal expression of the rescue construct (Baron et al., 1997). However, leaky expression of the transgene is unavoidable with this system (Yamazoe et al., 2004).

1.8.4.2 Conditional deletion of targeting genes

The Cre-mediated deletion system, which is commonly used in knockout mice, is also employed to disrupt essential genes in DT40 cells (Yamazoe et al., 2004). The 32-bp loxP recognition sites for the Cre recombinase are knocked-in to the flanking region of the essential gene locus (Matsudo et al., 2005). In another case, the knockout cells are transfected with the rescue construct containing the cDNA flanked by two loxP sites (Fujimori et al., 2001). The gene continues to express unless the Cre recombinase, MerCreMer, is induced to delete the region between the two loxP

sites. 4-hydroxytamoxifen (TAM), the antagonist of estrogen receptor, can bind the two mutated hormone-binding domains of MerCreMer (Zhang et al., 1998). MerCreMer binding with Hsp90 (a heat-shock protein) localises in the cytoplasm without the presence of TAM. After addition of TAM, MerCreMer translocates into the nucleus and recognises loxP signal for excision. This Cre-mediated deletion system works very efficiently. The targeted region of the gene is removed 24 hours after addition of TAM and no leaky expression happens (Yamazoe et al., 2004). Unfortunately, the recombination does not progress in all cells in a synchronous manner and results in a genetically heterogeneous population of cells (Sonoda et al., 2003). Therefore, whole population-based biochemical analyses are not feasible, whereas individual cell-based microscopy analyses can be conducted.

DT40 cells are viable when they are cultured at temperatures from 34 to 43 °C, allowing DT40 to be used for generating temperature-sensitive (TS) mutants (Yamazoe et al., 2004). TS mutations in *CENP-C* which disrupt the protein function immediately after the culture temperature shifts to 43 °C, have been reported (Fukagawa et al., 2001). This strategy is very useful for studying the proteins which have distinct functions at different cell cycle phases (Yamazoe et al., 2004). However, it is technically difficult to perform this strategy, due to the need for identification of appropriate TS mutations. Furthermore, the phenotype observed at a restrictive temperature may not be restored after reverting to permissive temperatures because of the changed culture conditions (Yamazoe et al., 2004).

1.8.4.3 Conditional deletion of proteins

Transcriptional repression of genes causes slow depletion of proteins. However, rapid depletion of a protein sometimes may be very important for observation of the proper phenotypes probably due to compensatory function of relative proteins arised in slow depletion (Kanemaki et al., 2003; Nishimura et al., 2009). Thus, direct and rapid degradation of targeting proteins has been developed in DT40 cells. A domain

to reduce the half-life of the target protein, known as a 'degron', is fused to the protein of interest.

It has been reported that ORC6 and RAD51, whose genes are essential for DT40 cells, were conditionally degraded using a temperature-sensitive degron system which was originally applied in budding yeast (Bernal and Venkitaraman, 2011; Dohmen et al., 1994; Su et al., 2008). The targeting genes were fused at their 5' ends with an N-end rule protein degron, the mutant dihydrofolate reductase, which is characterised by temperature-sensitive unfolding and degradation (Dohmen et al., 1994). The fusion protein was rapidly degraded to <10% of its initial levels within 90 min and undetectable within 120 min when cells were incubated at a nonpermissive temperature of 42 °C. The expression of the targeted protein was restored to normal level within 150 min when the cells were shifted back to the permissive temperature of 35 °C (Bernal and Venkitaraman, 2011; Su et al., 2008) .

An alternative auxin-inducible degron (AID) system facilitates the maintaining of cell culture at a constant temperature (Nishimura et al., 2009). The AID degron sequence can be integrated into either N or C terminus of the coding region of the targeting gene. Auxins are a family of plant hormones, including indole-3-acetic acid (IAA; a natural auxin) and 1-naphthaleneacetic acid (NAA; a synthetic auxin) (Teale et al., 2006). Auxin works as a bridge to achieve the binding of the AID-fused protein to the F-box transport inhibitor response 1 (TIR1) protein which is a part of the E3 ubiquitin ligase SCF (Skp1, Cullin and F-box)-TIR1 complex. SCF-TIR1 recruits an E2 ubiquitin conjugating proteosome which in turn induces poly-ubiquitination and degradation of the fusion protein (Nishimura et al., 2009). As auxin is only active in plants but silent in nonplant eukaryotes, it was shown that addition of 500 μM IAA did not affect growth and global gene expression of DT40 cells. It has been reported that this system resulted in depletion of CENP-H within 30 min after the presence of IAA whereas CENP-H was still detected 24 h after addition

of tetracycline in a CENP-H conditional DT40 cell line (Nishimura et al., 2009). This system could be applied in most eukaryotes, such as budding yeast, cell lines derived from mouse, hamster, monkey and human because Skp1, especially its C-terminal F-box binding domain, is highly conserved among all eukaryotes.

1.9 Aims of the thesis

The research described in this thesis aimed to better understand the roles of pericentrin in centrosome organisation, cell cycle progression and the responses to DNA damage.

The experimental system used in this research is the chicken DT40 cell line which is characterised by high recombinogenic efficiencies. To define the genomic locus for targeting vector construction, we cloned and sequenced chicken *Pcnt*. We then generated a *Pcnt*-deficient chicken cell line and analysed the phenotype caused by *Pcnt* deficiency. Cell cycle progression was analysed by flow cytometry and live cell imaging. Light and electron microscopy analyses were employed to study the roles of *Pcnt* in centrosome structure and function. In order to define the roles of *Pcnt* in DNA damage, cell cycle arrest, centrosome amplification and clonogenic survival were examined after DNA damage. Given the central role of CHK1 in DNA damage response, we also followed CHK1 activation after DNA damage by Western blot and immunofluorescence microscopy. In addition, we attempted to use reverse genetics to define the functional relationships between *Pcnt* and *Mcph1*, which are both linked to primary dwarfism. We characterised the DNA damage response in *Pcnt* and *Mcph1* double knockout cells. The research presented in this thesis helps to define the centrosomal functions of pericentrin and to establish a model for CHK1 activation after DNA damage.

Chapter 2. Materials and methods

2.1 Materials

2.1.1 Chemical reagents

Chemicals used throughout this study were of analytical grade and were purchased from Sigma (Arklow, Ireland), BDH (Hertfordshire, UK), Fisher (Leicestershire, UK) or GE Healthcare (Bucks, UK). All solutions were prepared using ddH_2O or Milli-Q purified water (Millipore, Billerica, USA) and were autoclaved prior to use if necessary.

All common reagents and buffers used throughout this study are shown in Table 2.1 (in alphabetical order).

Table 2.1 Commonly used reagents and buffers

Solutions	Composition	Notes and references
Annexin buffer	10 mM Hepes pH 7.4, 150 mM NaCl, 5 mM KCl, 1 mM $MgCl_2$, 1.8 mM $CaCl_2$	For desalting of FITC-conjugated Annexin V
Blocking solution (immunofluorescence microscopy)	1% BSA in 1 x PBS. Filter sterilise and store with 0.1% sodium azide	For blocking cells and diluting antibody
Blocking solution (Southern blot)	10% Caseine in Maleic acid wash buffer	For blocking of Southern blot membranes
Blocking solution (Western blot)	1 x PBS, 0.1% Tween 20, 5% dried milk	To decrease the unspecific binding of antibodies
1 x Ca^{2+} buffer	10 mM Hepes pH 7.5, 140 mM NaCl, 2.5 mM $CaCl_2$	For Annexin V staining
CLAP	1000 x stock solution of Chymotrypsin, Leupeptin, Antipain, Pepstatin A	Protease inhibitors, each at 1 mg/ml in DMSO
Coomassie Brilliant Blue R	0.5% Coomassie in 35% Methanol, 14% acetic acid	For SDS-PAGE analysis
2 x Cytoskeleton buffer (CB)	137 mM NaCl, 5 mM KCL, 1.1 mM Na_2HPO_4, 0.4 mM KH_2PO_4, 2 mM $MgCl_2$, 2 mM EGTA, 5 mM PIPES, 5.5 mM Glucose pH to 6.1 and filter sterilize.	For fixation and permeabilisation of cells in immunofluorescence microscopy

DABCO (1,4-diazabicyclo [2.2.2]octane)	2.5% DABCO, 50 mM Tris pH 8, 90% glycerol	For mounting slides
Denaturation solution	1.5 M NaCl, 0.5 M NaOH	For denaturation of Southern gels
DEPC water	0.1% DEPC in dH_2O	For RNA work
Depurination solution	250 mM HCl	For depurination of Southern gels
Detection buffer	0.1 M Tris pH 9.5, 0.1 M NaCl	For detection of DIG labeled probes
Destain solution	30% methanol, 10% acetic acid	For destaining Coomassie gels
6 x DNA loading dye	20% Sucrose, 0.1 M EDTA pH 8.0, 1% SDS, 0.25% Bromophenol blue, 0.25% Xylene cyanol.	For loading of DNA samples on agarose gels
Elution buffer	1 x PBS, 200 mM Imidazole	For elution of Annexin V from beads
Extraction buffer	20 mM HEPES pH 7.7, 1.5 mM $MgCl_2$, 0.42 M NaCl, 0.2 mM EDTA, and 25% (v/v) Glycerol supplemented with protease inhibitors and 1 mM DTT	For extraction of nuclear proteins in nuclear and cytoplasmic proteins isolation
Fixation solution	4% Paraformaldehyde in 1 x CB Methanol supplemented with 5 mM EGTA	For fixation of cells in immunofluorescence microscopy
High Stringency Buffer	0.5 x SSC, 0.1% SDS	For membrane washes in Southern blot
Isotonic lysis buffer	10 mM Tris-HCl pH 7.5, 2 mM $MgCl_2$, 3 mM $CaCl_2$, 0.32 M Sucrose supplemented with protease inhibitors and 1mM DTT	For lysis of cells in nuclear and cytoplasmic proteins isolation
Low Stringency Buffer	2 x SSC, 0.1% SDS	For membrane washes in Southern Blot
Luria-Bertani (LB) Medium	1% tryptone, 0.5% yeast extract, 1% NaCl, pH adjusted to 7.0 with 4 M NaOH	For growth of bacterial (*Escherichia coli*) cultures
Lysis buffer (Annexin V purification)	1 x PBS, 20 mM Imidazole, 350 mM NaCl, 1% Triton X-100	For lysis of bacteria expressing Annexin V
Lysis buffer (Centrosome purification)	1 mM Hepes pH 7.2, 0.5% NP40, 0.5 mM $MgCl_2$, 0.1% β-mercaptoethanol, 1 x CLAP, 1 mM PMSF	For lysis of cells in centrosome purification

Neutralisation solution	1.5 M NaCl, 0.5 M Tris-HCl pH7.5	For neutralisation of Southern gels
Permeabilisation buffer	0.15% Triton-X-100 in 1 x CB	For permeabilisation of cells in immuno-fluorescence microscopy
1 x Phosphate buffered saline (PBS)	137 mM NaCl, 2.7 mM KCl, 1.4 mM NaH_2PO_4, 4.3 mM Na_2HPO_4, pH 7.4	For washing cells
PBS-Tween	1 x PBS with 0.1% Tween 20	For washing Western blots
Ponceau S	0.5% Ponceau S, 5% acetic acid	For staining Western blot membranes
Primary antibody dilution buffer	1 x PBS, 0.1% Tween 20, 1% dried milk	For dilution of primary antibodies in Western blot
	1 x PBS, 0.1% Tween 20, 5% BSA	For dilution of primary phospho-antibodies in Western blot
Reaction buffer	160 mM Na_2CO_3, 333 mM $NaHCO_3$ pH 9.5	For desalting of Annexin V
RIPA buffer	50 mM Tris-HCl pH 7.4, 1% NP-40, 0.25% sodium deoxycholate, 150 mM NaCl, 1 mM EDTA	For extraction of protein
Running buffer	1 x TG, 0.1% SDS	For running acrylamide gels
3 x Sample buffer	150 mM Tris pH 6.8, 9% SDS, 45% sucrose, 6 mM EDTA pH 7.4, 0.03% bromophenol blue.	For loading protein samples on SDS-PAGE gels
10 x SSC	1.5 M NaCl, 0.15 M Na citrate, pH adjust to 7.0 with citric acid	For transfer of DNA from gels to nylon membranes
Sucrose gradient buffer	10 mM Pipes pH 7.2, 0.1% Triton X-100, 0.1% β-mercaptoethanol	For preparation of a discontinuous sucrose gradient
1 x TAE	40 mM Tris-acetate pH 8.0, 1 mM EDTA	For preparation and running of agarose gels
Tail Buffer	50 mM Tris pH 8.8, 100 mM EDTA, 100 mM NaCl, 1% SDS	For extraction of genomic DNA
TBS Buffer	20 mM Tris-HCI pH 7.4, 150 mM NaCl	For washing cell for centrosome purification
TFBI	30 mM Potassium Acetate, 100 mM RbCl, 10 mM $CaCl_2$, 50 mM $MnCl_2$, 15% glycerol, pH to 5.8 with dilute HCl, filter sterilise and store at 4ºC	For preparation of chemically competent *E.coli*

TFBII	30 mM Potassium Acetate, 100 mM RbCL, 10mM $CaCl_2$, 50 mM $MnCl_2$, 15% glycerol, pH to 6.5 with KOH, filter sterilise and store at 4ºC	For preparation of chemically competent *E.coli*
10 x TG	0.25 M Tris, 1.92 M Glycine, pH 8.3	For making running buffer and transfer buffer in Western blot
1 x Transfer buffer	48 mM Tris, 39 mM glycine, 20% methanol, 0.0375% SDS	For semi-dry transfer of proteins from SDS-PAGE gels to nitrocellulose membranes
	1 x TG 20% methanol, 1% SDS	For wet transfer
Tris buffered saline (TBS)	20 mM Tris pH 7.4, 150 mM NaCl	For washing cells in centrosome purification
Washing buffer	0.1 M Maleic acid, 0.15 M NaCl, pH 7.5, 0.3% (v/v) Tween 20	For washing Southern blot membranes

2.1.2 Molecular biology reagents

All of the restriction enzymes for DNA digestion and T4 DNA ligase were obtained from New England Biolabs (NEB, Hertfordshire, UK). Shrimp Alkaline Phosphatase (SAP) was from United States Biochemical (USB, Cleveland, USA). The DNA polymerases LA Taq, KOD Hot Star and Taq were purchased from Takara (Shiga, Japan), Novagen (Darmstadt, Germany) and Sigma, respectively. DNA and protein size markers were supplied by Invitrogen (Carlsbad, USA) and BioRad (Hercules, USA), respectively. Oligodeoxynucleotide primers were synthesized by Sigma. Total RNA was extracted from tissue culture cells using TRIzol obtained from Invitrogen. Molecular biology kits used throughout this study are listed in Table 2.2.

Table 2.2 Molecular biology kits used in this study

Name	Use	References
HiYield Plasmid Mini kit	Small scale plasmid DNA extraction	RBC Bioscience (Taipei, Taiwan)
GenElute^{TM} Plasmid Miniprep Kit	Small scale plasmid DNA extraction	Sigma
Midi/Maxi Prep Kit (Endotoxin-free)	Large scale plasmid DNA extraction	Qiagen (Crawley, UK)
QIAquick Gel Extraction	Extraction and purification of	Qiagen

Kit	DNA fragments from the agarose gel	
QIAquickPCR Purification Kit	Purification of DNA fragments	Qiagen
SigmaSpin™ Sequencing Reaction Clean-Up	Purification of DNA fragments	Sigma
Superscript First-Strand Synthesis for RT-PCR kit	cDNA synthesis	Invitrogen
2 x Precision^{TM} Mastermix	Real-time PCR	Primer Design (Southampton, UK)
PCR DIG Probe Synthesis Kit	Probe labeling for Southern blot	Roche (Mannheim, Germany)
pGEM-T Easy Vector kit	Cloning	Promega (Madison, USA)

A number of cloning and expression plasmids were used in this study, as shown in Table 2.3.

Table 2.3 Plasmids used in this study

Plasmid name	**Use**	**References**
pGEMT-Easy	General cloning	Promega
pBlueScript(SK/KS)		Stratagene (La Jolla, USA)
pEGFP-C1/N1	Expression of transgene	Clontech (Palo Alto, USA)
pmRFP-N1-H2B	Live cell imaging	(Dodson et al., 2007)
ptTA2 (Kif4a^{Pro})	Rescue expression of *Pcnt*	(Samejima et al., 2008)
pANMerCreMer	Recycling of resistance cassettes	(Arakawa et al., 2001)

DNA transformation was performed on competent *Escherichia coli* Top10 cultures. The strain used in this study has the following genotype: F^{-}*mcrAΔ (mrr-hsdRNS-mcrBC)* φ*80lacZΔM15 ΔlacX74deoR recA1 araD139 Δ(araleu) 7697 galU galK rpsL(StrR) endA1 nupG.*

Antibodies used throughout this study were mainly employed for immunodetection in Western blot (WB) and imaging of cells by immunofluorescence microscopy (IF). Tables 2.4 and 2.5 include sources of each antibody, host species and polyclonal serial number and the working dilutions used for IF and WB.

Table 2.4 Primary antibodies used in this study

Reactivity	Serial No.	Host species	Dilution for IF	Dilution for WB	Source
α-tubulin	B512	Mouse monoclonal	1:5000	1:10000	Sigma
Aurora A	35C1	Mouse polyclonal	1:500		Abcam (Cambridge, UK)
BubR1	R895	Rabbit polyclonal	1:500		(Vagnarelli et al., 2004)
Centrin-2	Poly 6288	Rabbit polyclonal	1:300	1:1000	BioLegend (San Diego, USA)
Centrin-3	M01 3E6	Mouse monoclonal	1:1000	1:1000	Abnova (Taipei, Taiwan)
Cep76		Rabbit polyclonal	1:200		(Tsang et al., 2009)
Chk1	DCS-310	Mouse monoclonal		1:1000	Sigma
FLAG	M2, F1804	Mouse monoclonal	1:1000	1:1000	Sigma
γ-tubulin	T3559	Rabbit polyclonal	1:1000		Sigma
	GTU88	Mouse monoclona	1:200		Sigma
	sc-7396	Goat polyclonal	1:200	1:1000	Santa Cruz (Santa Cruz, USA)
Glutamylated tubulin	GT335	Mouse monoclonal	1:300		(Wolff et al., 1992)
Ninein	AB 4447	Rabbit polyclonal	1:100		Abcam
PCM-1	817	Rabbit polyclonal	1:10000		(Dammermann and Merdes, 2002)
Phospho-Cdc 2 Tyr15	4539	Rabbit polyclonal		1:500	Cell Signaling (Danvers, USA)
Phospho-Cdk 2 Thr160	2561	Rabbit polyclonal		1:500	Cell Signaling
Phospho-Chk 1 Ser345	2348	Rabbit monoclonal	1:300	1:500	Cell Signaling
Phospho-H3	06-570	Rabbit polyclonal	1:500		Millipore
TPX2	BL 1679	Rabbit polyclonal	1:500		Bethyl Labs (Montgomery,USA)

Table 2.5 Secondary antibodies used in this study

Reactivity	Conjugation	Host species	Dilution for IF	Dilution for IB	Source
Rabbit IgG	Rhodamine Red	Goat	1:200		Jackson Labs (Bar Harbor, USA)
Rabbit IgG	FITC (fluorescein isothiocyanate)	Goat	1:200		Jackson Labs
Rabbit IgG	FITC	Donkey	1:200		Jackson Labs
Mouse IgG	Texas Red	Goat	1:200		Jackson Labs
Mouse IgG	FITC	Goat	1:200		Jackson Labs
Mouse IgG	FITC	Donkey	1:200		Jackson Labs
Goat IgG	Rhodamine Red	Donkey	1:200		Jackson Labs
Rabbit IgG	HRP (horseradish peroxidase)	Goat		1:5000	Invitrogen
Mouse IgG	HRP	Goat		1:5000	Invitrogen
Goat IgG	HRP	Donkey		1:5000	Abcam

Different SDS-polyacrylamide gels were used in this study depending on the size of the proteins that were analysed. Table 2.6 shows examples of the gel mixture used. All the reagents were purchased from Sigma except the 30% acrylamide/ bisacrylamide (37.5:1) mix, which was purchased from Severn Biotech Ltd (Worcestershire, UK).

Table 2.6 Example of SDS-polyacrylamide gel mixture

Running gel				
	High molecular weight		**Low molecular weight**	
Gel percentage	6.5%	8%	10%	12%
Acrylamide/Bis mix	80:1	37.5:1	37.5:1	37.5:1
Acrylamide	6.3%	7.9%	9.6%	11.7%
Bis-Acrylamide	0.08%	0.2%	0.26%	0.3%
Tris-HCl pH 8.8	368 mM	375 mM	375 mM	375 mM
Sodium dodecyl sulfate (SDS)	0.06%	0.1%	0.1%	0.1%
Ammonium persulfate (APS)	0.055%	0.1%	0.1%	0.1%
Tetramethylethylenediamine (TEMED)	0.18%	0.04%	0.04%	0.04%

Stacking gel (5%)		
Acrylamide/Bis mix	80:1	37.5:1
Acrylamide	5.1%	4.9%
Bis-Acrylamide	0.14%	0.13%
Tris-HCl pH6.8	124 mM	125 mM

Sodium dodecyl sulfate (SDS)	0.05%	0.1%
Ammonium persulfate (APS)	0.05%	0.1%
Tetramethylethylenediamine (TEMED)	0.21%	0.1%

2.1.3 Tissue culture reagents and cell lines

All sterile plasticware used for tissue culture was obtained from Sarstedt (Numbrecht, Germany), Corning (Riverfront Plaza, USA) and Sigma. An Amaxa (Cologne, Germany) nucleofector was used for the transient transfection of chicken DT40 cells. Stable transfection was carried out with a Gene Pulser apparatus from Bio-Rad. Roswell Park Memorial Institute media (RPMI) 1640 and fetal bovine serum (FBS) were purchased from Lonza (Basel, Switzerland). DMSO (dimethyl sulfoxide), chicken serum and the antibiotics penicillin and streptomycin were obtained from Sigma. Different drugs at varying concentrations were used as selection markers in the generation of stable chicken cell lines, as listed in Table 2.7.

Table 2.7 Drugs used for stable cell line selection

Name of the drug	Final concentration
Blasticidin (Sigma)	25 μg/ml
Geneticin (Invitrogen)	2.5 mg/ml
Histidinol (Sigma)	1 mg/ml
Hygromycin (Sigma)	2.5 mg/ml
Puromycin (Sigma)	0.5 μg/ml

Semi-solid methylcellulose medium used in clonogenic survival assays, was composed of 1.5% methylcellulose (Sigma), 1 x DMEM/F-12, L-glutamine (+) (Invitrogen), 15% FBS, 15% chicken serum, 5% penicillin/streptomycin and 50 μM β-mercaptoethanol. Methylcellulose medium was prepared as follows: 7.5 g sterile methylcellulose was dissolved in 216 ml sterile hot ddH_2O. An equal volume of 2 x DMEM containing 0.2% $NaHCO_3$ was added, and the solution was mixed overnight at 4 °C. 75 ml FBS, 7.5 ml chicken serum, 100 U/ml penicillin, 100 μg/ml streptomycin, and 2 μl 12.5 M β-mercaptoethanol were added. The solution was mixed for 3 hours at 4 °C, and then stored at 4 °C for a maximum of 1 month.

Different drugs at varying concentrations were used for pharmacological treatment of chicken DT40 cells: 4 mM hydroxyurea (HU, Sigma), 0.1 μg/ml colcemid (Sigma), 0.1-2 μg/ml nocodazole (Sigma), and 10-40 nM Taxol (Sigma).

2.1.4 Computer programmes

DNA plasmid maps were created using pDRAW32 (http://www.acaclone.com/). Sequenced DNA samples were viewed using Chromas (http://www.technelysium.com. au/chromas.html). DNAMAN (http://www.lynnon.com/) and BlastN or BlastP (http://www.ncbi.nlm.nih.gov/BLAST) were employed for homology alignment. Primer Premier 5 (http://www.premierbiosoft.com/) was used for primer design. All images were imported as Photoshop CS version 8.0 files (Adobe Systems, Mountain View, USA). Quantitative analysis of IF images was performed using Harmony software version 3.0 (PerkinElmer, Waltham, USA). Statistical analysis was performed by GraphPad Prism 5 (La Jolla, USA).

2.2 Nucleic acid methods

2.2.1 Extraction of genomic DNA from tissue culture cells

1.5 ml of confluent cells were harvested and resuspended in 0.5 ml of tail buffer containing 0.2 mg/ml proteinase K. After incubation in tail buffer at 37 °C overnight or at 55 °C for 3 h, the cells were shaken vigorously at 1400 rpm for 5 min and supplied with 200 μl of 6 M NaCl (saturated). The samples were then spun down at 16000 g for 10 min following another vigorously shaking for 5 min. The supernatant was then transferred to a new eppendorf tube and 700 μl of isopropanol was added to precipitate the DNA. The samples were mixed by inversion and centrifuged at 16000 g for 10 min. The DNA pellet was washed with 1 ml of 70% ethanol and resuspended in 70 μl dH_2O.

2.2.2 Plasmid DNA preparation

Plasmid DNA extraction was carried out by ion-exchange chromatography using a

HiYield Plasmid Mini kit or GeneElute™ Plasmid MiniPrep Kit for miniprep and Qiagen Midi Prep kit or Qiagen Endotoxin free MidiPrep kit for midiprep, according to the manufacturers' instructions. Briefly, 2 ml and 100 ml of overnight bacterial cultures (in the presence of selective antibiotics at 37 °C with shaking) were used for mini and midi plasmid isolation, respectively. Cell debris and protein were precipitated by centrifugation after lysis. The supernatant was loaded to DNA-binding columns followed by washing with 70% ethanol. DNA was eluted in appropriate volumes of MilliQ water and stored at -20 °C.

2.2.3 RNA preparation

Total RNA was isolated from tissue culture cells using TRIzol according to the manufacturer's instructions. Briefly, 5 x 10^6 suspension cells were harvested and lysed in 1 ml TRIzol. RNA was precipitated by isopropanol and spun down at 16000 g for 15 min. After washing in 70% ethanol, the RNA pellet was resuspended in 100 µl of 0.1% DEPC water and stored at -80 °C.

2.2.4 cDNA synthesis

A cDNA pool was prepared from 2 µg of total RNA (see Section 2.2.3) using the Superscript First-Strand Synthesis for Reverse Transcriptase (RT)-PCR kit in a total volume of 20 µl. Reactions were performed exactly as the manufacturer's instructions. The first strand cDNA was generated using oligo dT as a primer. An appropriate volume of each RT reaction was used as template for the subsequent PCR reactions (see Section 2.2.5 and 2.2.7).

2.2.5 Polymerase chain reaction

Polymerase chain reaction (PCR) was performed on a TGradient (Biometra, Göttingen, Germany) using two different polymerases (LA Taq and KOD Hot Start). The programs varied depending on the melting temperature of the primers and the

length of the PCR product expected. The sequences of all primers used are given in Appendix I. Table 2.8 gives the PCR conditions and programmes used.

Table 2.8 Typical PCR reaction conditions

		LA Taq Polymerase	KOD Polymerase
Reagent concentrations	10 x buffer	1 x	1 x
	Primers	0.3 µM	0.3 µM
	dNTPs	400 µM	200 µM
	Mg^{2+}	(in buffer)	1.5-2.25 mM
	Polymerase	2.5 U	1 U
PCR steps	'Hot start'	94 °C - 1 min	95 °C - 2 min
	Denaturation	98 °C - 10 sec	95 °C - 20 sec
	Annealing	68 °C - X sec	60 °C - 10 sec
	Elongation		70 °C - X sec
	Final elongation	72 °C - 10 min	70 °C - 5 min
	No. of cycles	30	30

2.2.6 Digoxigenin (DIG) labeling of probes by PCR

The PCR DIG Probe Synthesis Kit was used to label probes with digoxigenin for non-radioactive Southern hybridization. Table 2.9 shows the conditions and programmes used for DIG labeling of probes.

Table 2.9 PCR conditions for DIG labeling of probes

Reagent concentrations		PCR steps	
10 x Buffer	1 x	'Hot start'	95 °C - 2 min
Template	100 pg plasmid	Denaturation	95 °C - 10 sec
Primers	0.3 µM	Annealing	60 °C - 30 sec
dNTPs	200 µM	Elongation	72 °C - 40 sec
DIG-dUTP	35 or 70 µM	Final elongation	72 °C - 7 min
Enzyme	2.5 U	No. of cycles	30

2.2.7 Real-time PCR

Real-time PCR was performed using the Applied Biosystem 7500 Real Time PCR System (ABI, Foster City, USA) and Precision™ 2 x Quantitative PCR Mastermix, following the manufacturers' instructions. 1:50 diluted cDNA (see Section 2.2.4) was used as a template for each PCR reaction. The conditions and programmes of Real-time PCR are listed in Table 2.10. The fluorescent dye, SYBRgreen, was

incorporated into double-stranded DNA during the extension steps of PCR. The fluorescence data were quantitated to indicate the relative abundance of the amplified fragments. A post-PCR run melt curve was used to prove the specificity of the primers. All the reactions were performed in triplicate. A relative standard curve was made according to the serially diluted samples of one of the experimental samples which were regarded as the calibrator or 1 x sample. The target quantity of each sample is expressed as the fold difference relative to the calibrator. The relative expression levels of the genes studied were obtained by normalising their expression to a housekeeping gene, *beta-actin*.

Table 2.10 Real-time PCR conditions

Reagent concentrations		PCR steps	
2 x Mastermix	1 x	'Hot start'	95 °C - 10 min
Template	5 µl of diluted cDNA	Denaturation	95 °C - 15 sec
Primers	0.3 µM	Annealing	60 °C - 60 sec
Water	up to 20 µl	Elongation	
		No. of cycles	40

2.2.8 Restriction digestion of DNA

The restriction digestion of plasmid or genomic DNA was performed with the appropriate amount of enzyme, the corresponding 1 x buffer and bovine serum albumin (BSA) if required. The reaction was carried out at the optimum temperature (usually 37 °C) for 2-16 h and terminated by incubation at recommended temperature if required.

2.2.9 Dephosphorylation of DNA 5' ends

The 5' ends of vectors were treated with SAP for dephosphorylation to prevent self-ligation after restriction digestion. Digested vector DNA was incubated with 1 µl SAP in any NEB restriction endonuclease buffer or its own buffer at 37 °C for 1-2 h followed by 15 min incubation at 65 °C in order to inactivate SAP.

2.2.10 Agarose gel electrophoresis

Unless otherwise stated, 0.7% agarose gels containing 0.5 μg/ml ethidium bromide were prepared using electrophoresis grade agarose (Sigma) in 1 x TAE buffer. Gels were run in 1 x TAE buffer in Hoefer HE33 tanks (Mini Horizontal Submarine Unit, GE Healthcare) at 100 V (Electrophoresis Power Supply, GE Healthcare) until the required band resolution was achieved. 1 kb DNA ladders (Invitrogen) were always run in parallel to confirm the size of products. DNA bands in the gel were analysed using a MultiImage Light Cabinet (ChemiImager 5500, Alpha Innotech) and photographed using a digital camera.

2.2.11 DNA purification

DNA bands of interest were excised after electrophoresis from the agarose gel with a scalpel blade and placed in a pre-weighed tube. DNA was purified using the Qiagen QIAquick Gel Extraction kit according to the manufacturer's instructions. Briefly, the sliced agarose gel was dissolved and DNA bound to the column. The column was then washed by 70% ethanol. The DNA was eluted in 30-50 μl of MilliQ water and stored at -20 °C. Alternatively, DNA without agarose gel electrophoresis was purified by using SigmaSpin^{TM} Sequencing Reaction Clean-Up columns to remove buffer salts, enzymes and primers, according to the manufacturer's protocol. The samples were loaded to the column and spun down at 750 g for 4 min.

2.2.12 Ligation

Ligations were performed using T4 ligase supplemented with the reaction buffer in 10-15 μl total volume. Briefly, the ratios of purified vector and insert fragments were from 1:3 to 1:10. Ligations were carried out at room temperature (20-25 °C) for 1 h for sticky-end ligation, or overnight for blunt-end ligation. Control ligations were performed with either vector or insert alone to measure the background.

PCR products generated using KOD polymerase were incubated with Sigma Taq polymerase at 72 °C for 10 min to get A base overhangs (Zhou and Gomez-Sanchez,

2000). The purified PCR products were ligated into the pGEM-T Easy Vector at room temperature for 1 h.

2.2.13 Preparation of chemically competent *E. coli*

E. coli Top 10 cells were grown in 500 ml of LB broth at 37 °C with shaking until the A_{600nm} of the culture reached 0.5. The cells were then incubated on ice for 5 min and pelleted by centrifugation at 5000 g for 15 min. The cell pellet was resuspended in ice cold TfbI (40 ml per 100 ml culture). Cells were then pelleted as before and resuspended in ice cold TfbII (4 ml per 100 ml culture) and incubated on ice for 15 min. The high calcium concentration in those solutions creates small holes in the bacterial membranes making cells competent to take up exogenous DNA. The aliquoted cells were snap frozen in liquid nitrogen and stored at -80 °C.

2.2.14 *E. coli* transformations

E. coli Top10 cells were transformed by heat-shock at 42 °C for 90 s after incubation with DNA on ice for 20 min. The cells then were immediately chilled on ice for another 2 min and recovered in 1 ml of LB broth at 37 °C for 45 min with shaking. The concentrated cells (in 50 µl LB broth) were spread onto LB agar plates containing the appropriate antibiotic selection and incubated inverted at 37 °C overnight. The cells transformed with the ligation of pGEM-T Easy Vector and PCR products were spread onto LB agar plates containing ampicillin and X-gal (Vieira and Messing, 1982). The next day single white colonies were picked and incubated in 2 ml of LB broth containing the appropriate antibiotic selection overnight for the miniprep.

2.2.15 DNA sequencing

DNA samples were sent to either Cogenics (Takeley, UK) or Agowa GmbH (Berlin, Germany) for commercial sequencing.

2.2.16 Southern blot

Approximately 10 µg genomic DNA was digested in 50 µl total volume overnight as described in Section 2.2.8 with additional RNaseA (1 mg/ml). Subsequent analysis was performed at room temperature, unless otherwise stated. The samples were then run on a 0.7% agarose gel at 105 V for 3 h. The gel was immersed in 0.25 M HCl, denaturation buffer and then neutralization buffer with shaking for 20 min, respectively. The DNA was transferred overnight to a Hybond N nitrocellulose membrane (GE Healthcare) by upwards capillary transfer in 10 x SSC. Following transfer, the DNA was cross-linked to membrane with UV (3000 J/cm^2) using a UV Cross-linker (Hoefer UVC500, GE Healthcare).

The DIG labeled probes (see Section 2.2.6) were denatured in 50 µl of MilliQ water at 95 °C for 5 min and immediately chilled on ice. The membrane was incubated in a hybridisation incubator (Techne, Stone, UK) with Pre-Hyb buffer for 30 min and then with DIG Probe in Pre-Hyb buffer for 16 h at appropriate hybridization temperature (T_{hyb}), which was calculated according to the formula provided by the manufacturer[1]. The membrane was washed twice with low stringency buffer for 5 min, twice with high stringency buffer at 65 °C for 15 min. The membrane was then blocked with non-radioactive Southern blot blocking solution for 30 min and incubated with anti-digoxigenin antibody diluted in blocking solution (1:10000) for another 30 min. Unbound antibody was removed by 2 x 15 min washes in maleic acid washing buffer. The membrane was incubated with detection buffer for 3 min to equilibrate the membrane to the pH required for probe detection. The membrane was then transferred into a plastic bag and incubated with CSPD substrate (Disodium 3-(4-methoxyspiro {1,2-dioxetane-3,2'-(5'-chloro) tricyclo [3.3.1.1^{3,7}] decan}-4-yl) phenyl phosphate) for 5 min. Excess CSPD substrate was squeezed out of the bag. The membrane was sealed in the plastic bag and incubated at 37 °C for 10 min to

[1] $T_{hyb} = 49.82 + 0.41$ (% G + C) – 600/L – (20 to 25)
% G + C: % of G and C residues in probe sequence; L: length of hybrid in base pairs

enhance the signal. The membrane was exposed to an X-ray film for 5-18 h depending on the signal strength.

2.3 Protein methods

2.3.1 Protein sample preparation

Cells were harvested at 250 g for 5 min, washed once in 1 x PBS and pelleted again. The cells were then lysed by resuspension in RIPA buffer containing protease inhibitors and phosphatase inhibitors if required. The lysis reaction was proceeded on ice for 1 h, with vortexing every 15 min. The sample was then centrifuged at 16000 g for 15 min at 4 °C. The supernatant containing soluble proteins was transferred to a new tube and the protein yield was determined by Bradford analysis (see Section 2.3.3).

2.3.2 Isolation of nuclear and cytoplasmic proteins

Cells were cultured to at least 80% confluency and harvested by centrifuging at 250 g for 5 min. All the following procedures were carried out at 4 °C. Cell pellets were washed twice with equal volume cold PBS. The cells were then resuspended gently in appropriate volume (50 μl/10^7 cells) of isotonic lysis buffer and incubated on ice for 15 min to allow the cells to swell. 10% IGEPAL CA-630 was added to the lysate to a final concentration of 0.3% and mixed thoroughly. After incubation on ice for another 5 min, cells were spun at 2900 g for 1 min. The supernatant (cytoplasmic protein fraction) was transferred to a fresh tube and spun at 16000 g for 15 min to remove the debris. The pellet (containing nuclear protein) was washed with same volume isotonic lysis buffer, re-pelleted at 250 g for 5 min and resuspended in the appropriate volume (10 μl/10^7 cells) of extraction buffer. The tube was then placed on a mixer and agitated for 15 min at 700 rpm followed by 15 min at 1400 rpm. After centrifuging at 8500 g for 15 min, the supernatant (nuclear protein fraction) was transferred to a fresh tube. The protein concentration was determined by Bradford analysis (see Section 2.3.3).

2.3.3 Bradford protein assay

The Bradford assay is a spectroscopic method based on the change of colour of the Coomassie Blue G dye from red to blue upon binding to proteins in a concentration-dependent manner (Zor and Selinger, 1996). Bradford reagent (Sigma) was employed to determine protein concentration as described in the manufacturer's protocol. Briefly, 1 µl of a protein sample was diluted in 1 ml 1:1 Bradford : MilliQ water solution. The absorbance at 595 nm was measured by a spectrophotometer (Eppendorf, Hamburg, Germany). The protein concentration was calculated based on a BSA standard curve, in which absorbance was plotted *vs.* varying known concentrations of the BSA protein.

2.3.4 SDS-polyacrylamide gel electrophoresis

50-100 µg of total proteins were boiled in 1 x sample buffer containing β-mercaptoethanol at 95 °C for 10 min to completely denature proteins. Samples were then loaded into the wells of a SDS-PAGE gel. Polyacrylamide gel percentages varied depending on the protein size being analysed (see Table 2.6). Generally, samples were separated at 100 V through the stacking gel and 150 Volts through the resolving gel in 1 x running buffer.

2.3.5 Coomassie staining

Proteins were resolved using an acrylamide gel (see Section 2.3.4). Gels were stained with Coomassie Blue R for 20 min at room temperature, with gentle agitation, then destained overnight at room temperature with several changes of the destain solution.

2.3.6 Transfer of proteins to membrane

Proteins separated by SDS-PAGE were transferred to nitrocellulose membranes (GE Healthcare) using either wet or semi-dry transfer systems in 1 x transfer buffer. Small proteins (up to 100 kDa) were transferred by a semi-dry transfer system which was carried out at room temperature for 75 min at appropriate constant amperage

depending on the size of the membrane. The wet transfer which was used to transfer large proteins (>100 kDa), was carried out at 4 °C for 2 h at 350 mA. Following transfer, the membrane was washed in dH_2O and stained with Ponceau S for 5-10 min, to evaluate the quality of protein transfer.

2.3.7 Immunoblotting

Membranes with bound protein (see Section 2.3.6) were blocked with blocking solution at room temperature for 30 min on a rocking platform to decrease non-specific antibody binding. Following blocking, membranes were then incubated with diluted primary antibody (Table 2.4) overnight at 4 °C or at room temperature for 1 h with gentle agitation. Unbound antibody was removed with 3 times 10 min washes. The membrane was then incubated with the secondary antibody at room temperature for 1 h with gentle agitation. After another 3 x 10 min washes, the specific proteins were detected with ECL detection kit (GE Healthcare) according to the manufacturer's instructions and exposed to autoradiograph film (Hartenstein, Germany). The exposed film was then fixed and developed by passing it through a developing machine (CP 1000, AGFA, Brentford, UK).

2.3.8 Expression of Annexin V protein in *E. coli*

A starter culture expressing Annexin V protein (a kind gift from Prof. Afshin Samali) was incubated in 5 ml LB broth containing selective antibiotics overnight at 37 °C. The next day the culture was diluted 1:100 in LB broth containing selective antibiotics and grown at 37 °C until OD_{600} reached 0.5. 1 ml of cells ('un-induced' sample) was collected for SDS-PAGE analysis. After 2 h induction with 600 µM IPTG at 37 °C, the cells were pelleted and frozen at -80 °C. 1 ml of cells ('induced' sample) was collected.

2.3.9 Affinity purification of Annexin V

All the purification steps were performed at 4 °C. The *E. coli* pellet (see Section 2.3.8) was thawed on ice and resuspended in 20 ml lysis buffer. The cell suspension was sonicated for 6 x 5 s cycles at 35% amplitude on ice, and centrifuged at 16000 g for 30 min. The supernatant was removed to a new tube containing 200 µl of Ni Sepharose^{TM} 6 Fast Flow beads (GE Healthcare) which were prewashed in 1 x PBS. The binding of proteins with the beads was performed for 2 h on a rotating mixer. The supernatant was incubated with another 400 µl of fresh prewashed beads overnight on a rotating mixer. The beads were then washed once in 10 ml 1 x PBS, 5 times in 1 ml lysis buffer and 3 times in 200 µl elution buffer. The beads were finally washed in 1 ml lysis buffer. All the washes and elutions were kept and checked on Coomassie gel (see Sections 2.3.4 and 2.3.5). All the elutions were pooled and the concentration measured by Bradford assay (see Section 2.3.3).

2.3.10 Desalting and FITC-conjuation of purified Annexin V

All the steps were performed at 4 °C unless otherwise stated. A PD-10 desalting column (GE Healthcare) was equilibrated with 25 ml reaction buffer. 2.5 ml of pooled samples were loaded onto the column. The column was eluted with 3.5 ml reaction buffer. The concentration of elution was determined using Bradford (see Section 2.3.3). 10 mg FITC (Invitrogen) was dissolved in 1 ml DMSO and added to Annexin V at the ration of 20 µg FITC per 1 mg Annexin V. The conjugation reaction was performed in darkness for 1 h at room temperature on a rotating mixer. The desalting procedure was repeated to remove unconjugated FITC with Annexin buffer. 0.01% sodium azide was added to the conjugated protein for prevention of microbial contamination. The FITC labeled Annexin V was titrated against a commercial Annexin-V-FLUOS staining kit (Roche) to assess its efficiency.

2.4 Cell culture techniques

2.4.1 Maintenance of DT40 cells

DT40 cells were cultured in RPMI 1640 (with L-glutamine and sodium bicarbonate), supplemented with 10% FBS, 1% chicken serum, 100 U/ml penicillin, and 100 μg/ml streptomycin, at 39.5 °C, 5.0% CO_2, in humidified conditions. Cultures were maintained at cell densities between 1 x 10^5 cells/ml and 1 x 10^6 cells/ml, which is confluent for DT40. Experiments described here were performed using exponentially growing cells (50-80% confluent).

2.4.2 Freezing cells

1 x 10^7 cells were harvested by centrifugation at 250 g for 5 min. The pellet was resuspended in 200 μl freezing media (10% DMSO in FBS) and transferred to cryovials. Cells could be kept at -80 °C for up to a year and in liquid nitrogen for longer-term storage. Cells were woken up by thawing as soon as possible to re-culture as usual (see Section 2.4.1).

2.4.3 DT40 proliferation analysis

Cells were counted using a haemocytometer as described in the manufacturer's protocol. Each cell line was diluted into triplicate wells to start with equal cell densities (5 x 10^4 cells/ml). The cells were cultured as usual (see Section 2.4.1) and counted every 24 hours for at least 96 hours. When cells were approaching confluency, the cultures were diluted to 5 x 10^4 cells/ml again. The dilution factor was recorded to calculate the actual cell numbers for plotting of growth curve.

2.4.4 Stable transfection of DT40 cells

Stable cell lines for gene targeting or expression of exogenous transgene were generated by electroporation of a linearised DNA construct using a Gene Pulser electroporation apparatus. 1 x 10^7 cells were harvested and washed once in sterile 1 x PBS. The cell pellet was then resuspended in 500 μl 1 x PBS and mixed with 20 μg of linearised and purified plasmid DNA. The mixture was transferred to an electroporation cuvette (BioRad, 0.4 cm gap) and incubated on ice for 10 min.

Electroporation was performed at either 550 V/25 μF or 300 V/600 μF. Following electroporation, the mixture was again incubated on ice for 10 min, and then pipetted into 20 ml of prewarmed media for growing as usual (see Section 2.4.1). 18-24 h later, 20 ml of prewarmed media and the appropriate selection drug were added to the culture. The transfected cells were seeded into four 96-well plates (100 μl per well). The plates were then placed in the incubator for 8-10 days until single colonies were visible through the bottom of the plate. Each single colony was then expanded to 3 ml of media without drug in 24-well plates and incubated for 3-4 days until cultures reached confluency. Half of the each culture was frozen at -80 °C for temporary storage. The other half was analysed by Southern blot, immunofluorescence microscopy or Western blot.

2.4.5 Transient transfection

Transient transfection was performed using endotoxin-free circular plasmids and the Amaxa nucleofection system (cell line nucleofection kit T (VCA-1002)) in an Amaxa nucleofector (Cologne, Germany), as described in the manufacturer's protocol. 5 x 10^6 cells were harvested and resuspended in the 100 μl of Solution T provided in the kit. 10-15 μg of endotoxin-free circular DNA (in less than 15 μl) was mixed with cells sufficiently. The mixture was then transferred to the Amaxa transfection cuvette and nucleofected using programme B-23. The transfected cells were pipetted into 5 ml of prewarmed media for growing as normal (see Section 2.4.1). 24 hours later, cells were harvested for analysis by immunofluorescence microscopy or Western blot.

2.4.6 Resistance cassette recycling

Transient transfections were carried out as Section 2.4.5 with the chimeric Cre recombinase expression plasmid pMerCreMer (Verrou et al., 1999). After 24 hours recovery, cells were counted and serially diluted to 1 cell/100 μl. 100 μl of diluted cells were than plated into each well of two to four 96-well plates. The plates were placed in the incubator for 8-10 days until single colonies were visible through the

bottom of the plate. Each single colony was expanded and replica plated to two 24-well plates. Half of the each colony was grown in fresh medium without drug. The other half was grown in replica wells with appropriate drug. After 4-6 days' incubation, colonies that were no longer drug-resistant in the replica wells were frozen and confirmed for resistance cassette recycling by Southern blot.

2.4.7 Irradiation of cultures

For ionising radiation, cultures were irradiated with a ^{137}Cs source at 23.5 Gy/min (Mainance Engineering, Waterlooville, UK). For UV-C irradiation, cells were irradiated in PBS using a 254 nm UV-C lamp at 23 J/m^2/min (NU-6 lamp; Benda, Wiesloch, Germany).

2.4.8 Clonogenic survival

Clonogenic survival assays were performed to determine the sensitivity of cells to different DNA damage agents as previously described (Takata *et al*., 1998). Serially diluted cells (1 x 10^3 cells/ml-1 x 10^5 cells/ml) were plated in 7 ml of semi-solid methylcellulose medium (see Section 2.1.3) which had been pre-warmed in a 39.5 °C incubator for at least 1 h. After one hour recovery, the plated cells were irradiated at various doses (2, 4, 8 Gy) using a ^{137}Cs source (see Section 2.4.7). In general, colonies were counted 10-14 days after seeding. Cell survival was expressed as a percentage of the survival of untreated cells.

2.4.9 DT40 centrosome purification

Centrosome purification was performed as previously described (Barr et al., 2010). Briefly, 100 ml of 80% confluent cells were arrested in mitosis by incubation with 500 ng/ml nocodazole for 12 h. The microtubule and actin cytoskeletons were then depolymerised by treatment with 1 μg/ml nocodazole (final concentration) and 1 μg/ml cytochalasin D for 1 h. Cells were pelleted and washed in TBS buffer and 8% sucrose in 1/10 TBS buffer. Cells were then resuspended in 1 ml of TBS 1/10 8%

sucrose buffer and lysed in 8 ml lysis buffer. After spinning at 2500 g for 10 min, the supernatant was filtered through a nylon mesh (40-µm pore size) and incubated with 10 mM Hepes and 1 µg/ml DNase I on ice for 30 min. The supernatant was spun onto 2 ml of 60% sucrose cushion in a SW32 rotor (Beckman Coulter, Brea, USA) at 10000 g for 30 min. The discontinuous sucrose gradient consisted of 1 ml 70% sucrose, 600 µl 50% sucrose and 600 µl 40% sucrose. After addition of the centrosome-containing supernatant onto this gradient, samples were centrifuged for 2 h at 120000 g in a SW55 Ti rotor (Beckman Coulter). 500 µl of fractions were collected by punching a small hole in the bottom of the centrifuge tube and collecting droplets. After addition of 10 mM PIPES-KOH, pH 7.2, centrosomes in each fraction were pelleted at 115000 g in a S45A rotor in a Sorvall Discovery ultracentrifuge (Thermo Scientific, Basingstoke, UK). The supernatant was discarded and centrosome pellets were resuspended in 40 µl boiling 1 x SDS-Loading buffer. Samples were analysed by Western blotting.

2.4.10 Microtubule regrowth assays

DT40 cultures were incubated with 2 µg/ml nocodazole for 3 h in a 39.5 °C incubator and for another 1 h on ice to depolymerise microtubules. Cells were washed three times in ice-cold 1 x PBS (supplemented with 1:1000 volume DMSO) by centrifugation at 250 g for 2 min. Cells were then resuspended in 100 µl cold 1 x PBS and adhered to poly-L-lysine slides for 30 min at 4 °C. The slides were submerged in 1% FBS in 1 x PBS at 40 °C for 30 s or 1 min and immediately fixed in methanol. Immunofluorescence microscopy analysis with antibodies to α-tubulin (see Section 2.4.12) was used to assess microtubule growth.

2.4.11 Electron microscopy

DT40 cells were processed for transmission electron microscopy (TEM) using an established protocol (Liptrot and Gull, 1992). All the following experiments were performed at room temperature unless otherwise stated. Briefly, 1 x 10^7 cells were

washed in 0.1 M sodium cacodylate buffer and pelleted at 250 g for 5 min. The cell pellet was fixed with a combination of 2% glutaraldehyde and 2% paraformaldehyde in 0.1 M cacodylate buffer for 1 h. Following 1 h post-fixation in a solution of 2% osmium tetroxide in 0.1 M cacodylate buffer, cell pellets were dehydrated through an alcohol gradient (30%; 60%; 90%; 100%) which was then replaced by propylene oxide. Subsequently, cell pellets were equilibrated in 1:1 100% ethanol:final epoxy mixture and then in 1:2 100% ethanol:epoxy embedding medium, each for 90 min. Cell pellets were embedded in Agar Low Viscosity Resin (Agarscientific, Essex, UK). Sample containing moulds were polymerised at 60 °C for 24 h. Sections were cut on a Reichert-Jung Ultracut E microtome (Leica, Wetzlar, Germany), using a diamond knife. Serials sections were collected onto Formvar-coated copper grids and stained with uranyl acetate and lead citrate, then viewed on an H-7000 Electron Microscope (Hitachi, Maidenhead, UK). Images were taken with an ORCA-HRL camera (Hamamatsu Photonics, Hamamatsu City, Japan) and processed using AMT version 6 (AMT Imaging, Danvers, MA, USA).

2.4.12 Immunofluorescence microscopy

Cells were left to attach to poly-L-lysine-coated slides (Fisher) for 15 min at room temperature. The media was aspirated, and cells were fixed/ permeabilised for 10 min in pre-chilled 95% methanol containing 5 mM EGTA at -20 °C. Alternatively, cells were fixed in 4% paraformaldehyde in 1 x cytoskeleton buffer (CB) or PBS for 10 min and permeabilised in 0.15% Triton X-100 in 1 x CB or PBS for 2 min at room temperature. Thereafter, the cells were blocked in 1% BSA in 1 x PBS for 30 min at room temperature or overnight at 4 °C. The cells were than incubated with primary antibodies for 1 h at 37 °C followed by 45 min incubation at 37 °C with secondary antibodies in a humid atmosphere. The exact blocking and antibody binding conditions for each antibody used for immunofluorescence microscopy are given in Table 2.4 and 2.5. Slides were mounted with DABCO supplemented with 1 µg/ml DAPI (4,6-diamidino-2-phenylindole) and sealed with nail varnish.

For fixed cell imaging, images were taken as Z-sections (0.2 μm steps) with a DeltaVision integrated microscope system controlled by SoftWorx software (Applied Precision, Issaquah, USA) mounted on an IX71 microscope (Olympus, Melville, USA) with a PlanApo N100 x oil objective, (N.A. 1.40). Images were deconvolved and quick projection was made by SoftWorx software. For the measurement of centrosomal γ-tubulin, PCM1, and nuclear phospho-CHK1 foci intensities, cells were imaged by an Operetta high content imaging system (PerkinElmer) with a 40 x air objective. The centrosome spots or nuclear foci were identified and analysed automatically by Harmony software version 3.0 (PerkinElmer). All images from a single experiment were treated in exactly the same way. Cell counting was performed blind using a BX51 microscope (Olympus, Tokyo, Japan), using 60 x oil (N.A. 1.4) or 100 x oil, (N.A. 1.35) objectives.

For live cell imaging, cells that stably expressed H2B-RFP were allowed to attach to poly-D-lysine-coated dishes (MatTek, Ashland, USA) for 2-3 h in the media supplemented with 12.5 mM Hepes, pH 7.5. Images were taken at 3 min intervals for 3 h on a DeltaVision integrated microscope system using a PlanApo N60 x oil objective (N.A. 1.42) and a 39.5 °C environmental chamber (WeatherStation, Precision Control, Sammamish, USA).

2.4.13 Flow cytometry

For analysis of cell cycle profiles, 5 x 10^6 cells were centrifuged at 250 g for 5 min and resuspended in 1 ml of 70% ethanol in 1 x PBS for fixation at -20 °C. For propidium iodide (PI) FACS, cells were washed in 1 x PBS and incubated in 40 μg/ml PI and 200 μg/ml RNaseA in 1 x PBS overnight at 4 °C in the dark. For bromodeoxyuridine (BrdU) FACS, cells were cultured with 20 μM BrdU for 10 min and fixed. Cells were then washed in 1 x PBS with 1% BSA and resuspended in 2 M HCl/ 0.5% Triton X-100 in 1 x PBS. After 30 min incubation at 37 °C, cells were washed again and then

incubated with 30% anti-BrdU (BD Biosciences, Erembodegem, Belgium) in 1 x PBS with 1% BSA/0.5% Triton X-100 for 1 h with shaking at 37 °C followed by washing and 30 min incubation with FITC anti-mouse antibody at 1:50 in 1 x PBS with 1% BSA at room temperature in the dark. Finally, cells were resuspended in PI/RNaseA solution as above. For phospho-Ser10 Histone H3 (pH3) FACS, fixed cells were washed in 1 x PBS and resuspended in 1 ml of 1 x PBS containing 0.25% Triton X-100. After 15 min incubation on ice, cells were pelleted and then incubated with 1% anti-pH3 in 1 x PBS with 1% BSA for 2 h with shaking at room temperature followed by washing and 30 min incubation with FITC anti-rabbit antibody at 1:30 in PBS with 1% BSA at room temperature in the dark. Finally, cells were resuspended in PI/RNaseA solution as above. Flow cytometry was performed on a FACS Canto (Becton Dickinson (BD), San Jose, USA) and analysed using BD FACS Diva Software.

Annexin V-FITC, which specifically binds to negatively charged phospholipids surface exposed on the cell membrane, was used for identifying apoptotic cells. Cells were centrifuged at 250 g for 5 min and re-suspended in 1 x Ca^{2+} buffer supplemented with 1 µl of Annexin V-FITC and 2 µg/ml PI. After 15 min incubation at room temperature in the dark, cells were analysed immediately using flow cytometry as above.

Chapter 3. Cloning and characterisation of chicken *Pcnt*

3.1 Introduction

Pericentrin is a large coiled-coil centrosomal protein which was first identified in mouse as a 220 kDa protein (Doxsey et al., 1994). A larger protein (~ 380 kDa) with an N-terminal region homologous to the original protein and a unique C-terminal calmodulin-binding domain was later found in humans (Li et al., 2001). It is now believed that both isoforms are encoded by alternatively-spliced transcripts and expressed in both humans and mice (Flory and Davis, 2003; Miyoshi et al., 2006). The calmodulin-binding domain, the PACT domain, is the best studied domain of pericentrin. It is responsible for the centrosomal localisation of the protein (Gillingham and Munro, 2000). No other distinctive domains have been described. Pericentrin plays important roles in a variety of fundamental cellular processes through its multifunctional scaffold ability to anchor numerous proteins to the centrosome (Delaval and Doxsey, 2009). Recently, it has been indicated that *PCNT* mutations which lead to premature protein truncation are linked with a rare autosomal recessive genetic disorder, MOPD II (Rauch et al., 2008). To better understand the function of pericentrin, we proposed to use reverse genetics to study the phenotypes after the *Pcnt* gene was disrupted in chicken DT40 cells. We decided to clone and characterise chicken *Pcnt* first so that we could define the genomic locus for targeting vector construction.

3.2 Cloning of chicken *Pcnt*

The human *PCNT* gene maps to chromosome 21 (21q.22.3) and the chicken *Pcnt* localises on chromosome 7. *PCNT* and *Pcnt* are directly flanked on both sides by homologous genes (5' end, *C21orf58*; 3' end, *DIP2A* and *S100B*). The predicted mRNA sequences of chicken *Pcnt* are available in the NCBI and Ensembl databases. The genomic sequences are almost identical between these two databases. However, the protein predicted in the NCBI database (XP_421895) is 404 kDa with 3477

residues in 48 exons, whereas there are three isoforms in the Ensembl database, a 220 kDa protein with 1905 residues in 44 exons (ENSGALP00000011342), a 182 kDa protein with 1550 residues in 33 exons (ENSGALP00000011498) and a 46 kDa protein with 399 residues in 8 exons (ENSGALP00000012030). When we aligned the Ensembl and NCBI sequences, all three Ensembl sequences were found within the NCBI sequence. This suggests that the three transcripts predicted by the Ensembl database are different splice isoforms of that in the NCBI database. In addition, a 380 kDa pericentrin form has been described in both human and mouse (Miyoshi et al., 2006). Therefore, we used the NCBI *Pcnt* sequence for further alignments. Next, we searched the expression sequence tag (EST) database (dbEST, NCBI) with the candidate *Pcnt* mRNA sequence to confirm that it is expressed in chicken cells. Multiple EST clones covered 62% of the entire *Pcnt* mRNA sequence, including 2 kb of the 5' end and 1.7 kb of the 3' end. Four fragments covering a total of 4 kb in the middle of the mRNA were not found in any of the EST clones. A BLAST search against the entire nucleotide collection revealed that there was no other similar gene in the *Gallus gallus* genome.

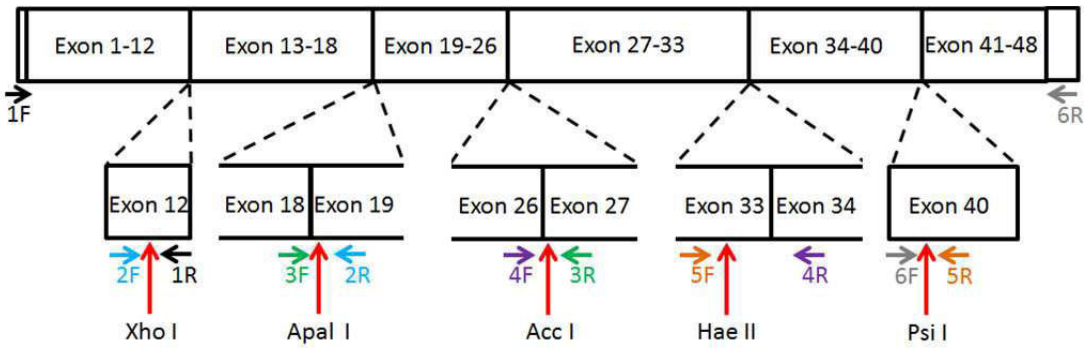

Figure 3.1 Strategy of cloning chicken *Pcnt* cDNA.
Six small fragments of *Pcnt* cDNA were amplified separately and combined using the indicated unique restriction endonuclease sites predicted in the NCBI *Pcnt* sequence. Each pair of primers is indicated by the same colour.

We then amplified the chicken *Pcnt* cDNA according to the mRNA sequence predicted in the NCBI database. As the predicted coding sequence of *Pcnt* is 10434 bp flanked by a 90 bp 5'-UTR and a 416 bp 3'-UTR, it would be technically difficult

to amplify such a long fragment without mutations. Therefore, we amplified 6 small fragments (1.3-2.5 kb each) of the *Pcnt* cDNA and combined them using the unique restriction endonuclease sites (Figure 3.1). The 6 fragments were amplified from the cDNA and then cloned into a pEGMT-easy vector. Only one band was observed in

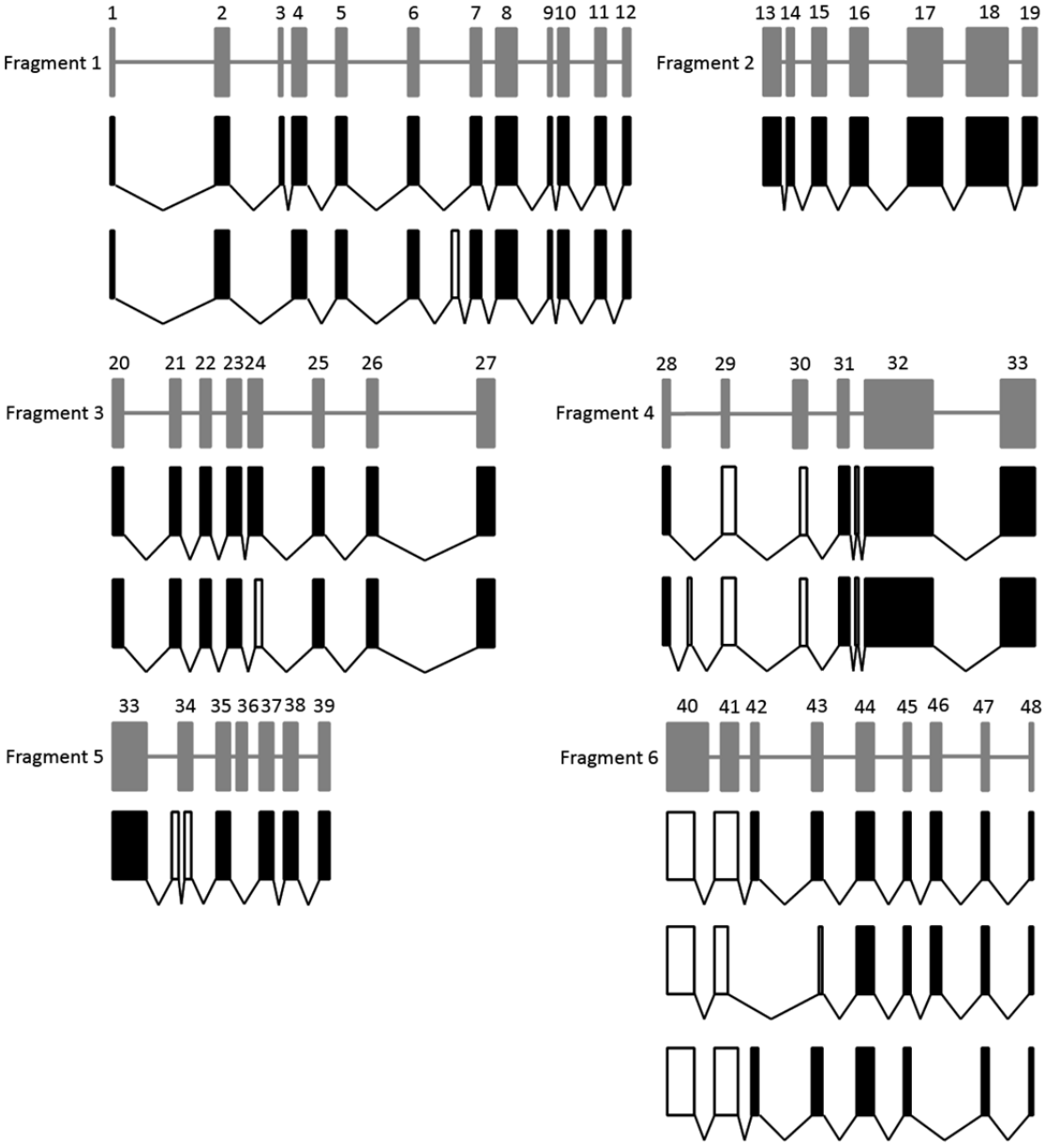

Figure 3.2 Comparison of the cloned *Pcnt* sequence with the predicted sequence in the NCBI database.

A schematic representation of the chicken *Pcnt* locus is shown. The predicted exons are presented as grey boxes. The exons in our cDNA which are the same as the predicted ones are presented as black boxes. The exons in our cDNA that differ from the predicted ones are presented as white boxes. Numbers indicate exons, based on the NCBI sequence.

all the 6 PCR reactions (data not shown), suggesting there were no isoforms with distinctly different sizes. At least 3 clones of each fragment were sent for sequencing. A total of 5 additional splice isoforms were found in the 4 assembled fragments. However, the difference in size between each isoform was less than 300 bp. Compared with our cDNA sequence, exons 3, 42 and 46 in the NCBI sequence were spliced out in some clones. Exons 29, 30, 34, 40 and 41 were partially consistent with our cDNA. We found extra exons before exons 7, 32 and 34, respectively. Predicted exon 36 did not exist in our cDNA. The summary of the differences between the cloned cDNA and predicted sequence is shown in Figure 3.2. The point mutations in each fragment were corrected before the final ligation. When we compared the 6 fragments against the entire nucleotide collection, there was no similarity to any other gene. The longest isoform of each fragment for assembly was chosen for the ligation. Our full-length chicken pericentrin cDNA is 10479 bp in length and encodes a protein of 3492 amino acid residues with a predicted size of 405.96 kDa. However, we cannot exclude the possibility that there are some other truncated splice isoforms because we failed to amplify the full length *Pcnt* cDNA in a single reaction. Full chicken *Pcnt* sequence information is shown in Appendix 2.

3.3 Sequence analyses of pericentrin protein

Pericentrin homologues have been identified in a variety of organisms, including budding yeast, fission yeast, *Drosophila*, mouse and human (Flory et al., 2002; Flory et al., 2000; Martinez-Campos et al., 2004). So far, at least two isoforms of pericentrin have been found in human, mouse and *Drosophila*. We used the longer available isoforms of *Pcnt* in these species to construct a phylogenetic tree based on the neighbor-joining method. This tree showed that chicken pericentrin is not highly conserved, compared with the other species analysed. However, the chicken pericentrin showed a higher similarity to mammalian pericentrins than to its homologues from non-vertebrate organisms (Figure 3.3A). The analysis of domain architectures by SMART (Simple Modular Architecture Research Tool, http://smart.embl-heidelberg.de/) showed that these pericentrin proteins contained extensive

coiled-coil secondary structure and a conserved C-terminal PACT domain (a calmodulin-binding domain) (residues 3285 to 3366 in the chicken peptide, Figure 3.3B).

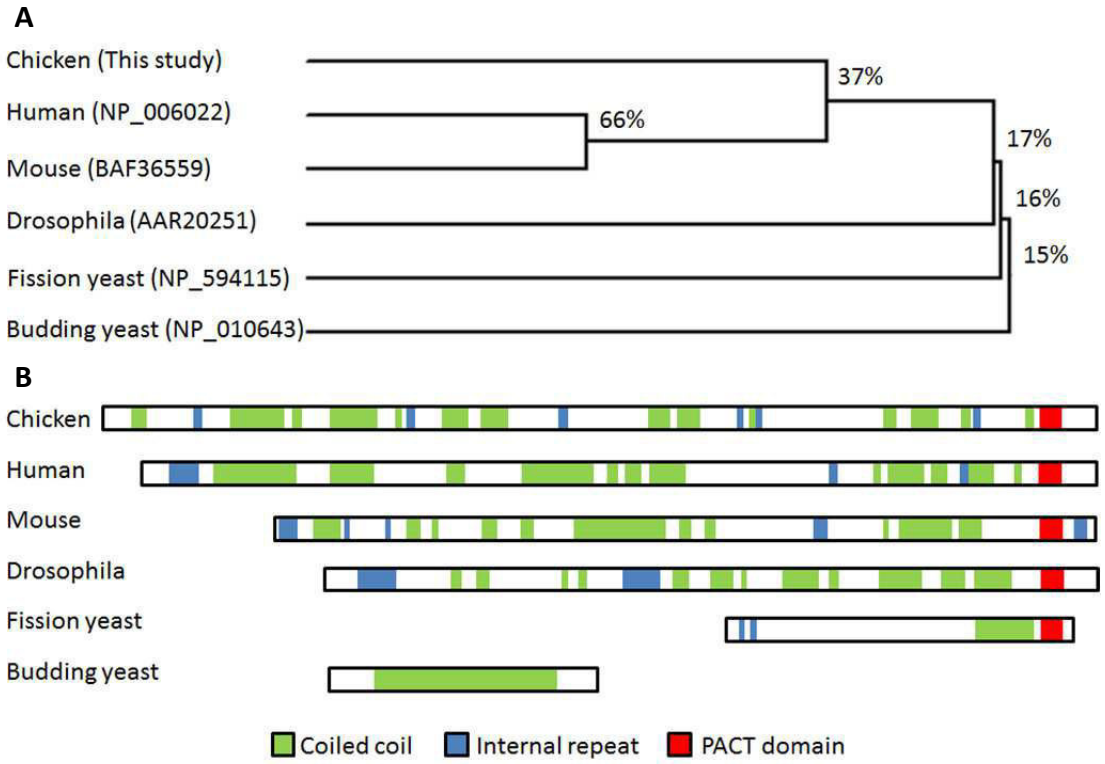

Figure 3.3 Analyses of *Pcnt* protein sequences.
A. Phylogenetic tree showing an evolutionary conservation of pericentrin protein sequences among human, mouse, chicken, *Drosophila*, budding and fission yeast. The taxa joined together indicate that the species are descended from a common ancestor. Numerical values show the similarity between the species.
B. Predicted secondary structure of pericentrin proteins. The protein sequences of each species were analysed with SMART software to identify protein domains and motifs.

3.4 Mapping of the chicken *Pcnt* genomic locus

These results indicated that we had cloned chicken *Pcnt* and that the bulk of the information about chicken *Pcnt* in the NCBI database was correct. The chicken *Pcnt* locus is on chromosome 7. However, the human *PCNT* locus is on chromosome 21 and the mouse *Pcnt* locus is on chromosome 10. To confirm that chicken *Pcnt* is the orthologue of human *PCNT*, we examined whether chicken, human and mouse pericentrins were encoded by syntenic loci. As shown in Figure 3.4, chicken, human and mouse pericentrins are flanked on both sides by homologous genes. Therefore,

we concluded that chicken, human and mouse pericentrins are in syntenic genomic regions. However, there are more homologues of human genes on the mouse chromosome than those on the chicken chromosome. In addition, the relative positions of human genes are more similar to the mouse homologues than to the chicken homologues. These data also suggest that human and mouse pericentrins have a closer evolutionary relationship, which is consistent with the results shown in Figure 3.3A and with the mammal-bird split.

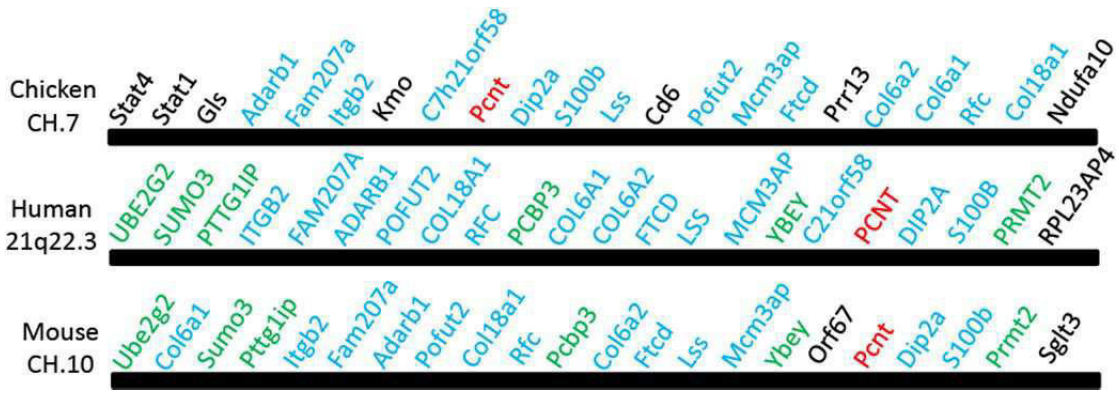

Figure 3.4 Synteny map of chicken, human and mouse *pericentrin* loci.
The related regions of chicken chromosome 7, human chromosome 21 (21q22.3) and mouse chromosome 10 were analysed according to the NCBI database. The homologous genes flanking all chicken, human and mouse pericentrins are shown in blue, whereas those only flanking human and mouse pericentrins are shown in green.

Our aim was to investigate the function of pericentrin by targeted gene disruption in the DT40 cell line. Therefore we needed detailed genomic information about this locus to design the targeting vectors for *Pcnt* disruption. *Pcnt* spans about 100 kb and localises on chromosome 7, which means there are 2 copies of the gene in DT40 cells. Our full-length *Pcnt* cDNA consists of 49 exons. We aligned the full-length chicken *Pcnt* cDNA sequence with its genomic sequence using Spidey (NCBI) to analyse the exon and intron structure of the locus (Table 3.1). Most of the exons are very small (about 200 bp), whereas the introns are larger (up to 6 kb). A similar distribution also occurs in the human *PCNT* locus, which has 47 exons. This means the conventional strategies were not applicable for knocking out chicken *Pcnt* (see Chapter 4).

Table 3.1 The length of exons and introns of chicken *Pcnt* genes.

Exon		Intron		Exon		Intron	
No.	**Length (bp)**	**No.**	**Length (bp)**	**No.**	**Length (bp)**	**No.**	**Length (bp)**
1	45	**1**	5791	**26**	144	**26**	5997
2	204	**2**	3636	**27**	230	**27**	454
3	180	**3**	1659	**28**	120	**28**	2970
4	144	**4**	3510	**29**	228	**29**	3695
5	165	**5**	2866	**30**	171	**30**	2521
6	93	**6**	220	**31**	153	**31**	544
7	177	**7**	932	**32**	168	**32**	353
8	254	**8**	1803	**33**	1113	**33**	4017
9	61	**9**	194	**34**	516	**34**	1499
10	175	**10**	1507	**35**	97	**35**	367
11	137	**11**	1031	**36**	155	**36**	1278
12	112	**12**	2248	**37**	198	**37**	1154
13	265	**13**	287	**38**	196	**38**	607
14	91	**14**	949	**39**	223	**39**	1387
15	217	**15**	1395	**40**	151	**40**	1572
16	239	**16**	2294	**41**	522	**41**	762
17	476	**17**	1373	**42**	284	**42**	758
18	577	**18**	770	**43**	100	**43**	3179
19	234	**19**	1981	**44**	165	**44**	1964
20	165	**20**	2695	**45**	239	**45**	1848
21	147	**21**	1228	**46**	89	**46**	1115
22	152	**22**	995	**47**	154	**47**	2382
23	215	**23**	458	**48**	119	**48**	2264
24	212	**24**	2901	**49**	44		
25	163	**25**	2525				

3.5 Structure-function analysis of chicken pericentrin

Previous reports have suggested that pericentrin localises at the centrosome in human, mouse and *Drosophila* cells (Endoh-Yamagami et al., 2010; Kawaguchi and Zheng, 2004; Lüders et al., 2005). To further confirm that the gene we cloned is the pericentrin orthologue in chicken, we next investigated the centrosomal localisation of the candidate pericentrin protein. The GFP-pericentrin (full-length) fusion protein was expressed transiently in *Pcnt* null DT40 cells (see Chapter 4) and imaged by immunofluorescence microscopy. The cells were counter-stained with a centrosome

marker, γ-tubulin, and examined for co-localisation with the GFP-pericentrin signal. Immunofluorescence microscopy on fixed cells demonstrated that GFP-pericentrin (full-length) only localised to centrosomes as a very small dot (Figure 3.5), suggesting that we had successfully cloned the chicken pericentrin.

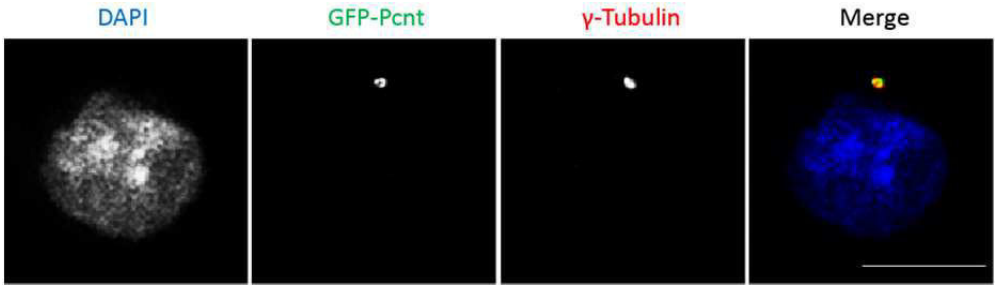

Figure 3.5 Centrosomal localisation of the GFP-pericentrin fusion protein.
Pericentrin null DT40 cells were transiently transfected with the GFP-tagged pericentrin fragment (full length), fixed with methanol, and counter stained with γ-tubulin (red) which indicates the location of the centrosome. Scale bar, 10 μm.

So far, there is very little information about the functional domains of pericentrin. The only domain characterised to date is the PACT domain at its C-terminal end, which is responsible for the centrosomal anchoring of the protein (Gillingham and Munro, 2000). The PACT domain consists of ~200 amino acid residues, whereas there are 3492 residues in the pericentrin protein. To determine whether there is another region(s) of pericentrin required for its centrosomal targeting or function

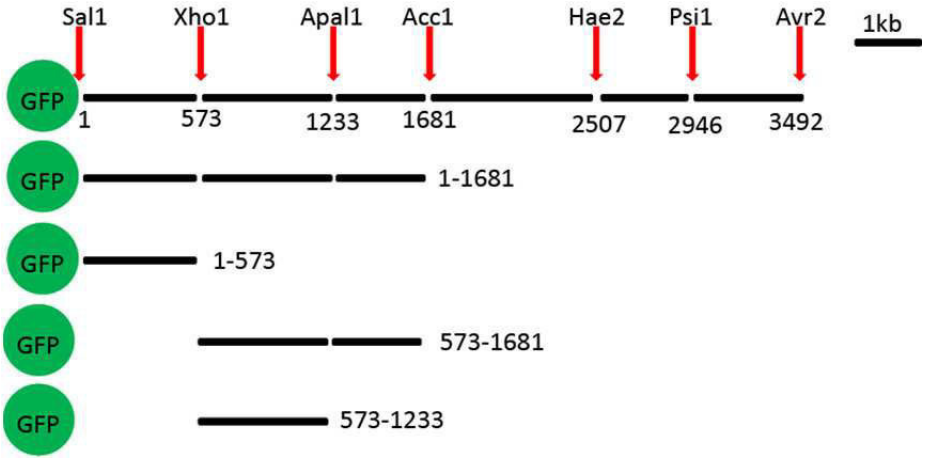

Figure 3.6 Schematic representation of pericentrin and its deletion mutants.
Positions of deletion mutants are shown with amino acid residues indicated. Individual fragments were assembled to generate full length *Pcnt* and 4 deletion mutants.

folding, we performed preliminary structure-function analysis of chicken pericentrin. As we used 6 fragments to assemble the full-length pericentrin, we also constructed several deletion mutants by linking some of the fragments. A schematic representation of Pcnt and its deletion mutants is shown in Figure 3.6. Deletion mutants are named as PcntX-X, where X-X represents amino acid residues. All the deletion mutants were N-terminally tagged with GFP.

We then transiently expressed the various deletion mutants in the *Pcnt* null DT40 cells and analysed their subcellular localisation by fluorescence microscopy. The cells were counter stained with γ-tubulin to label their centrosomes. As shown in Figure 3.7, most of the deletions were distributed in the cytosol. Truncated

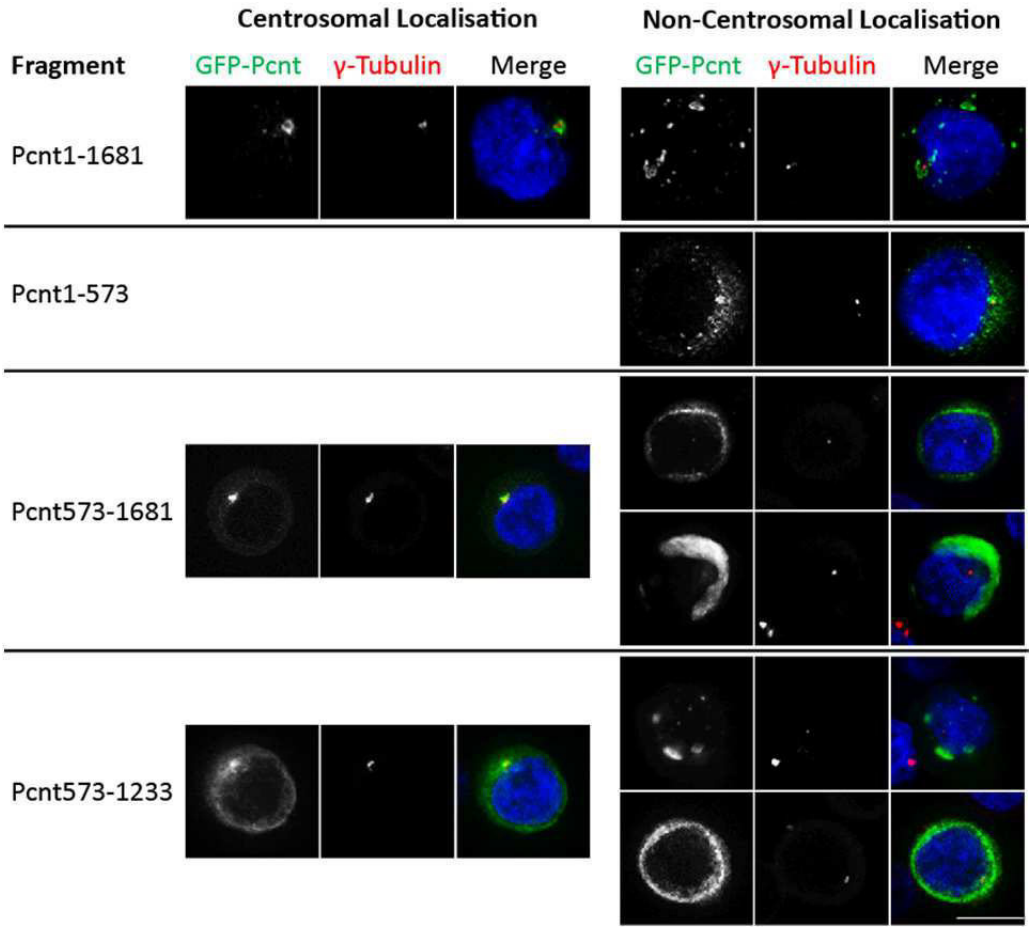

Figure 3.7 Structure-function analysis of chicken pericentrin.
Pericentrin null DT40 cells were transiently transfected with the GFP-tagged pericentrin fragments (deletion mutants), fixed with methanol, and counter stained with γ-tubulin (red) which indicates the location of the centrosome. Scale bar, 10 μm.

pericentrin cannot form a single sharp spot or localise at the centrosome in some cases, which never happened in the full-length pericentrin transfected cells. These data suggest that the C-terminal end, which contains the PACT domain, is required for pericentrin to form the correct structure. However, we observed a single green spot colocalising with γ-tubulin in some cells transfected with truncated pericentrin. This indicates that some part of the protein, distinct from the PACT domain, is also able to assemble pericentrin at the centrosome. If the truncated protein expressed only one distinct green spot which colocalised with γ-tubulin in more than 50% of the positive cells, we concluded that the fragment was centrosomally localised. A summary of the colocalisation of each truncation mutant with γ-tubulin is shown in Table 3.2. At least 100 positive cells per transfection were analysed. We found that more than 50% of the cells transfected with GFP-Pcnt1-1681 and GFP-Pcnt573-1681 had bright spots that colocalised with γ-tubulin at the centrosomes, while only 10% of cells transfected with GFP-Pcnt573-1233 had detectable spots at centrosomes. The truncated mutant GFP-Pcnt1-573 distributed diffusely in the cytosol without any obvious centrosomal localization. We speculate that the fragment from residues 573 to 1681 is sufficient for pericentrin association with centrosomes and the main functional domain of the protein may be narrowed to the smaller fragment from residues 1233 to 1681 because the fragment from residues 573 to 1233 did not form any centrosomal foci.

Table 3.2 Results of the co-localisation of pericentrin mutants with γ-tubulin.

Fragment	% of cells colocalised with γ-Tubulin	Centrosome localisation
Pcnt1-3492	100	Yes
Pcnt1-573	0	No
Pcnt1-1681	69	Yes
Pcnt574-1681	57	Yes
Pcnt574-1233	10	No

3.6 Discussion

3.6.1 Cloning of chicken *Pcnt*

As the aim of the project was the targeted disruption of chicken *Pcnt* gene, we required detailed information on the locus. So we first analysed the genomic and mRNA sequences of pericentrin in detail. Pericentrin was originally cloned from mouse, which sequence is now named pericentrin A (Doxsey et al., 1994; Flory and Davis, 2003). A homologous protein, pericentrin B was later identified in humans with a unique C-terminal calmodulin-binding domain (Flory et al., 2000; Li et al., 2001). Northern blot analysis revealed that pericentrin B exists in most tissues in both organisms while pericentrin A was found only in a subset of tissues. Pericentrin A and B are encoded by alternatively spliced transcripts (Miyoshi et al., 2006). In the same paper, the authors found an additional isoform, pericentrin S, in mouse. Pericentrin S contains the C-terminal two-thirds region of pericentrin B, which means that it is an N-terminally truncated isoform. In addition, a smaller pericentrin isoform corresponding to the C-terminal half of the larger isoform was also found in *Drosophila* (Martinez-Campos et al., 2004).

Chicken *Pcnt* is on chromosome 7, which is predicted by both the NCBI and Ensembl databases. However, the mRNA sequence given by the two databases is not consistent. The putative chicken Pcnt protein in the NCBI database is a 400 kDa coiled-coil protein with a PACT domain in its C-terminus, which is similar to pericentrin B. Moreover, the mutations which have recently been linked to MOPD II and Seckel syndrome were identified in the Pericentrin B mRNA sequence (Griffith et al., 2008; Piane et al., 2009; Rauch et al., 2008; Willems et al., 2009). Therefore, we decided to follow the chicken *Pcnt* mRNA sequence in the NCBI database for cloning of chicken *Pcnt* cDNA.

To confirm that the predicted *Pcnt* is really expressed, we next carried out RT-PCR using total RNA from DT40 cells as a template. Since the predicted mRNA of *Pcnt* is about 11 kb, it is difficult to amplify such a big fragment. As an alternative, we amplified 6 smaller fragments and assembled the full length cDNA using restriction endonuclease sites. We found 6 splice isoforms in the 4 fragments. However, all the

isoforms are in the middle of the sequence and very small (<300 bp). When we compared our cDNA sequence with the predicted sequence in the NCBI database, most of the sequence was identical. When we aligned the cDNA with the genomic sequence, all the exons were found in the genome in order. The homologous neighbouring genes indicate that human and mouse pericentrins were encoded by syntenic loci. We then analysed the sequence and secondary structure of chicken pericentrin with its orthologues identified in other species. Despite the fact that the homology of overall pericentrin sequence is low between the chicken and other species, these pericentrins all have a conserved PACT domain in the C-terminus, suggesting we have cloned the orthologous pericentrin in chicken.

Pericentrin is a critical centrosomal component and it interacts with other components such as the γ-TuRC complex (Dictenberg et al., 1998). To confirm that our *Pcnt* is functional, we tagged the *Pcnt* cDNA with a GFP-coding sequence and investigated the subcellular localisation of pericentrin. We transiently expressed a GFP-Pcnt fusion protein in *Pcnt*-deficient cells. Examination of the transfected cells revealed a very small green dot at the centrosome indicated by γ-tubulin, suggesting the chicken pericentrin we cloned is a centrosomal protein. Although we could not amplify the 11 kb cDNA in a single PCR reaction, it is likely that the *Pcnt* sequence we cloned is expressed in chicken. The existence of an N-terminally truncated isoform (like Pericentrin S) or C-terminally truncated isoform (like Pericentrin A) in chicken was not determined in our study.

3.6.2 Structure-function analysis of chicken pericentrin

Previous studies involving ectopic expression of GFP-PACT in human and *Drosophila* tissue culture cells have demonstrated that the C-terminal calmodulin-binding PACT domain of pericentrin directs it to the centrosome (Gillingham and Munro, 2000; Martinez-Campos et al., 2004). A potential problem is that ectopic expression may not accurately reflect the localisation of the endogenous protein because the overexpression of the PACT domain can displace

endogenous pericentrin and AKAP450 from the centrosome (Gillingham and Munro, 2000; Keryer et al., 2003). Moreover, it is interesting that the N-terminal isoform lacking the PACT domain, pericentrin A, shares some biological functions with pericentrin B or S including its centrosomal localisation (Doxsey et al., 1994). A very straightforward explanation is that some other part(s) of the protein can mediate the centrosomal localisation of the protein. To test this possibility, we carried out a structure-function analysis to study the region responsible for centrosomal localisation.

In this study, we have shown that the N-terminal half of the chicken pericentrin, Pcnt1-1681, localised to centrosomes, suggesting that the PACT domain may be not the only domain responsible for centrosomal localisation of pericentrin. Our data showed that even the shorter fragment, Pcnt573-1681 still localised at centrosomes while Pcnt573-1233 did not. This raises the possibility that fragment 1233-1681 may be sufficient for its location at centrosomes. It has been noticed that the N-terminal region of pericentrin B indirectly associates with γ-tubulin through binding with other components of γ-TuRC, GCP-2 and/or -3 (Takahashi et al., 2002; Zimmerman et al., 2004). Here we used γ-tubulin as a centrosome marker. We cannot draw any conclusion regarding as interaction between pericentrin domain and γ-tubulin itself because the centrosome is intact in *Pcnt*-deficient cells (see Chapter 4). Our fragment Pcnt574-1681 still colocalised with γ-tubulin but its direct association may be lost.

Diverse frameshift and premature termination mutations have been reported in human pericentrin B as the cause of MOPD II and Seckel syndrome (Griffith et al., 2008; Piane et al., 2009; Rauch et al., 2008; Willems et al., 2009). All the patients were either homozygous or compound heterozygous for biallelic null *PCNT* mutations, which meant pericentrin was a truncated and non-functional protein in these patients. Several mutations have been well studied, including a nonsense mutation in exon 4 (E220X) and single base pair deletion in exon 12 (S629fs). Pericentrin protein was absent in lymphoblastoid cell lines from patients with these

mutations, as shown by western blot (Griffith et al., 2008). Furthermore, centrosomal pericentrin staining was lost in these cell lines. Our fragment Pcnt1-573 truncated in exon 12, Pcnt1-1233 in exon 19 and Pcnt1-1681 in exon 26. In agreement with previous results in human lymphoblastoid cell lines, fragment Pcnt1-573 did not localise at centrosomes either. Some mutations were found in the exons after exon 12 in the patients, even in exon 39 (Rauch et al., 2008). However, no information about their centrosomal localisation is available. According to our results, it is also logical to expect that the patients with the mutations in later exons might have less severe symptoms because the longer truncated proteins might be functional at the centrosomes.

Chapter 4. Generation and characterisation of *Pcnt* knockout cells

4.1 Introduction

Pericentrin works as a multifunctional scaffold protein that anchors proteins to the centrosomes for spindle organisation and microtubule nucleation (Doxsey *et al.*, 1994; Takahashi *et al.*, 2002; Kawaguchi and Zheng, 2003; Keryer *et al.*, 2003). The γ-TuRC is the best studied component that is anchored to the centrosomes by pericentrin to participate in microtubule nucleation. Silencing of pericentrin reduced centrosomal γ-tubulin, inhibited astral microtubule nucleation, caused formation of monopolar spindles and led to chromosome mis-segregation (Dictenberg et al., 1998; Zheng et al., 1995). Pericentrin is also involved in cell cycle progression. Several studies have shown cell cycle defects in pericentrin-deficient cells. An increased G1 population, along with decreased S and G2 cell number were observed in pericentrin-depleted cells and in cells expressing a dominant-negative pericentrin domain (Matsuo et al., 2010; Mikule et al., 2007; Srsen et al., 2006). The impaired pericentrin-γ-TuRC interaction ultimately induces G2/antephase delay and apoptosis (Zimmerman et al., 2004). However, some contradictory data have also been reported. It was shown that pericentrin deficiency had no impact on microtubule nucleation or cell cycle progression in these studies (Li et al., 2001; Martinez-Campos et al., 2004). Here we investigated the function of pericentrin using reverse genetics in a genetically tractable experimental system, DT40 cells.

4.2 Targeting of the chicken *Pcnt* locus

As described in Chapter 3, we identified and cloned the chicken *Pcnt* cDNA and used it to define its genomic locus. The chicken *Pcnt* locus spans almost 100 kb on chicken chromosome 7. The gene contains about 49 exons that encode a protein with few defined function domains. Thus the conventional strategy of gene targeting in DT40 cells, which is to disrupt the whole gene or several important exons, is not

feasible (Arakawa and Buerstedde, 2006). In addition, a C-terminally truncated isoform in human and an N-terminally truncated isoform in mouse have been characterised respectively. Our structure-function analysis of chicken pericentrin in DT40 cells indicated that other isoform(s) might exist in chicken as well (see Chapter 3). It was likely that these different isoforms were encoded by alternatively spliced products of the one gene, as occurs in the case of human *PCNT* (Flory and Davis, 2003). Therefore, we had to abolish the expression of all *Pcnt* isoforms at the same time, assuming they exist.

A recently-published promoter hijack strategy offered us an ideal way to conditionally shut down multiply spliced essential genes (Samejima et al., 2008). The gene targeting strategy is shown in Figure 4.1A. The putative endogenous promoter (5.5 kb of the 5'-UTR of the *Pcnt* gene) was replaced by the minimal tTA-responsive promoter (tetO). Both alleles were targeted by the same promoter-hijack targeting vector. The recyclable puromycin cassette was excised by transient transfection of a plasmid encoding Cre recombinase after each round of targeting (Arakawa, 2006). As we speculated that *Pcnt* was an essential gene, the heterozygous clones were stably transfected with a rescue plasmid expressing tTA2 driven by a compatible promoter (the promoter of *Kif4a*) (Baron and Bujard, 2000; Gossen and Bujard, 1992). The coding region of the gene is intact so that any possible transcripts, depending on different splicing, can be restored indirectly through tTA. Subsequently, a second round of targeting was performed to replace the promoter of the other allele with tetO. Addition of doxycycline would block tTA binding to tetO, which in turn would shut off *Pcnt* expression. We also carried out the second round of targeting without the introduction of the rescue plasmid in case *Pcnt* was not essential for DT40 cells. Each transfection step of the targeting is shown in Figure 4.1B. The cells without endogenous promoter of *Pcnt* were defined as $Pcnt^{\Delta/\Delta}$ cells. $Pcnt^{\Delta/\Delta}$ cells containing a tTA expression vector were defined as "rescue" or "over-expressing" cells, depending on the mRNA levels of *Pcnt* (130%

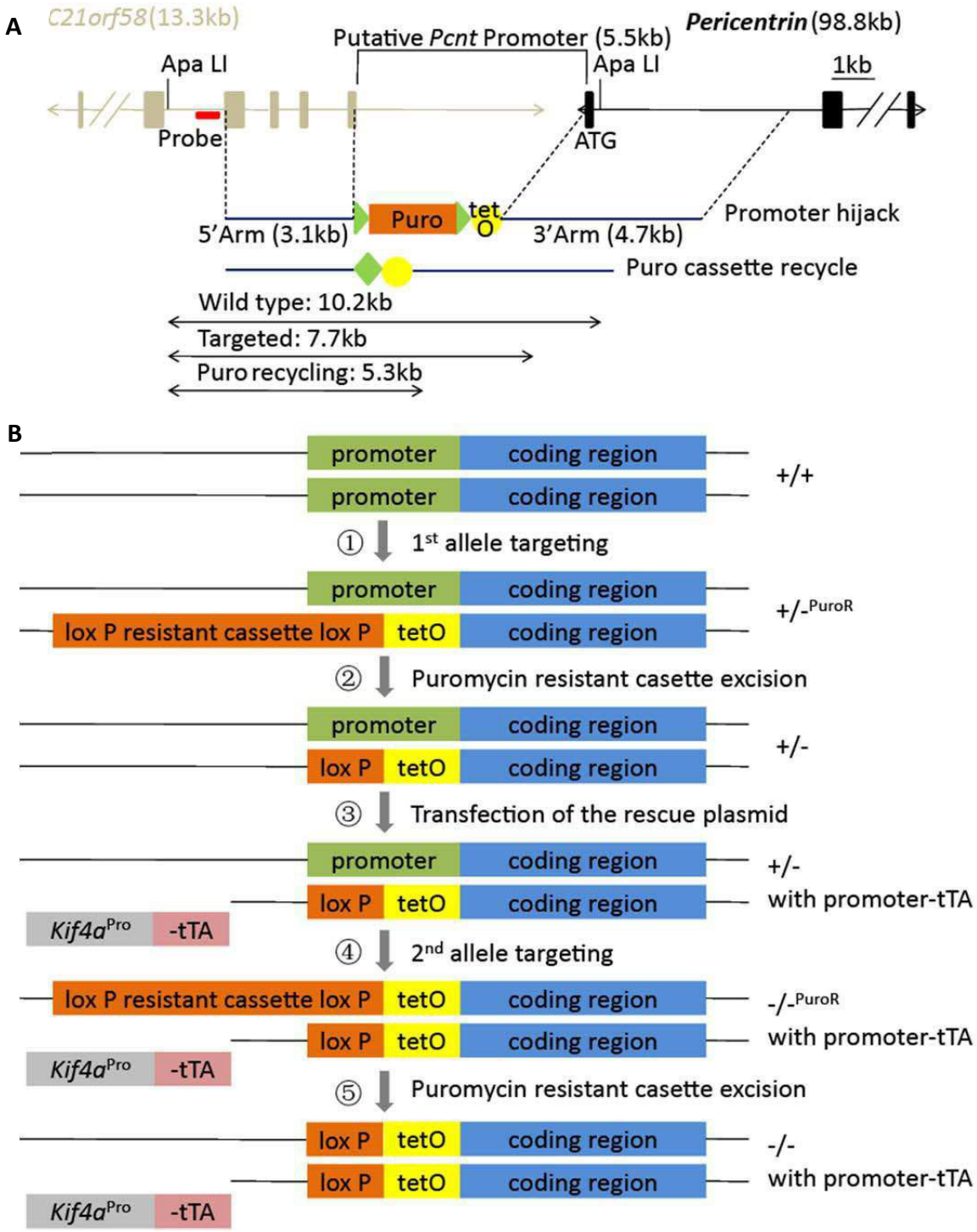

Figure 4.1 Promoter-hijack strategy for generating *Pcnt* conditional knockout cell lines.

A. Physical map of the *Pcnt* locus with promoter-hijack knockout strategy and schematic diagram for Southern blotting. The putative *Pcnt* promoter was replaced by tetO. The coding region from ATG was intact.

B. The promoter-hijack knockout strategy. +, wild-type allele; -, promoter-hijack vector-targeted allele. The clones generated following all the steps were named as rescue or over-expressing cells in this study. Step ③ was omitted in generating *Pcnt* knockout cell lines, which were named as $Pcnt^{\Delta/\Delta}$ cells in the study.

of the WT level in rescue cells and 900 times of WT level in over-expressing cells.

Both the 5' and 3' homology arms of the disruption construct were amplified from the genomic DNA of DT40 cells and sequenced to confirm their sequence. The first exon, which is inside the 3' homology arm, did not contain any mutations. The 5' homology arm (3.1 kb) was cloned into a modified pTRE-Tight Vector (a kind gift from Prof. W. C. Earnshaw), which contains a Tet-responsive promoter and a recyclable puromycin cassette, via a SpeI restriction site. The 3' homology arm (4.7 kb) was inserted using an MluI restriction site. A non-radioactive Southern blot was employed to screen for positive clones after targeting transfection. The specificity of the probe was identified by several genomic DNA digestions in WT cells. All of the bands were consistent with predicted sizes (Figure 4.2).

A

Specificity of 5' probe		
Genotype	Enzyme	Size (kb)
WT	Afl II	5.8
	Apa LI	10.2
	Sac I	7.3
	Spe I	7.2

B

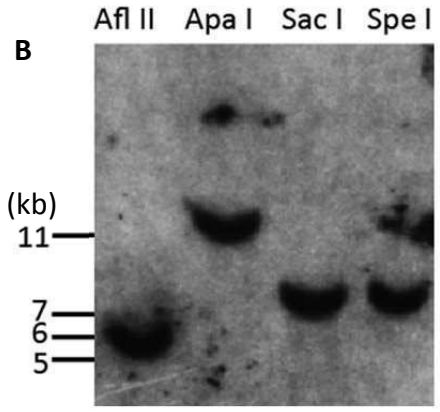

Figure 4.2 Specificity testing of the probe used for knockout clones screening.
Genomic DNA extracted from the WT cells was digested with indicated restriction nucleases and probed with a 5' probe.
A. Predicted size of Southern blot fragments.
B. A representative Southern blot result, using the indicated restriction nucleases.

A total of 162 clones were screened for the first allele targeting and 11 clones were positive. For the second allele targeting, a total of 514 (with the rescue plasmid) and 89 clones (without the rescue plasmid) were screened. We obtained one positive clone in each case. A representative Southern blot result for each genotype and the gene targeting frequencies are shown in Figure 4.3.

A

Screening of targeted clones		
Genotype	Size (kb)	Frequencies
WT	10.2	-
WT/Targeted	10.2+7.7	6.8%
WT/Floxed	10.2+5.3	-
Floxed/Targeted	5.3+7.7	0.3%
Floxed/Floxed	5.3	-

B

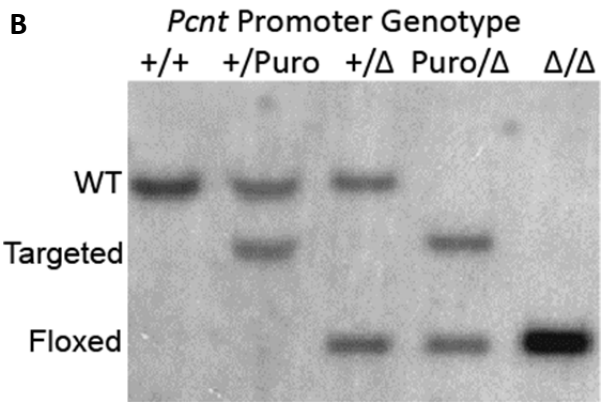

Figure 4.3 Screening of positive clones after targeting transfection.
Genomic DNA extracted from cells with the indicated genotype was digested with Apa LI and probed with a 5' probe.
A. Predicted size of Southern blot fragments and targeting frequencies at the *Pcnt* locus.
B. A representative Southern blot result of indicated genotypes. +: WT allele; Puro: targeted allele containing puromycin cassette; Δ: cassette recycled targeted allele.

4.3 Knock-in of a FLAG tag to the *Pcnt* locus

As no pericentrin antibody worked in DT40 cells, we decided to tag the endogenous *Pcnt* by knocking FLAG-encoding sequences into both alleles. Thus we would be able to detect the expression of pericentrin using a FLAG antibody. A 230 bp fragment, which consists of part of the last intron and entire last exon but without the stop codon, was amplified and ligated to a FLAG fragment using an artificial NotI restriction site. The combined fragment was then inserted into a pBlueScript vector via BamHI and XhoI restriction sites. The 5' homology arm (1.9 kb) was inserted using BamHI and SpeI restriction sites. The 3' homology arm (3.6 kb) was inserted using XhoI and KpnI restriction sites. A recyclable blasticidin resistant cassette was cloned into the targeting construct behind the 5' arm using BamHI restriction sites. Since the integrity of the 3'UTR may affect the transcription of mRNA and the sequence of the intron may affect the splicing, both 5' and 3' homology arms were sequenced completely to ensure there were no mutations in the arms. The recyclable blasticidin cassette was excised by transient transfection of a plasmid encoding Cre recombinase after each round of targeting. The remaining fragment after recycling is inside the intron and should be removed by splicing. The knock-in strategy is shown in Figure 4.4.

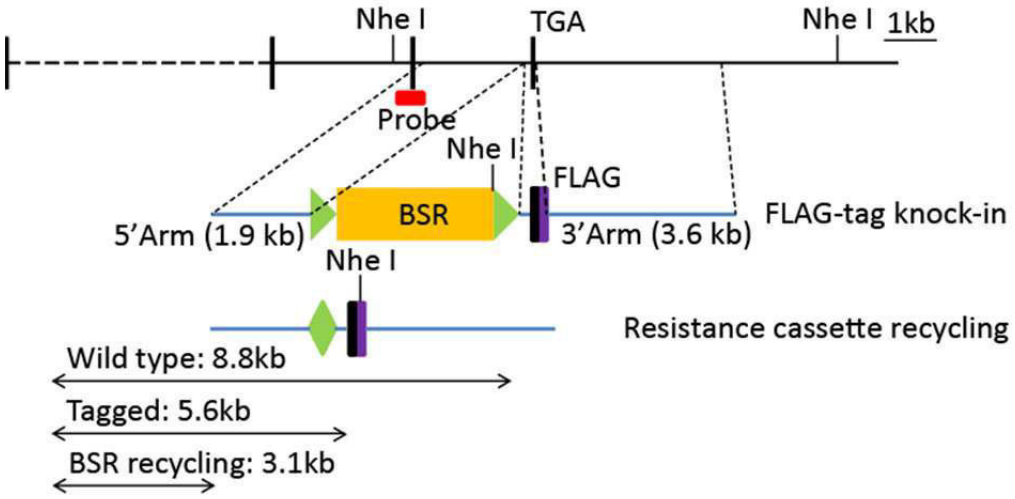

Figure 4.4 FLAG-tag knock-in strategy of *Pcnt* locus.
The stop codon was replaced by a FLAG-tag fragment. The 3' arm was sequenced to make sure the 3'UTR of *Pcnt* was intact. The blasticidin cassette, which localised inside of the last intron, was excised to minimise its potential effect on mRNA splicing.

A non-radioactive Southern blot was employed to screen the positive clones after targeting transfection. The specificity of the probe was confirmed by several genomic DNA digestions in WT cells (Figure 4.5). All the bands were consistent with predicted sizes. However, we saw an extra band in the sample digested by NheI. Several lines of evidence suggested that the extra band was caused by a SNP in one

A

Specificity of 5' probe		
Genotype	Enzyme	Size (kb)
WT	Afl II	5.9
	Eco RI	7.4
	Hind III	2.6
	Nde I	2.7
	Nhe I	8.8

B

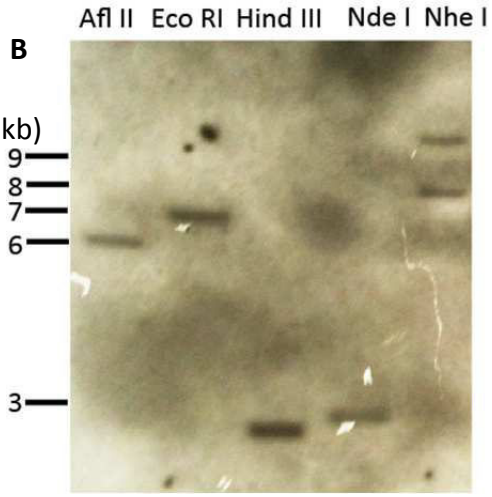

Figure 4.5 Specificity testing of the probe used for knock-in clones screening.
Genomic DNA extracted from the WT cells was digested with indicated restriction nucleases and probed with a 5' probe.
A. Predicted size of Southern blot fragments.
B. A representative Southern blot result, using the indicated restriction nucleases. An extra band was seen after digestion with Nhe I.

of the *Pcnt* alleles. First, all the other four samples showed a single band with the expected size, which meant the probe was specifically hybridized with the region it was expected to bind. Second, this extra band was not the same size of the band generated by digestion of targeting samples. Third, the intensity of the extra band was equal to that of the other "right size" band, which suggested that the two bands were from the two alleles respectively.

We inserted the FLAG-tag fragment into the *Pcnt* locus of all WT, $Pcnt^{\Delta/\Delta}$, rescue and over-expressing (OverExp) cell lines that we used for *Pcnt* function analysis. A total of 144 clones were screened for the first allele targeting and 122 clones were positive. A total of 144 clones (36 clones per cell line) were screened for the second allele targeting and 17 clones were positive. A representative Southern blot result for each genotype and the gene targeting frequencies are shown in Figure 4.6.

A

Screening of targeted clones		
Genotype	Size (kb)	Frequencies
WT	8.8	-
WT/Targeted	8.8+5.5	85%
WT/Floxed	8.8+3.1	-
Floxed/Targeted	5.5+3.1	12%
Floxed/Floxed	3.1	-

B

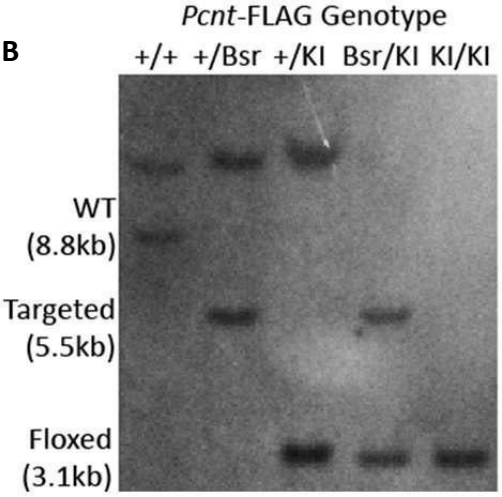

Figure 4.6 Screening of positive clones after knock-in transfection.
Genomic DNA extracted from cells with the indicated genotype was digested with Nhe I and probed with a 5' probe.
A. Predicted size of Southern blot fragments and targeting frequencies at the *Pcnt* locus.
B. A representative Southern blot result of indicated genotypes. +: WT allele; Bsr: targeted allele containing blasticidin cassette; KI: cassette recycled targeted allele.

4.4 Characterisation of *Pcnt* knockout DT40 cells

To confirm that *Pcnt* was disrupted in the positive clones screened by the Southern blot, the RNA levels of *Pcnt* in each cell line were checked by RT-PCR. The

successful amplification of the 5'end of *Pcnt* mRNA after 40 cycles but not after 30 cycles in $Pcnt^{\Delta/\Delta}$ cells suggests that *Pcnt* is still expressed but at a reduced level in the knockout cells (Figure 4.7A). We hypothesized that the disrupted promoter could not drive the transcription of the full length mRNA. Therefore, another pair of primers was used to amplify the 3'UTR of *Pcnt* mRNA. The results were the same as the previous amplification, indicating that the full-length mRNA of *Pcnt* may be expressed in the $Pcnt^{\Delta/\Delta}$ cells. It was confirmed by real-time PCR that *Pcnt* mRNA drops to about 2% of control levels in the $Pcnt^{\Delta/\Delta}$ cells (Figure 4.7B).

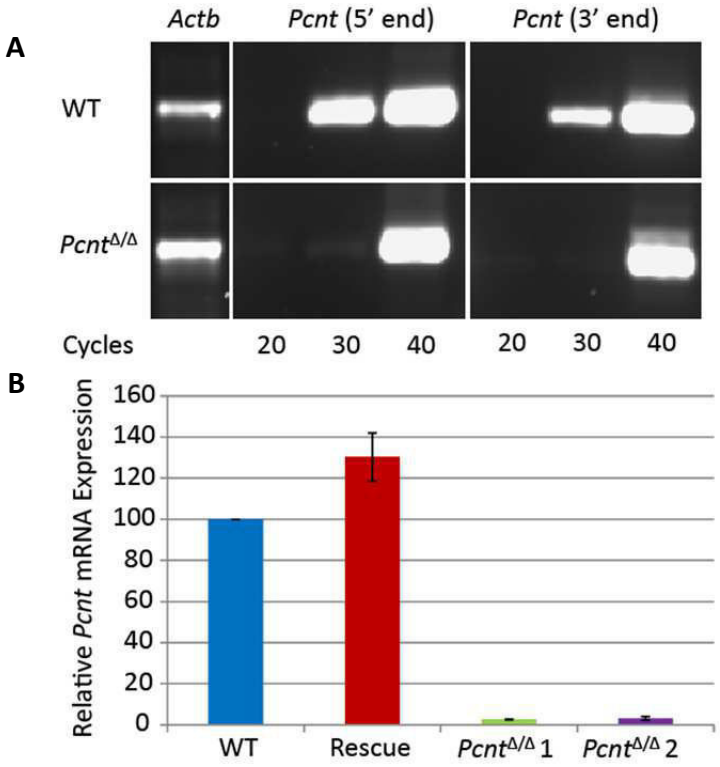

Figure 4.7 RT-PCR analyses of *Pcnt* expression in $Pcnt^{\Delta/\Delta}$ cells.
A. RT-PCR with total mRNA isolated from the WT and $Pcnt^{\Delta/\Delta}$ cells. Two sets of primers located at 5' end and 3' end of the mRNA were used for PCR.
B. Quantitative RT-PCR of total mRNA isolated from the WT, rescue and two $Pcnt^{\Delta/\Delta}$ cell lines. The primers were located at the 5' end of the cDNA sequence.

As the *Pcnt* transcript was not completely eliminated, we needed to determine the levels of the pericentrin protein in $Pcnt^{\Delta/\Delta}$ cells, because this directly controls *Pcnt* function. As shown by immunofluorescence microscopy in Figure 4.8, FLAG-tagged pericentrin was found at centrosomes in WT, rescue and OverExp cells but not in

Pcnt$^{\Delta/\Delta}$ cells. In the OverExp cells, overexpressed pericentrin is coupled with increased γ-tubulin, which confirms pericentrin's function (Loncarek et al., 2008). The predicted size of full-length pericentrin is ~400 kDa. Western blot analysis was then performed to examine the expression level of the pericentrin protein in whole cell lysates. However, we could only detect pericentrin in the total protein extracts of OverExp cells by western blot (data not shown). We next tried the immuno-precipitation of Pcnt-FLAG with anti-FLAG beads but again failed to detect the predicted band in WT cells. These results suggest that the abundance of pericentrin is very low, which is consistent with a previous report in human cells (Doxsey et al., 1994). Together, our Southern blot, RT-PCR, real-time PCR, and in particular, our immunofluorescence microscopy analysis demonstrate that we have successfully generated a *Pcnt*-deficient DT40 cell line.

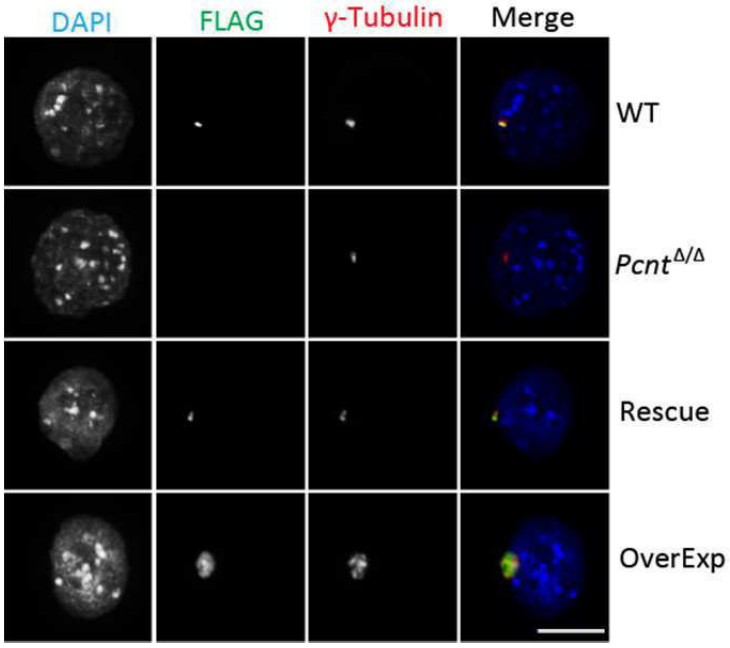

Figure 4.8 Immunofluorescence microscopy analysis of expression of pericentrin in *Pcnt*$^{\Delta/\Delta}$ cells.
WT, *Pcnt*$^{\Delta/\Delta}$, rescue and over-expressing cells were stained with anti-FLAG antibody to indicate pericentrin (green) and with γ-tubulin (red) as a reference marker. Cells were counter-stained with DAPI to visualise the DNA (blue) prior to imaging. Scale bar, 10 μm.

4.5 *Pcnt*$^{\Delta/\Delta}$ cells are viable

To determine the consequences of loss of *Pcnt*, we first monitored the proliferative capacity of $Pcnt^{\Delta/\Delta}$ cells. As *PCNT* is involved in the primordial dwarfism (Rauch et al., 2008), we speculated that *Pcnt* played a role in cell growth. The *Pcnt*-deficient chicken cells were viable. A 96-hour growth curve was determined by seeding cells at 5 x 10^4/ml and counting them every 24 hours using a haemocytometer. Under standard growth conditions, the proliferation rate of $Pcnt^{\Delta/\Delta}$ cell lines was slightly slower than that of WT cells (Figure 4.9). The doubling time of WT cells was 7.52 ± 0.34 h whereas that of the two $Pcnt^{\Delta/\Delta}$ cell lines analysed was 8.91 ± 0.58 h and 8.54 ± 0.51 h. The growth retardation was restored after pericentrin was re-expressed. The doubling time of rescued cells was 7.86 ± 0.40 h, which was close to that of WT cells. These data suggested that *Pcnt* has a function in controlling cell proliferation.

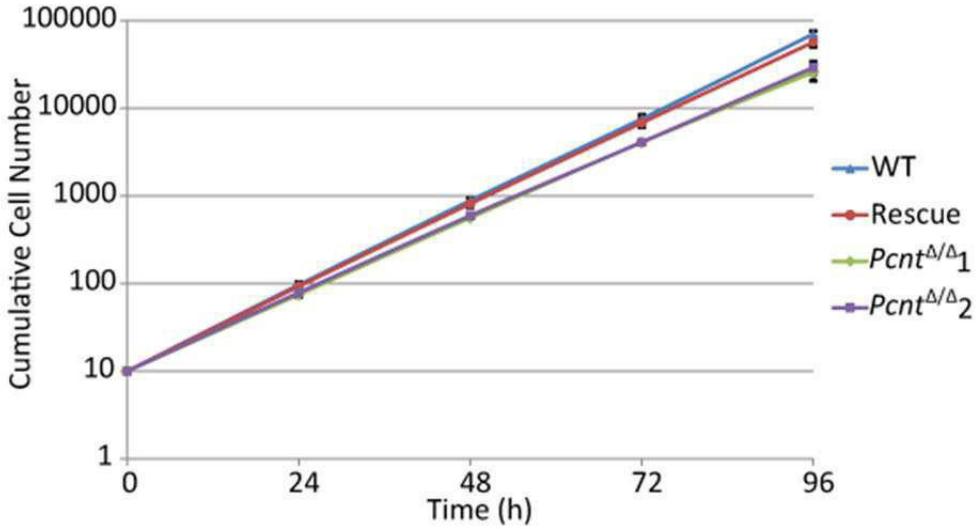

Figure 4.9 Proliferation analysis of $Pcnt^{\Delta/\Delta}$ cells.
Cells were seeded at 5×10^4 /ml and cell numbers were counted every 24 hours for a 96-hour duration. Data show the mean ± s.d. of three separate experiments.

4.5.1 Cell cycle analysis

To explore whether loss of *Pcnt* disturbed cell cycle progression *per se*, flow cytometry was performed to determine the cell cycle distribution of each cell line. The resulting patterns of one-dimensional PI staining looked identical with regard to distribution of DNA content between WT cells and $Pcnt^{\Delta/\Delta}$ cells (Figure 4.10A). To quantify the cell distribution at the each stage of the cell cycle, two more accurate

analyses, using two dimensional BrdU and phospho-histone H3 (pH3) stainings were carried out. *Pcnt*$^{\Delta/\Delta}$ cells exhibited similar percentages of cells in G1, S and G2/M phases of the cell cycle as compared to the WT cells (Figure 4.10B). However, the mitotic index, which was evaluated by DNA content and phosphorylation at the Ser10 residue of histone H3, a marker of mitosis, was slightly elevated in *Pcnt*$^{\Delta/\Delta}$

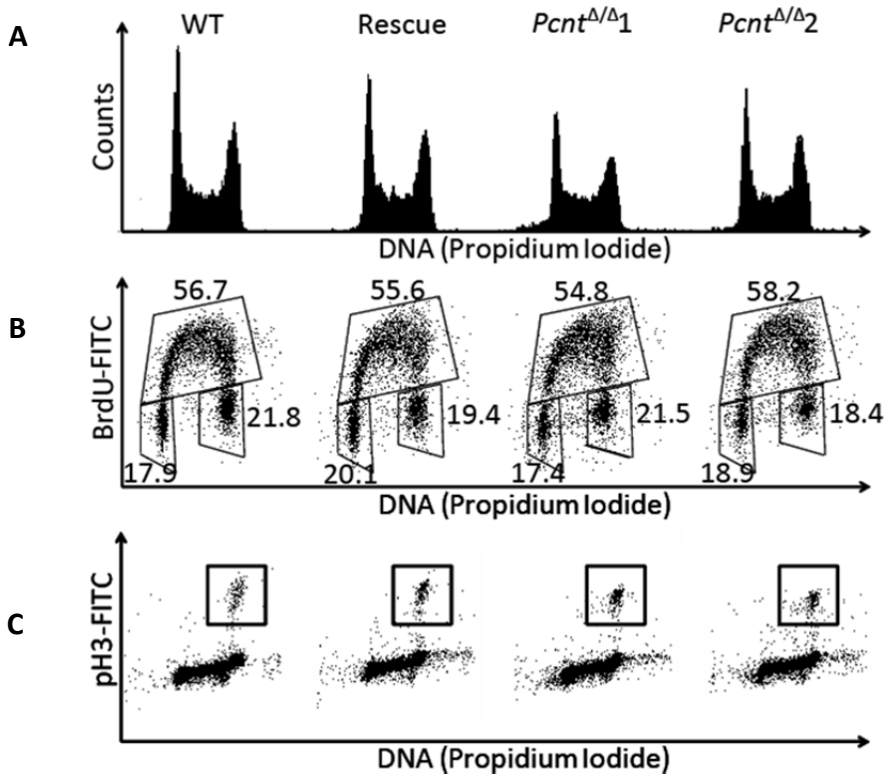

Cell line	WT	Rescue	*Pcnt*$^{\Delta/\Delta}$ 1	*Pcnt*$^{\Delta/\Delta}$ 2
Mitotic Index	2.53 ± 0.15%	3.27 ± 0.15%	3.93 ± 0.40%	4.33 ± 0.50%

Figure 4.10 Cell cycle analyses of asynchronous *Pcnt*$^{\Delta/\Delta}$ cells.

A. Cell cycle profile of cells of the indicated genotypes stained with propidium iodide.

B. Quantitative cell cycle analysis of cells of the indicated genotypes was measured by bromodeoxyuridine (BrdU) incorporation and DNA content. Cells were pulse-labeled with BrdU and stained with FITC-anti-BrdU to detect BrdU incorporation (vertical axis) and propidium iodide to detect total DNA (horizontal axis). The G1 (bottom left), S (top), and G2/M (bottom right) gates are indicated by boxes, and the numbers refer to the percentage of cells detected in each of the gates.

C. Mitotic index was determined by flow cytometry of the late G2/M phases marker, phosphorylated histone H3 (pH3). Cells of the indicated genotypes were stained with FITC-anti-pH3 to detect mitotic cells (vertical axis) and propidium iodide to detect total DNA (horizontal axis). Statistical analysis of the mitotic index is shown in the table as mean ± s.d. of three separate experiments.

cells compared with WT cells. (Figure 4.10C). Our data suggest that the reduced proliferation rates of *Pcnt*$^{\Delta/\Delta}$ cells were due to an accumulation of late G2 or mitotic populations.

4.5.2 Live cell imaging

To confirm the presence of a delay at mitosis in the *Pcnt*$^{\Delta/\Delta}$ cells, the duration of mitosis was measured through live cell imaging. Each cell line was stably transfected with an expression vector for histone H2B-RFP. Thereafter, we could visualise the morphological changes of chromosomes during the cell cycle. Time-lapse imaging was carried out for 3 hours with a 3 minute interval (Figure 4.11). The time from chromosome condensation to decondensation was defined as mitotic duration. Although most *Pcnt*$^{\Delta/\Delta}$ cells progressed through mitosis, the two cell lines took 57.8 ± 22.3 min and 58.0 ± 21.6 min to complete mitosis, which is longer than the time observed in WT cells (40.9 ± 7.5 min and 44.6 ± 10.3 min in 2 WT cell lines) (Figure 4.11A, B and Figure 4.12A). In addition, we observed that some of the cells were arrested at prometaphase and metaphase during the entire imaging time (Figure 4.11C). We grouped the cells which stayed in prometaphase and metaphase for longer than 45 min, in which time most WT cells completed the mitosis. We found that more cells were arrested at mitosis if pericentrin was deficient (10% of WT cells *vs* 39% of *Pcnt*$^{\Delta/\Delta}$ cells) (Figure 4.12B). Furthermore, the mitotic timing was restored to WT levels after pericentrin was re-expressed (45.5 ± 14.2 min and 46.0 ± 11.0 min in 2 rescue cell lines). Taken together, we conclude that pericentrin plays a role in cell cycle progression, particularly in proper mitotic progression in DT40 cells.

4.6 Pericentrin deficiency has no detectable impact on centrosome composition

Pericentrin works as a multifunctional scaffold for anchoring centrosomal proteins to the centrosomes. These proteins are involved in centrosome composition and/or microtubule nucleation (Badano et al., 2005; Delaval and Doxsey, 2009). To

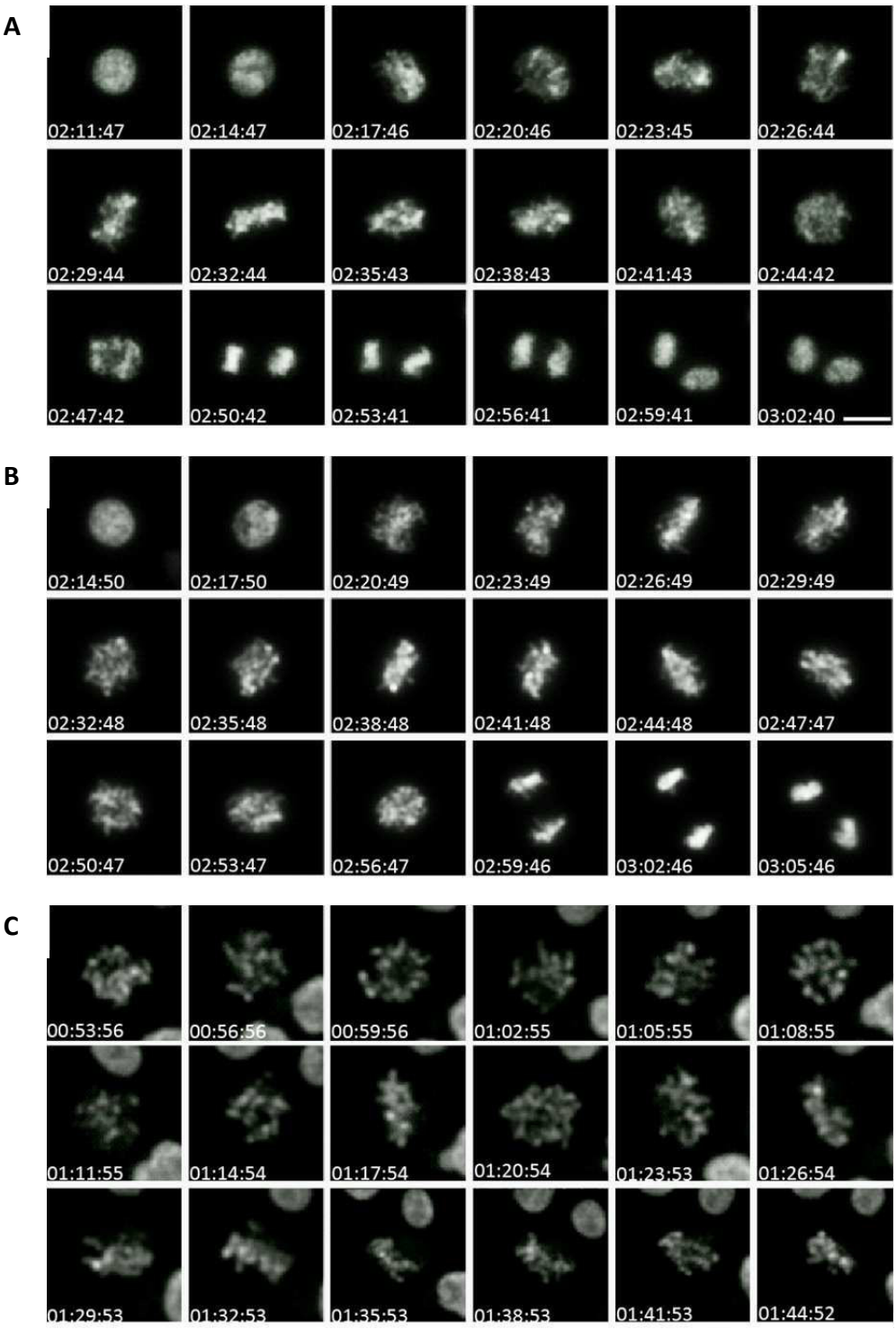

Figure 4.11 Selected frames from live-cell imaging of mitotic cells.

Cells of each genotype were stably transfected with an expression vector for histone H2B-RFP. 2 clones of each genotype after the transfection were analysed by time-lapse microscopy. Time is shown in HH:MM:SS format. Scale bar, 10 μm.

A. WT cells completed mitosis in about 45 min.

B. *Pcnt*$^{\Delta/\Delta}$ cells took a longer time to go through mitosis than WT cells.

C. A *Pcnt*$^{\Delta/\Delta}$ cell arrested in mitosis during the entire imaging time.

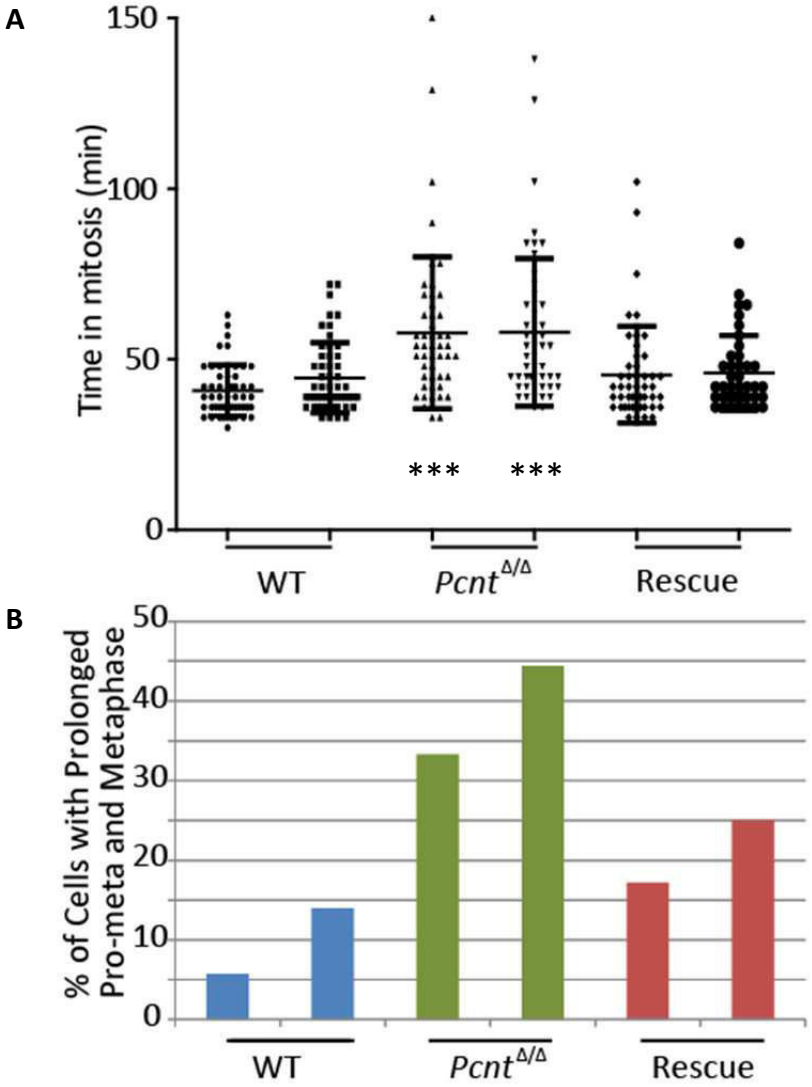

Figure 4.12 Live-cell imaging analysis of mitotic timing.

A. Mitotic duration of cells of the indicated genotypes (*n*>50).Data is shown as mean ± s.d. ***, p<0.001, compared to WT cells.

B. Percentage of cells which were arrested at prometaphase/metaphase for more than 45 min in each cell line (n>50).

investigate the impact of pericentrin deficiency on centrosome structure and organisation, a series of centrosome markers were used to identify various centrosome components in both WT and *Pcnt*$^{\Delta/\Delta}$ cells by immunofluorescence microscopy. Centrin3 has been reported to be required for microtubule organisation and centrosome reproduction (Dammermann and Merdes, 2002; Middendorp et al., 2000). Ninein is a marker of mother centrioles, as it is a component of the subdistal appendages of mature centrioles. It is involved in microtubule anchoring and

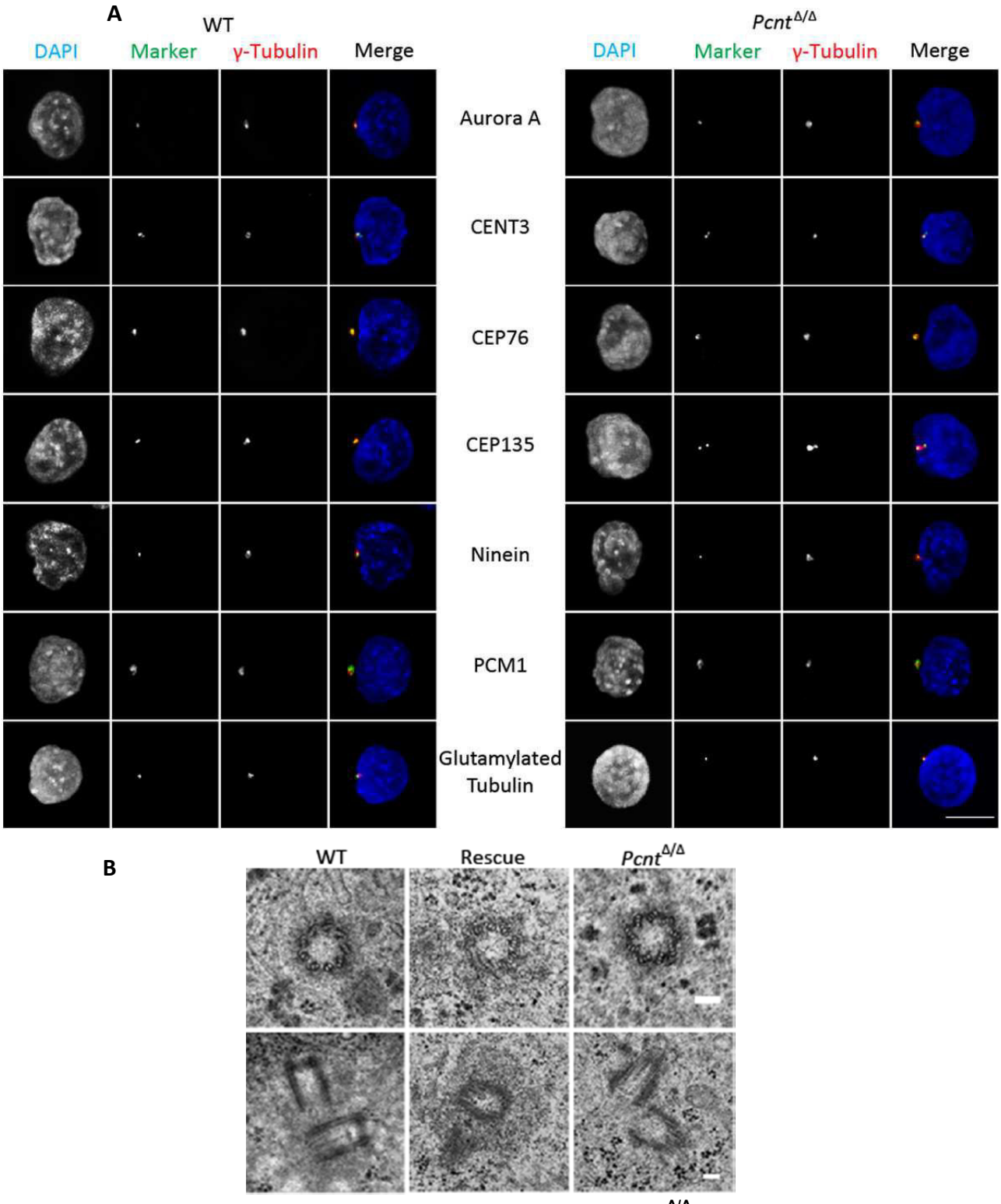

Figure 4.13 Structural integrity of the centrosomes in *Pcnt*$^{\Delta/\Delta}$ cells.

A. Immunofluorescence microscopy analysis of WT and *Pcnt*$^{\Delta/\Delta}$ DT40 cells stained with antibodies to the indicated centrosome components (green) with γ-tubulin (red) as a reference marker. Cells were counter-stained with DAPI to visualise the DNA (blue) prior to imaging. Scale bar, 10 μm.

B. Transmission electron microscopy of centrosomes in WT, rescue and *Pcnt*$^{\Delta/\Delta}$ DT40 cells. Scale bars, 100 nm.

nucleation (Mogensen et al., 2000; Ou et al., 2002). Cep76 restrains centriole reduplication (Tsang et al., 2009). Cep135 is involved in centriole biogenesis and microtubule organisation (Kim et al., 2008b; Ohta et al., 2002). The centrosome-associated kinase, Aurora A, plays a role in centrosome maturation and separation (Barr and Gergely, 2007). PCM-1 is a major component of pericentriolar satellites and is involved in microtubule organisation (Dammermann and Merdes, 2002). Immunofluorescence microscopy imaging revealed that these proteins still localised at the centrosome (Figure 4.13A), suggesting that there were no defects of centrosome composition in $Pcnt^{\Delta/\Delta}$ cells and *Pcnt*-deficient centrosomes could duplicate and organise microtubules like WT controls. The presence of glutamylated tubulin suggested that *Pcnt*-deficient centrosomes could also nucleate polyglutamylated, stabilised microtubules (Kann et al., 2003).

These light microscopy observations were confirmed by transmission electron microscopy at higher resolution. As shown in Figure 4.13B, centrioles in $Pcnt^{\Delta/\Delta}$ cells were composed of nine triplet microtubules with mean diameters of 216.8 ± 9.6 nm (n=11) in WT cells and 212.5 ± 8.7 nm (n=6) in $Pcnt^{\Delta/\Delta}$ cells. The two centrioles were orthogonally arranged and surrounded by electron-dense PCM in both WT and $Pcnt^{\Delta/\Delta}$ cells. However, we were not able to quantify the PCM to determine whether there was any difference in this assembly in the absence of pericentrin. These observations indicate that *Pcnt* deficiency has no impact on the characteristic ultrastructure of the centrosome.

4.7 Pericentrin disruption decreases centrosomal γ-tubulin

Although centrosomal proteins localised at the centrosome without pericentrin, we observed large aggregates of pericentriolar material proteins, PCM-1 and γ-tubulin, in OverExp cells (Figure 4.14A). This observation is consistent with previous reports and confirms that pericentrin recruits pericentriolar materials to the centrosome (Loncarek et al., 2008; Pihan et al., 1998). This also promoted us to ask whether

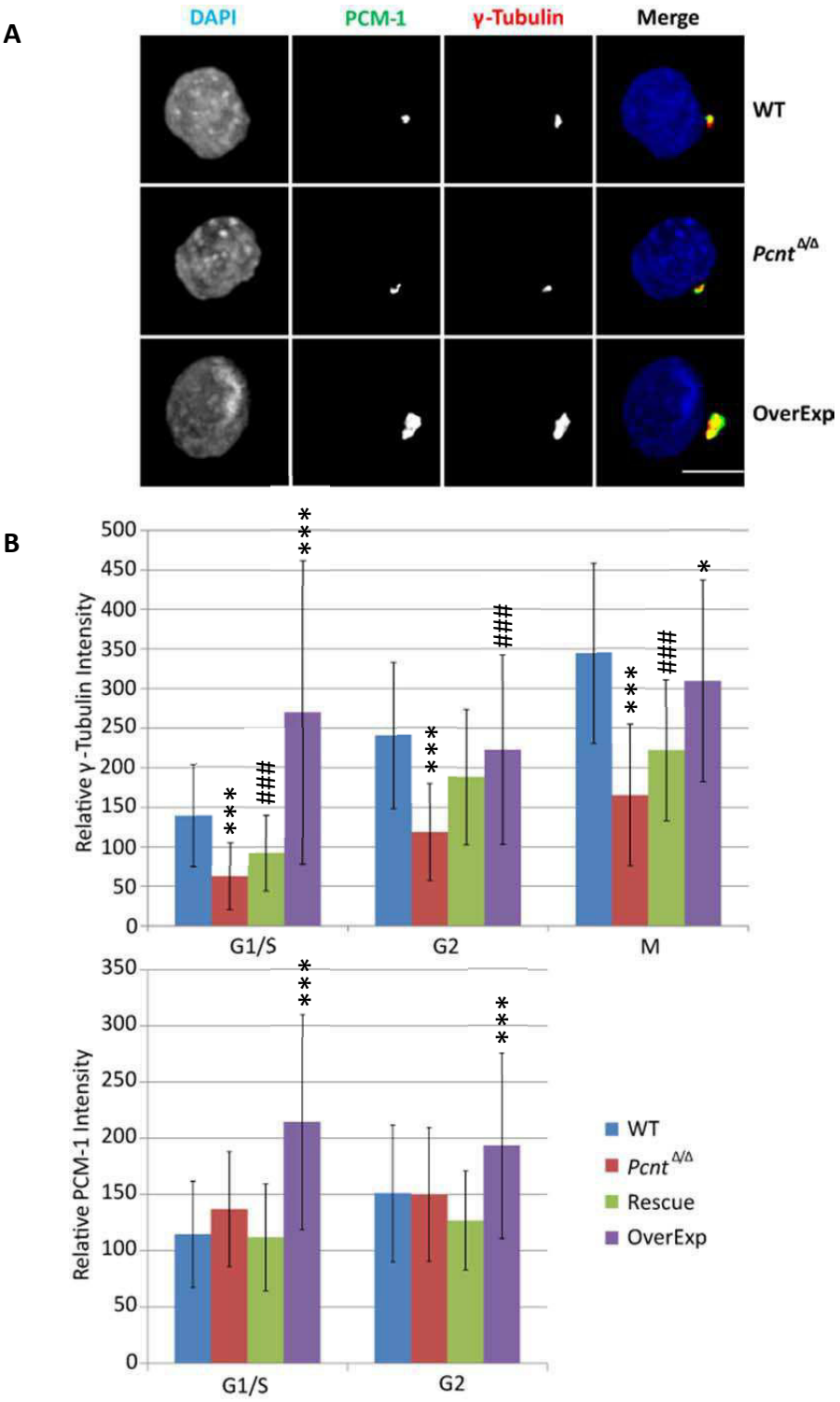

Figure 4.14 Reduced centrosomal γ-tubulin recruitment at the centrosomes in *Pcnt*$^{\Delta/\Delta}$ cells.

A. Immunofluorescence staining of PCM-1 (green) and γ-tubulin (red) in WT, *Pcnt*$^{\Delta/\Delta}$ and OverExp cells. Cells were counter-stained with DAPI to visualise the DNA (blue) prior to imaging. Scale bar, 10 μm.

B. Statistical analysis of centrosomal levels of γ-tubulin and PCM-1 in each cell cycle stage of the indicated genotypes (n>100). Data is shown as mean ± s.d. ***, p<0.001, compared to WT cells. ###, p<0.001, compared to *Pcnt*$^{\Delta/\Delta}$ cells.

levels of these proteins were reduced at centrosomes in *Pcnt*$^{\Delta/\Delta}$ cells. We quantified the centrosomal levels of each protein by measuring the fluorescence intensity of staining with specific antibodies in the centrosomal region. To precisely compare the signals, the immunofluorescence staining was done in a 96-well plate and imaged by the Operetta imaging system. The centrosome markers were identified automatically and the intensities were calculated by the coupled software. Since it was shown that centrosomal γ-tubulin rises progressively from G1 until mitosis and then drops precipitously to basal levels (Dictenberg et al., 1998), we compared the cell lines at different cell cycle stages. Consistently, we observed cell cycle-dependent recruitment of γ-tubulin in all the cell lines except OverExp cells (Figure 4.14B). However, the relative centrosomal intensity of γ-tubulin was significantly reduced in *Pcnt*$^{\Delta/\Delta}$ cells. Re-expression of pericentrin restored the loss of γ-tubulin but overexpression of pericentrin only caused a dramatic aggregation of γ-tubulin at the centrosome in G1 cells. To our surprise, centrosomal recruitment of PCM-1 was not impacted in *Pcnt*$^{\Delta/\Delta}$ cells. PCM-1 was not found on the centrosome in mitiotic cells. Thus, we conclude that *Pcnt* plays an important role in recruiting γ-tubulin to centrosomes.

4.8 Altered mitotic spindles in *Pcnt*$^{\Delta/\Delta}$ cells

The above data suggest that loss of pericentrin leads to the reduction of γ-tubulin anchored at the centrosome, which may in turn cause defects in mitotic spindle formation and microtubule nucleation. We then investigated spindle organisation by immunofluorescence microscopy. The morphology of the spindle was visualised with antibodies to α-tubulin (green), the centrosome was indicated by γ-tubulin (red) and DNA was visualised with DAPI (Figure 4.15A). The spindles of *Pcnt*$^{\Delta/\Delta}$ cells were bipolar, with γ-tubulin localised exclusively at the spindle poles and the chromosomes aligned at the metaphase plate as in WT cells. To ensure that the observation was accurate, we then examined 50 metaphase spindles of both WT and *Pcnt*$^{\Delta/\Delta}$ cells, as determined by BUBR1 staining at kinetochores (Figure 4.15A). We

found that there was no detectable abnormality in the arrangement of microtubules and chromosomes in *Pcnt*$^{\Delta/\Delta}$ cells.

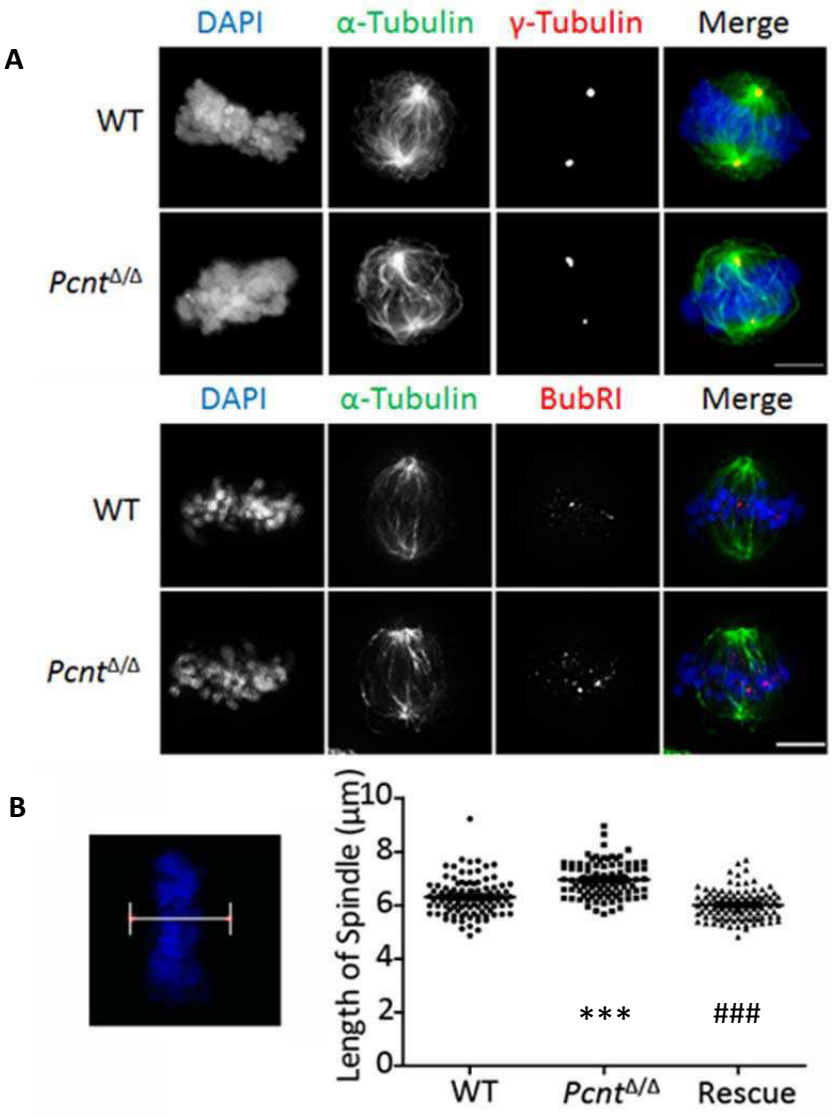

Figure 4.15 Altered mitotic spindle organisation in *Pcnt*$^{\Delta/\Delta}$ cells.
A. Immunofluorescence microscopy images of mitotic WT and *Pcnt*$^{\Delta/\Delta}$ cells stained with antibodies to α-tubulin (green) which showed the morphology of the spindle. The cells were co-stained with either anti-γ-tubulin or anti-BubR1 antibody (red). DNA was visualised with DAPI (blue). Scale bar, 10μm.
B. Pole-pole spindle length was defined as the distance between the two γ-tubulin spots of the metaphase cell. Graph showing the spindle length in the indicated cell lines. Data show the mean ± s.d. At least 90 metaphase cells were analysed per cell line. ***, p<0.001, compared to WT cells. ###, p<0.001, compared to *Pcnt*$^{\Delta/\Delta}$ cells.

However, when we checked the spindles in detail we found the spindles of *Pcnt*$^{\Delta/\Delta}$ cells were longer than those of WT cells (Figure 4.15B). We defined the distance

between the two γ-tubulin spots of metaphase cells as the length of the spindles. To ensure that the distance between the two γ-tubulin spots exactly represented the real spindle length, we only scored the metaphase cells with clearly defined metaphase plates and whose γ-tubulin spots could be seen on the same section in parallel with the surface of the slides. Metaphase spindle lengths were increased in $Pcnt^{\Delta/\Delta}$ cells to 6.95 ± 0.65 μm (*n*=103) from 6.31 ± 0.68 μm (*n*=93) in WT cells. Re-expression of pericentrin in $Pcnt^{\Delta/\Delta}$ cells can reverse the elongated spindle lengths to 6.02 ± 0.55 μm (*n*=104).

4.9 Pericentrin is dispensable for microtubule nucleation

It has been demonstrated that γ-tubulin plays an important role in centrosomal microtubule nucleation (Kollman et al., 2011). The reduced centrosomal γ-tubulin seen in our study (see Section 4.6) suggests there may be a defect in microtubule nucleation in $Pcnt^{\Delta/\Delta}$ cells. We therefore directly examined the dependence of centrosomal microtubule nucleation on *Pcnt* by an assay that monitors microtubule regrowth after microtubule destabilisation, which was accomplished by combined cold and nocodazole treatment. Immunofluorescence microscopy was employed to assess the formation of microtubule asters, which was indicated by α-tubulin. Microtubules of DT40 cells were completely depolymerised after the cold and nocodazole treatment. The microtubule asters extended from the centrosomes after the cells were immersed in PBS at 40 ºC for 30 s or 1 min (Figure 4.16A). Small microtubules were nucleated at 30 s after recovery. Numerous radial arrays of microtubule extended to the cell cortex at 1 min after recovery (Figure 4.16B). We adopted a fixed diameter for sub-grouping positive asters (extend outside of the ring) and negative asters (within the ring). As we had found the capacity of microtubule nucleation was weaker in mitotic cells, we set different criterion ring for interphase cells (2.5μm in diameter) and mitotic cells (2 μm in diameter) (Figure 4.16B). Unexpectedly, we found that both interphase and mitotic $Pcnt^{\Delta/\Delta}$ cells were as capable as WT cells of nucleating microtubule asters longer than the threshold

(Figure 4.16C). These results suggest that the loss of *Pcnt* does not affect the MTOC activity of the centrosomes in DT40 cells, at least within the resolution limits of this assay.

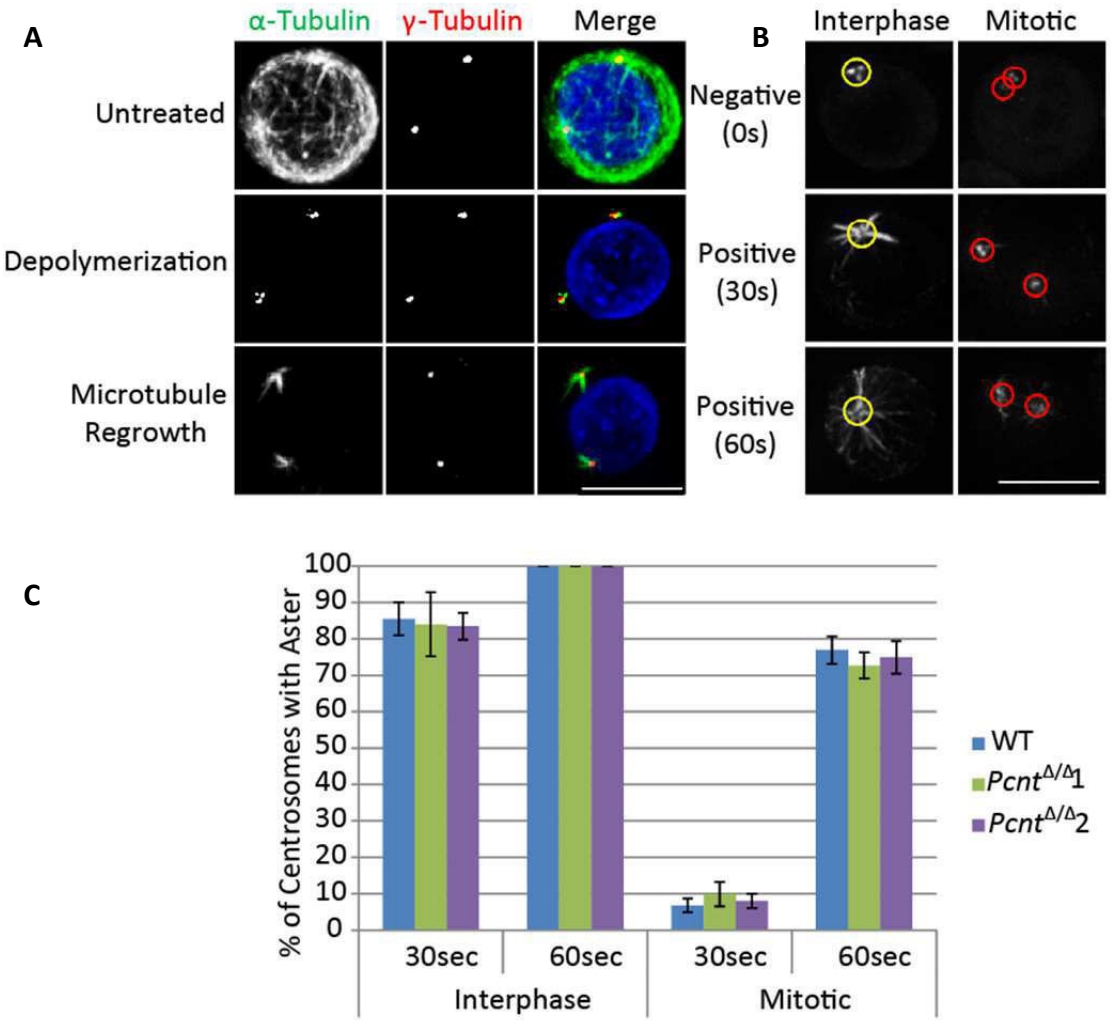

Figure 4.16 Normal microtubule nucleation ability in *Pcnt*$^{\Delta/\Delta}$ cells.

A. Immunofluorescence microscopy analysis of microtubule nucleation in DT40 cells before and after release from arrest in nocodazole and cold. Cells were stained with antibodies to α-tubulin (green) to show the formation of microtubulin asters and γ-tubulin (red) to indicate the position of the centrosomes. DNA was visualised with DAPI (blue). Scale bar, 10μm.

B. A positive aster was defined as an α-tubulin (in green channel) structure beyond 2.5 μm (yellow circles) or 2 μm (red circles) diameter in interphase or mitotic cells, respectively. The mitotic cells were demonstrated as phospho-histone H3 (in red channel) positive cells. Scale bar, 10μm.

C. Quantification of the percentage of cells with positive aster at 30 s and 1 min after microtubule recovery at 40 °C. Histogram shows mean ± s.d. of three separate experiments in which at least 50 centrosomes per experiment were counted.

4.10 Delayed satisfaction of the SAC in *Pcnt*$^{\Delta/\Delta}$ cells

Although pericentrin deficiency had no detectable impact on the microtubule nucleation, we speculated that this assay might not be sensitive enough to detect a difference in MTOC functions. Therefore, we examined the cellular responses to spindle poisons through analysis of the cell cycle. We first performed a nocodazole block and release experiment. The cells were treated with nocodazole for 12 h, then washed and entered into the next cell cycle. The cells were examined by FACS for PI staining at the indicated time points. As shown in Figure 4.17A, both WT and *Pcnt*$^{\Delta/\Delta}$ cells were arrested at mitosis after a 12-hour incubation with 0.1 μM nocodazole. After nocodazole was washed out using fresh medium, the cells started to re-enter into cell cycle (G1 phase). However, fewer *Pcnt*$^{\Delta/\Delta}$ cells proceeded to G1 phase, instead remaining arrested in mitosis. The re-expression of pericentrin partly alleviated this effect (Figure 4.17A).

Taxol is another microtubule-targeted drug. Unlike nocodazole, which depolymerises microtubules, taxol stabilises microtubules and induces activation of the SAC, which in turn leads to cell arrest at mitosis (Jordan et al., 1992; Yang et al., 2009). As shown in figure 4.17B, increasing number of cells were arrested at mitosis when they were incubated with increasing concentrations of taxol for 12 hours. The difference in the percentage of mitotically-arrested cells between *Pcnt*$^{\Delta/\Delta}$ cells and WT cells was most significant when the cells were treated with 20 nM taxol. As we hypothesised that satisfaction of the SAC was delayed in *Pcnt*$^{\Delta/\Delta}$ cells, *Pcnt*$^{\Delta/\Delta}$ cells should complete and exit mitosis later than WT cells after taxol treatment. We then carried out a time-course analysis of incubation with 20 nM taxol which confirmed that cells first accumulated at mitosis and then exited (Figure 4.17C). The mitotic index of *Pcnt*$^{\Delta/\Delta}$ cells remained higher than that of WT cells after 9 hours incubation with taxol. In addition, we also observed that *Pcnt*$^{\Delta/\Delta}$ cells accumulated at mitosis as quickly as WT cells. Together with the observation that *Pcnt*$^{\Delta/\Delta}$ cells had slower mitotic progression (see Section 4.4), we concluded that it took longer for *Pcnt*

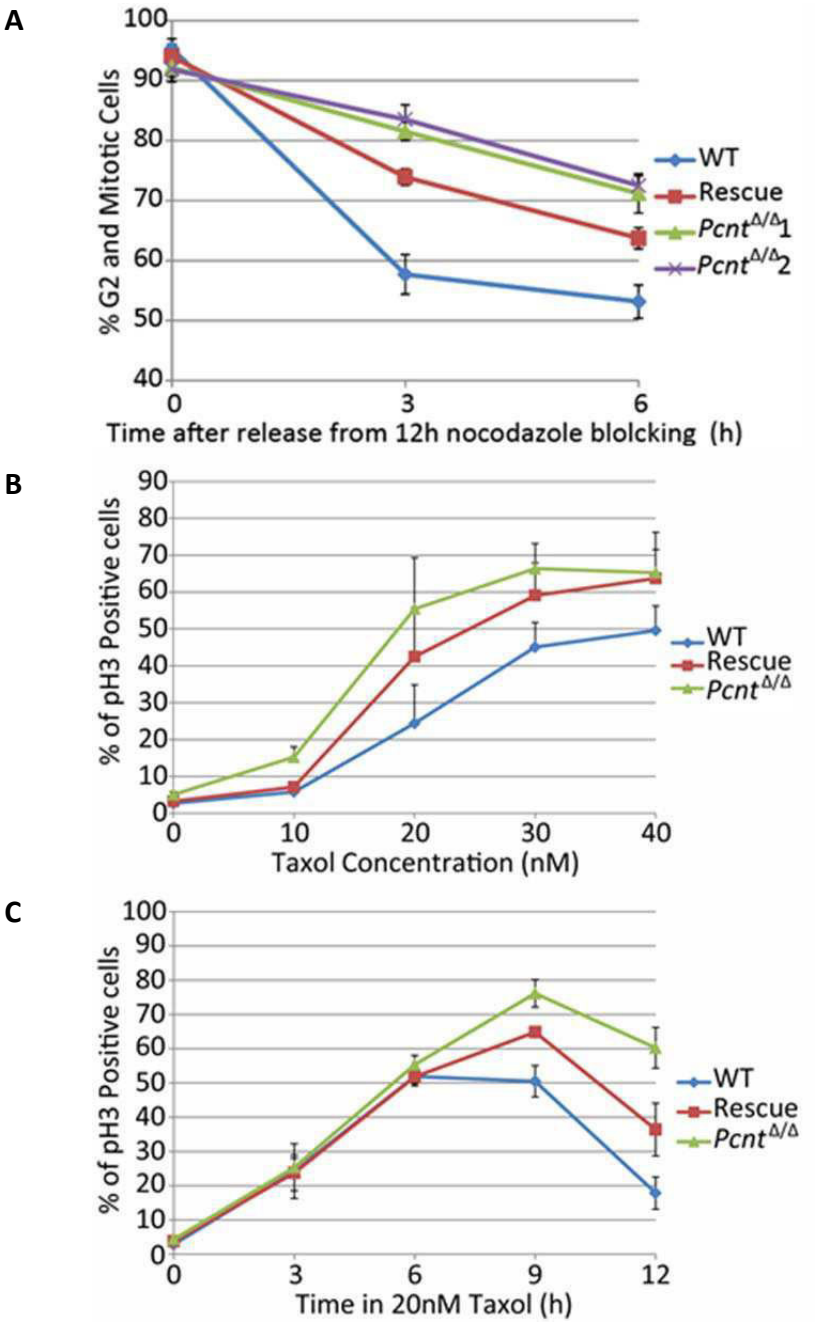

Figure 4.17 Delayed satisfaction of the SAC in *Pcnt*$^{\Delta/\Delta}$ cells.

The percentage of G2 and mitotic cells (Figure A) was measured by flow cytometry of propidium iodide. The percentage of mitotic cells (Figure B and C) was determined by flow cytometry of phosphorylated histone H3. All graphs show mean ± s.d. of 3 experiments in which 10000 events were scored.

A. Fewer *Pcnt*$^{\Delta/\Delta}$ cells exit mitosis after release from nocodazole blocking, as compared to WT and rescue cells.

B. Dose-dependence of mitotic arrest imposed by increasing doses of taxol. More *Pcnt*$^{\Delta/\Delta}$ cells were arrested at mitosis after 12 hours incubation of taxol.

C. Time-course analysis of taxol-induced arrest and satisfaction of the SAC. *Pcnt*$^{\Delta/\Delta}$ cells were arrested at mitosis as quickly as WT cells but exited from mitosis later than WT cells.

deficient cells to satisfy the SAC than WT cells.

4.11 *Pcnt*$^{\Delta/\Delta}$ cells show resistance to taxol induced cell death

Taxol has been used extensively to treat diverse types of cancer. However, the mechanism by which it kills tumour cells has not been fully understood. It has been demonstrated that mitotic arrest caused by taxol treatment determines cell death after

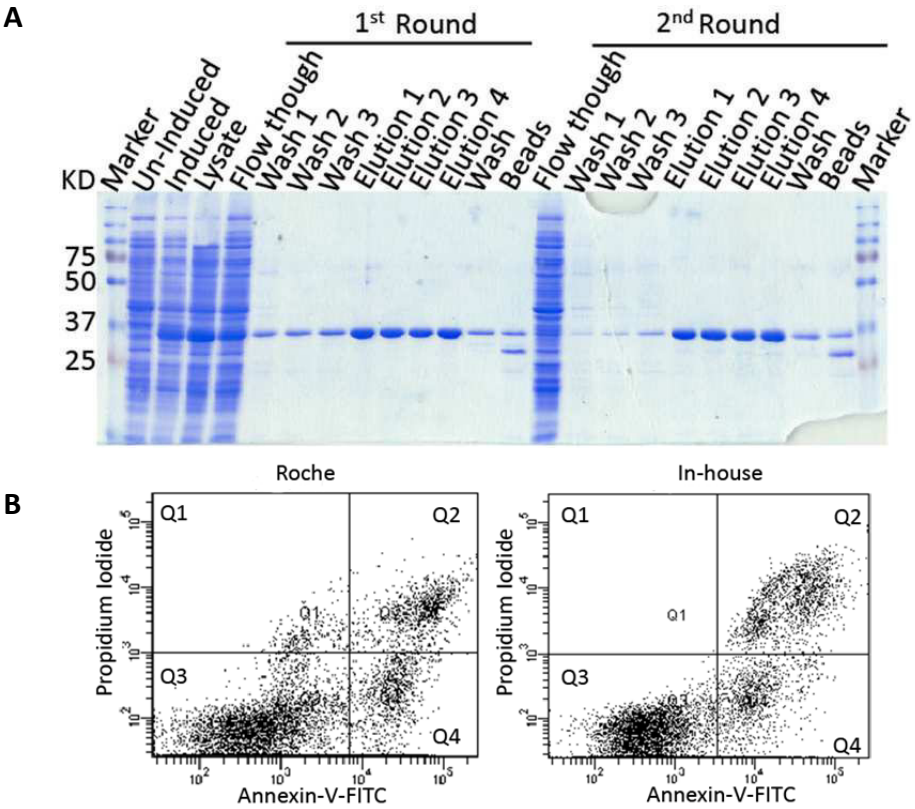

	Roche	In-house
Q2 (necrotic cells)	9.0 %	14.2 %
Q3 (live cells)	61.3 %	65.0 %
Q4 (apoptotic cells)	16.4 %	12.9 %
Q2+Q4 (dead cells)	25.4 %	27.1 %

Figure 4.18 Validation of in-house produced Annexin V Staining kit.
A. Coomassie-stained SDS-polyacrylamide gel showing expression and purification of Annexin V. Two rounds of purification were carried out with Ni-TA beads and the pooled elution was then labeled with FITC.
B. Evaluation of the in-house produced Annexin V staining kit against a commercial kit. The population was sorted by FACS as: live cells (Q3) with low Annexin and low PI staining, apoptotic cells (Q4) with high Annexin and low PI staining, and necrotic cells (Q2) with high Annexin and high PI staining.

mitotic exit (Bekier et al., 2009; Yang et al., 2009). If the SAC cannot be satisfied, cells escape mitosis after a prolonged delay and form multinucleated G1 cells, termed mitotic slippage. The aberrant G1 cells in turn undergo apoptosis (Brito and Rieder, 2006). As *Pcnt*$^{\Delta/\Delta}$ cells show delayed satisfaction of SAC, we next measured the number of cells which underwent apoptosis after the taxol treatment using an in-house produced Annexin V Staining kit. Annexin V is a protein which binds to phosphatidylserine in a calcium-dependent manner (Andree et al., 1990). Since phosphatidylserine becomes exposed at the external cell surface in both apoptotic and necrotic cells, dye exclusion of propidium iodide is performed to detect integrity of the cell membrane (Vermes et al., 1995). The necrotic cells (Annexin V high/PI high) whose membrane is not intact can be discriminated from live cells (Annexin V low/PI low) and apoptotic cells (Annexin V high/PI low). In this study, we grouped apoptotic and necrotic cells together as dead cells (Annexin V high).

The Annexin V protein was purified by Ni-TA beads (Figure 4.18A) and then conjugated with FITC. The efficiency of the in-house produced Annexin V-FITC kit was evaluated by comparing it with a commercial Annexin-V-FLUOS Staining Kit (Roche). Cell death was determined by flow cytometry, measuring Annexin V and DNA content. As shown in Figure 4.18B, the results obtained using the in-house produced Annexin V-FITC were similar to those with the commercial kit.

Considering that the cells started to exit from mitosis at 9 hours after blocking with 20 nM taxol, we examined cell death from 12 hours post-taxol treatment until 24 h. FACS analysis showed that the percentage of Annexin V positive cells in *Pcnt*$^{\Delta/\Delta}$ cells was lower than that in WT cells (Figure 4.19). As expected, *Pcnt*$^{\Delta/\Delta}$ cells showed resistance to taxol-induced cell death. The prolonged block of *Pcnt*$^{\Delta/\Delta}$ cells at mitosis in the presence of taxol may provide protection from cell death during the time course of the experiment. These data further support our hypothesis that *Pcnt*-deficient cells show delayed satisfaction of the spindle assembly checkpoint.

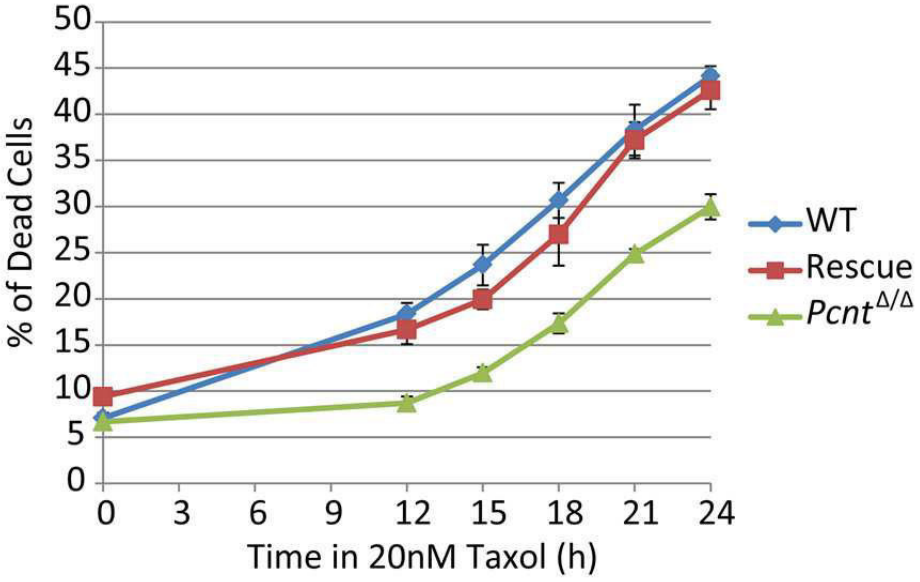

Figure 4.19 *Pcnt*$^{\Delta/\Delta}$ cells show resistance to taxol induced cell death.
Cell death induced by low-dose taxol treatment in cells of the indicated genotypes was measured by flow cytometric analysis of Annexin V staining. "Dead cells" were all those with a high Annexin V signal. The graph shows mean ± s.d. of 3 experiments in which 10000 events were scored.

4.12 Discussion

4.12.1 Generation of *Pcnt*-deficient cell lines

As we cloned the *Pcnt* cDNA, we then used it to map the genomic locus of *Pcnt* gene and to design a knockout strategy. The *Pcnt* locus is on chicken chromosome 7 and spans 98.8 kb. The neighbouring genes are *C21orf58* on its 5' end and *DIP2A* on its 3'end which are the same with the human *PCNT* gene. Further comparison of *Pcnt* cDNA sequence with the genomic sequence revealed the gene consists of 49 exons. Knocking out of the best studied PACT domain, which localises on exon 45 and 46, was a potential strategy for us to disrupt pericentrin function. The two exons are only 239 and 89 bp in length and the intron between them is 1.8 kb. We could knock out the region from exon 44 to 47 using a conventional strategy. However, the possibility that N-terminal or C-terminal truncated isoforms may exist in chicken suggests that we would be unable to abolish all the isoforms using a single targeting construct. Structure-function analysis also confirmed that this 49-exon pericentrin could localise at the centrosome as a small spot without the PACT domain (see Chapter 3).

Even if we achieved disruption of the whole *Pcnt* locus using a 3-lox P system (Arakawa et al., 2012), we would need to restore the phenotype by re-expression of *Pcnt* in knockout cells to confirm its function. However, expression of a single isoform might fail to restore full *Pcnt* function. In addition, the overexpression of *Pcnt* could cause overduplication of centrosome as it has been observed in tumour cells (Pihan et al., 1998). Therefore, we needed a different approach.

A recently published "promoter-hijack" strategy allows experiments to conditionally knock out essential, multiply-spliced genes and large genes (Samejima et al., 2008). The strategy is ideal for us to generate *Pcnt*-deficient DT40 cells. As the cDNA we cloned is the largest one, any other isoforms should be spliced from this one. So we proposed that the 5.5 kb upstream the ATG were the promoter region. As shown in Figure 4.1A, the promoter region of pericentrin and its upstream gene *C21orf58* overlap. Thereby, we actually disrupted the promoters of pericentrin and *C21orf58* at the same time. As the directions of the two genes are opposite, we can only rescue the expression of *Pcnt* when tTA is expressed. However, there is no literature about the function of *C21orf58*. Furthermore, we could not detect its expression by RT-PCR using the primers based on the predicted mRNA sequence (data not shown). We assume that *C21orf58* is not expressed in DT40 cells. On the other hand, if we could rescue the phenotype observed in knockout cells by re-expression of *Pcnt*, we could exclude any contribution of *C21orf58*.

The targeting vector was constructed from a modified pTRE-tight plasmid which contains a minimal tet-responsive promoter and puromycin resistance cassette flanked by Lox P sites. As there are two copies of *Pcnt* gene and we only generated one targeting vector, a transient transfection of a pMerCreMer plasmid was performed to recycle the puromycin cassette between the two lox P sites in the correct heterozygotes after first round targeting transfection. Considering that *PCNT* mutations are involved in growth retardation (Griffith et al., 2008; Reed et al., 2004),

we speculated that *Pcnt* was an essential gene in DT40 cells. Therefore, heterozygous clones after recycling of the puromycin cassette were transfected with a *Kif4a*^{pro}-tTA2 plasmid prior to the second round targeting transfection. The *Kif4a* promoter is a weak promoter which was not expected to induce over-expression of *Pcnt* (Samejima et al., 2008). In the meantime, we also performed the second round of targeting directly in the heterozygous clones, in case *Pcnt* was not an essential gene. In addition, the activity of *Kif4a* promoter varied between the clones. We thus generated several rescue clones that showed both wild-type and increased *Pcnt* expression.

We then confirmed the absence of *Pcnt* using RT-PCR. However, we detected the mRNA in knockout clones after 40 cycles of amplification, even though it was undetectable after 30 cycles. One possible reason may be that the promoter region of *Pcnt* is longer than 5.5 kb. As the primers were located at the 5'end of the mRNA, we supposed that the residual promoter could not drive the transcription of full length mRNA. However, the primers located at the 3'end gave the same results, suggesting that the expression of *Pcnt* was not completely abolished. The real-time PCR demonstrated that 2% of wild-type level mRNA was transcribed in our knockout cells. Leaky expression is an inherent problem with this strategy because the promoter of a gene is very difficult to define exactly. It is more important to examine the protein level in the knockout cells. We tried several commercial anti-pericentrin antibodies (Ab4448 from Abcam, A301-349A from Bethyl and PRB-432C from Covance) and one in-house produced antibody from Prof. R. Kuriyama. However, none of them worked for either immunofluorescence microscopy or Western blot. Therefore, we tried to check the pericentrin protein indirectly by knocking a FLAG-tag into the *Pcnt* locus. The tag could be knocked in either 5' end or 3'end of the gene. As the promoter region differs between *Pcnt*$^{\Delta/\Delta}$ cells and WT cells, we required a different targeting construct to put the tag in the 5'end. Therefore, we chose to replace the stop codon with the tag. A drug-resistant cassette was put inside

the intron so that the 3'UTR remained intact. Thus, any changes that might affect the stability of the mRNA were minimised. Immunofluorescence microscopy showed that the FLAG-tag was successfully knocked into the 3'end of the gene locus and that no signal was detected in the $Pcnt^{\Delta/\Delta}$ cells. We conclude that we successfully generated a *Pcnt*-deficient cell line.

4.12.2 *Pcnt*-deficient cell are delayed in mitosis

In addition to the MTOC function, centrosomes also serve as platforms for multiple signaling networks and regulatory complexes. Thus, centrosomes are involved in numerous cell cycle regulatory events such as entry into mitosis, cytokinesis and G1/S transition (Hinchcliffe et al., 2001; Khodjakov and Rieder, 2001). As the main centrosomal scaffold protein, pericentrin has been shown to anchor centrosome structure proteins and signaling proteins to the centrosome, suggesting it controls cell cycle progression. Depletion of pericentrin in human cells and in budding and fission yeast (but not flies) leads to cell death via impaired centrosome and spindle integrity (Flory et al., 2002; Martinez-Campos et al., 2004; Stirling et al., 1996; Zimmerman et al., 2004). Therefore, we hypothesised that *Pcnt* was an essential gene in DT40 cells. Although we finally obtained *Pcnt*-deficient cell lines, it is likely that loss of pericentrin could lead to growth restriction, but not cell death. Our cell proliferation results confirmed that $Pcnt^{\Delta/\Delta}$ cell grew slower than WT cells. We next tried to define the stage where $Pcnt^{\Delta/\Delta}$ cells were arrested. Pericentrin depletion in cultured human cells prevents cells from entering S phase. However, this G1 phase arrest is p53-dependent because pericentrin depletion in *p53* null cells does not inhibit cell cycle progress (Mikule et al., 2007; Srsen et al., 2006). Consistent with this idea, was the observation that we did not detect higher proportion of G1 cells in $Pcnt^{\Delta/\Delta}$ cells. The flow cytometry analysis and live cell imaging showed that mitotic progression was delayed in $Pcnt^{\Delta/\Delta}$ cells. Similar defects were also observed in fission yeast (Fong et al., 2009). It is likely that altered mitotic spindle organisation causes the

mitosis delay in *Pcnt*-deficient cells. We conclude that pericentrin is required for normal cell growth but the mechanism may be varied in different cell types.

4.12.3 Centrosome structure and its MTOC function in *Pcnt*-deficient cells

Pericentrin has been suggested to serve as a molecular scaffold which anchors centrosomal structural proteins. It has also been suggested that pericentrin is involved in centrosome duplication by preventing premature centrosome splitting during interphase (Matsuo et al., 2010; Matsuo et al., 2012). Therefore, we examined the components of the centrosome in order to establish whether centrosome structure was affected by the absence of pericentrin. The centrosome-associated kinase, Aurora A; centriole proteins, centrin3, Ninein, CEP76, CEP135, and pericentriolar proteins, PCM-1, γ-tubulin were all localised at centrosomes in $Pcnt^{\Delta/\Delta}$ cells. These data indicate that centrosome biogenesis and maturation are normal in $Pcnt^{\Delta/\Delta}$ cells, which was confirmed by transmission electron microscopy analysis. There is no direct evidence showing pericentrin interacts with the above centrosomal proteins except PCM-1 and γ-tubulin (Dictenberg et al., 1998). It has been reported that the centrosomal levels of pericentrin and γ-tubulin increase progressively from early G1 to metaphase and then drop dramatically to basal levels (Dictenberg et al., 1998). γ-tubulin was significantly reduced or absent at centrosomes in pericentrin-deficient cells (Griffith et al., 2008; Tibelius et al., 2009). Pericentrin anchors the γ-TuRC to centrosomes through interaction with GCP-2 and GCP-3 (Takahashi et al., 2002; Zimmerman et al., 2004).

We then quantified the centrosomal localisation of the two proteins in detail. Consistent with previous studies, quantitative analysis of the intensities of centrosomal components during the cell cycle indicated that centrosomal recruitment of γ-tubulin was reduced at all the cell cycle stages in $Pcnt^{\Delta/\Delta}$ cells. The remaining protein may be anchored by other proteins. We also observed the cell cycle-dependent assembly of centrosomal γ-tubulin in all our cell lines except the

pericentrin overexpression cells. To our surprise, overexpression of pericentrin only resulted in significant exaggeration of γ-tubulin at centrosome in G1/S cells. It is possible that the cytoplasmic pool of γ-tubulin is not controlled by pericentrin or that there is a threshold for centrosomal pool of γ-tubulin. Depletion of PCM-1 has been shown to result in defective assembly of pericentrin (Dammermann and Merdes, 2002). We found that the centrosomal anchoring of PCM-1 was not impaired in the absence of *Pcnt*, suggesting that PCM-1 mediates centrosomal recruitment of pericentrin. The elevated expression of PCM-1 in OverExp cells may be caused through a separate mechanism.

We next examined the effects of *Pcnt* loss on the established MTOC function of centrosomes. In higher eukaryotes, microtubule nucleation at the centrosome is initiated from γ-TuRC (Moritz et al., 1995; Zheng et al., 1995). The impaired centrosomal γ-tubulin in $Pcnt^{\Delta/\Delta}$ cells indicated that *Pcnt* was required for centrosome-dependent microtubule nucleation. However, we found that microtubule asters formed efficiently from *Pcnt*-deficient centrosome in both interphase and mitotic cells after cells recovered from cold and nocodazole induced microtubules depolymerisation. The roles of pericentrin in microtubule nucleation have been widely studied but a consolidated conclusion has not been reached. Depletion of pericentrin inhibited microtubule nucleation *in vitro* from purified centrosomes of *Drosophila* embryo, mouse oocytes and *Xenopus laevis* embryos (Doxsey et al., 1994; Kawaguchi and Zheng, 2004; Takahashi et al., 2002). RNAi depletion of pericentrin A but not pericentrin B only impaired the centrosomal localisation of γ-tubulin and microtubule organisation in mitotic cells (Zimmerman et al., 2004). However, it was also reported that pericentrin silencing had no significant effect on microtubule anchoring at the centrosome (Srsen et al., 2006). It is of interest that centrosomes can organise microtubules in the absence of functional γ-tubulin or other γ-TuRC proteins (Sampaio et al., 2001; Strome et al., 2001). Therefore, we

suggest that pericentrin plays a role in microtubule nucleation but microtubules can also be organised by centrosomes in a pericentrin-independent pathway.

In mitotic cells, centrosomes and microtubules play an important role in the assembly and function of mitotic spindles. Abnormal mitotic morphology was observed in MOPD II fibroblast cells (Rauch et al., 2008). Monopolar spindles formed in pericentrin-depleted cells (Lee and Rhee, 2011; Rauch et al., 2008; Zimmerman et al., 2004). In contrast, we observed bipolar spindles in mitotic $Pcnt^{\Delta/\Delta}$ cells, which is in agreement with our results of normal composition and MTOC function of centrosomes in these cells. In addition, centrosome-independent microtubule generation may also contribute to spindle assembly in $Pcnt^{\Delta/\Delta}$ cells (Karsenti and Vernos, 2001). Extensive studies have demonstrated that chromosomal microtubule assembly can be triggered by GTP-bound Ran and the chromosomal passenger complex (Sampath et al., 2004; Zhang et al., 1999). Microtubule nucleation on preexisting microtubules through a complex called Augmin causes microtubule branching and amplification, which in turn build a bipolar spindle (Goshima et al., 2008). However, the bipolar spindle in $Pcnt^{\Delta/\Delta}$ cells is not well organised, as we found the pole-to-pole distance was longer in $Pcnt^{\Delta/\Delta}$ cells than WT cells. A key step in spindle assembly is the nucleation of stable microtubules from the centrosome. Our microtubule regrowth assay may not be sufficiently sensitive to detect the nucleation of fiber microtubules. Therefore, we tried to determine the microtubule extension rates by live-cell imaging of the microtubule plus end marker EB1 (microtubule end-binding protein 1). Unfortunately, it was not possible to track the movement of EB1 in suspension cells.

To highlight the role of pericentrin in mitotic spindle organisation, we treated $Pcnt^{\Delta/\Delta}$ cells with nocodazole or taxol to disrupt spindle function and activate the SAC, then examined the ability of cells to re-enter the cell cycle from mitotic arrest. Although nocodazole and taxol function via different mechanisms, both drugs impair the

functional connections or tension between kinetochores and spindle microtubules during mitosis which in turn activate the SAC and induce cell arrest at metaphase. Nocodazole depolymerises microtubules but the microtubules can re-polymerise after withdrawal of the drug (Jordan et al., 1992; Minoshima et al., 2005). We found that fewer $Pcnt^{\Delta/\Delta}$ cells exited mitotic arrest than WT cells when they were released from nocodazole blocking, suggesting that bipolar spindles become re-established more slowly in $Pcnt^{\Delta/\Delta}$ cells. Taxol stabilises the microtubules, but cells can overcome low dose taxol-induced prolonged mitotic arrest in a dose-dependent manner through regeneration of the connection between microtubules and kinetochores (Barboule et al., 1997; Rieder et al., 1994; Yang et al., 2009). $Pcnt^{\Delta/\Delta}$ cells also exited mitotic arrest later than WT cells after taxol incubation. Studies with cultured cells have suggested that cell death is a subsequent event of the SAC-mediated mitotic arrest induced by antimitotic drugs (Bekier et al., 2009; Jordan et al., 1996; Lee et al., 2004). Consistently, we observed that cell death was inhibited in $Pcnt^{\Delta/\Delta}$ cells after treatment with taxol because $Pcnt^{\Delta/\Delta}$ cells were still under arrest in mitosis when WT cells re-entered cell cycle and underwent cell death. Taken together, we propose that efficient spindle microtubule organisation from centrosomes requires pericentrin. Impaired spindle microtubules in turn delays satisfaction of the SAC. Findings in support of this idea include our observation that $Pcnt^{\Delta/\Delta}$ cells showed a delay in mitosis in normal cell cycle progression.

4.12.4 Interplay of AKAP450 and pericentrin

AKAP450, also named CG-NAP (Centrosome and Golgi localized PKN-associated protein), is a giant coiled-coil protein. It is localised to the centrosome throughout the cell cycle and to the Golgi apparatus in interphase (Takahashi et al., 1999). However, its localisation to the Golgi apparatus but not centrosomes can be disrupted by microtubule depolymerisation (Kim et al., 2007). Both AKAP450 and pericentrin contain three coiled-coil regions flanked by noncoiled regions. The middle and C-terminal coiled-coil regions of the two proteins show relatively high homology

(Takahashi et al., 2002). The PACT domain in their C-terminus is particularly conserved (Gillingham and Munro, 2000). In addition, only one protein containing a PACT domain has been identified in *Drosophila* (Martinez-Campos et al., 2004). These data suggest that there may be some functional redundancy between these two structurally related proteins.

Indeed, it has been demonstrated that AKAP450 mediates protein-protein interaction which can also be mediated by pericentrin. AKAP450 anchors various signaling components such as protein kinases (PKN, PKC and PKA) and phosphatases (PP1 and PP2A) (Takahashi et al., 2000; Takahashi et al., 1999), whereas pericentrin interacts with PKA and PKC (Chen et al., 2004; Diviani et al., 2000; Kim et al., 2008a). Similar to pericentrin, displacement of the endogenous AKAP450 from centrosomes in Hela cells induced defects in cytokinesis and centriole replication (Keryer et al., 2003). Furthermore, AKAP450 and pericentrin indirectly associate with γ-TuRC via the binding of their N-terminal region with GCP-2 and/or GCP-3. Co-immunoprecipitation experiments also suggest AKP450 and pericentrin interact with each other (Takahashi et al., 2002). Therefore, AKP450 and pericentrin may form a structural framework of the PCM at the centrosome to provide anchoring sites for the γ-TuRCs (Dictenberg et al., 1998; Takahashi et al., 2002). Consistently, pretreatment of isolated centrosomes with antibodies to AKAP450 or pericentrin moderately inhibited microtubule nucleation, whereas the combination of two antibodies caused stronger inhibition (Takahashi et al., 2002).

As we did not observe significant defects in either centrosome or microtubule organisation in $Pcnt^{\Delta/\Delta}$ cells, we speculated that some compensatory mechanisms were generated in $Pcnt^{\Delta/\Delta}$ cells. It is possible that other centrosome scaffold proteins took the place of pericentrin during the selection of *Pcnt*-deficient clones. Considering the structural relationship, AKAP450 is the most conceivable candidate.

Functional redundancy and the differences between pericentrin and AKAP450 remain to be addressed.

Chapter 5. Pericentrin function in the DNA damage responses

5.1 Introduction

It has been reported that the UV-induced G2/M checkpoint was defective in *PCNT*-mutant lymphoblastoid cells and *PCNT*-depleted Hela cells (Griffith et al., 2008). A similar defect was also observed in *MCPH1*-mutant lymphoblastoid cells (Alderton et al., 2006). These data suggest that both *PCNT* and *MCPH1* have a function in the ATR-signaling pathway. In addition, mutations in *PCNT* cause MOPD II and mutations in *MCPH1* cause primary microcephaly (Jackson et al., 2002; Rauch et al., 2008). Both syndromes are autosomal recessive disorders and are characterised by a markedly reduced brain size. Therefore, we hypothesised there is a genetic interaction between *PCNT* and *MCPH1*. A paper published recently has proposed that pericentrin mediates MCPH1-dependent recruitment of CHK1 to centrosomes, which in turn controls activation of cyclin B-CDK1 (Tibelius et al., 2009). To explore this idea, we targeted *Mcph1* in $Pcnt^{\Delta/\Delta}$ cells and investigated the function of pericentrin in DNA damage responses.

5.2 Targeting of the chicken *Mcph1* locus

The targeting strategy and vectors for *Mcph1* disruption were described previously (Figure 5.1A, (Brown et al., 2010)). A non-radioactive Southern blot was employed to screen for positive clones after targeting transfection. The specificity of the probe was confirmed by several genomic DNA digestions in WT cells. All of the bands were consistent with the predicted sizes (Figure 5.1B). WT, $Pcnt^{\Delta/\Delta}$ and rescue cells were all transfected with *Mcph1* targeting vectors to disrupt the *Mcph1* gene in these cells. A total of 216 clones (72 clones per cell line) were screened for the first allele targeting and 48 clones were positive. For the second allele targeting, a total of 266 clones (108 $Pcnt^{\Delta/\Delta}$ clones, 108 rescue clones and 50 WT clones) were screened. We identified 4 $Mcph1^{-/-}$ clones, 32 double knockout ($Pcnt^{\Delta/\Delta}$/$Mcph1^{-/-}$) clones and 16 double knockout clones but with *Pcnt* restored. A representative Southern blot result

A

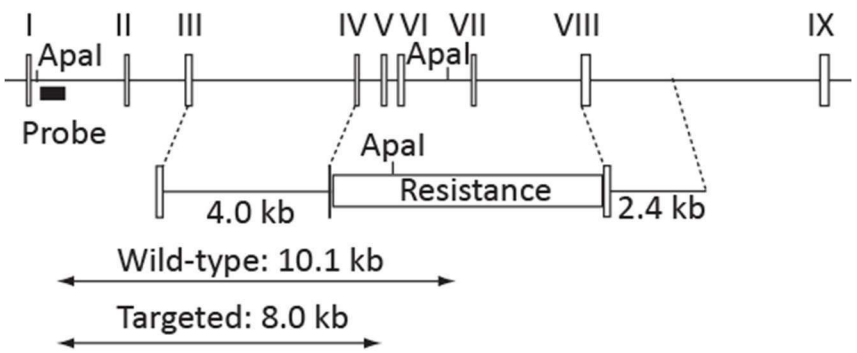

B

Specificity of 5' probe		
Genotype	Enzyme	Size (kb)
WT	Acc I	9.2
	Eco RI	7.9
	Hind III	5.1
	Nde I	7.0
	Xba I	8.0
	Apa I	10.1

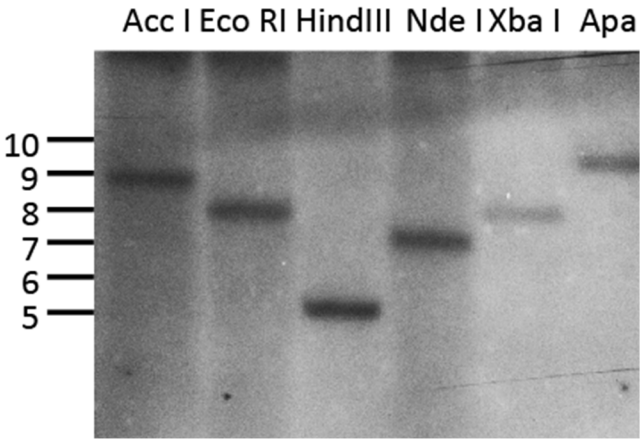

C

Screening of targeted clones		
Genotype	Size (kb)	Frequencies
WT	10.1	-
WT/Targeted	8.0+10.1	22%
Targeted	8.0	20%

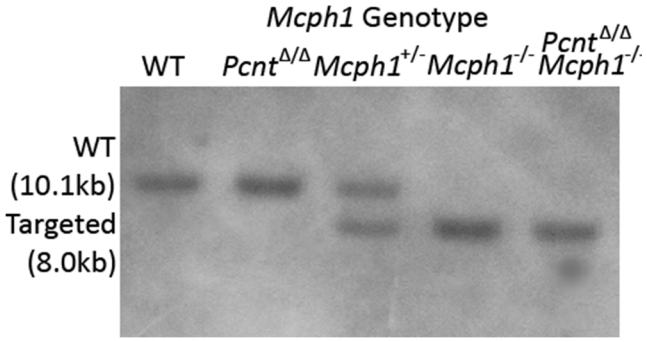

Figure 5.1 Targeting of the chicken *Mcph1* locus.

A. Map of the *Mcph1* locus with knockout strategy and schematic diagram for Southern blotting (Brown et al., 2010).

B. Specificity testing of the probe used for positive clones screening. Genomic DNA extracted from the WT cells was digested with indicated restriction nucleases and probed with a 5' probe. The predicted size of Southern blot fragments is shown in the table.

C. Screening of positive clones after each round of transfection. Genomic DNA extracted from cells with the indicated genotype was digested with Apa I and probed with a 5' probe. The predicted size of Southern blot fragments and targeting frequencies at the *Mcph1* locus are shown in the table.

with each genotype and the gene targeting frequencies are shown in Figure 5.1C.

To confirm that *Mcph1* was disrupted in the positive clones screened by the Southern blot, total RNA was isolated from cells of each genotype and used to examine the expression of *Mcph1* by RT-PCR. As shown in Figure 5.2, the expression of *Mcph1* was abrogated in all *Mcph1*-deficient cell lines.

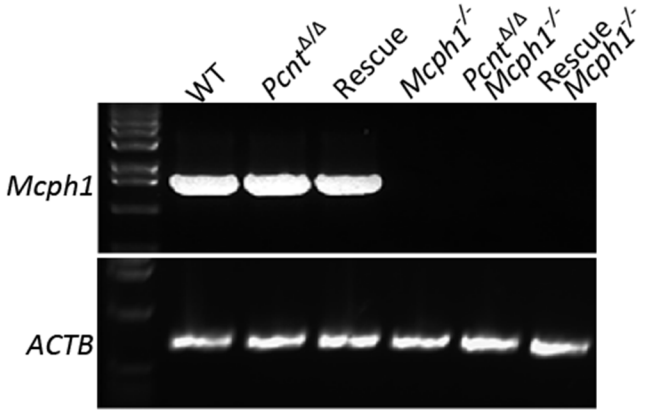

Figure 5.2 RT-PCR analysis of *Mcph1* expression.
A RT-PCR with total mRNA isolated from cells of the indicated genotypes. Primers against full-length *Mcph1* mRNA were used for PCR, as previously described (Jeffers et al., 2008).

5.3 Neither *Pcnt* nor *Mcph1* deficiency has a significant impact on IR-induced cell cycle checkpoint responses

It has been reported that *PCNT* mutant cells have a defect in UV-induced G2/M checkpoint arrest (Griffith et al., 2008). Although UV causes activation of the ATR pathway, additional evidence indicates that ATR is also activated in response to IR (Adams et al., 2006; Myers and Cortez, 2006). Furthermore, the method of analysing IR-induced G2/M checkpoint has been well established in DT40 cells using combinations of flow cytometry (Rainey et al., 2006). Therefore, we tested whether *Pcnt* deficiency impacted on the initiation of G2/M checkpoint after IR. Cells were incubated in medium containing colcemid, with or without prior exposure to 2 Gy IR damage. Colcemid traps cells in mitosis for several hours (Rieder and Palazzo, 1992) while the G2/M checkpoint induced by IR causes cells to accumulate in G2 phase (Rieder, 2011). Samples were collected at different time points and the mitotic index

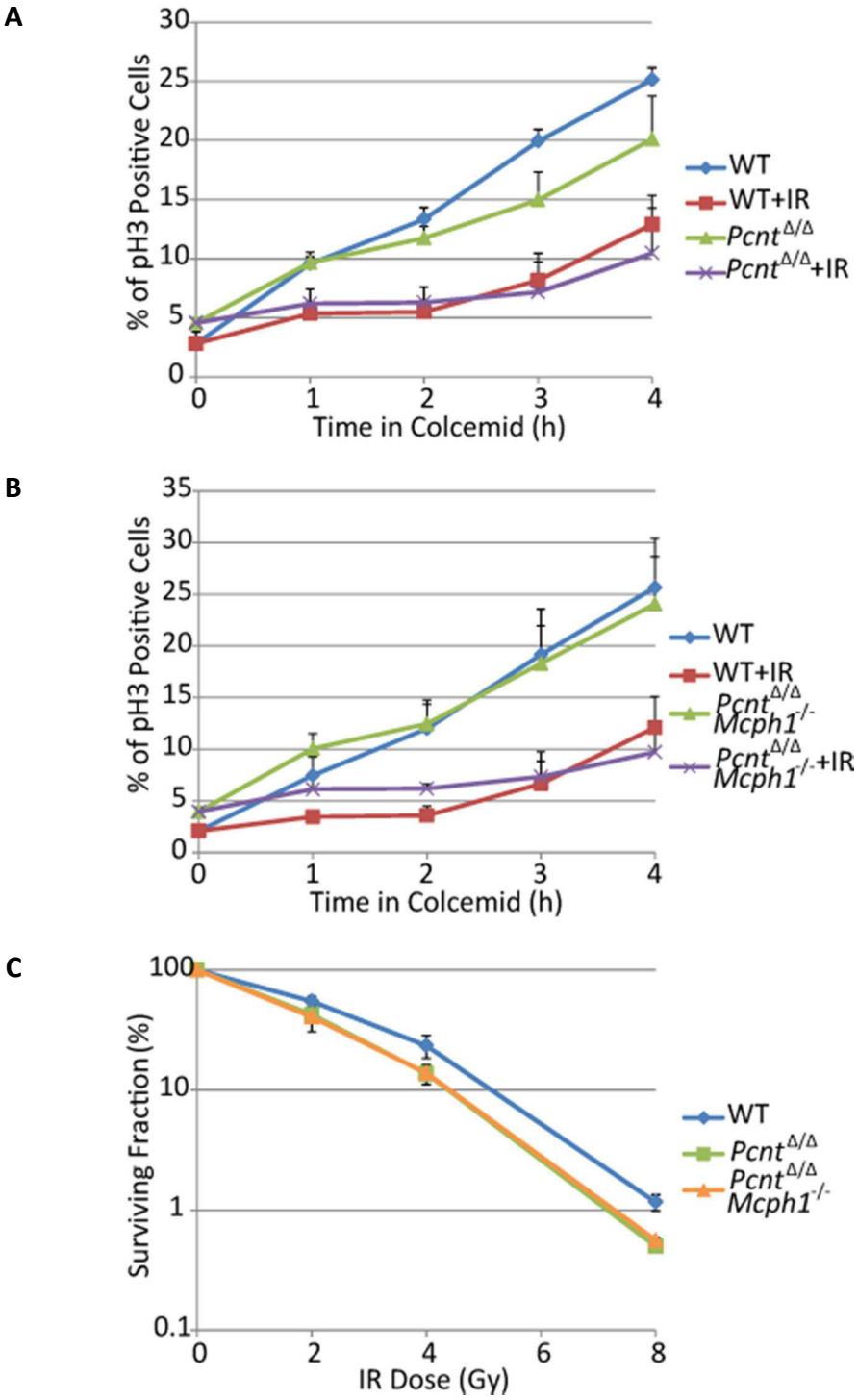

Figure 5.3 Cell cycle checkpoint responses of *Pcnt*$^{\Delta/\Delta}$ and *Pcnt*$^{\Delta/\Delta}$/*Mcph1*$^{-/-}$ cells after IR damage.

A. Analysis of the G2/M checkpoint of *Pcnt*$^{\Delta/\Delta}$ cells.

B. Analysis of the G2/M checkpoint of double knockout cells.

Colcemid was added to non-irradiated and irradiated cells at the time of irradiation for the time indicated. Mitotic index was assessed by flow cytometry for phospho-histone H3.The graphs show mean ± s.d. of 3 experiments in which 10000 events were scored.

C. Clonogenic survival analysis of *Pcnt*$^{\Delta/\Delta}$ and double knockout cells after treatment with the indicated doses of IR. Data points show mean ± s.d. of 3 separate experiments.

was determined by flow cytometric analysis of phospho-histone H3. As shown in Figure 5.3A, cells incubated with colcemid showed an increase in mitotic index over time. However, the mitotic indices of both *Pcnt*$^{\Delta/\Delta}$ and WT cells remained static after DNA damage, indicating that the G2/M checkpoint was induced in the absence of *Pcnt*.

It has been demonstrated that *MCPH1* knock-down results in a defect in the G2/M checkpoint after IR damage in U2OS cells (Lin et al., 2005; Xu et al., 2004). However, this checkpoint is intact in *Mcph1*-deficient DT40 cells (Brown et al., 2010). Considering the potential genetic interactions between *PCNT* and *MCPH1*, we asked whether simultaneous loss of *Pcnt* and *Mcph1* led to a G2/M checkpoint defect in DT40 cells. We therefore carried out the same experiments using WT and double knockout cells. However, the G2/M checkpoint induced by IR was still intact after both genes were disrupted (Figure 5.3B). Therefore, we conclude that neither *Pcnt* nor *Mcph1* is required for IR-induced G2/M checkpoint activation in DT40 cells.

We then examined the ability of cells to survive genotoxic stress by comparing the clonogenic survival of *Pcnt*$^{\Delta/\Delta}$ cells, double knockout cells and WT cells after exposure to increasing doses of IR. As shown in Figure 5.3C, *Pcnt*$^{\Delta/\Delta}$ cells were only slightly more sensitive to IR than WT controls, which was similar to *Mcph1*$^{-/-}$ cells (Brown et al., 2010). Double knockout cells showed similar levels of radiosensitivity as the single mutants. In summary, we found that the DSB repair capacity of the cells was not significantly altered in the absence of *Pcnt*, *Mcph1* or both.

5.4 Pericentrin limits IR-induced centrosome hyperamplification in *Mcph1*-deficient cells

Centrosome amplification is a frequent consequence of the DNA damage response (Sato et al., 2000). It also occurs when cell cycle progression is perturbed (Balczon et

al., 1995; Dodson et al., 2004). It has been reported that pericentrin plays pivotal roles in centrosome duplication and cell cycle progression (Matsuo et al., 2010; Mikule et al., 2007; Zimmerman et al., 2004). Therefore we explored the potential role of *Pcnt* in multiple centrosome production. To address this we treated $Pcnt^{\Delta/\Delta}$ cells, $Mcph1^{-/-}$ cells, double knockout cells and WT cells with 5 Gy IR or 4 mM hydroxyurea (HU), which cause centrosome amplification in DT40 cells (Dantas et al., 2011). Centrosome numbers, as determined by γ-tubulin spots in each genotype, were analyzed by immunofluorescence microscopy (Figure 5.4). Centrosomes were amplified after either IR or HU treatment in the absence of *Pcnt*.

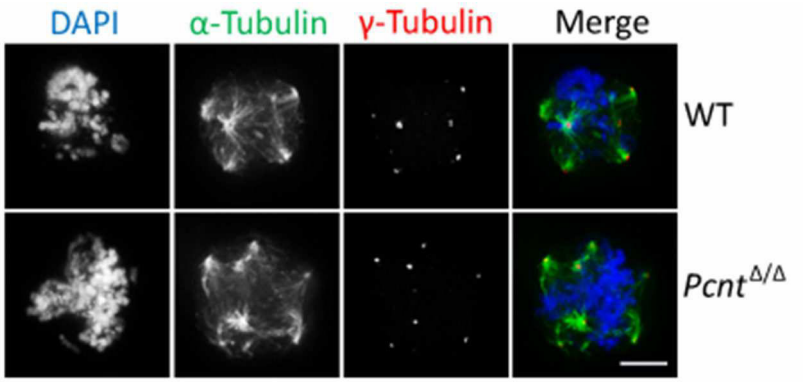

Figure 5.4 Representative immunofluorescence microscopy images of cells with amplified centrosomes.
Cells of the indicated genotype were treated with 5 Gy IR for 24h and then stained with antibodies to α-tubulin (green) and γ-tubulin (red). DNA was visualised with DAPI (blue). Scale bar, 10 μm.

$Pcnt^{\Delta/\Delta}$ and $Mcph1^{-/-}$ single mutants, double knockout cells and WT cells all showed similar levels of centrosome amplification in response to treatment with HU (Figure 5.5A). These data suggest that neither gene is required for centrosome overduplication caused by HU-induced extended S phase arrest. However, the hyperamplification of centrosomes in response to IR, as previously seen in $Mcph1^{-/-}$ cells (Brown et al., 2010), was suppressed by the deletion of *Pcnt* (Figure 5.5B). Importantly, this suppression was solely due to the absence of *Pcnt*, since the levels of centrosome amplification after re-expression of *Pcnt* in double knockout cells

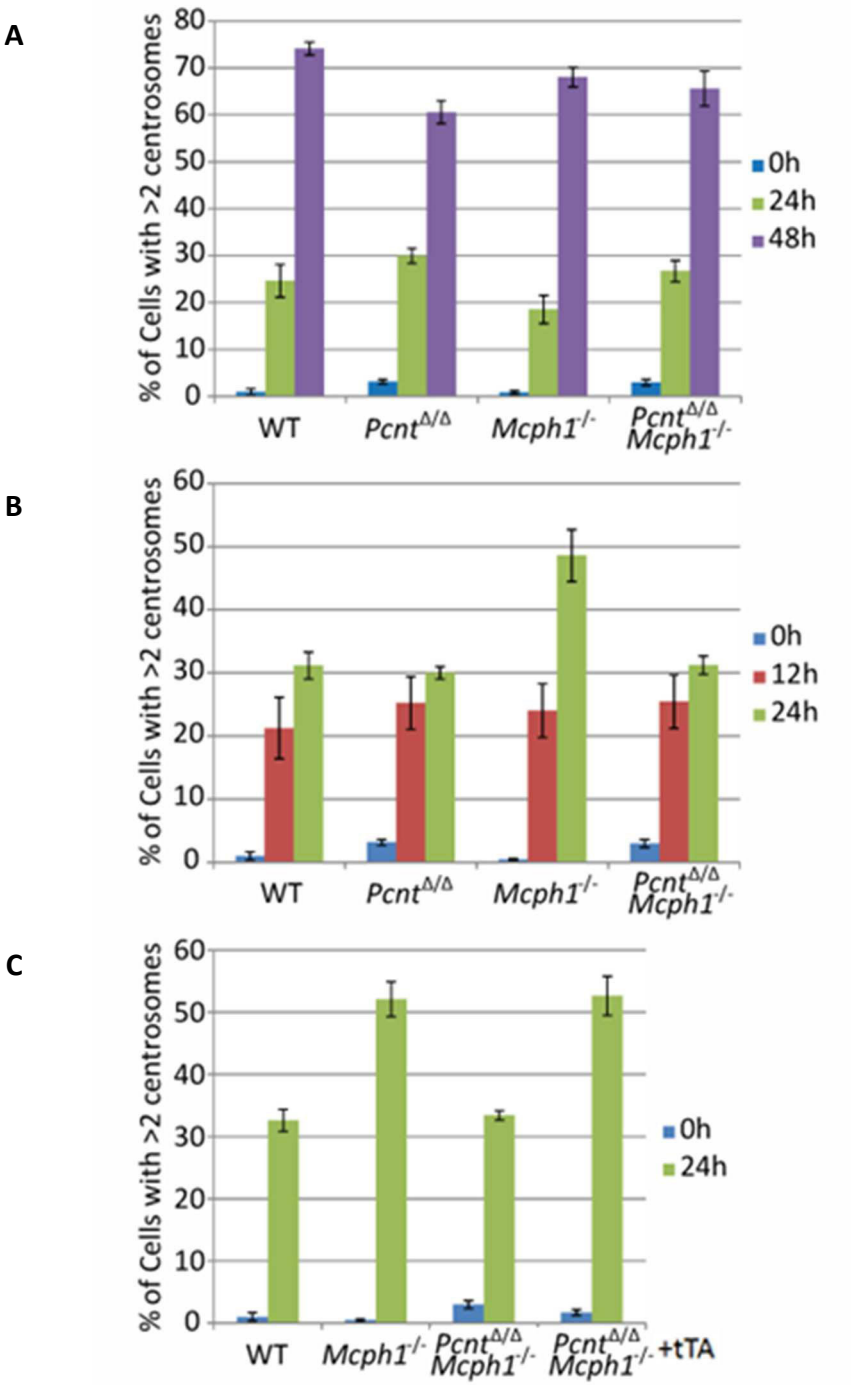

Figure 5.5 *Pericentrin* deficiency rescues IR-induced centrosome hyper-amplification in *Mcph1*-deficient cells.

A. Centrosome amplification in the cells of the indicated genotypes was similar at the described time points after 4 mM HU treatment.

B. Centrosome hyperamplification in *Mcph1*$^{-/-}$ cells at 24 h after 5 Gy IR treatment was reduced to WT cells level when *Pcnt* was abrogated in *Mcph1*$^{-/-}$ cells.

C. Levels of centrosome amplification were restored to those in *Mcph1*$^{-/-}$ cells after re-expression of *Pcnt* in double knockout cells.

All histograms show mean ± s.d. of 3 separate experiments in which at least 300 cells per experiment were counted.

were indistinguishable from those in *Mcph1*$^{-/-}$ cells (Figure 5.5C). Our results provide clear evidence for the genetic interaction of *Pcnt* and *Mcph1* in IR-induced centrosome amplification.

5.5 Pericentrin is required for efficient CHK1 response to IR

We have demonstrated that CHK1 is required to promote centrosome over-duplication after DNA damage (Bourke et al., 2007). Inhibition of CHK1 by RNAi or drug treatment suppressed centrosome amplification after DNA damage. In addition, centrosome amplification was abrogated in *Chk1*$^{-/-}$ DT40 cells. CHK1 is activated by IR in DT40 cells and its activity requires increased phosphorylation of Ser345 (human sequence), a site phosphorylated by ATM/ATR (Lopez-Girona et al., 2001; Zhao and Piwnica-Worms, 2001). We hypothesised that pericentrin controls the activity of CHK1, which in turn determines centrosomal responses to IR. We

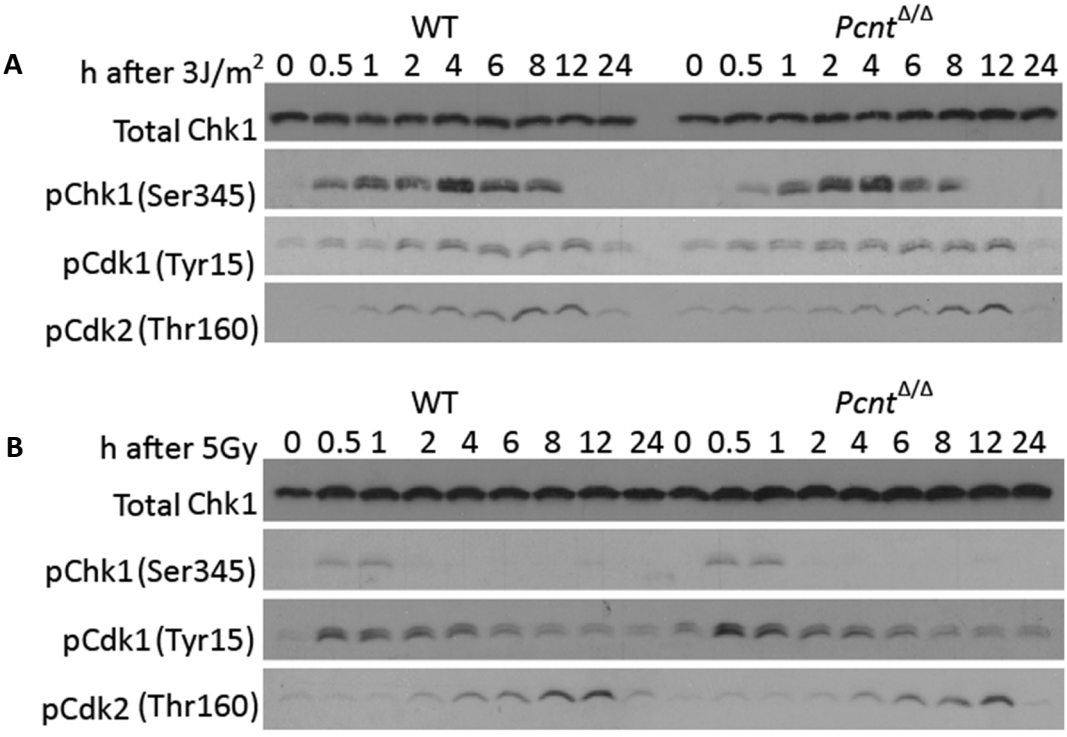

Figure 5.6 Immunoblot analyses of activation of CHK1, CDK1 and CDK2 in *Pcnt*$^{\Delta/\Delta}$ cells after DNA damage.

The soluble whole cell extracts from WT and *Pcnt*$^{\Delta/\Delta}$ cells at indicated time points after UV (A) and IR (B) damage were used for immunoblot analyses, using antibodies to phospho-CHK1, phospho-CDK1, phospho-CDK2 and total CHK1 as loading control.

then tested the impact of *Pcnt* on CHK1 activation after DNA damage. As shown in Figure 5.6, CHK1 was activated immediately after the treatment and remained activated for a short period after IR damage but for a longer time after UV treatment. However, the dynamics of CHK1 phosphorylation after IR and UV irradiation were not affected by *Pcnt* deficiency.

It has been suggested that pericentrin might mediate the centrosomal localisation of CHK1 (Griffith et al., 2008). Centrosome-associated CHK1 in turn prevents premature activation of cyclin B-CDK1 which controls G2/M transition (Kramer et al., 2004). Furthermore, our group has shown that CDK2 activation induced by CHK1-dependent phosphorylation on Thr160 is associated with IR-induced centrosome amplification in DT40 cells (Bourke et al., 2010). However, our immunoblotting analysis did not show any defects in CHK1 phosphorylation in $Pcnt^{\Delta/\Delta}$ cells. This may be due to the Western blot samples which contained the total soluble proteins from whole cell extracts rather than a limited chromatin-associated fraction. Unfortunately, the anti-CHK1 antibodies in our hands were not suitable for immunofluorescence staining in DT40 cells so we could not examine the centrosomal localisation of CHK1 in $Pcnt^{\Delta/\Delta}$ cells. As an alternative approach, we instead checked the activation of downstream targets of CHK1 to assess whether CHK1 works normally in $Pcnt^{\Delta/\Delta}$ cells. As shown in Figure 5.6, the kinetics of CDK1 and CDK2 phosphorylation after DNA damage were identical between WT and $Pcnt^{\Delta/\Delta}$ cells.

As immunoblot analysis may not fully capture the intracellular dynamics of checkpoint activation, we then carried out immunofluorescence microscopy to test the subcellular localisation of phosphorylated CHK1 after IR treatment. A monoclonal antibody to phospho-CHK1 (Ser345) detected nuclear foci in irradiated cells which colocalised with γ-H2AX foci (Figure 5.7B). CHK1 was found to exclusively localise at the centrosome in U2OS cells (Kramer et al., 2004; Tibelius et

al., 2009). Unexpectedly, we did not see any phospho-CHK1 foci which localised at centrosomes in either WT cells or *Pcnt*$^{\Delta/\Delta}$ cells (Figure 5.7A). We next quantified the cellular intensity of IRIF of phospho-CHK1 to monitor dynamics of CHK1 activation at DNA breaks. It should be noted that the anti-phospho-CHK1 (Ser345) antibody gave some background signal because it was detected in *Chk1*$^{-/-}$ DT40 cells, but this signal did not increase after IR treatment (Figure 5.8). The background signal was then subtracted from each sample. As shown in Figure 5.8B, we found that the intensity of phospho-CHK1 IRIF was greatly attenuated in *Pcnt*$^{\Delta/\Delta}$ cells over time after 5 Gy IR. This decreased activation was restored to control level by the deletion of *Mcph1* in *Pcnt*$^{\Delta/\Delta}$ cells (Figure 5.8B).

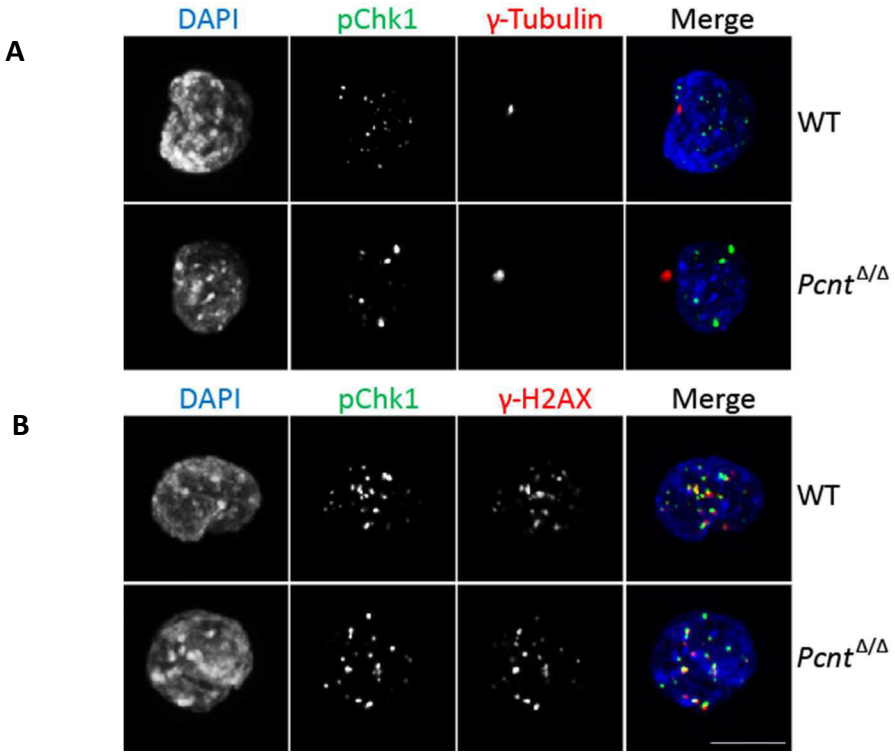

Figure 5.7 Subcellular localisation of phospho-CHK1 (Ser345) in DT40 cells.
Immunofluorescence microscopy showing that phospho-CHK1 (green) formed foci 1 h after irradiation at DNA breaks indicated by γ-H2AX (B) but not at centrosomes, as indicated by γ-tubulin (A). DNA was visualised with DAPI (blue). Scale bar, 10 μm.

The immunofluorescence microscopy data suggest CHK1 activation was impaired in the nucleus of *Pcnt*$^{\Delta/\Delta}$ cells which was not observed in the immunoblot analyses of CHK1 activation from whole cell extracts (Figure 5.6). To confirm the results, we

next performed the immunoblotting analyses of nuclear and cytoplasmic fractions after DNA damage. SCC1 and Actin were used as the markers of nuclear and cytoplasmic fractions, respectively. The nuclear and cytoplasmic proteins were fractionated successfully and we found CHK1 localised in both fractions (Figure 5.9A). phospho-CHK1 was also found in nucleus and cytoplasm but several bands were observed in nucleus (Figure 5.9B). To exclude the non-specific reactivity of the antibodies, we tested the CHK1 and phospho-CHK1 (Ser345) by using samples from

WT and *Chk1*$^{-/-}$ cells. We did not detect any signals for the two antibodies in *Chk1*$^{-/-}$ cells (Figure 5.9B). Therefore, it is possible that CHK1 is activated in a different manner in nucleus and cytoplasm. Those with bigger size might be multiply phosphorylated or ubiquitylated CHK1. Those with smaller size might be due to degradation of phospho-CHK1. The activation of CHK1 in cytoplasm was identical between the different cell lines and similar to what we saw in whole cell extracts (Figure 5.6). No matter how many isoforms of phospho-CHK1 exist in nucleus, the overall signal of phospho-CHK1 in nucleus was much weaker in *Pcnt*$^{\Delta/\Delta}$ cells than in

WT cells over time after IR. The signals of phospho-CHK1 in nucleus were a little stronger in *Mcph1*$^{-/-}$ cells but they were restored to WT levels in double knockout cells (Figure 5.9C). Taken together with the immunofluorescence microscopy results, we conclude that pericentrin is required for efficient CHK1 activation in nucleus after DNA damage.

5.6 Discussion

5.6.1 Neither *Pcnt* nor *Mcph1* deficiency impacts on G2/M checkpoint

When DNA damage or replication errors occur, the cell cycle is delayed or arrested by multiple checkpoints, which provides cells with additional time to complete replication and repair damaged DNA. These checkpoints ensure the faithful transmission of fully replicated and undamaged genome to the daughter cells. There are several cell cycle checkpoints. The G1/S checkpoint, which is p53-mediated, blocks entry to S phase in order to avoid replicating damaged DNA (Bates and Vousden, 1996). The G2/M checkpoint prevents cells with damaged genomes from entering mitosis, so that genomic integrity is maintained after cell division (O'Connell et al., 2000). Many proteins are involved in cell cycle checkpoint pathways. It is generally believed that CHK2 is primarily activated by DNA DSBs via ATM, whereas CHK1 is activated by diverse stimuli such as stalled replication forks and UV via both ATR and ATM (Abraham, 2001).

Since the G1/S checkpoint is absent in DT40 cells due to the lack of functional p53, WT DT40 cells are always arrested at G2 phase after IR damage through activated G2/M checkpoints (Takao et al., 1999). Previous studies have suggested that mutations in *PCNT* caused defective ATR-dependent DNA damage signaling because UV-induced but not IR-induced G2/M checkpoint arrest were affected in both *PCNT*-mutant and *PCNT*-deficient cells (Griffith et al., 2008). However, *Pcnt*$^{\Delta/\Delta}$ cells were arrested as efficiently as WT cells after IR treatment, indicating that *Pcnt* is not required for G2/M checkpoint activation in DT40 dells. Although one could

argue that the effect of pericentrin on G2/M checkpoint might be also UV-dependent in DT40 cells, this does not appear to be the case. Recent evidence has shown that ATR is activated via ATM and that both ATM and ATR are required for CHK1 phosphorylation in response to DSBs (Jazayeri et al., 2006). Moreover, IR failed to induce measurable mitotic delay in *Chk1*$^{-/-}$ DT40 cells but did so in *Chk2*$^{-/-}$ cells (Rainey et al., 2008; Zachos et al., 2007). Thus ATR-dependent DNA damage signaling can be activated by IR in DT40 cells. In addition, the kinetics of the phosphorylation of CHK1 and its downstream factors after UV irradiation were identical between WT and *Pcnt*$^{\Delta/\Delta}$ cells, indicating that the UV-induced G2/M checkpoint is also intact in *Pcnt*$^{\Delta/\Delta}$ cells.

It has been reported that transient G2/M arrest following exposure to IR was severely impaired in *MCPH1*-depleted U2OS cells (Lin et al., 2005; Xu et al., 2004). However, an elevated proportion of cells entering mitosis were not observed in *MCPH1* patient cells after IR damage (Gavvovidis et al., 2010; Neitzel et al., 2002). In fact, these irradiated *MCPH1* patient cells showed a delay in release from G2/M checkpoint arrest (Gavvovidis et al., 2010). Moreover, the IR-induced G2/M checkpoint was unaffected in *Mcph1*-deficient mouse fibroblasts in which the BRCT domains of *Mcph1* were deleted (Trimborn et al., 2010). Our previous studies also demonstrated that IR-induced G2/M checkpoint was intact in *Mcph1*$^{-/-}$ DT40 cells (Brown et al., 2010). Here, we found that the G2/M checkpoint was still functional even when both *Pcnt* and *Mcph1* were disrupted. We conclude that neither *Pcnt* nor *Mcph1* is required for the G2/M checkpoint. One possibility is that the defective G2/M checkpoint observed in *MCPH1*-depleted U2OS cells may be caused by the off-target effects of siRNA. It is also possible that the knockouts or patient cells have adapted to the absence of *Pcnt* and *Mcph1*.

5.6.2 Pericentrin limits IR-induced centrosome hyperamplification in *Mcph1*-deficient cells

The precise duplication of centrosomes must be tightly coupled with the cell cycle to ensure faithful transmission of the genome to the daughter cells. If cell cycle progression is perturbed, cells may acquire abnormal numbers of centrosomes. Supernumerary centrosomes can result in multipolar spindle formation which in turn leads to abnormal chromosome segregation and aneuploidy (Brinkley, 2001; Ganem et al., 2009; Sluder and Nordberg, 2004). Thus centrosome amplification, a common characteristic of tumour cells, is thought to contribute to the genomic instability in cancer (Fukasawa, 2005).

Centrosome amplification also frequently occurs in response to DNA damage. It is plausible that centrosome amplification works as a backup checkpoint to eliminate damaged cells by mitotic catastrophe (Dodson et al., 2004; Sato et al., 2000). Depletion of *MCPH1* resulted in centrosome amplification and subsequent mitotic spindle malformation in U2OS cell (Rai et al., 2008). Our previous studies also showed that *Mcph1*$^{-/-}$ DT40 cells contained supernumerary centrosomes after exposure to IR (Brown et al., 2010), which is in agreement with observations in *MCPH1* patient cells (Alderton et al., 2006). Interesting, the IR-induced centrosome amplification was restored to WT levels if *Pcnt* was abolished in *Mcph1*$^{-/-}$ cells, although *Pcnt*$^{\Delta/\Delta}$ cells also showed similar proportion of amplified centrosomes.

Mostly, centrosome amplification has been interpreted as a consequence of cell cycle defects. It was first reported by Balczon et al. that centrosomes overduplicated during hydroxyurea-induced S phase arrest in some mammalian cells (Balczon et al., 1995). Failure in cytokinesis also led to numerical centrosome aberrations (Meraldi et al., 2002). Our group has suggested that centrosome amplification occurs during an extended G2/M arrest after DNA damage induced by irradiation (Dodson et al., 2004). Our data suggest that there is a genetic relationship between *Pcnt* and *Mcph1* in response to DNA damage. We and other groups have shown that signaling to CHK1 and CHK1 catalytic activity are necessary for efficient DNA damage-induced

centrosome amplification after IR (Bourke et al., 2007; Dodson et al., 2004; Loffler et al., 2007). Therefore, the altered CHK1 activation caused by *Pcnt* deficiency may explain why the IR-induced centrosome amplification in *Mcph1*$^{-/-}$ cells was restored to WT levels in double knockouts.

5.6.3 Pericentrin is required for an efficient CHK1 response to IR

CHK1 was first identified in the fission yeast (Walworth et al., 1993). Disruption of CHK1 function in yeast, mammalian and chicken cells causes the cells to bypass the G2/M checkpoint and enter mitosis with damaged DNA (Liu et al., 2000; Takai et al., 2000; Walworth et al., 1993; Zachos et al., 2007). The current model proposes that CHK1 works as the critical mediator of the DNA damage response. Inhibition of CDC25 phosphatases by CHK1/2 prevents cyclin B-CDK1 activation which is required for the initiation of mitosis (Bartek and Lukas, 2003). However, it remains controversial whether CHK1 inhibits CDK1 at the centrosome or in the nucleus before the G2/M transition.

CDK1 and cyclin B were previously shown to accumulate at centrosomes during interphase (Bailly et al., 1992) and their activation initiates on centrosomes in prophase (Jackman et al., 2003). Kramer et al. found that CHK1 localised to centrosomes in interphase and disappeared in mitosis in U2OS cells by immunofluorescence microscopy using a monoclonal anti-CHK1 antibody (DCS-310). Therefore, they proposed that CDK1 was inactivated by centrosome-associated CHK1 until CHK1 dissociated from the centrosome at the onset of mitosis (Kramer et al., 2004). A similar observation was also described in mouse neuroprogenitors (Gruber et al., 2011). In addition, the forced immobilisation of kinase-dead CHK1 within centrosomes by fusing it to the PACT domain induced the premature activation of CDK1 at centrosomes (Kramer et al., 2004). As pericentrin is one of two proteins containing the PACT domain and as it localises at centrosomes, it is reasonable to speculate that pericentrin contributes to the centrosomal

localisation of CHK1. Indeed, centrosomal CHK1 was lost in *PCNT*-deficient cells (Tibelius et al., 2009).

However, a very recent study has demonstrated that CHK1 localises in the nucleus but not at the centrosomes in mouse embryonic fibroblasts and human colon adenocarcinoma cells. Mitotic entry was delayed by forced nuclear localisation of the CHK1 mutant (Matsuyama et al., 2011). The centrosomal reactivity of anti-CHK1 antibody (DCS-310) appears to be partly due to its cross reactivity with another protein, Ccdc151 (Matsuyama et al., 2011). It is interesting that the CHK1-PACT fusion protein was also detected in the nucleus and mitotic entry was delayed in cells with high expression levels of CHK1-PACT. In agreement with its nuclear localisation, an NLS and an NES sequences have been described in CHK1 (Dunaway et al., 2005). It has also been reported that pericentrin contains five NESs and an NLS (Liu et al., 2010). Thus, it is possible that pericentrin is also involved in the nuclear localisation of CHK1.

In unperturbed DT40 cells, it was shown that CHK1-GFP fusion protein localised at kinetochores in prometaphase cells. CHK1 disappeared during metaphase and anaphase but reappeared at the midbody during cytokinesis (Zachos et al., 2007). Consistently, our fractionation experiments demonstrated that CHK1 localises in both nucleus and cytoplasm. As we cannot examine the subcellular localisation of CHK1 by immunofluorescence microscopy, we assessed CHK1 function in $Pcnt^{\Delta/\Delta}$ cells by monitoring the activation of its downstream targets and itself after DNA damage. CHK1, CDK1 and CDK2 were all efficiently phosphorylated in $Pcnt^{\Delta/\Delta}$ cells after either IR or UV treatment, suggesting that *Pcnt* deficiency may not impact on CHK1 activation or its phosphorylation activity. Since the total soluble protein from the whole cell extracts may not reveal the actual kinetics of CHK1 activation in the cells, we examined CHK1 activation *in situ* after exposure to IR by immuno-fluorescence microscopy using anti-phospho-CHK1 (Ser345) antibody.

CHK1 is phosphorylated on multiple C-terminal residues, including Ser317 and Ser345 in response to a variety of genotoxic insults (Jiang et al., 2003; Liu et al., 2000; Zhao and Piwnica-Worms, 2001). Ser345 is essential for CHK1 function whereas Ser317 may play a contributory role (Walker et al., 2009; Wilsker et al., 2008). CHK1 is also physiologically activated in unperturbed cells (Jiang et al., 2003; Kramer et al., 2004; Smits et al., 2006; Wilsker et al., 2008). Like CHK1, phosphorylated CHK1 has been reported to accumulate preferentially at centrosomes in some studies (Loffler et al., 2007; Niida et al., 2007; Wilsker et al., 2008) but not all (Jiang et al., 2003; Smits et al., 2006). We observed that phospho-CHK1 formed foci which colocalised with γ-H2AX in the nucleus of interphase cells and disappeared in mitotic cells. We did not find any centrosomal signal of phospho-CHK1 (Ser345) either in $Pcnt^{\Delta/\Delta}$ or in WT cells. The nuclear phospho-CHK1 foci are likely to contain several different isoforms of phospho-CHK1. In agreement with phospho-CHK1 being found in the cytoplasmic fraction, it has also been proposed that phosphorylation of CHK1 results in its release from chromatin to the cytoplasm, which is important for transmitting the DNA damage signal (Smits et al., 2006). The absence of detectable cytoplasmic phospho-CHK1 foci in our experiments may be because cytoplasmic phospho-CHK1 does not aggregate but distributes diffusely.

Nuclear foci of MCPH1 were formed rapidly and colocalised with IRIF of γ-H2AX and other numerous DNA damage response proteins associated with both ATM and ATR signaling pathways (Jeffers et al., 2008; Lin et al., 2005; Rai et al., 2006; Xu et al., 2004). In addition, MCPH1 has also been shown to colocalise with γ-tubulin throughout the cell cycle (Jeffers et al., 2008; Rai et al., 2008; Zhong et al., 2006). These data suggest that MCPH1 has nuclear and centrosomal functions. Thus, it is possible that MCPH1 may control or interact with CHK1. Consistently, the expression of *BRCA1* and *CHK1* decreased at both mRNA and protein levels in

MCPH1 knock-down cells (Lin et al., 2005; Xu et al., 2004). In addition, impaired centrosome localisation of CHK1 and decreased centrosomal CHK1 were also observed in *MCPH1*-deficient cells (Gruber et al., 2011; Tibelius et al., 2009). However, the expression of *BRCA1* and *CHK1* was normal in *Mcph1*-deficient mouse fibroblasts and in cells derived from microcephaly patients (Alderton et al., 2006; Trimborn et al., 2010). Therefore, the direct role of MCPH1 in regulation of CHK1 remains controversial. Our data showed that the CHK1 was activated in $Mcph1^{-/-}$ cells as efficiently as in WT cells. However, phospho-CHK1 foci intensity and nuclear phospho-CHK1 signals were significantly reduced in $Pcnt^{\Delta/\Delta}$ cells, consistent with pericentrin having a role in CHK1 activation. Thus, we proposed that CHK1 activation occurs on the centrosome. Once the CHK1 is activated, the phospho-CHK1 is disassociated from the centrosome and shuttled to the nucleus, where it regulates its downstream effectors. Pericentrin is likely to be required for CHK1 activation and migration. Although the CHK1 activation foci results are not fully consistent with those of centrosome amplification, we confirmed the genetic interaction between *Pcnt* and *Mcph1* as WT levels of phospho-CHK1 were seen in double knockout cells.

Chapter 6. Conclusions and future perspectives

In this study, we investigated the roles of vertebrate pericentrin in centrosome composition, cell cycle progression and DNA damage responses by using reverse genetics.

We analysed the chicken genome and cloned the chicken *Pcnt* cDNA, confirming its genomic locus. It has been demonstrated that there are two isoforms in human and three isoforms in mouse (Flory and Davis, 2003; Miyoshi et al., 2006a). However, we only cloned one isoform from the total mRNA of DT40 cells which we termed chicken full-length *Pcnt*. As we failed to generate the full-length product in a single PCR reaction, it cannot be excluded that there are other truncated isoforms in DT40 cells. Our structure-function analysis suggests that the best studied domain of pericentrin structure, the PACT domain, perhaps is not the only domain responsible for the centrosomal localisation of the protein (Gillingham and Munro, 2000). More work is required for analysis of pericentrin structure in detail, such as characterising of specific binding domains for each centrosome proteins. New anti-chicken pericentrin antibodies may help to identify the other isoforms in chicken.

We successfully substituted the endogenous promoter of *Pcnt* with the minimal tTA-responsive promoter and replaced the stop code with a FLAG-tag fragment. The expression of *Pcnt* was reduced to 2% of WT at the mRNA level and undetectable at the protein level, measured by real-time PCR and immunofluorescence microscopy, respectively. Since the two *PCNT* isoforms identified in human are encoded by alternatively spliced transcripts (Flory and Davis, 2003), it is reasonable to speculate that other potential isoforms are also impacted by the promoter removal.

We first examined the proliferation of *Pcnt*-deficient cells. *PCNT* mutations are associated with MOPD II, a growth retardation symptom, indicating that *Pcnt* may

be an essential gene (Rauch et al., 2008). However, our *Pcnt*$^{\Delta/\Delta}$ cells were viable but showed a growth delay compared to WT cells. Cell cycle analysis suggested that *Pcnt* deficiency caused a mitotic arrest, which was confirmed by live cell imaging. Depletion of pericentrin resulted in inhibition of S phase entry in primary human fibroblasts and diploid epithelial cells through the activation of the *p53*-dependent checkpoint (Mikule et al., 2007; Srsen et al., 2006). Consistently, we found similar proportion of S phase cells in WT and *Pcnt*$^{\Delta/\Delta}$ cells due to the absence of *p53* in DT40 cells. Although no direct evidence has shown that pericentrin deficiency leads to mitotic arrest, the defective mitotic spindles described in *PCNT* mutant cells indicate a disturbance of mitosis (Rauch et al., 2008), which is supported by our observations. We next checked the mitotic spindles in *Pcnt*$^{\Delta/\Delta}$ cells. Previous studies revealed that *PCNT* depletion resulted in abnormal morphology of the bipolar spindles (Lee and Rhee, 2011; Rauch et al., 2008). However, other studies reported that PCNT was not important for spindle formation in vertebrate cell lines (Dammermann and Merdes, 2002; Zimmerman et al., 2004). In this study, we showed that bipolar spindles were formed in *Pcnt*$^{\Delta/\Delta}$ cells but with a longer distance between the two poles. We concluded that these altered spindles contributed to the mitosis defect in *Pcnt*$^{\Delta/\Delta}$ cells.

As a centrosome scaffold protein, depletion of pericentrin causes centriole loss and centriole separation in human diploid epithelial cells (Mikule et al., 2007). Recently, it has been shown that pericentrin can be cleaved by separase and that it protects engaged centrioles from premature disengagement (Matsuo et al., 2012). Furthermore, pericentrin also prevents premature centrosome splitting by anchoring NEK2A at the centrosomes and suppressing its kinase activity (Matsuo et al., 2010). In addition, PLK1 phosphorylation of pericentrin is essential for recruitment of the PCM proteins for centrosome maturation (Lee and Rhee, 2011). Taken together, these results suggest that pericentrin is involved in centrosome duplication and centrosome structure. However, our detailed analysis by light and electron

microscopy showed that *Pcnt*-deficient centrosomes had a robust composition and ultrastructure. Although the centrosome constituents are not completely lost, it is possible that they are recruited to the centrosomes less efficiently due to the loss of *Pcnt*. We then determined the centrosomal levels of γ-tubulin and PCM-1 by immunofluorescence microscopy. Consistent with previous results (Griffith et al., 2008; Lee and Rhee, 2011), we observed reduced centrosomal levels of γ-tubulin but not PCM-1 on *Pcnt*-deficient centrosomes. It is interesting that overexpression of *Pcnt* increased centrosomal γ-tubulin in G1 cells, but not in G2 or mitotic cells.

Pericentrin is also involved in formation of cilia, a centrosome-derived structure. Pericentrin is a low abundance protein in proliferating cells but is preferentially expressed in quiescent G0 phase cells throughout the embryo (Miyoshi et al., 2006b). Pericentrin is localised to the base of primary cilia in multiple mouse embryonic tissues (Miyoshi et al., 2006b; Muhlhans et al., 2011) and is required for olfactory cilia assembly in mice (Miyoshi et al., 2009). Moreover, a mutation in the pericentrin gene causes abnormal interneuron migration to the olfactory bulb in mice (Endoh-Yamagami et al., 2010). Sensory cilia are absent or severely shortened in *d-plp* mutant flies (Martinez-Campos et al., 2004). Unfortunately, we were unable to investigate pericentrin function in ciliogenesis in our *Pcnt*-deficient cells because primary cilia are not assembled in lymphoid cells (Alieva and Vorobjev, 2004). However, pericentrin has been demonstrated to be required for primary cilia formation in cultured mammalian cells (Graser et al., 2007; Jurczyk et al., 2004).

It has been hypothesized that pericentrin may provide microtubule nucleation sites at the centrosome (Takahashi et al., 2002). Similar to spindle organisation, pericentrin has been shown to be required for microtubule organisation in some studies (Lee and Rhee, 2011; Zimmerman et al., 2004), but not all (Li et al., 2001; Srsen et al., 2006). As both γ-tubulin and PCM-1 play important roles in microtubule nucleation (Dammermann and Merdes, 2002), our quantification of centrosomal γ-tubulin, but

not PCM-1, supported the role of *Pcnt* in microtubule nucleation. The microtubule regrowth assay showed that astral microtubules efficiently nucleated in $Pcnt^{\Delta/\Delta}$ cells after their deploymerisation, suggesting that the *Pcnt*-deficient centrosomes retain MTOC functions. However, we found that $Pcnt^{\Delta/\Delta}$ cells had a defect in re-entry into the cell cycle after a mitotic arrest caused by microtubule poisons. It is likely that the SAC satisfaction is delayed in $Pcnt^{\Delta/\Delta}$ cells because the microtubules can not reach the kinetochores as efficiently as in WT cells. This also explains why $Pcnt^{\Delta/\Delta}$ cells spent a longer time completing mitosis than WT cells during the normal proliferation cycle. Although we failed to determine the microtubule extension rates by using the microtubule plus end marker EB1, we speculate that pericentrin plays an important role in SAC function through the organisation of kinetochore microtubules.

There are several other centrosome scaffold proteins, such as PCM-1, NuMA and AKAP450 (Zimmerman and Doxsey, 2000). AKAP450 is one of two proteins known to contain a PACT domain, suggesting it shares some similarities with pericentrin. It has been shown that both AKAP450 and pericentrin bind GCP-2 and play a role in microtubule nucleation in vertebrates and *Drosophila* (Kawaguchi and Zheng, 2004; Keryer et al., 2003; Takahashi et al., 2002). The mild defects in $Pcnt^{\Delta/\Delta}$ cells may be due to the compensation effects generated by other scaffold proteins and AKAP450 is the most conceivable candidate. Therefore, it may be worthwhile to disrupt *Pcnt* and *Akap450* simultaneously to characterise the PACT protein functions.

PCNT and *MCPH1* are linked to primary dwarfism. Furthermore, mutations in both genes lead to defective G2/M checkpoint (Alderton et al., 2006; Griffith et al., 2008). Therefore, we next targeted *Mcph1* in $Pcnt^{\Delta/\Delta}$ cells and investigated the function of pericentrin in DNA damage responses. To our surprise, $Pcnt^{\Delta/\Delta}$ cells, $Mcph1^{-/-}$ cells and double knockout cells were arrested at G2 phase as efficiently as WT cells after IR treatment, indicating that neither *Pcnt* nor *Mcph1* is required for G2/M checkpoint activation. Consistently, all three cell lines showed only moderate sensitivity to IR

damage (Brown et al., 2010). However, it is very interesting that the IR-induced centrosome hyperamplification was restored to WT levels if *Pcnt* was abolished in *Mcph1*$^{-/-}$ cells although *Pcnt*$^{\Delta/\Delta}$ cells also showed a similar proportion of amplified centrosomes. Since signaling to CHK1 and CHK1 catalytic activity are necessary for efficient DNA damage-induced centrosome amplification after IR (Bourke et al., 2007; Dodson et al., 2004; Loffler et al., 2007), it is possible that CHK1 activation depends on pericentrin. Although the kinetics of CHK1 and its downstream factors' phosphorylation after DNA damage were identical between WT and *Pcnt*$^{\Delta/\Delta}$ cells, CHK1 activation in nucleus was significantly impaired in *Pcnt*$^{\Delta/\Delta}$ cells. We conclude that there is a genetic interaction between *Pcnt* and *Mcph1* in the control of genome stability because nuclear CHK1 activation and amplified centrosomes, which were abnormal in either *Pcnt*$^{\Delta/\Delta}$ cells or *Mcph1*$^{-/-}$ cells, were at WT levels in the double knockout cells.

Current models propose that CHK1 activation occurs at centrosomes and depends on pericentrin (Rauch et al., 2008; Tibelius et al., 2009). MCPH1 can also target CHK1 to centrosomes but its recruitment is mediated by pericentrin (Tibelius et al., 2009). After CHK1 activation, phospho-CHK1 is shuttled to the nucleus. However, the centrosomal localisation of CHK1 remains under debate (Matsuyama et al., 2011). Thus, further studies are required to support this model, such as the identification of CHK1 subcellular localisation at centrosome in *Pcnt*$^{\Delta/\Delta}$ cells.

Taken together, our results demonstrate that *Pcnt*-deficient cells proceed through mitosis more slowly and are more sensitive to spindle poisons than controls. The centriolar ultrastructure of *Pcnt*-deficient cells is normal, but γ-tubulin was not recruited efficiently. Cell cycle arrest, centrosome amplification and survival rates after ionising radiation treatment were normal in *Pcnt*-deficient cells, but nuclear CHK1 activation was reduced. However, pericentrin deficiency abrogated the

centrosome hyperamplification noted in *Mcph1*$^{-/-}$ cells. Therefore, we propose that pericentrin controls genomic stability by both ensuring appropriate mitotic spindle activity and CHK1 activation after DNA damage.

References

Abdrakhmanov, I., Lodygin, D., Geroth, P., Arakawa, H., Law, A., Plachy, J., Korn, B., and Buerstedde, J.M. (2000). A large database of chicken bursal ESTs as a resource for the analysis of vertebrate gene function. Genome Res *10*, 2062-2069.

Abraham, R.T. (2001). Cell cycle checkpoint signaling through the ATM and ATR kinases. Genes Dev *15*, 2177-2196.

Adams, K.E., Medhurst, A.L., Dart, D.A., and Lakin, N.D. (2006). Recruitment of ATR to sites of ionising radiation-induced DNA damage requires ATM and components of the MRN protein complex. Oncogene *25*, 3894-3904.

Alderton, G.K., Galbiati, L., Griffith, E., Surinya, K.H., Neitzel, H., Jackson, A.P., Jeggo, P.A., and O'Driscoll, M. (2006). Regulation of mitotic entry by microcephalin and its overlap with ATR signalling. Nat Cell Biol *8*, 725-733.

Alderton, G.K., Joenje, H., Varon, R., Borglum, A.D., Jeggo, P.A., and O'Driscoll, M. (2004). Seckel syndrome exhibits cellular features demonstrating defects in the ATR-signalling pathway. Hum Mol Genet *13*, 3127-3138.

Alexandru, G., Uhlmann, F., Mechtler, K., Poupart, M.A., and Nasmyth, K. (2001). Phosphorylation of the cohesin subunit Scc1 by Polo/Cdc5 kinase regulates sister chromatid separation in yeast. Cell *105*, 459-472.

Alieva, I.B., and Vorobjev, I.A. (2004). Vertebrate primary cilia: a sensory part of centrosomal complex in tissue cells, but a "sleeping beauty" in cultured cells? Cell Biol Int *28*, 139-150.

Andersen, J.S., Wilkinson, C.J., Mayor, T., Mortensen, P., Nigg, E.A., and Mann, M. (2003). Proteomic characterization of the human centrosome by protein correlation profiling. Nature *426*, 570-574.

Andree, H.A., Reutelingsperger, C.P., Hauptmann, R., Hemker, H.C., Hermens, W.T., and Willems, G.M. (1990). Binding of vascular anticoagulant alpha (VAC alpha) to planar phospholipid bilayers. J Biol Chem *265*, 4923-4928.

Anitha, A., Nakamura, K., Yamada, K., Iwayama, Y., Toyota, T., Takei, N., Iwata, Y., Suzuki, K., Sekine, Y., Matsuzaki, H.*, et al.* (2008). Gene and expression analyses reveal enhanced expression of pericentrin 2 (PCNT2) in bipolar disorder. Biol Psychiatry *63*, 678-685.

Anitha, A., Nakamura, K., Yamada, K., Iwayama, Y., Toyota, T., Takei, N., Iwata, Y., Suzuki, K., Sekine, Y., Matsuzaki, H.*, et al.* (2009). Association studies and gene expression analyses of the DISC1-interacting molecules, pericentrin 2 (PCNT2) and DISC1-binding zinc finger protein (DBZ), with schizophrenia and with bipolar disorder. Am J Med Genet B Neuropsychiatr Genet *150B*, 967-976.

Arakawa, H. (2006). Excision of floxed-DNA sequences by transient induction of Mer-Cre-Mer. Subcell Biochem *40*, 347-349.

Arakawa, H., Bednar, T., Wang, M., Paul, K., Mladenov, E., Bencsik-Theilen, A.A., and Iliakis, G. (2012). Functional redundancy between DNA ligases I and III in DNA replication in vertebrate cells. Nucleic Acids Res *40*, 2599-2610.

Arakawa, H., and Buerstedde, J.M. (2006). Dt40 gene disruptions: a how-to for the design and the construction of targeting vectors. Subcell Biochem *40*, 1-9.

Arakawa, H., Lodygin, D., and Buerstedde, J.M. (2001). Mutant loxP vectors for selectable marker recycle and conditional knock-outs. BMC Biotechnol *1*, 1-7.

Arakawa, H., Saribasak, H., and Buerstedde, J.M. (2004). Activation-induced cytidine deaminase initiates immunoglobulin gene conversion and hypermutation by a common intermediate. PLoS Biol *2*, 967-974.

Arquint, C., Sonnen, K.F., Stierhof, Y.D., and Nigg, E.A. (2012). Cell-cycle-regulated expression of STIL controls centriole number in human cells. J Cell Sci *125*, 1342-1352.

Augustin, A., Spenlehauer, C., Dumond, H., Menissier-De Murcia, J., Piel, M., Schmit, A.C., Apiou, F., Vonesch, J.L., Kock, M., Bornens, M., *et al.* (2003). PARP-3 localizes preferentially to the daughter centriole and interferes with the G1/S cell cycle progression. J Cell Sci *116*, 1551-1562.

Azimzadeh, J., and Bornens, M. (2007). Structure and duplication of the centrosome. J Cell Sci *120*, 2139-2142.

Baba, T.W., Giroir, B.P., and Humphries, E.H. (1985). Cell lines derived from avian lymphomas exhibit two distinct phenotypes. Virology *144*, 139-151.

Badano, J.L., Teslovich, T.M., and Katsanis, N. (2005). The centrosome in human genetic disease. Nat Rev Genet *6*, 194-205.

Bahe, S., Stierhof, Y.D., Wilkinson, C.J., Leiss, F., and Nigg, E.A. (2005). Rootletin forms centriole-associated filaments and functions in centrosome cohesion. J Cell Biol *171*, 27-33.

Bailly, E., Pines, J., Hunter, T., and Bornens, M. (1992). Cytoplasmic accumulation of cyclin B1 in human cells: association with a detergent-resistant compartment and with the centrosome. J Cell Sci *101*, 529-545.

Bakkenist, C.J., and Kastan, M.B. (2003). DNA damage activates ATM through intermolecular autophosphorylation and dimer dissociation. Nature *421*, 499-506.

Balczon, R., Bao, L., Zimmer, W.E., Brown, K., Zinkowski, R.P., and Brinkley, B.R. (1995). Dissociation of centrosome replication events from cycles of DNA synthesis and mitotic division in hydroxyurea-arrested Chinese hamster ovary cells. J Cell Biol *130*, 105-115.

Bannigan, A., Lizotte-Waniewski, M., Riley, M., and Baskin, T.I. (2008). Emerging molecular mechanisms that power and regulate the anastral mitotic spindle of flowering plants. Cell Motil Cytoskeleton *65*, 1-11.

Barboule, N., Chadebech, P., Baldin, V., Vidal, S., and Valette, A. (1997). Involvement of p21 in mitotic exit after paclitaxel treatment in MCF-7 breast adenocarcinoma cell line. Oncogene *15*,

2867-2875.

Baron, M. (2002). Manic-depression genes and the new millennium: poised for discovery. Mol Psychiatry *7*, 342-358.

Baron, U., and Bujard, H. (2000). Tet repressor-based system for regulated gene expression in eukaryotic cells: principles and advances. Methods Enzymol *327*, 401-421.

Baron, U., Gossen, M., and Bujard, H. (1997). Tetracycline-controlled transcription in eukaryotes: novel transactivators with graded transactivation potential. Nucleic Acids Res *25*, 2723-2729.

Barr, A.R., and Gergely, F. (2007). Aurora-A: the maker and breaker of spindle poles. J Cell Sci *120*, 2987-2996.

Barr, A.R., Kilmartin, J.V., and Gergely, F. (2010). CDK5RAP2 functions in centrosome to spindle pole attachment and DNA damage response. J Cell Biol *189*, 23-39.

Barrera, J.A., Kao, L.R., Hammer, R.E., Seemann, J., Fuchs, J.L., and Megraw, T.L. (2010). CDK5RAP2 regulates centriole engagement and cohesion in mice. Dev Cell *18*, 913-926.

Bartek, J., Lukas, C., and Lukas, J. (2004). Checking on DNA damage in S phase. Nat Rev Mol Cell Biol *5*, 792-804.

Bartek, J., and Lukas, J. (2001). Pathways governing G1/S transition and their response to DNA damage. Febs Lett *490*, 117-122.

Bartek, J., and Lukas, J. (2003). Chk1 and Chk2 kinases in checkpoint control and cancer. Cancer Cell *3*, 421-429.

Bates, S., and Vousden, K.H. (1996). p53 in signaling checkpoint arrest or apoptosis. Curr Opin Genet Dev *6*, 12-18.

Bekier, M.E., Fischbach, R., Lee, J., and Taylor, W.R. (2009). Length of mitotic arrest induced by microtubule-stabilizing drugs determines cell death after mitotic exit. Mol Cancer Ther *8*, 1646-1654.

Belmont, L.D., Hyman, A.A., Sawin, K.E., and Mitchison, T.J. (1990). Real-time visualization of cell cycle-dependent changes in microtubule dynamics in cytoplasmic extracts. Cell *62*, 579-589.

Bernal, J.A., and Venkitaraman, A.R. (2011). A vertebrate N-end rule degron reveals that Orc6 is required in mitosis for daughter cell abscission. J Cell Biol *192*, 969-978.

Besson, A., Dowdy, S.F., and Roberts, J.M. (2008). CDK inhibitors: cell cycle regulators and beyond. Dev Cell *14*, 159-169.

Bharadwaj, R., and Yu, H. (2004). The spindle checkpoint, aneuploidy, and cancer. Oncogene *23*, 2016-2027.

Boardman, P.E., Sanz-Ezquerro, J., Overton, I.M., Burt, D.W., Bosch, E., Fong, W.T., Tickle, C., Brown, W.R., Wilson, S.A., and Hubbard, S.J. (2002). A comprehensive collection of chicken cDNAs. Curr Biol *12*, 1965-1969.

Bourke, E., Brown, J.A., Takeda, S., Hochegger, H., and Morrison, C.G. (2010). DNA damage

induces Chk1-dependent threonine-160 phosphorylation and activation of Cdk2. Oncogene *29*, 616-624.

Bourke, E., Dodson, H., Merdes, A., Cuffe, L., Zachos, G., Walker, M., Gillespie, D., and Morrison, C.G. (2007). DNA damage induces Chk1-dependent centrosome amplification. Embo Rep *8*, 603-609.

Brinkley, B.R. (2001). Managing the centrosome numbers game: from chaos to stability in cancer cell division. Trends Cell Biol *11*, 18-21.

Brito, D.A., and Rieder, C.L. (2006). Mitotic checkpoint slippage in humans occurs via cyclin B destruction in the presence of an active checkpoint. Curr Biol *16*, 1194-1200.

Brown, J.A., Bourke, E., Liptrot, C., Dockery, P., and Morrison, C.G. (2010). MCPH1/BRIT1 limits ionizing radiation-induced centrosome amplification. Oncogene *29*, 5537-5544.

Brunk, K., Vernay, B., Griffith, E., Reynolds, N.L., Strutt, D., Ingham, P.W., and Jackson, A.P. (2007). Microcephalin coordinates mitosis in the syncytial Drosophila embryo. J Cell Sci *120*, 3578-3588.

Buchman, J.J., Tseng, H.C., Zhou, Y., Frank, C.L., Xie, Z., and Tsai, L.H. (2010). Cdk5rap2 interacts with pericentrin to maintain the neural progenitor pool in the developing neocortex. Neuron *66*, 386-402.

Budhu, A.S., and Wang, X.W. (2005). Loading and unloading: orchestrating centrosome duplication and spindle assembly by Ran/Crm1. Cell Cycle *4*, 1510-1514.

Buerstedde, J.M., Reynaud, C.A., Humphries, E.H., Olson, W., Ewert, D.L., and Weill, J.C. (1990). Light chain gene conversion continues at high rate in an ALV-induced cell line. Embo J *9*, 921-927.

Buerstedde, J.M., and Takeda, S. (1991). Increased ratio of targeted to random integration after transfection of chicken B cell lines. Cell *67*, 179-188.

Bulavin, D.V., Higashimoto, Y., Popoff, I.J., Gaarde, W.A., Basrur, V., Potapova, O., Appella, E., and Fornace, A.J., Jr. (2001). Initiation of a G2/M checkpoint after ultraviolet radiation requires p38 kinase. Nature *411*, 102-107.

Campisi, J., and d'Adda di Fagagna, F. (2007). Cellular senescence: when bad things happen to good cells. Nat Rev Mol Cell Biol *8*, 729-740.

Cannon, T.D., Hennah, W., van Erp, T.G., Thompson, P.M., Lonnqvist, J., Huttunen, M., Gasperoni, T., Tuulio-Henriksson, A., Pirkola, T., Toga, A.W., *et al.* (2005). Association of DISC1/TRAX haplotypes with schizophrenia, reduced prefrontal gray matter, and impaired short- and long-term memory. Arch Gen Psychiatry *62*, 1205-1213.

Chen, D., Purohit, A., Halilovic, E., Doxsey, S.J., and Newton, A.C. (2004). Centrosomal anchoring of protein kinase C betaII by pericentrin controls microtubule organization, spindle function, and cytokinesis. J Biol Chem *279*, 4829-4839.

Chipuk, J.E., and Green, D.R. (2006). Dissecting p53-dependent apoptosis. Cell Death Differ *13*,

994-1002.

Choi, J.H., Lindsey-Boltz, L.A., Kemp, M., Mason, A.C., Wold, M.S., and Sancar, A. (2010a). Reconstitution of RPA-covered single-stranded DNA-activated ATR-Chk1 signaling. Proc Natl Acad Sci U S A *107*, 13660-13665.

Choi, Y.K., Liu, P., Sze, S.K., Dai, C., and Qi, R.Z. (2010b). CDK5RAP2 stimulates microtubule nucleation by the gamma-tubulin ring complex. J Cell Biol *191*, 1089-1095.

Chretien, D., Buendia, B., Fuller, S.D., and Karsenti, E. (1997). Reconstruction of the centrosome cycle from cryoelectron micrographs. J Struct Biol *120*, 117-133.

Chretien, D., Fuller, S.D., and Karsenti, E. (1995). Structure of growing microtubule ends: two-dimensional sheets close into tubes at variable rates. J Cell Biol *129*, 1311-1328.

Ciccia, A., and Elledge, S.J. (2010). The DNA damage response: making it safe to play with knives. Mol Cell *40*, 179-204.

Ciciarello, M., Mangiacasale, R., Casenghi, M., Zaira Limongi, M., D'Angelo, M., Soddu, S., Lavia, P., and Cundari, E. (2001). p53 displacement from centrosomes and p53-mediated G1 arrest following transient inhibition of the mitotic spindle. J Biol Chem *276*, 19205-19213.

Ciliberto, A., and Shah, J.V. (2009). A quantitative systems view of the spindle assembly checkpoint. Embo J *28*, 2162-2173.

Collado, M., Blasco, M.A., and Serrano, M. (2007). Cellular senescence in cancer and aging. Cell *130*, 223-233.

Cuschieri, L., Nguyen, T., and Vogel, J. (2007). Control at the cell center: the role of spindle poles in cytoskeletal organization and cell cycle regulation. Cell Cycle *6*, 2788-2794.

Dammermann, A., and Merdes, A. (2002). Assembly of centrosomal proteins and microtubule organization depends on PCM-1. J Cell Biol *159*, 255-266.

Dantas, T.J., Wang, Y., Lalor, P., Dockery, P., and Morrison, C.G. (2011). Defective nucleotide excision repair with normal centrosome structures and functions in the absence of all vertebrate centrins. J Cell Biol *193*, 307-318.

Delaval, B., and Doxsey, S.J. (2009). Pericentrin in cellular function and disease. J Cell Biol *188*, 181-190.

Dictenberg, J.B., Zimmerman, W., Sparks, C.A., Young, A., Vidair, C., Zheng, Y., Carrington, W., Fay, F.S., and Doxsey, S.J. (1998). Pericentrin and gamma-tubulin form a protein complex and are organized into a novel lattice at the centrosome. J Cell Biol *141*, 163-174.

Diviani, D., Langeberg, L.K., Doxsey, S.J., and Scott, J.D. (2000). Pericentrin anchors protein kinase A at the centrosome through a newly identified RII-binding domain. Curr Biol *10*, 417-420.

Dodson, H., Bourke, E., Jeffers, L.J., Vagnarelli, P., Sonoda, E., Takeda, S., Earnshaw, W.C., Merdes, A., and Morrison, C. (2004). Centrosome amplification induced by DNA damage occurs during a prolonged G2 phase and involves ATM. Embo J *23*, 3864-3873.

Dodson, H., Wheatley, S.P., and Morrison, C.G. (2007). Involvement of centrosome amplification in radiation-induced mitotic catastrophe. Cell Cycle *6*, 364-370.

Dohmen, R.J., Wu, P., and Varshavsky, A. (1994). Heat-inducible degron: a method for constructing temperature-sensitive mutants. Science *263*, 1273-1276.

Doubilet, S., and McKim, K.S. (2007). Spindle assembly in the oocytes of mouse and Drosophila--similar solutions to a problem. Chromosome Res *15*, 681-696.

Doxsey, S. (2001). Re-evaluating centrosome function. Nat Rev Mol Cell Biol *2*, 688-698.

Doxsey, S.J., Stein, P., Evans, L., Calarco, P.D., and Kirschner, M. (1994). Pericentrin, a highly conserved centrosome protein involved in microtubule organization. Cell *76*, 639-650.

Duensing, A., Liu, Y., Tseng, M., Malumbres, M., Barbacid, M., and Duensing, S. (2006). Cyclin-dependent kinase 2 is dispensable for normal centrosome duplication but required for oncogene-induced centrosome overduplication. Oncogene *25*, 2943-2949.

Dunaway, S., Liu, H.Y., and Walworth, N.C. (2005). Interaction of 14-3-3 protein with Chk1 affects localization and checkpoint function. J Cell Sci *118*, 39-50.

Dutertre, S., Cazales, M., Quaranta, M., Froment, C., Trabut, V., Dozier, C., Mirey, G., Bouche, J.P., Theis-Febvre, N., Schmitt, E.*, et al.* (2004). Phosphorylation of CDC25B by Aurora-A at the centrosome contributes to the G2-M transition. J Cell Sci *117*, 2523-2531.

Ekholm, S.V., and Reed, S.I. (2000). Regulation of G(1) cyclin-dependent kinases in the mammalian cell cycle. Curr Opin Cell Biol *12*, 676-684.

Elledge, S.J., and Harper, J.W. (1998). The role of protein stability in the cell cycle and cancer. Biochim Biophys Acta *1377*, M61-70.

Endoh-Yamagami, S., Karkar, K.M., May, S.R., Cobos, I., Thwin, M.T., Long, J.E., Ashique, A.M., Zarbalis, K., Rubenstein, J.L.R., and Peterson, A.S. (2010). A mutation in the pericentrin gene causes abnormal interneuron migration to the olfactory bulb in mice. Dev Biol *340*, 41-53.

Falck, J., Mailand, N., Syljuasen, R.G., Bartek, J., and Lukas, J. (2001). The ATM-Chk2-Cdc25A checkpoint pathway guards against radioresistant DNA synthesis. Nature *410*, 842-847.

Faragher, A.J., and Fry, A.M. (2003). Nek2A kinase stimulates centrosome disjunction and is required for formation of bipolar mitotic spindles. Mol Biol Cell *14*, 2876-2889.

Fletcher, L., Cerniglia, G.J., Nigg, E.A., Yend, T.J., and Muschel, R.J. (2004). Inhibition of centrosome separation after DNA damage: a role for Nek2. Radiat Res *162*, 128-135.

Flory, M., and Davis, T.N. (2003). The centrosomal proteins pericentrin and kendrin are encoded by alternatively spliced products of one gene. Genomics *82*, 401-405.

Flory, M.R., Morphew, M., Joseph, J.D., Means, A.R., and Davis, T.N. (2002). Pcp1p, an Spc110p-related calmodulin target at the centrosome of the fission yeast Schizosaccharomyces pombe. Cell Growth Differ *13*, 47-58.

Flory, M.R., Moser, M.J., Monnat, R.J., Jr., and Davis, T.N. (2000). Identification of a human

centrosomal calmodulin-binding protein that shares homology with pericentrin. Proc Natl Acad Sci U S A *97*, 5919-5923.

Fong, C.S., Sato, M., and Toda, T. (2009). Fission yeast Pcp1 links polo kinase-mediated mitotic entry to γ-tubulin-dependent spindle formation. Embo J *29*, 120-130.

Fornerod, M., Ohno, M., Yoshida, M., and Mattaj, I.W. (1997). CRM1 is an export receptor for leucine-rich nuclear export signals. Cell *90*, 1051-1060.

Friedberg, E.C. (2003). DNA damage and repair. Nature *421*, 436-440.

Fry, A.M. (2002). The Nek2 protein kinase: a novel regulator of centrosome structure. Oncogene *21*, 6184-6194.

Fry, A.M., Meraldi, P., and Nigg, E.A. (1998). A centrosomal function for the human Nek2 protein kinase, a member of the NIMA family of cell cycle regulators. Embo J *17*, 470-481.

Fujimori, A., Tachiiri, S., Sonoda, E., Thompson, L.H., Dhar, P.K., Hiraoka, M., Takeda, S., Zhang, Y., Reth, M., and Takata, M. (2001). Rad52 partially substitutes for the Rad51 paralog XRCC3 in maintaining chromosomal integrity in vertebrate cells. Embo J *20*, 5513-5520.

Fukagawa, T., Regnier, V., and Ikemura, T. (2001). Creation and characterization of temperature-sensitive CENP-C mutants in vertebrate cells. Nucleic Acids Res *29*, 3796-3803.

Fukasawa, K. (2005). Centrosome amplification, chromosome instability and cancer development. Cancer Lett *230*, 6-19.

Fukasawa, K., Choi, T., Kuriyama, R., Rulong, S., and Vande Woude, G.F. (1996). Abnormal centrosome amplification in the absence of p53. Science *271*, 1744-1747.

Fung, T.K., and Poon, R.Y. (2005). A roller coaster ride with the mitotic cyclins. Semin Cell Dev Biol *16*, 335-342.

Gadde, S., and Heald, R. (2004). Mechanisms and molecules of the mitotic spindle. Curr Biol *14*, R797-805.

Ganem, N.J., Godinho, S.A., and Pellman, D. (2009). A mechanism linking extra centrosomes to chromosomal instability. Nature *460*, 278-282.

Gavvovidis, I., Pohlmann, C., Marchal, J.A., Stumm, M., Yamashita, D., Hirano, T., Schindler, D., Neitzel, H., and Trimborn, M. (2010). MCPH1 patient cells exhibit delayed release from DNA damage-induced G2/M checkpoint arrest. Cell Cycle *9*, 4893-4899.

Gillingham, A.K., and Munro, S. (2000). The PACT domain, a conserved centrosomal targeting motif in the coiled-coil proteins AKAP450 and pericentrin. Embo Rep *1*, 524-529.

Gitig, D.M., and Koff, A. (2000). Cdk pathway: cyclin-dependent kinases and cyclin-dependent kinase inhibitors. Methods Mol Biol *142*, 109-123.

Gorlich, D., and Kutay, U. (1999). Transport between the cell nucleus and the cytoplasm. Annu Rev Cell Dev Biol *15*, 607-660.

Goshima, G., Mayer, M., Zhang, N., Stuurman, N., and Vale, R.D. (2008). Augmin: a protein

complex required for centrosome-independent microtubule generation within the spindle. J Cell Biol *181*, 421-429.

Gossen, M., and Bujard, H. (1992). Tight control of gene expression in mammalian cells by tetracycline-responsive promoters. Proc Natl Acad Sci U S A *89*, 5547-5551.

Graser, S., Stierhof, Y.D., Lavoie, S.B., Gassner, O.S., Lamla, S., Le Clech, M., and Nigg, E.A. (2007a). Cep164, a novel centriole appendage protein required for primary cilium formation. J Cell Biol *179*, 321-330.

Graser, S., Stierhof, Y.D., and Nigg, E.A. (2007b). Cep68 and Cep215 (Cdk5rap2) are required for centrosome cohesion. J Cell Sci *120*, 4321-4331.

Griffin, C.S., Simpson, P.J., Wilson, C.R., and Thacker, J. (2000). Mammalian recombination-repair genes XRCC2 and XRCC3 promote correct chromosome segregation. Nat Cell Biol *2*, 757-761.

Griffith, E., Walker, S., Martin, C.A., Vagnarelli, P., Stiff, T., Vernay, B., Al Sanna, N., Saggar, A., Hamel, B., Earnshaw, W.C., *et al.* (2008). Mutations in pericentrin cause Seckel syndrome with defective ATR-dependent DNA damage signaling. Nat Genet *40*, 232-236.

Gromley, A., Jurczyk, A., Sillibourne, J., Halilovic, E., Mogensen, M., Groisman, I., Blomberg, M., and Doxsey, S. (2003). A novel human protein of the maternal centriole is required for the final stages of cytokinesis and entry into S phase. J Cell Biol *161*, 535-545.

Gruber, R., Zhou, Z., Sukchev, M., Joerss, T., Frappart, P.O., and Wang, Z.Q. (2011). MCPH1 regulates the neuroprogenitor division mode by coupling the centrosomal cycle with mitotic entry through the Chk1-Cdc25 pathway. Nat Cell Biol *13*, 1325-1334.

Guderian, G., Westendorf, J., Uldschmid, A., and Nigg, E.A. (2010). Plk4 trans-autophosphorylation regulates centriole number by controlling betaTrCP-mediated degradation. J Cell Sci *123*, 2163-2169.

Guillet, V., Knibiehler, M., Gregory-Pauron, L., Remy, M.H., Chemin, C., Raynaud-Messina, B., Bon, C., Kollman, J.M., Agard, D.A., Merdes, A., *et al.* (2011). Crystal structure of gamma-tubulin complex protein GCP4 provides insight into microtubule nucleation. Nat Struct Mol Biol *18*, 915-919.

Habedanck, R., Stierhof, Y.D., Wilkinson, C.J., and Nigg, E.A. (2005). The Polo kinase Plk4 functions in centriole duplication. Nat Cell Biol *7*, 1140-1146.

Hagting, A., Den Elzen, N., Vodermaier, H.C., Waizenegger, I.C., Peters, J.M., and Pines, J. (2002). Human securin proteolysis is controlled by the spindle checkpoint and reveals when the APC/C switches from activation by Cdc20 to Cdh1. J Cell Biol *157*, 1125-1137.

Hakem, R. (2008). DNA-damage repair; the good, the bad, and the ugly. Embo J *27*, 589-605.

Halazonetis, T.D., Gorgoulis, V.G., and Bartek, J. (2008). An oncogene-induced DNA damage model for cancer development. Science *319*, 1352-1355.

Hall, J.G., Flora, C., Scott, C.I., Jr., Pauli, R.M., and Tanaka, K.I. (2004). Majewski

osteodysplastic primordial dwarfism type II (MOPD II): natural history and clinical findings. Am J Med Genet A *130A*, 55-72.

Harbour, J.W., Luo, R.X., Dei Santi, A., Postigo, A.A., and Dean, D.C. (1999). Cdk phosphorylation triggers sequential intramolecular interactions that progressively block Rb functions as cells move through G1. Cell *98*, 859-869.

Haren, L., and Merdes, A. (2002). Direct binding of NuMA to tubulin is mediated by a novel sequence motif in the tail domain that bundles and stabilizes microtubules. J Cell Sci *115*, 1815-1824.

Haren, L., Stearns, T., and Luders, J. (2009). Plk1-dependent recruitment of gamma-tubulin complexes to mitotic centrosomes involves multiple PCM components. PLoS One *4*, e5976.

Harper, J.W., and Elledge, S.J. (2007). The DNA damage response: ten years after. Mol Cell *28*, 739-745.

Hashimoto, S., and Egly, J.M. (2009). Trichothiodystrophy view from the molecular basis of DNA repair/transcription factor TFIIH. Hum Mol Genet *18*, R224-230.

Heald, R., Tournebize, R., Blank, T., Sandaltzopoulos, R., Becker, P., Hyman, A., and Karsenti, E. (1996). Self-organization of microtubules into bipolar spindles around artificial chromosomes in Xenopus egg extracts. Nature *382*, 420-425.

Heald, R., Tournebize, R., Habermann, A., Karsenti, E., and Hyman, A. (1997). Spindle assembly in Xenopus egg extracts: respective roles of centrosomes and microtubule self-organization. J Cell Biol *138*, 615-628.

Hennah, W., Thomson, P., Peltonen, L., and Porteous, D. (2006). Genes and schizophrenia: beyond schizophrenia: the role of DISC1 in major mental illness. Schizophr Bull *32*, 409-416.

Herwig, S., and Strauss, M. (1997). The retinoblastoma protein: a master regulator of cell cycle, differentiation and apoptosis. Eur J Biochem *246*, 581-601.

Hildebrandt, F., and Otto, E. (2005). Cilia and centrosomes: a unifying pathogenic concept for cystic kidney disease? Nat Rev Genet *6*, 928-940.

Hinchcliffe, E.H., Li, C., Thompson, E.A., Maller, J.L., and Sluder, G. (1999). Requirement of Cdk2-cyclin E activity for repeated centrosome reproduction in Xenopus egg extracts. Science *283*, 851-854.

Hinchcliffe, E.H., Miller, F.J., Cham, M., Khodjakov, A., and Sluder, G. (2001). Requirement of a centrosomal activity for cell cycle progression through G1 into S phase. Science *291*, 1547-1550.

Hirano, T. (2006). At the heart of the chromosome: SMC proteins in action. Nat Rev Mol Cell Biol *7*, 311-322.

Hirota, T., Kunitoku, N., Sasayama, T., Marumoto, T., Zhang, D., Nitta, M., Hatakeyama, K., and Saya, H. (2003). Aurora-A and an interacting activator, the LIM protein Ajuba, are required for mitotic commitment in human cells. Cell *114*, 585-598.

Hochegger, H., Dejsuphong, D., Sonoda, E., Saberi, A., Rajendra, E., Kirk, J., Hunt, T., and

Takeda, S. (2007). An essential role for Cdk1 in S phase control is revealed via chemical genetics in vertebrate cells. J Cell Biol *178*, 257-268.

Hoffmann, I., Clarke, P.R., Marcote, M.J., Karsenti, E., and Draetta, G. (1993). Phosphorylation and activation of human cdc25-C by cdc2--cyclin B and its involvement in the self-amplification of MPF at mitosis. Embo J *12*, 53-63.

Holland, A.J., Lan, W., Niessen, S., Hoover, H., and Cleveland, D.W. (2010). Polo-like kinase 4 kinase activity limits centrosome overduplication by autoregulating its own stability. J Cell Biol *188*, 191-198.

Hornig, N.C., Knowles, P.P., McDonald, N.Q., and Uhlmann, F. (2002). The dual mechanism of separase regulation by securin. Curr Biol *12*, 973-982.

Howell, B.J., McEwen, B.F., Canman, J.C., Hoffman, D.B., Farrar, E.M., Rieder, C.L., and Salmon, E.D. (2001). Cytoplasmic dynein/dynactin drives kinetochore protein transport to the spindle poles and has a role in mitotic spindle checkpoint inactivation. J Cell Biol *155*, 1159-1172.

Hoyt, M.A., Totis, L., and Roberts, B.T. (1991). S. cerevisiae genes required for cell cycle arrest in response to loss of microtubule function. Cell *66*, 507-517.

Hudson, D.F., Morrison, C., Ruchaud, S., and Earnshaw, W.C. (2002). Reverse genetics of essential genes in tissue-culture cells: 'dead cells talking'. Trends Cell Biol *12*, 281-287.

Hurd, T.W., and Hildebrandt, F. (2011). Mechanisms of nephronophthisis and related ciliopathies. Nephron Exp Nephrol *118*, e9-14.

Hut, H.M., Lemstra, W., Blaauw, E.H., Van Cappellen, G.W., Kampinga, H.H., and Sibon, O.C. (2003). Centrosomes split in the presence of impaired DNA integrity during mitosis. Mol Biol Cell *14*, 1993-2004.

Hutchins, J.R., Toyoda, Y., Hegemann, B., Poser, I., Heriche, J.K., Sykora, M.M., Augsburg, M., Hudecz, O., Buschhorn, B.A., Bulkescher, J., *et al.* (2010). Systematic analysis of human protein complexes identifies chromosome segregation proteins. Science *328*, 593-599.

Inanc, B., Dodson, H., and Morrison, C.G. (2010). A centrosome-autonomous signal that involves centriole disengagement permits centrosome duplication in G2 phase after DNA damage. Mol Biol Cell *21*, 3866-3877.

Jackman, M., Lindon, C., Nigg, E.A., and Pines, J. (2003). Active cyclin B1-Cdk1 first appears on centrosomes in prophase. Nat Cell Biol *5*, 143-148.

Jackson, A.P., Eastwood, H., Bell, S.M., Adu, J., Toomes, C., Carr, I.M., Roberts, E., Hampshire, D.J., Crow, Y.J., Mighell, A.J., *et al.* (2002). Identification of microcephalin, a protein implicated in determining the size of the human brain. Am J Hum Genet *71*, 136-142.

Jackson, A.P., McHale, D.P., Campbell, D.A., Jafri, H., Rashid, Y., Mannan, J., Karbani, G., Corry, P., Levene, M.I., Mueller, R.F., *et al.* (1998). Primary autosomal recessive microcephaly (MCPH1) maps to chromosome 8p22-pter. Am J Hum Genet *63*, 541-546.

Jaken, S., and Parker, P.J. (2000). Protein kinase C binding partners. Bioessays *22*, 245-254.

Jakobsen, L., Vanselow, K., Skogs, M., Toyoda, Y., Lundberg, E., Poser, I., Falkenby, L.G., Bennetzen, M., Westendorf, J., Nigg, E.A., *et al.* (2011). Novel asymmetrically localizing components of human centrosomes identified by complementary proteomics methods. Embo J *30*, 1520-1535.

Jamieson, C.R., Govaerts, C., and Abramowicz, M.J. (1999). Primary autosomal recessive microcephaly: homozygosity mapping of MCPH4 to chromosome 15. Am J Hum Genet *65*, 1465-1469.

Jazayeri, A., Falck, J., Lukas, C., Bartek, J., Smith, G.C., Lukas, J., and Jackson, S.P. (2006). ATM- and cell cycle-dependent regulation of ATR in response to DNA double-strand breaks. Nat Cell Biol *8*, 37-45.

Jeffers, L.J., Coull, B.J., Stack, S.J., and Morrison, C.G. (2008). Distinct BRCT domains in Mcph1/Brit1 mediate ionizing radiation-induced focus formation and centrosomal localization. Oncogene *27*, 139-144.

Jiang, K., Pereira, E., Maxfield, M., Russell, B., Goudelock, D.M., and Sanchez, Y. (2003). Regulation of Chk1 includes chromatin association and 14-3-3 binding following phosphorylation on Ser-345. J Biol Chem *278*, 25207-25217.

Jin, J., Shirogane, T., Xu, L., Nalepa, G., Qin, J., Elledge, S.J., and Harper, J.W. (2003). SCFbeta-TRCP links Chk1 signaling to degradation of the Cdc25A protein phosphatase. Genes Dev *17*, 3062-3074.

Jordan, M.A., Thrower, D., and Wilson, L. (1992). Effects of vinblastine, podophyllotoxin and nocodazole on mitotic spindles. Implications for the role of microtubule dynamics in mitosis. J Cell Sci *102*, 401-416.

Jordan, M.A., Wendell, K., Gardiner, S., Derry, W.B., Copp, H., and Wilson, L. (1996). Mitotic block induced in HeLa cells by low concentrations of paclitaxel (Taxol) results in abnormal mitotic exit and apoptotic cell death. Cancer Res *56*, 816-825.

Jurczyk, A., Gromley, A., Redick, S., San Agustin, J., Witman, G., Pazour, G.J., Peters, D.J., and Doxsey, S. (2004). Pericentrin forms a complex with intraflagellar transport proteins and polycystin-2 and is required for primary cilia assembly. J Cell Biol *166*, 637-643.

Kalab, P., Pu, R.T., and Dasso, M. (1999). The ran GTPase regulates mitotic spindle assembly. Curr Biol *9*, 481-484.

Kaldis, P. (1999). The cdk-activating kinase (CAK): from yeast to mammals. Cell Mol Life Sci *55*, 284-296.

Kanai, M., Tong, W.M., Sugihara, E., Wang, Z.Q., Fukasawa, K., and Miwa, M. (2003). Involvement of poly(ADP-Ribose) polymerase 1 and poly(ADP-Ribosyl)ation in regulation of centrosome function. Mol Cell Biol *23*, 2451-2462.

Kanai, M., Uchida, M., Hanai, S., Uematsu, N., Uchida, K., and Miwa, M. (2000). Poly(ADP-ribose) polymerase localizes to the centrosomes and chromosomes. Biochem Biophys

Res Commun *278*, 385-389.

Kanemaki, M., Sanchez-Diaz, A., Gambus, A., and Labib, K. (2003). Functional proteomic identification of DNA replication proteins by induced proteolysis in vivo. Nature *423*, 720-724.

Kann, M.L., Soues, S., Levilliers, N., and Fouquet, J.P. (2003). Glutamylated tubulin: diversity of expression and distribution of isoforms. Cell Motil Cytoskeleton *55*, 14-25.

Kapoor, T.M., Mayer, T.U., Coughlin, M.L., and Mitchison, T.J. (2000). Probing spindle assembly mechanisms with monastrol, a small molecule inhibitor of the mitotic kinesin, Eg5. J Cell Biol *150*, 975-988.

Karsenti, E., and Vernos, I. (2001). The mitotic spindle: a self-made machine. Science *294*, 543-547.

Kastan, M.B., and Bartek, J. (2004). Cell-cycle checkpoints and cancer. Nature *432*, 316-323.

Katsetos, C.D., Reddy, G., Draberova, E., Smejkalova, B., Del Valle, L., Ashraf, Q., Tadevosyan, A., Yelin, K., Maraziotis, T., Mishra, O.P., *et al.* (2006). Altered cellular distribution and subcellular sorting of gamma-tubulin in diffuse astrocytic gliomas and human glioblastoma cell lines. J Neuropathol Exp Neurol *65*, 465-477.

Kawaguchi, S., and Zheng, Y. (2004). Characterization of a Drosophila centrosome protein CP309 that shares homology with Kendrin and CG-NAP. Mol Biol Cell *15*, 37-45.

Kawamura, K., Izumi, H., Ma, Z., Ikeda, R., Moriyama, M., Tanaka, T., Nojima, T., Levin, L.S., Fujikawa-Yamamoto, K., Suzuki, K., *et al.* (2004). Induction of centrosome amplification and chromosome instability in human bladder cancer cells by p53 mutation and cyclin E overexpression. Cancer Res *64*, 4800-4809.

Keryer, G., Di Fiore, B., Celati, C., Lechtreck, K.F., Mogensen, M., Delouvee, A., Lavia, P., Bornens, M., and Tassin, A.M. (2003a). Part of Ran is associated with AKAP450 at the centrosome: involvement in microtubule-organizing activity. Mol Biol Cell *14*, 4260-4271.

Keryer, G., Witczak, O., Delouvee, A., Kemmner, W.A., Rouillard, D., Tasken, K., and Bornens, M. (2003b). Dissociating the centrosomal matrix protein AKAP450 from centrioles impairs centriole duplication and cell cycle progression. Mol Biol Cell *14*, 2436-2446.

Khodjakov, A., and Rieder, C.L. (2001). Centrosomes enhance the fidelity of cytokinesis in vertebrates and are required for cell cycle progression. J Cell Biol *153*, 237-242.

Kiley, S.C., and Parker, P.J. (1995). Differential localization of protein kinase C isozymes in U937 cells: evidence for distinct isozyme functions during monocyte differentiation. J Cell Sci *108*, 1003-1016.

Kilmartin, J.V., and Goh, P.Y. (1996). Spc110p: assembly properties and role in the connection of nuclear microtubules to the yeast spindle pole body. Embo J *15*, 4592-4602.

Kim, H.S., Takahashi, M., Matsuo, K., and Ono, Y. (2007). Recruitment of CG-NAP to the Golgi apparatus through interaction with dynein-dynactin complex. Genes Cells *12*, 421-434.

Kim, J., Choi, Y.L., Vallentin, A., Hunrichs, B.S., Hellerstein, M.K., Peehl, D.M., and

Mochly-Rosen, D. (2008a). Centrosomal PKCbetaII and pericentrin are critical for human prostate cancer growth and angiogenesis. Cancer Res *68*, 6831-6839.

Kim, K., Lee, S., Chang, J., and Rhee, K. (2008b). A novel function of CEP135 as a platform protein of C-NAP1 for its centriolar localization. Exp Cell Res *314*, 3692-3700.

Kirschner, M., and Mitchison, T. (1986). Beyond self-assembly: from microtubules to morphogenesis. Cell *45*, 329-342.

Kitagawa, R., Bakkenist, C.J., McKinnon, P.J., and Kastan, M.B. (2004). Phosphorylation of SMC1 is a critical downstream event in the ATM-NBS1-BRCA1 pathway. Genes Dev *18*, 1423-1438.

Kleylein-Sohn, J., Westendorf, J., Le Clech, M., Habedanck, R., Stierhof, Y.D., and Nigg, E.A. (2007). Plk4-induced centriole biogenesis in human cells. Dev Cell *13*, 190-202.

Knop, M., and Schiebel, E. (1997). Spc98p and Spc97p of the yeast gamma-tubulin complex mediate binding to the spindle pole body via their interaction with Spc110p. Embo J *16*, 6985-6995.

Kollman, J.M., Merdes, A., Mourey, L., and Agard, D.A. (2011). Microtubule nucleation by gamma-tubulin complexes. Nat Rev Mol Cell Biol *12*, 709-721.

Komarova, Y.A., Vorobjev, I.A., and Borisy, G.G. (2002). Life cycle of MTs: persistent growth in the cell interior, asymmetric transition frequencies and effects of the cell boundary. J Cell Sci *115*, 3527-3539.

Kozlov, S.V., Graham, M.E., Peng, C., Chen, P., Robinson, P.J., and Lavin, M.F. (2006). Involvement of novel autophosphorylation sites in ATM activation. Embo J *25*, 3504-3514.

Kramer, A., Mailand, N., Lukas, C., Syljuasen, R.G., Wilkinson, C.J., Nigg, E.A., Bartek, J., and Lukas, J. (2004). Centrosome-associated Chk1 prevents premature activation of cyclin-B-Cdk1 kinase. Nat Cell Biol *6*, 884-891.

Kramer, A., Neben, K., and Ho, A.D. (2005). Centrosome aberrations in hematological malignancies. Cell Biol Int *29*, 375-383.

Kramer, E.R., Scheuringer, N., Podtelejnikov, A.V., Mann, M., and Peters, J.M. (2000). Mitotic regulation of the APC activator proteins CDC20 and CDH1. Mol Biol Cell *11*, 1555-1569.

Krek, W., Xu, G., and Livingston, D.M. (1995). Cyclin A-kinase regulation of E2F-1 DNA binding function underlies suppression of an S phase checkpoint. Cell *83*, 1149-1158.

Kumagai, A., Lee, J., Yoo, H.Y., and Dunphy, W.G. (2006). TopBP1 activates the ATR-ATRIP complex. Cell *124*, 943-955.

Kumar, A., Girimaji, S.C., Duvvari, M.R., and Blanton, S.H. (2009). Mutations in STIL, encoding a pericentriolar and centrosomal protein, cause primary microcephaly. Am J Hum Genet *84*, 286-290.

Kwon, M., Godinho, S.A., Chandhok, N.S., Ganem, N.J., Azioune, A., Thery, M., and Pellman, D. (2008). Mechanisms to suppress multipolar divisions in cancer cells with extra centrosomes.

Genes Dev *22*, 2189-2203.

Le Breton, M., Cormier, P., Belle, R., Mulner-Lorillon, O., and Morales, J. (2005). Translational control during mitosis. Biochimie *87*, 805-811.

Leal, G.F., Roberts, E., Silva, E.O., Costa, S.M., Hampshire, D.J., and Woods, C.G. (2003). A novel locus for autosomal recessive primary microcephaly (MCPH6) maps to 13q12.2. J Med Genet *40*, 540-542.

Lee, E.A., Keutmann, M.K., Dowling, M.L., Harris, E., Chan, G., and Kao, G.D. (2004). Inactivation of the mitotic checkpoint as a determinant of the efficacy of microtubule-targeted drugs in killing human cancer cells. Mol Cancer Ther *3*, 661-669.

Lee, J., Kumagai, A., and Dunphy, W.G. (2003). Claspin, a Chk1-regulatory protein, monitors DNA replication on chromatin independently of RPA, ATR, and Rad17. Mol Cell *11*, 329-340.

Lee, K., and Rhee, K. (2011). PLK1 phosphorylation of pericentrin initiates centrosome maturation at the onset of mitosis. J Cell Biol *195*, 1093-1101.

Leidel, S., Delattre, M., Cerutti, L., Baumer, K., and Gonczy, P. (2005). SAS-6 defines a protein family required for centrosome duplication in C. elegans and in human cells. Nat Cell Biol *7*, 115-125.

Lew, D.J., and Burke, D.J. (2003). The spindle assembly and spindle position checkpoints. Annu Rev Genet *37*, 251-282.

Li, Q., Hansen, D., Killilea, A., Joshi, H.C., Palazzo, R.E., and Balczon, R. (2001). Kendrin/pericentrin-B, a centrosome protein with homology to pericentrin that complexes with PCM-1. J Cell Sci *114*, 797-809.

Li, R., and Murray, A.W. (1991). Feedback control of mitosis in budding yeast. Cell *66*, 519-531.

Liang, Y., Gao, H., Lin, S.Y., Peng, G., Huang, X., Zhang, P., Goss, J.A., Brunicardi, F.C., Multani, A.S., Chang, S., *et al.* (2010). BRIT1/MCPH1 is essential for mitotic and meiotic recombination DNA repair and maintaining genomic stability in mice. PLoS Genet *6*, e1000826.

Lin, P.I., McInnis, M.G., Potash, J.B., Willour, V.L., Mackinnon, D.F., Miao, K., Depaulo, J.R., and Zandi, P.P. (2005a). Assessment of the effect of age at onset on linkage to bipolar disorder: evidence on chromosomes 18p and 21q. Am J Hum Genet *77*, 545-555.

Lin, S.Y., and Elledge, S.J. (2003). Multiple tumor suppressor pathways negatively regulate telomerase. Cell *113*, 881-889.

Lin, S.Y., Rai, R., Li, K., Xu, Z.X., and Elledge, S.J. (2005b). BRIT1/MCPH1 is a DNA damage responsive protein that regulates the Brca1-Chk1 pathway, implicating checkpoint dysfunction in microcephaly. Proc Natl Acad Sci U S A *102*, 15105-15109.

Lindahl, T., and Barnes, D.E. (2000). Repair of endogenous DNA damage. Cold Spring Harb Symp Quant Biol *65*, 127-133.

Lipska, B.K., Peters, T., Hyde, T.M., Halim, N., Horowitz, C., Mitkus, S., Weickert, C.S., Matsumoto, M., Sawa, A., Straub, R.E., *et al.* (2006). Expression of DISC1 binding partners is

reduced in schizophrenia and associated with DISC1 SNPs. Hum Mol Genet *15*, 1245-1258.

Liptrot, C., and Gull, K. (1992). Detection of viruses in recombinant cells by electron microscopy. In Animal Cell Technology: Development, Processes and Production, R.E. Spiers, J.B. Griffiths, and C. MacDonald, eds. (Oxford, Butterworth-Heinemann), pp. 653–657.

Liu, Q., Guntuku, S., Cui, X.S., Matsuoka, S., Cortez, D., Tamai, K., Luo, G., Carattini-Rivera, S., DeMayo, F., Bradley, A., *et al.* (2000). Chk1 is an essential kinase that is regulated by Atr and required for the G(2)/M DNA damage checkpoint. Genes Dev *14*, 1448-1459.

Liu, Q., Jiang, Q., and Zhang, C. (2009). A fraction of Crm1 locates at centrosomes by its CRIME domain and regulates the centrosomal localization of pericentrin. Biochem Biophys Res Commun *384*, 383-388.

Liu, Q., Yu, J., Zhuo, X., Jiang, Q., and Zhang, C. (2010). Pericentrin contains five NESs and an NLS essential for its nucleocytoplasmic trafficking during the cell cycle. Cell Res *20*, 948-962.

Lodish, H., Berk, A., Zipursky, S.L., Matsudaira, P., and Darnell, J. (2003). Molecular Cell Biology, Fifth Edition

Loffler, H., Bochtler, T., Fritz, B., Tews, B., Ho, A.D., Lukas, J., Bartek, J., and Kramer, A. (2007). DNA damage-induced accumulation of centrosomal Chk1 contributes to its checkpoint function. Cell Cycle *6*, 2541-2548.

Loncarek, J., Hergert, P., and Khodjakov, A. (2010). Centriole reduplication during prolonged interphase requires procentriole maturation governed by Plk1. Curr Biol *20*, 1277-1282.

Loncarek, J., Hergert, P., Magidson, V., and Khodjakov, A. (2008). Control of daughter centriole formation by the pericentriolar material. Nat Cell Biol *10*, 322-328.

Lopez-Girona, A., Tanaka, K., Chen, X.B., Baber, B.A., McGowan, C.H., and Russell, P. (2001). Serine-345 is required for Rad3-dependent phosphorylation and function of checkpoint kinase Chk1 in fission yeast. Proc Natl Acad Sci U S A *98*, 11289-11294.

Lukasiewicz, K.B., and Lingle, W.L. (2009). Aurora A, centrosome structure, and the centrosome cycle. Environ Mol Mutagen *50*, 602-619.

Lundberg, A.S., and Weinberg, R.A. (1998). Functional inactivation of the retinoblastoma protein requires sequential modification by at least two distinct cyclin-cdk complexes. Mol Cell Biol *18*, 753-761.

Mack, G., and Rattner, J.B. (1993). Centrosome repositioning immediately following karyokinesis and prior to cytokinesis. Cell Motil Cytoskeleton *26*, 239-247.

Mailand, N., Falck, J., Lukas, C., Syljuasen, R.G., Welcker, M., Bartek, J., and Lukas, J. (2000). Rapid destruction of human Cdc25A in response to DNA damage. Science *288*, 1425-1429.

Majewski, F., Ranke, M., and Schinzel, A. (1982). Studies of microcephalic primordial dwarfism II: the osteodysplastic type II of primordial dwarfism. Am J Med Genet *12*, 23-35.

Manke, I.A., Lowery, D.M., Nguyen, A., and Yaffe, M.B. (2003). BRCT repeats as phosphopeptide-binding modules involved in protein targeting. Science *302*, 636-639.

Mapelli, M., Filipp, F.V., Rancati, G., Massimiliano, L., Nezi, L., Stier, G., Hagan, R.S., Confalonieri, S., Piatti, S., Sattler, M., *et al.* (2006). Determinants of conformational dimerization of Mad2 and its inhibition by p31comet. Embo J *25*, 1273-1284.

Martinez-Campos, M., Basto, B., Baker, J., and M, K. (2004). The Drosophila pericentrin-like protein is essential for cilia/flagella function, but appears to be dispensable for mitosis. J Cell Biol *165*, 673-683.

Matsudo, H., Osano, K., Arakawa, H., and Ono, M. (2005). Effect of deletion of the DNase I hypersensitive sites on the transcription of chicken Ig-beta gene and on the maintenance of active chromatin state in the Ig-beta locus. Febs J *272*, 422-432.

Matsumoto, Y., and Maller, J.L. (2004). A centrosomal localization signal in cyclin E required for Cdk2-independent S phase entry. Science *306*, 885-888.

Matsuo, K., Nishimura, T., Hayakawa, A., Ono, Y., and Takahashi, M. (2010). Involvement of a centrosomal protein kendrin in the maintenance of centrosome cohesion by modulating Nek2A kinase activity. Biochem Biophys Res Commun *398*, 217-223.

Matsuo, K., Ohsumi, K., Iwabuchi, M., Kawamata, T., Ono, Y., and Takahashi, M. (2012). Kendrin Is a Novel Substrate for Separase Involved in the Licensing of Centriole Duplication. Curr Biol *27*, 589-605.

Matsushime, H., Ewen, M.E., Strom, D.K., Kato, J.Y., Hanks, S.K., Roussel, M.F., and Sherr, C.J. (1992). Identification and properties of an atypical catalytic subunit (p34PSK-J3/cdk4) for mammalian D type G1 cyclins. Cell *71*, 323-334.

Matsuura, S., Tauchi, H., Nakamura, A., Kondo, N., Sakamoto, S., Endo, S., Smeets, D., Solder, B., Belohradsky, B.H., Der Kaloustian, V.M., *et al.* (1998). Positional cloning of the gene for Nijmegen breakage syndrome. Nat Genet *19*, 179-181.

Matsuyama, M., Goto, H., Kasahara, K., Kawakami, Y., Nakanishi, M., Kiyono, T., Goshima, N., and Inagaki, M. (2011). Nuclear Chk1 prevents premature mitotic entry. J Cell Sci *124*, 2113-2119.

Matsuzaki, S., and Tohyama, M. (2007). Molecular mechanism of schizophrenia with reference to disrupted-in-schizophrenia 1 (DISC1). Neurochem Int *51*, 165-172.

Mayor, T., Stierhof, Y.D., Tanaka, K., Fry, A.M., and Nigg, E.A. (2000). The centrosomal protein C-Nap1 is required for cell cycle-regulated centrosome cohesion. J Cell Biol *151*, 837-846.

Meek, K., Dang, V., and Lees-Miller, S.P. (2008). DNA-PK: the means to justify the ends? Adv Immunol *99*, 33-58.

Meraldi, P., Honda, R., and Nigg, E.A. (2002). Aurora-A overexpression reveals tetraploidization as a major route to centrosome amplification in p53-/- cells. Embo J *21*, 483-492.

Meyerson, M., and Harlow, E. (1994). Identification of G1 kinase activity for cdk6, a novel cyclin D partner. Mol Cell Biol *14*, 2077-2086.

Middendorp, S., Kuntziger, T., Abraham, Y., Holmes, S., Bordes, N., Paintrand, M., Paoletti, A.,

and Bornens, M. (2000). A role for centrin 3 in centrosome reproduction. J Cell Biol *148*, 405-416.

Mikule, K., Delaval, B., Kaldis, P., Jurcyzk, A., Hergert, P., and Doxsey, S. (2007). Loss of centrosome integrity induces p38-p53-p21-dependent G1-S arrest. Nat Cell Biol *9*, 160-170.

Minoshima, Y., Hori, T., Okada, M., Kimura, H., Haraguchi, T., Hiraoka, Y., Bao, Y.C., Kawashima, T., Kitamura, T., and Fukagawa, T. (2005). The constitutive centromere component CENP-50 is required for recovery from spindle damage. Mol Cell Biol *25*, 10315-10328.

Mitchison, T., and Kirschner, M. (1984). Dynamic instability of microtubule growth. Nature *312*, 237-242.

Miyoshi, K., Asanuma, M., Miyazaki, I., Diaz-Corrales, F.J., Katayama, T., Tohyama, M., and Ogawa, N. (2004). DISC1 localizes to the centrosome by binding to kendrin. Biochem Biophys Res Commun *317*, 1195-1199.

Miyoshi, K., Asanuma, M., Miyazaki, I., Matsuzaki, S., Tohyama, M., and Ogawa, N. (2006a). Characterization of pericentrin isoforms in vivo. Biochem Biophys Res Commun *351*, 745-749.

Miyoshi, K., Kasahara, K., Miyazaki, I., Shimizu, S., Taniguchi, M., Matsuzaki, S., Tohyama, M., and Asanuma, M. (2009). Pericentrin, a centrosomal protein related to microcephalic primordial dwarfism, is required for olfactory cilia assembly in mice. Faseb J *23*, 3289-3297.

Miyoshi, K., Onishi, K., Asanuma, M., Miyazaki, I., Diaz-Corrales, F.J., and Ogawa, N. (2006b). Embryonic expression of pericentrin suggests universal roles in ciliogenesis. Dev Genes Evol *216*, 537-542.

Mochly-Rosen, D. (1995). Localization of protein kinases by anchoring proteins: a theme in signal transduction. Science *268*, 247-251.

Mogensen, M.M., Malik, A., Piel, M., Bouckson-Castaing, V., and Bornens, M. (2000). Microtubule minus-end anchorage at centrosomal and non-centrosomal sites: the role of ninein. J Cell Sci *113*, 3013-3023.

Morgan, D.O. (1997). Cyclin-dependent kinases: engines, clocks, and microprocessors. Annu Rev Cell Dev Biol *13*, 261-291.

Moritz, M., and Agard, D.A. (2001). Gamma-tubulin complexes and microtubule nucleation. Curr Opin Struct Biol *11*, 174-181.

Moritz, M., Braunfeld, M.B., Sedat, J.W., Alberts, B., and Agard, D.A. (1995). Microtubule nucleation by gamma-tubulin-containing rings in the centrosome. Nature *378*, 638-640.

Moskalewski, S., and Thyberg, J. (1992). Synchronized shift in localization of the Golgi complex and the microtubule organizing center in the terminal phase of cytokinesis. J Submicrosc Cytol Pathol *24*, 359-370.

Moynihan, L., Jackson, A.P., Roberts, E., Karbani, G., Lewis, I., Corry, P., Turner, G., Mueller, R.F., Lench, N.J., and Woods, C.G. (2000). A third novel locus for primary autosomal recessive microcephaly maps to chromosome 9q34. Am J Hum Genet *66*, 724-727.

Muhlhans, J., Brandstatter, J.H., and Giessl, A. (2011). The centrosomal protein pericentrin identified at the basal body complex of the connecting cilium in mouse photoreceptors. PLoS One *6*, e26496.

Musacchio, A., and Hardwick, K.G. (2002). The spindle checkpoint: structural insights into dynamic signalling. Nat Rev Mol Cell Biol *3*, 731-741.

Musacchio, A., and Salmon, E.D. (2007). The spindle-assembly checkpoint in space and time. Nat Rev Mol Cell Biol *8*, 379-393.

Mussman, J.G., Horn, H.F., Carroll, P.E., Okuda, M., Tarapore, P., Donehower, L.A., and Fukasawa, K. (2000). Synergistic induction of centrosome hyperamplification by loss of p53 and cyclin E overexpression. Oncogene *19*, 1635-1646.

Myers, J.S., and Cortez, D. (2006). Rapid activation of ATR by ionizing radiation requires ATM and Mre11. J Biol Chem *281*, 9346-9350.

Nakamura, A., Arai, H., and Fujita, N. (2009). Centrosomal Aki1 and cohesin function in separase-regulated centriole disengagement. J Cell Biol *187*, 607-614.

Nakazawa, Y., Hiraki, M., Kamiya, R., and Hirono, M. (2007). SAS-6 is a cartwheel protein that establishes the 9-fold symmetry of the centriole. Curr Biol *17*, 2169-2174.

Neben, K., Ott, G., Schweizer, S., Kalla, J., Tews, B., Katzenberger, T., Hahn, M., Rosenwald, A., Ho, A.D., Muller-Hermelink, H.K.*, et al.* (2007). Expression of centrosome-associated gene products is linked to tetraploidization in mantle cell lymphoma. Int J Cancer *120*, 1669-1677.

Neben, K., Tews, B., Wrobel, G., Hahn, M., Kokocinski, F., Giesecke, C., Krause, U., Ho, A.D., Kramer, A., and Lichter, P. (2004). Gene expression patterns in acute myeloid leukemia correlate with centrosome aberrations and numerical chromosome changes. Oncogene *23*, 2379-2384.

Neitzel, H., Neumann, L.M., Schindler, D., Wirges, A., Tonnies, H., Trimborn, M., Krebsova, A., Richter, R., and Sperling, K. (2002). Premature chromosome condensation in humans associated with microcephaly and mental retardation: a novel autosomal recessive condition. Am J Hum Genet *70*, 1015-1022.

Neuber, A., Franke, J., Wittstruck, A., Schlenstedt, G., Sommer, T., and Stade, K. (2008). Nuclear export receptor Xpo1/Crm1 is physically and functionally linked to the spindle pole body in budding yeast. Mol Cell Biol *28*, 5348-5358.

Newton, A.C. (1997). Regulation of protein kinase C. Curr Opin Cell Biol *9*, 161-167.

Nezi, L., and Musacchio, A. (2009). Sister chromatid tension and the spindle assembly checkpoint. Curr Opin Cell Biol *21*, 785-795.

Nguyen, T., Vinh, D.B., Crawford, D.K., and Davis, T.N. (1998). A genetic analysis of interactions with Spc110p reveals distinct functions of Spc97p and Spc98p, components of the yeast gamma-tubulin complex. Mol Biol Cell *9*, 2201-2216.

Nicklas, R.B., Ward, S.C., and Gorbsky, G.J. (1995). Kinetochore chemistry is sensitive to tension and may link mitotic forces to a cell cycle checkpoint. J Cell Biol *130*, 929-939.

Nigg, E.A., and Stearns, T. (2011). The centrosome cycle: Centriole biogenesis, duplication and inherent asymmetries. Nat Cell Biol *13*, 1154-1160.

Niida, H., Katsuno, Y., Banerjee, B., Hande, M.P., and Nakanishi, M. (2007). Specific role of Chk1 phosphorylations in cell survival and checkpoint activation. Mol Cell Biol *27*, 2572-2581.

Nishimura, K., Fukagawa, T., Takisawa, H., Kakimoto, T., and Kanemaki, M. (2009). An auxin-based degron system for the rapid depletion of proteins in nonplant cells. Nat Methods *6*, 917-922.

Nogales, E., Whittaker, M., Milligan, R.A., and Downing, K.H. (1999). High-resolution model of the microtubule. Cell *96*, 79-88.

Nogales, E., Wolf, S.G., and Downing, K.H. (1998). Structure of the alpha beta tubulin dimer by electron crystallography. Nature *391*, 199-203.

Numata, S., Iga, J., Nakataki, M., Tayoshi, S., Tanahashi, T., Itakura, M., Ueno, S., and Ohmori, T. (2009). Positive association of the pericentrin (PCNT) gene with major depressive disorder in the Japanese population. J Psychiatry Neurosci *34*, 195-198.

Nyberg, K.A., Michelson, R.J., Putnam, C.W., and Weinert, T.A. (2002). Toward maintaining the genome: DNA damage and replication checkpoints. Annu Rev Genet *36*, 617-656.

O'Connell, M.J., Walworth, N.C., and Carr, A.M. (2000). The G2-phase DNA-damage checkpoint. Trends Cell Biol *10*, 296-303.

O'Driscoll, M., and Jeggo, P.A. (2006). The role of double-strand break repair - insights from human genetics. Nat Rev Genet *7*, 45-54.

O'Driscoll, M., Ruiz-Perez, V.L., Woods, C.G., Jeggo, P.A., and Goodship, J.A. (2003). A splicing mutation affecting expression of ataxia-telangiectasia and Rad3-related protein (ATR) results in Seckel syndrome. Nature Genetics *33*, 497-501.

O'Regan, L., Blot, J., and Fry, A.M. (2007). Mitotic regulation by NIMA-related kinases. Cell Div *2*, 25.

Oegema, K., Wiese, C., Martin, O.C., Milligan, R.A., Iwamatsu, A., Mitchison, T.J., and Zheng, Y. (1999). Characterization of two related Drosophila gamma-tubulin complexes that differ in their ability to nucleate microtubules. J Cell Biol *144*, 721-733.

Ohta, T., Essner, R., Ryu, J.H., Palazzo, R.E., Uetake, Y., and Kuriyama, R. (2002). Characterization of Cep135, a novel coiled-coil centrosomal protein involved in microtubule organization in mammalian cells. J Cell Biol *156*, 87-99.

Ono, T., Fang, Y., Spector, D.L., and Hirano, T. (2004). Spatial and temporal regulation of Condensins I and II in mitotic chromosome assembly in human cells. Mol Biol Cell *15*, 3296-3308.

Oricchio, E., Saladino, C., Iacovelli, S., Soddu, S., and Cundari, E. (2006). ATM is activated by default in mitosis, localizes at centrosomes and monitors mitotic spindle integrity. Cell Cycle *5*, 88-92.

Osborn, A.J., Elledge, S.J., and Zou, L. (2002). Checking on the fork: the DNA-replication stress-response pathway. Trends Cell Biol *12*, 509-516.

Ou, Y.Y., Mack, G.J., Zhang, M., and Rattner, J.B. (2002). CEP110 and ninein are located in a specific domain of the centrosome associated with centrosome maturation. J Cell Sci *115*, 1825-1835.

Paintrand, M., Moudjou, M., Delacroix, H., and Bornens, M. (1992). Centrosome organization and centriole architecture: their sensitivity to divalent cations. J Struct Biol *108*, 107-128.

Pan, J., Wang, Q., and Snell, W.J. (2005). Cilium-generated signaling and cilia-related disorders. Lab Invest *85*, 452-463.

Patel, H., and Gordon, M.Y. (2009). Abnormal centrosome-centriole cycle in chronic myeloid leukaemia? Br J Haematol *146*, 408-417.

Pattison, L., Crow, Y.J., Deeble, V.J., Jackson, A.P., Jafri, H., Rashid, Y., Roberts, E., and Woods, C.G. (2000). A fifth locus for primary autosomal recessive microcephaly maps to chromosome 1q31. Am J Hum Genet *67*, 1578-1580.

Pazour, G.J., Dickert, B.L., Vucica, Y., Seeley, E.S., Rosenbaum, J.L., Witman, G.B., and Cole, D.G. (2000). Chlamydomonas IFT88 and its mouse homologue, polycystic kidney disease gene tg737, are required for assembly of cilia and flagella. J Cell Biol *151*, 709-718.

Pazour, G.J., San Agustin, J.T., Follit, J.A., Rosenbaum, J.L., and Witman, G.B. (2002). Polycystin-2 localizes to kidney cilia and the ciliary level is elevated in orpk mice with polycystic kidney disease. Curr Biol *12*, R378-380.

Peel, N., Stevens, N.R., Basto, R., and Raff, J.W. (2007). Overexpressing centriole-replication proteins in vivo induces centriole overduplication and de novo formation. Curr Biol *17*, 834-843.

Peng, C.Y., Graves, P.R., Thoma, R.S., Wu, Z., Shaw, A.S., and Piwnica-Worms, H. (1997). Mitotic and G2 checkpoint control: regulation of 14-3-3 protein binding by phosphorylation of Cdc25C on serine-216. Science *277*, 1501-1505.

Peng, G., Yim, E.K., Dai, H., Jackson, A.P., Burgt, I., Pan, M.R., Hu, R., Li, K., and Lin, S.Y. (2009). BRIT1/MCPH1 links chromatin remodelling to DNA damage response. Nat Cell Biol *11*, 865-872.

Pereira, G., and Schiebel, E. (1997). Centrosome-microtubule nucleation. J Cell Sci *110*, 295-300.

Peters, J.M. (2002). The anaphase-promoting complex: proteolysis in mitosis and beyond. Mol Cell *9*, 931-943.

Piane, M., Della Monica, M., Piatelli, G., Lulli, P., Lonardo, F., Chessa, L., and Scarano, G. (2009). Majewski osteodysplastic primordial dwarfism type II (MOPD II) syndrome previously diagnosed as Seckel syndrome: Report of a novel mutation of thePCNTgene. Am J Med Genet A *149A*, 2452-2456.

Piehl, M., Tulu, U.S., Wadsworth, P., and Cassimeris, L. (2004). Centrosome maturation:

measurement of microtubule nucleation throughout the cell cycle by using GFP-tagged EB1. Proc Natl Acad Sci U S A *101*, 1584-1588.

Piel, M., Nordberg, J., Euteneuer, U., and Bornens, M. (2001). Centrosome-dependent exit of cytokinesis in animal cells. Science *291*, 1550-1553.

Pihan, G.A., Purohit, A., Wallace, J., Knecht, H., Woda, B., Quesenberry, P., and Doxsey, S.J. (1998). Centrosome defects and genetic instability in malignant tumors. Cancer Res *58*, 3974-3985.

Pines, J., and Hunter, T. (1991). Human cyclins A and B1 are differentially located in the cell and undergo cell cycle-dependent nuclear transport. J Cell Biol *115*, 1-17.

Puklowski, A., Homsi, Y., Keller, D., May, M., Chauhan, S., Kossatz, U., Grunwald, V., Kubicka, S., Pich, A., Manns, M.P., *et al.* (2011). The SCF-FBXW5 E3-ubiquitin ligase is regulated by PLK4 and targets HsSAS-6 to control centrosome duplication. Nat Cell Biol *13*, 1004-1009.

Purohit, A., Tynan, S.H., Vallee, R., and Doxsey, S.J. (1999). Direct interaction of pericentrin with cytoplasmic dynein light intermediate chain contributes to mitotic spindle organization. J Cell Biol *147*, 481-492.

Quintyne, N.J., Reing, J.E., Hoffelder, D.R., Gollin, S.M., and Saunders, W.S. (2005). Spindle multipolarity is prevented by centrosomal clustering. Science *307*, 127-129.

Rai, R., Dai, H., Multani, A.S., Li, K., Chin, K., Gray, J., Lahad, J.P., Liang, J., Mills, G.B., Meric-Bernstam, F., *et al.* (2006). BRIT1 regulates early DNA damage response, chromosomal integrity, and cancer. Cancer Cell *10*, 145-157.

Rai, R., Phadnis, A., Haralkar, S., Badwe, R.A., Dai, H., Li, K., and Lin, S.Y. (2008). Differential regulation of centrosome integrity by DNA damage response proteins. Cell Cycle *7*, 2225-2233.

Rainey, M.D., Black, E.J., Zachos, G., and Gillespie, D.A. (2008). Chk2 is required for optimal mitotic delay in response to irradiation-induced DNA damage incurred in G2 phase. Oncogene *27*, 896-906.

Rainey, M.D., Zachos, G., and Gillespie, D.A. (2006). Analysing the DNA damage and replication checkpoints in DT40 cells. Subcell Biochem *40*, 107-117.

Rauch, A., Thiel, C.T., Schindler, D., Wick, U., Crow, Y.J., Ekici, A.B., van Essen, A.J., Goecke, T.O., Al-Gazali, L., Chrzanowska, K.H., *et al.* (2008). Mutations in the pericentrin (PCNT) gene cause primordial dwarfism. Science *319*, 816-819.

Raynaud-Messina, B., and Merdes, A. (2007). Gamma-tubulin complexes and microtubule organization. Curr Opin Cell Biol *19*, 24-30.

Reed, J.R., Vukmanovic-Stejic, M., Fletcher, J.M., Soares, M.V., Cook, J.E., Orteu, C.H., Jackson, S.E., Birch, K.E., Foster, G.R., Salmon, M., *et al.* (2004). Telomere erosion in memory T cells induced by telomerase inhibition at the site of antigenic challenge in vivo. J Exp Med *199*, 1433-1443.

Reynaud, C.A., Anquez, V., Dahan, A., and Weill, J.C. (1985). A single rearrangement event

generates most of the chicken immunoglobulin light chain diversity. Cell *40*, 283-291.

Reynaud, C.A., Anquez, V., Grimal, H., and Weill, J.C. (1987). A hyperconversion mechanism generates the chicken light chain preimmune repertoire. Cell *48*, 379-388.

Reynaud, C.A., Bertocci, B., Dahan, A., and Weill, J.C. (1994). Formation of the chicken B-cell repertoire: ontogenesis, regulation of Ig gene rearrangement, and diversification by gene conversion. Adv Immunol *57*, 353-378.

Rieder, C.L. (2011). Mitosis in vertebrates: the G2/M and M/A transitions and their associated checkpoints. Chromosome Res *19*, 291-306.

Rieder, C.L., Cole, R.W., Khodjakov, A., and Sluder, G. (1995). The checkpoint delaying anaphase in response to chromosome monoorientation is mediated by an inhibitory signal produced by unattached kinetochores. J Cell Biol *130*, 941-948.

Rieder, C.L., and Palazzo, R.E. (1992). Colcemid and the mitotic cycle. J Cell Sci *102*, 387-392.

Rieder, C.L., Schultz, A., Cole, R., and Sluder, G. (1994). Anaphase onset in vertebrate somatic cells is controlled by a checkpoint that monitors sister kinetochore attachment to the spindle. J Cell Biol *127*, 1301-1310.

Roberts, E., Jackson, A.P., Carradice, A.C., Deeble, V.J., Mannan, J., Rashid, Y., Jafri, H., McHale, D.P., Markham, A.F., Lench, N.J.*, et al.* (1999). The second locus for autosomal recessive primary microcephaly (MCPH2) maps to chromosome 19q13.1-13.2. Eur J Hum Genet *7*, 815-820.

Saladino, C., Bourke, E., Conroy, P.C., and Morrison, C.G. (2009). Centriole separation in DNA damage-induced centrosome amplification. Environ Mol Mutagen *50*, 725-732.

Samejima, K., Ogawa, H., Cooke, C.A., Hudson, D.F., Macisaac, F., Ribeiro, S.A., Vagnarelli, P., Cardinale, S., Kerr, A., Lai, F.*, et al.* (2008). A promoter-hijack strategy for conditional shutdown of multiply spliced essential cell cycle genes. Proc Natl Acad Sci U S A *105*, 2457-2462.

Sampaio, P., Rebollo, E., Varmark, H., Sunkel, C.E., and Gonzalez, C. (2001). Organized microtubule arrays in gamma-tubulin-depleted Drosophila spermatocytes. Curr Biol *11*, 1788-1793.

Sampath, S.C., Ohi, R., Leismann, O., Salic, A., Pozniakovski, A., and Funabiki, H. (2004). The chromosomal passenger complex is required for chromatin-induced microtubule stabilization and spindle assembly. Cell *118*, 187-202.

Sancar, A., Lindsey-Boltz, L.A., Unsal-Kacmaz, K., and Linn, S. (2004). Molecular mechanisms of mammalian DNA repair and the DNA damage checkpoints. Annu Rev Biochem *73*, 39-85.

Sato, N., Mizumoto, K., Nakamura, M., and Tanaka, M. (2000). Radiation-induced centrosome overduplication and multiple mitotic spindles in human tumor cells. Exp Cell Res *255*, 321-326.

Schmidt, T.I., Kleylein-Sohn, J., Westendorf, J., Le Clech, M., Lavoie, S.B., Stierhof, Y.D., and Nigg, E.A. (2009). Control of centriole length by CPAP and CP110. Curr Biol *19*, 1005-1011.

Schneeweiss, A., Sinn, H.-P., Ehemann, V., Khbeis, T., Neben, K., Krause, U., Ho, A.D., Bastert,

G., and Kramer, A. (2003). Centrosomal aberrations in primary invasive breast cancer are associated with nodal status and hormone receptor expression. Int J Cancer Suppl *107*, 346-352.

Schreiber, V., Dantzer, F., Ame, J.C., and de Murcia, G. (2006). Poly(ADP-ribose): novel functions for an old molecule. Nat Rev Mol Cell Biol *7*, 517-528.

Schwarz, J.K., Lovly, C.M., and Piwnica-Worms, H. (2003). Regulation of the Chk2 protein kinase by oligomerization-mediated cis- and trans-phosphorylation. Mol Cancer Res *1*, 598-609.

Semmler, K., Meyer, H.W., and Quinn, P.J. (2000). The structure and thermotropic phase behaviour of dipalmitoylphosphatidylcholine codispersed with a branched-chain phosphatidylcholine. Biochim Biophys Acta *1509*, 385-396.

Sewing, A., Burger, C., Brusselbach, S., Schalk, C., Lucibello, F.C., and Muller, R. (1993). Human cyclin D1 encodes a labile nuclear protein whose synthesis is directly induced by growth factors and suppressed by cyclic AMP. J Cell Sci *104*, 545-555.

Shimada, M., and Komatsu, K. (2009). Emerging connection between centrosome and DNA repair machinery. J Radiat Res (Tokyo) *50*, 295-301.

Shimada, M., Sagae, R., Kobayashi, J., Habu, T., and Komatsu, K. (2009). Inactivation of the Nijmegen breakage syndrome gene leads to excess centrosome duplication via the ATR/BRCA1 pathway. Cancer Res *69*, 1768-1775.

Shimizu, S., Matsuzaki, S., Hattori, T., Kumamoto, N., Miyoshi, K., Katayama, T., and Tohyama, M. (2008). DISC1-kendrin interaction is involved in centrosomal microtubule network formation. Biochem Biophys Res Commun *377*, 1051-1056.

Sillibourne, J.E., Delaval, B., Redick, S., Sinha, M., and Doxsey, S.J. (2007). Chromatin remodeling proteins interact with pericentrin to regulate centrosome integrity. Mol Biol Cell *18*, 3667-3680.

Skoufias, D.A., Andreassen, P.R., Lacroix, F.B., Wilson, L., and Margolis, R.L. (2001). Mammalian mad2 and bub1/bubR1 recognize distinct spindle-attachment and kinetochore-tension checkpoints. Proc Natl Acad Sci U S A *98*, 4492-4497.

Sluder, G., and Nordberg, J.J. (2004). The good, the bad and the ugly: the practical consequences of centrosome amplification. Curr Opin Cell Biol *16*, 49-54.

Smits, V.A., Reaper, P.M., and Jackson, S.P. (2006). Rapid PIKK-dependent release of Chk1 from chromatin promotes the DNA-damage checkpoint response. Curr Biol *16*, 150-159.

Somers, M., and Engelborghs, Y. (1990). Kinetics of the spontaneous organization of microtubules in solution. Eur Biophys J *18*, 239-244.

Sonoda, E., Okada, T., Zhao, G.Y., Tateishi, S., Araki, K., Yamaizumi, M., Yagi, T., Verkaik, N.S., van Gent, D.C., Takata, M.*, et al.* (2003). Multiple roles of Rev3, the catalytic subunit of polzeta in maintaining genome stability in vertebrates. Embo J *22*, 3188-3197.

Sonoda, E., Sasaki, M.S., Buerstedde, J.M., Bezzubova, O., Shinohara, A., Ogawa, H., Takata, M., Yamaguchi-Iwai, Y., and Takeda, S. (1998). Rad51-deficient vertebrate cells accumulate

chromosomal breaks prior to cell death. Embo J *17*, 598-608.

Sorokin, A.V., Kim, E.R., and Ovchinnikov, L.P. (2007). Nucleocytoplasmic transport of proteins. Biochemistry (Mosc) *72*, 1439-1457.

Srsen, V., Gnadt, N., Dammermann, A., and Merdes, A. (2006). Inhibition of centrosome protein assembly leads to p53-dependent exit from the cell cycle. J Cell Biol *174*, 625-630.

Steere, N., Wagner, M., Beishir, S., Smith, E., Breslin, L., Morrison, C.G., Hochegger, H., and Kuriyama, R. (2011). Centrosome amplification in CHO and DT40 cells by inactivation of cyclin-dependent kinases. Cytoskeleton (Hoboken) *68*, 446-458.

Stirling, D.A., Rayner, T.F., Prescott, A.R., and Stark, M.J. (1996). Mutations which block the binding of calmodulin to Spc110p cause multiple mitotic defects. J Cell Sci *109*, 1297-1310.

Strnad, P., Leidel, S., Vinogradova, T., Euteneuer, U., Khodjakov, A., and Gonczy, P. (2007). Regulated HsSAS-6 levels ensure formation of a single procentriole per centriole during the centrosome duplication cycle. Dev Cell *13*, 203-213.

Strome, S., Powers, J., Dunn, M., Reese, K., Malone, C.J., White, J., Seydoux, G., and Saxton, W. (2001). Spindle dynamics and the role of gamma-tubulin in early Caenorhabditis elegans embryos. Mol Biol Cell *12*, 1751-1764.

Su, X., Bernal, J.A., and Venkitaraman, A.R. (2008). Cell-cycle coordination between DNA replication and recombination revealed by a vertebrate N-end rule degron-Rad51. Nat Struct Mol Biol *15*, 1049-1058.

Subba Rao, K. (2007). Mechanisms of disease: DNA repair defects and neurological disease. Nat Clin Pract Neurol *3*, 162-172.

Sudakin, V., Chan, G.K., and Yen, T.J. (2001). Checkpoint inhibition of the APC/C in HeLa cells is mediated by a complex of BUBR1, BUB3, CDC20, and MAD2. J Cell Biol *154*, 925-936.

Sui, G., Affar el, B., Shi, Y., Brignone, C., Wall, N.R., Yin, P., Donohoe, M., Luke, M.P., Calvo, D., and Grossman, S.R. (2004). Yin Yang 1 is a negative regulator of p53. Cell *117*, 859-872.

Sundberg, H.A., Goetsch, L., Byers, B., and Davis, T.N. (1996). Role of calmodulin and Spc110p interaction in the proper assembly of spindle pole body compenents. J Cell Biol *133*, 111-124.

Swedlow, J.R., and Hirano, T. (2003). The making of the mitotic chromosome: modern insights into classical questions. Mol Cell *11*, 557-569.

Takahashi, M., Mukai, H., Oishi, K., Isagawa, T., and Ono, Y. (2000). Association of immature hypophosphorylated protein kinase cepsilon with an anchoring protein CG-NAP. J Biol Chem *275*, 34592-34596.

Takahashi, M., Shibata, H., Shimakawa, M., Miyamoto, M., Mukai, H., and Ono, Y. (1999). Characterization of a novel giant scaffolding protein, CG-NAP, that anchors multiple signaling enzymes to centrosome and the golgi apparatus. J Biol Chem *274*, 17267-17274.

Takahashi, M., Yamagiwa, A., Nishimura, T., Mukai, H., and Ono, Y. (2002). Centrosomal proteins CG-NAP and kendrin provide microtubule nucleation sites by anchoring gamma-tubulin

ring complex. Mol Biol Cell *13*, 3235-3245.

Takai, H., Tominaga, K., Motoyama, N., Minamishima, Y.A., Nagahama, H., Tsukiyama, T., Ikeda, K., Nakayama, K., and Nakanishi, M. (2000). Aberrant cell cycle checkpoint function and early embryonic death in Chk1(-/-) mice. Genes Dev *14*, 1439-1447.

Takao, N., Kato, H., Mori, R., Morrison, C., Sonada, E., Sun, X., Shimizu, H., Yoshioka, K., Takeda, S., and Yamamoto, K. (1999). Disruption of ATM in p53-null cells causes multiple functional abnormalities in cellular response to ionizing radiation. Oncogene *18*, 7002-7009.

Tang, C.J., Fu, R.H., Wu, K.S., Hsu, W.B., and Tang, T.K. (2009). CPAP is a cell-cycle regulated protein that controls centriole length. Nat Cell Biol *11*, 825-831.

Taylor, S.S., Scott, M.I., and Holland, A.J. (2004). The spindle checkpoint: a quality control mechanism which ensures accurate chromosome segregation. Chromosome Res *12*, 599-616.

Teale, W.D., Paponov, I.A., and Palme, K. (2006). Auxin in action: signalling, transport and the control of plant growth and development. Nat Rev Mol Cell Biol *7*, 847-859.

Terada, Y., Tatsuka, M., Jinno, S., and Okayama, H. (1995). Requirement for tyrosine phosphorylation of Cdk4 in G1 arrest induced by ultraviolet irradiation. Nature *376*, 358-362.

Thoms, K.M., Kuschal, C., and Emmert, S. (2007). Lessons learned from DNA repair defective syndromes. Exp Dermatol *16*, 532-544.

Thomson, P.A., Wray, N.R., Millar, J.K., Evans, K.L., Hellard, S.L., Condie, A., Muir, W.J., Blackwood, D.H., and Porteous, D.J. (2005). Association between the TRAX/DISC locus and both bipolar disorder and schizophrenia in the Scottish population. Mol Psychiatry *10*, 657-668, 616.

Tibelius, A., Marhold, J., Zentgraf, H., Heilig, C.E., Neitzel, H., Ducommun, B., Rauch, A., Ho, A.D., Bartek, J., and Kramer, A. (2009). Microcephalin and pericentrin regulate mitotic entry via centrosome-associated Chk1. J Cell Biol *185*, 1149-1157.

Trimborn, M., Bell, S.M., Felix, C., Rashid, Y., Jafri, H., Griffiths, P.D., Neumann, L.M., Krebs, A., Reis, A., Sperling, K.*, et al.* (2004). Mutations in microcephalin cause aberrant regulation of chromosome condensation. Am J Hum Genet *75*, 261-266.

Trimborn, M., Ghani, M., Walther, D.J., Dopatka, M., Dutrannoy, V., Busche, A., Meyer, F., Nowak, S., Nowak, J., Zabel, C.*, et al.* (2010). Establishment of a mouse model with misregulated chromosome condensation due to defective Mcph1 function. PLoS One *5*, e9242.

Trimborn, M., Schindler, D., Neitzel, H., and Hirano, T. (2006). Misregulated chromosome condensation in MCPH1 primary microcephaly is mediated by condensin II. Cell Cycle *5*, 322-326.

Tritarelli, A., Oricchio, E., Ciciarello, M., Mangiacasale, R., Palena, A., Lavia, P., Soddu, S., and Cundari, E. (2004). p53 localization at centrosomes during mitosis and postmitotic checkpoint are ATM-dependent and require serine 15 phosphorylation. Mol Biol Cell *15*, 3751-3757.

Tsang, W.Y., Spektor, A., Vijayakumar, S., Bista, B.R., Li, J., Sanchez, I., Duensing, S., and

Dynlacht, B.D. (2009). Cep76, a centrosomal protein that specifically restrains centriole reduplication. Dev Cell *16*, 649-660.

Tsou, M.F., and Stearns, T. (2006). Mechanism limiting centrosome duplication to once per cell cycle. Nature *442*, 947-951.

Tsou, M.F., Wang, W.J., George, K.A., Uryu, K., Stearns, T., and Jallepalli, P.V. (2009). Polo kinase and separase regulate the mitotic licensing of centriole duplication in human cells. Dev Cell *17*, 344-354.

Uetake, Y., and Sluder, G. (2004). Cell cycle progression after cleavage failure: mammalian somatic cells do not possess a "tetraploidy checkpoint". J Cell Biol *165*, 609-615.

Urnov, F.D., Miller, J.C., Lee, Y.L., Beausejour, C.M., Rock, J.M., Augustus, S., Jamieson, A.C., Porteus, M.H., Gregory, P.D., and Holmes, M.C. (2005). Highly efficient endogenous human gene correction using designed zinc-finger nucleases. Nature *435*, 646-651.

Vagnarelli, P., Morrison, C., Dodson, H., Sonoda, E., Takeda, S., and Earnshaw, W.C. (2004). Analysis of Scc1-deficient cells defines a key metaphase role of vertebrate cohesin in linking sister kinetochores. Embo Rep *5*, 167-171.

van Vugt, M.A., Gardino, A.K., Linding, R., Ostheimer, G.J., Reinhardt, H.C., Ong, S.E., Tan, C.S., Miao, H., Keezer, S.M., Li, J.*, et al.* (2010). A mitotic phosphorylation feedback network connects Cdk1, Plk1, 53BP1, and Chk2 to inactivate the G(2)/M DNA damage checkpoint. PLoS Biol *8*, e1000287.

Varon, R., Vissinga, C., Platzer, M., Cerosaletti, K.M., Chrzanowska, K.H., Saar, K., Beckmann, G., Seemanova, E., Cooper, P.R., Nowak, N.J.*, et al.* (1998). Nibrin, a novel DNA double-strand break repair protein, is mutated in Nijmegen breakage syndrome. Cell *93*, 467-476.

Vermes, I., Haanen, C., Steffens-Nakken, H., and Reutelingsperger, C. (1995). A novel assay for apoptosis. Flow cytometric detection of phosphatidylserine expression on early apoptotic cells using fluorescein labelled Annexin V. J Immunol Methods *184*, 39-51.

Verrou, C., Zhang, Y., Zurn, C., Schamel, W.W., and Reth, M. (1999). Comparison of the tamoxifen regulated chimeric Cre recombinases MerCreMer and CreMer. Biol Chem *380*, 1435-1438.

Vieira, J., and Messing, J. (1982). The pUC plasmids, an M13mp7-derived system for insertion mutagenesis and sequencing with synthetic universal primers. Gene *19*, 259-268.

Wadsworth, P., and Khodjakov, A. (2004). E pluribus unum: towards a universal mechanism for spindle assembly. Trends Cell Biol *14*, 413-419.

Walker, M., Black, E.J., Oehler, V., Gillespie, D.A., and Scott, M.T. (2009). Chk1 C-terminal regulatory phosphorylation mediates checkpoint activation by de-repression of Chk1 catalytic activity. Oncogene *28*, 2314-2323.

Walworth, N., Davey, S., and Beach, D. (1993). Fission yeast chk1 protein kinase links the rad checkpoint pathway to cdc2. Nature *363*, 368-371.

Wang, W., Budhu, A., Forgues, M., and Wang, X.W. (2005). Temporal and spatial control of nucleophosmin by the Ran-Crm1 complex in centrosome duplication. Nat Cell Biol *7*, 823-830.

Wang, X., Yang, Y., Duan, Q., Jiang, N., Huang, Y., Darzynkiewicz, Z., and Dai, W. (2008). sSgo1, a major splice variant of Sgo1, functions in centriole cohesion where it is regulated by Plk1. Dev Cell *14*, 331-341.

Wang, Z., Wu, T., Shi, L., Zhang, L., Zheng, W., Qu, J.Y., Niu, R., and Qi, R.Z. (2010). Conserved motif of CDK5RAP2 mediates its localization to centrosomes and the Golgi complex. J Biol Chem *285*, 22658-22665.

Waters, J.C., Chen, R.H., Murray, A.W., and Salmon, E.D. (1998). Localization of Mad2 to kinetochores depends on microtubule attachment, not tension. J Cell Biol *141*, 1181-1191.

Wiese, C., and Zheng, Y. (2006). Microtubule nucleation: gamma-tubulin and beyond. J Cell Sci *119*, 4143-4153.

Willems, M., Genevieve, D., Borck, G., Baumann, C., Baujat, G., Bieth, E., Edery, P., Farra, C., Gerard, M., Heron, D.*, et al.* (2009). Molecular analysis of pericentrin gene (PCNT) in a series of 24 Seckel/microcephalic osteodysplastic primordial dwarfism type II (MOPD II) families. J Med Genet *47*, 797-802.

Wilsker, D., Petermann, E., Helleday, T., and Bunz, F. (2008). Essential function of Chk1 can be uncoupled from DNA damage checkpoint and replication control. Proc Natl Acad Sci U S A *105*, 20752-20757.

Winding, P., and Berchtold, M.W. (2001). The chicken B cell line DT40: a novel tool for gene disruption experiments. J Immunol Methods *249*, 1-16.

Wojcik, E., Basto, R., Serr, M., Scaerou, F., Karess, R., and Hays, T. (2001). Kinetochore dynein: its dynamics and role in the transport of the Rough deal checkpoint protein. Nat Cell Biol *3*, 1001-1007.

Wolff, A., de Nechaud, B., Chillet, D., Mazarguil, H., Desbruyeres, E., Audebert, S., Edde, B., Gros, F., and Denoulet, P. (1992). Distribution of glutamylated alpha and beta-tubulin in mouse tissues using a specific monoclonal antibody, GT335. Eur J Cell Biol *59*, 425-432.

Wollman, R., Civelekoglu-Scholey, G., Scholey, J.M., and Mogilner, A. (2008). Reverse engineering of force integration during mitosis in the Drosophila embryo. Mol Syst Biol *4*, 195.

Wong, C., and Stearns, T. (2003). Centrosome number is controlled by a centrosome-intrinsic block to reduplication. Nat Cell Biol *5*, 539-544.

Wood, J.L., Singh, N., Mer, G., and Chen, J. (2007). MCPH1 functions in an H2AX-dependent but MDC1-independent pathway in response to DNA damage. J Biol Chem *282*, 35416-35423.

Woods, C.G., Bond, J., and Enard, W. (2005). Autosomal recessive primary microcephaly (MCPH): a review of clinical, molecular, and evolutionary findings. Am J Hum Genet *76*, 717-728.

Wu, X., Mondal, G., Wang, X., Wu, J., Yang, L., Pankratz, V.S., Rowley, M., and Couch, F.J.

(2009). Microcephalin regulates BRCA2 and Rad51-associated DNA double-strand break repair. Cancer Res *69*, 5531-5536.

Xia, G., Luo, X., Habu, T., Rizo, J., Matsumoto, T., and Yu, H. (2004). Conformation-specific binding of p31(comet) antagonizes the function of Mad2 in the spindle checkpoint. Embo J *23*, 3133-3143.

Xu, B., O'Donnell, A.H., Kim, S.T., and Kastan, M.B. (2002). Phosphorylation of serine 1387 in Brca1 is specifically required for the Atm-mediated S-phase checkpoint after ionizing irradiation. Cancer Res *62*, 4588-4591.

Xu, X., Lee, J., and Stern, D.F. (2004). Microcephalin is a DNA damage response protein involved in regulation of CHK1 and BRCA1. J Biol Chem *279*, 34091-34094.

Yamazoe, M., Sonoda, E., Hochegger, H., and Takeda, S. (2004). Reverse genetic studies of the DNA damage response in the chicken B lymphocyte line DT40. DNA Repair (Amst) *3*, 1175-1185.

Yang, Z., Kenny, A.E., Brito, D.A., and Rieder, C.L. (2009). Cells satisfy the mitotic checkpoint in Taxol, and do so faster in concentrations that stabilize syntelic attachments. J Cell Biol *186*, 675-684.

Young, A., Dictenberg, J.B., Purohit, A., Tuft, R., and Doxsey, S.J. (2000). Cytoplasmic dynein-mediated assembly of pericentrin and gamma tubulin onto centrosomes. Mol Biol Cell *11*, 2047-2056.

Yu, X., Chini, C.C., He, M., Mer, G., and Chen, J. (2003). The BRCT domain is a phospho-protein binding domain. Science *302*, 639-642.

Zachos, G., Black, E.J., Walker, M., Scott, M.T., Vagnarelli, P., Earnshaw, W.C., and Gillespie, D.A. (2007). Chk1 is required for spindle checkpoint function. Dev Cell *12*, 247-260.

Zhang, C., Hughes, M., and Clarke, P.R. (1999). Ran-GTP stabilises microtubule asters and inhibits nuclear assembly in Xenopus egg extracts. J Cell Sci *112*, 2453-2461.

Zhang, S., Hemmerich, P., and Grosse, F. (2007). Centrosomal localization of DNA damage checkpoint proteins. J Cell Biochem *101*, 451-465.

Zhang, Y., Wienands, J., Zurn, C., and Reth, M. (1998). Induction of the antigen receptor expression on B lymphocytes results in rapid competence for signaling of SLP-65 and Syk. Embo J *17*, 7304-7310.

Zhao, H., and Piwnica-Worms, H. (2001). ATR-mediated checkpoint pathways regulate phosphorylation and activation of human Chk1. Mol Cell Biol *21*, 4129-4139.

Zheng, Y., Wong, M.L., Alberts, B., and Mitchison, T. (1995). Nucleation of microtubule assembly by a gamma-tubulin-containing ring complex. Nature *378*, 578-583.

Zhong, X., Pfeifer, G.P., and Xu, X. (2006). Microcephalin encodes a centrosomal protein. Cell Cycle *5*, 457-458.

Zhou, B.B., and Elledge, S.J. (2000). The DNA damage response: putting checkpoints in

perspective. Nature *408*, 433-439.

Zhou, J., Yao, J., and Joshi, H.C. (2002). Attachment and tension in the spindle assembly checkpoint. J Cell Sci *115*, 3547-3555.

Zhou, M.Y., and Gomez-Sanchez, C.E. (2000). Universal TA cloning. Curr Issues Mol Biol *2*, 1-7.

Zimmerman, W., and Doxsey, S.J. (2000). Construction of centrosomes and spindle poles by molecular motor-driven assembly of protein particles. Traffic *1*, 927-934.

Zimmerman, W.C., Sillibourne, J., Rosa, J., and Doxsey, S.J. (2004). Mitosis-specific anchoring of gamma tubulin complexes by pericentrin controls spindle organization and mitotic entry. Mol Biol Cell *15*, 3642-3657.

Zor, T., and Selinger, Z. (1996). Linearization of the Bradford protein assay increases its sensitivity: theoretical and experimental studies. Anal Biochem *236*, 302-308.

Appendix 1. List of primers

Primers Used for	Sequence (5' to 3')
Pcnt targeting 5' Arm	agactagtGCTGTGGGAGCTGCTGGATGATAG
	ctactagtTTGCCTGCCTGCTCTTTCAGAAG
Pcnt targeting 3' Arm	agacgcgtGACCGAAACTTCTGTGCCTGCC
	ctacgcgtGCCAGATGCTCTATTGATTTGCCA
Pcnt targeting 5' Probe	GCTCTAAGGATATTGAACAGCAGGT
	GCCCAGCCTTTTGCTCATC
Pcnt cDNA 5' end RT-PCR	ACAACTTAGCCAGCATAGGGACT
	GCTGTGAAGTGTCTGTGATTGGA
Pcnt cDNA 3' end RT-PCR	TGCTCCTCCAAATCCTCTCAC
	TGAAAAATAAACACCAAACAGACTC
Pcnt cDNA qRT-PCR	ACAACTTAGCCAGCATAGGGACT
	GTTTGTTGAAGGCAGCTTGTTAG
Actb cDNA RT-PCR	GCTAGAGGCAGCTGTGGC
	ATGGATGATGATATTGCT
Actb cDNA qRT-PCR	GACACAGATCATGTTTGAGACCTTC
	ACCAGAGTCCATCACAATACCAGT
Pcnt cDNA Cloning Fragment1	gtcgacgTTGTTTGTGTCTTGTACGGGATG
	CACTTAACTCTTGCCGATTTGCT
Pcnt cDNA Cloning Fragment2	GAGCTGGAAAAACTTCAGGTCAT
	CTTATGCTTCTTAATTTCTGCCTCA
Pcnt cDNA Cloning Fragment3	ATTATGGCTGTAGAAGCAGAAGAAG
	GAGAGCGTAAGTTAGAATGGTCCT
Pcnt cDNA Cloning Fragment4	TCTAAAAGAAGAATCTGAGCGTCG
	GGTCTGATGTTTGTAACTGCTCCT
Pcnt cDNA Cloning Fragment5	GGGATTCGCCTGAGATTATGA
	CTTGGGACAATAATGCTTCACAG
Pcnt cDNA Cloning Fragment6	AGCTGTCTGTATCCTTAGAGCATGA
	cctaggACAGATTTCAGAAGCATTCGGAT
Pcnt cDNA Cloning Fragment2 Sequencing	AAGCGAGTGTCTGTGCTGGAG
Pcnt cDNA Cloning Fragment4 Sequencing	GGATGAAGTGAGGCATGGAGTAC
	AGAGTACAGCCTTCTCCAAACACA
Pcnt cDNA Cloning Fragment6 Sequencing	CTACTCTGCAAGGTGAGGGAACT
FLAG-tag Knockin 5' Arm	actagTCAATCGTACTTCAAGTTAGTCCAAG
	ggatccACCAATGCTCAATCAGAAGAGTACA
FLAG-tag Knockin 3' Arm	ctcgagTCCGAATGCTTCTGAAATCTGT
	ggtacCAGCACACTCGAAAGAGGACAC

FLAG-tag Knockin Intermediate Fragment	ggatcCTTTATGTGTGAATGTTTGCTTTTG
	gcggccgcCTTTTTCATGTTTCTTTGGCAAG
FLAG-tag Knockin 5' Probe	TAGACTTTAACCTGCTGTGGACTTG
	GAAAACCCATGCAAAGAGGATC
FLAG-tag Knockin 5' Arm Sequencing	TTCTCCATACACTCAGTCAAAACCT
FLAG-tag Knockin 3' Arm Sequencing	CTCCCACATGGAAACTCTGATACT
	CGCTTCGGATCTCAGACCTC
	TCCTATGTAGCAGGGCTGTCAG
Eb1 cDNA Cloning	gtcgacATGGCAGTGAATGTGTACTCCA
	actagtTAATACTCTTCTTGCTCCTCCTG

Appendix 2. Full length chicken *Pcnt* cDNA

```
   1 ATGGAGGAGG CGCGGATGCG CAAGCTGGAG GCTGGTAGAG CTAAGTTTGC
  51 TCACTTCAGA GAACGAAAAG CAAAAAGCAA TGTCACGCAG TCGCAGAAAA
 101 AGACGACGAA GAGGAAGGGC TCGTCTGTCC ACACACATGA CGTTCCACAG
 151 GAAGAGCACG CAGCAATGGG CCAAGGCTGT GATGTCGGTA AGGGTATAGA
 201 GAGTAAGGCT GAAGACACCA ACTTCCTAGA GACAACAACA GAGACAGAGA
 251 AAGTTGCAGT ACATTCTGCT GCAGAATATA GTGAGCTTGA TGATAAGATG
 301 CGTCAAACAA GAATAGCTGA GTTAGAGAAG AGACTTCTGG AGAAACAGCA
 351 AGCAGTTGGA AGACTTACTG TGCAGATGAA TGAACTACAG GAACAACTTA
 401 GCCAGCATAG GGACTCAATG CAGCTTCAGG AAACAACTAT TCAAGAGCAG
 451 AATGAAGTCA TAAGGAAACT AACAAGCTGC CTTCAACAAA CAAGGAAGGA
 501 TTGGGATGAC TTGCAAGAAG AGGCTTCACA TGTAGCTGAT CAGATCCATG
 551 GCTTACAACT TCAGTTGCAT GAGGTTAATG TGATGCTGAA GAGTAAAGGC
 601 TCTGGGAAGA AAGAGGTATT AGAAGCCCAG CAGCAAATGT CCTTGTTTCA
 651 GAGCAGTCTC CAAGAACAAA ATGCACGTTT GGAGATGCTG CATCAGAGAG
 701 CATATGACCT GGAGGTACAG CTTGAGTCTT CTCAAAAGAT AGAAGAATTA
 751 AATGCTGAAA TAAAAGATAA AGTTGAAAAG CAAAAGAGGT TGGAGGAAGA
 801 AAGAGTAGAA CAGCTTGCTT TAGTAAAAAA GGTACATGAA CGAGAGCATG
 851 ACCGTGAAAT TTCTGAACTG ATTGCTAAAC ATAAAGAGGA AATGGAGGAG
 901 CTCCGTGCTG AACTTCATAA AGAAAAGCTA CACCTGTTGG ATGAACTTCA
 951 GCAGCAAATG GCAGCCACAC ATAAAGCAGA GATTGAGTAT GCCCAGCTCC
1001 AATCACAGAC ACTTCACAGC CTTGAATTGG AAGCATTACG CCTAAGCTTA
1051 AACAATTTGC ATACCTCTCA GCTTGAGCTT ACTCAGTCCA ACTTGAGAAA
1101 AGAAAAGGAA ACTGCACTTG TGGAGCTACG GGAGATGCTC AATGATAAGC
1151 GTGCTCAGGA GATAGCAATT CTACAAAGCC GCCATCAGCT GGAGTGGGAG
1201 AAAATTAAAG AACGTTGTTT GAAGGAAAAA GAAGACCTAA CGTCAAAGTA
1251 TCAGCAAGAA TTAGTTGATC AGAGAAAGAA AATAGAATTG GAAATGGAAG
1301 AGAAACATAT CCAGATATTA GAGACTCTCA AAAGAGACTG GGAATTGGAG
1351 TCTGAGATGC GTTTAAAATA CACATGTGAG GAGCTGTCTA AAAAACATAA
```

```
1401 GGCTGAAATA GCAGAGCTGC AGAAAACTCT GGAAATGGAA TTAGAAAAAG
1451 TCAAAGCAGA GCTGGGACTT CTTTCTCTTG AGAAGGAGCA ATCTGAAATG
1501 AAATGTGTAG ATTTGGAGAA ACAACAGCAG TTAGCAATCA CAACGTTAAC
1551 TAAACAACTG CAGTCTGAAC ACAACCAACT CCTAGAAGAT GTGAAGATAG
1601 AAAGCCAAGA AAAAGAACAG AATCTACAGA AGGAGCTGGA AAAACTTCAG
1651 GTCATGCACG AAGAATTCAA GACTCGATCA CAAGAAGAAG TCAAGCAGCT
1701 TTGGTCTCAA CTTGGCAGTA CTCGAGCAAA TCGGCAAGAG TTAAGTGAGC
1751 TGAAAGAGCA GCTCATGGCT CGTGCATCAC AGGTGGAAGA AATAGAGCAT
1801 TTAAAGCAAA AATTTGAAGA GCAGCAGCAG CAAACAAAAA GTGAGCATGA
1851 AGCTGAATTA GAACAGCTTA GAATCTACTT TGAAAGAAAG TTAAGAGTCA
1901 CTGAGGAAAA CTACAGAGAA GAATTGACTT TGCTGCATCA GAAACTGCAA
1951 GAACTGAAAG AATATTCCGT ATCTGGGGTT GATGTGAGCC ATAATCAAGC
2001 AGGGAATATC AGTTCTTCTG TCATAGTTTT TGGAGAGGCT GTTGAGAAAG
2051 AGAGAAAAGA CTTTTTCCTA GATCAACTGA ATCAACAGCT GGAGCAACAT
2101 AAGGAAGAAA TTGCCTGTTT GCAAGGACAA CTTAAAGAAG ATCACAGACA
2151 TGAACTAGAT TCCTTAAAGT CTTCCCTTGC ACTTCAATAT AAAGGGGACC
2201 TACTGAAAAT GAAGATGGAG CTCTCAGACA AGTATATAGC AGAAATAGAG
2251 GAGATGAAAA GAAAGCATTG TTTAGAACTT GAGCAGCTCC GTGCCAGACT
2301 TTCAGAAGAA CATATCAAAG AAATCACTAA ACTGCGCCTA CAGAGTGCTC
2351 AAGATGCAGC ACGTCAAGTT GAAATGGAGG TGGCCAAGCG AGTGTCTGTG
2401 CTGGAGGAAG AACACAAAGT TAAGCTCTCT CTCCTCCACT CTGAGGAACA
2451 GCATATTGCA GAGCTTTCAG AAGAAATAAA GTGTTTAAAA GAAGAGATGA
2501 CTAAACAAAA AGACTTTTTT GTGCAGAATG AAAAGCATCT GAAAGAGCAA
2551 ATGGAACAGG TAAAATTTAA AATCGCTGAG GATCACGAGA ATGAATTAAA
2601 GGAAGCCAGG GAAGAAGTTC TGAAAATAGA GACTTTGTAC AAAGAGAAAG
2651 AGAAGAAATG GAAATGTGAA AGTGAGGACC AGAGAGTCCA AGCGGAGGAG
2701 AAATTATCAT TGTTGCACAC AGAACTGCAA AATAGGTTGG AATATGAGAA
2751 GCAGAATTTA CAGAAGGAGT TTGAAGTTCG TGAAGCTCAA ATGAATCAGC
2801 TCCAAGATCA CCAGGCTGCC AAAATTGTAG AATTAGAGAA GTTGGTAAAA
2851 GAGCAGCAAA ACAACTTGAA ACAGTTAGAG GACAGCCTTG CAGTTGCACA
2901 GGCTACACGT AAGTCTCAGG AACAATATGA CAGTGACCTG CAGGCAGCCA
2951 AAGAGCTTAT GGCAAAAGAA ATGGAGAAGG CCGAGCTTTG TCTGCAGGAA
3001 GAATGTGCGC TGAAACTTAT GAAAGCACAA AACAAGTTTA TGGAGGAACA
3051 CAAAGCTTTG ACTCAGAAGT TCACAGCTGA GCAAGAGATT CTTCTCCAAG
3101 AGCTGAAGAA GAGACATGTT GATGAGCTAG AACTCCAAAG TCAGCAGCTA
3151 CAGGAGAAGC ATAAGCAGGA AATTTTATCT CTGACAGCTG AGTTTCAGAG
3201 AAAGCACCAA GCTGAAATTA AGACACTTAA ATCTACACTA GAAAGTAAAC
3251 AGCAAATTCA GCTTGAAGCT TTTGTTGCTG AACTTCAGAC AAAACATCAA
3301 GCACAAGTTG ATGCCCTGGA GGCTAAACAC TTATCAAACC TGGATTCCTT
3351 GGAGTCATCC TACCTATCTG AAATTCAGAA TATAAGAGGT GAACATAGGC
3401 TGGTTCTTGA GAAACTACAG CTGCATCACA CAGAGCAGCT CCATGAAAAG
3451 GATAAAATGA ATCAAGCATG CCTGGCTCAG GAGATAGAGA TATTGAAATT
3501 AAAGCACTCT GAAGAACTTC AGCTAGCACA AAATAATTTG AAAATTGAGC
3551 TAGCTACTGT GCATATGGAA AAACTTAAAA TTATGGCTGT AGAAGCAGAA
```

```
3601 GAAGCTCATA AGGATGATTT AAAAGCAGCT CTGCAAAATC AGAGAAGTTT
3651 ACTGGAAGAA GAAAAACGTC TAGCCTTGGA TATGTTACGT GAGGAAGTAG
3701 TGCACATGGA AGAAAAACAT AGAAAAGCAC TGCAAGAACT TCAGGATCTT
3751 CATGAGGCAG AAATTAAGAA GCATAAGGAA GAATACTCTA GGGAGCTGGA
3801 AAAGGAATTG GAGAAACTAA AAGCACAGCA TAAACATGAA CAGGAGATGT
3851 ATGCTTCTGC ATCAGCCTCT GAAATTGAAA CTGTGAGGAC AGCTCTTCTG
3901 TCTCAATTTG AGGCAGTGAA AATGAAGCAG CAGCTTCAGT TCCAGGAAGA
3951 GATTGAGCTG TTGAAGTGTC AGTCAGAAGT ACTCCTTGAA CAGCAAATTG
4001 CACAGCTGAA GGATGAATTT GAAGCTGAAA AAACAGCATT AATACATGAC
4051 CAGGAGCAGG TGTTAATTCA GGAAAGTGAG AAGGCACAGG CTGCTTGCCA
4101 AAAGGAGAAG GAGACATTAT CAGCACAGCT ACAGGAAAAA GCAGCAAGAA
4151 TTATCCAGCT GGAAAAGAGA GTAGAATCTT TAAATTGTGA AATACAGGAG
4201 ACCAACTGTG AACTGGAGAC ACTCATAGAG CGACGGGACA GAGAGAACCA
4251 AGAAGGAGGG AATTTGGTAG CCATGTTGAG ATCTGATATT GAGCAGTCCA
4301 AAGATGAAAG GAAGAAAATG CAGGACTCAT ATCAGTGTGT TTTGAAATGG
4351 CTTGTGGAGC TGGTGAAGGC CACAATTGCT GTTGAGGATC TTATCTGTAG
4401 CAAGATTGGT CTTTGCCTTG ATAACAGTAT GGCTTCTGCA GATTCTATGG
4451 AAAGTCACAG TATTGTGGAA GAAATAGGTT TCGCACAATA CTTCAAAGCT
4501 AAAGAAAAGA GTCACCTAGA GAAAGTAGAT GAACTGCTTG ATGAAACTCT
4551 CACAGAACAC AGCCAGCTGT CTCCAGTGAC TGAAGAGCAG TATGAGTTGA
4601 GCCAGTACTT ATATGAAAGT GTTTTTGCAA AGCCAGAAAT GGCATATGAA
4651 AACGAAGAAA TGATACTGAA AATTTGTCGT CGTTTGCGCA CTGCGGTGGA
4701 AAGACTTCTG GAACTGGTTA CAGAATCAAC TAAGCAACTG GAAAAAACAC
4751 ATGAAATCCA TGCACAGTTT GAAGAAGAAT TCACCCGCCG AAATCAGGAG
4801 ACTGCTCAGG TGGTTTGTCA ACATCGAGAA CTAATGGAGT GCCTCACTGA
4851 GGAAAGTGAG GCCAAGAATC AGCTGGCACT AGAGCTTCAT AAAGCAGAAG
4901 GCATTATTGA AGGCTATGTT GCAGAAAAAG CTGCGCTGGA GGAGGCCTTG
4951 AATCTAAAAG AAGAATCTGA GCGTCGCCTT GTTGTGGAGC TGGAGAATAT
5001 GCGTGAACGC TTCCAGGAAC TAACCCAGGA GCAGGCAATT CTTGGTCTAC
5051 TTAAGGAAGT AGAACTTTTA GCAAAGGAGA AATTGGAACT TGAGTGTCAG
5101 GCAGAAAAGG ACCATTCTAA CTTACGCTCT CAAATGAAAG TTCTGGAGAT
5151 GGAACTGGAA GAACAGCTGC ATAGTAATCA AGACTTGACT AAACAATTGA
5201 TGGAGACTGC TGAGTTAAAG CAGCAAATTG AAGTCCTTGA AAAACAGCTT
5251 AAAAACCAGC GACAATTCAT GGATGAACAA GCTATAGAAA GAGAAAATGA
5301 ACGTGATGAT TTTCAGCAAG AAATTAAAAA GCTGGAAGAA CAGTTGAAAC
5351 TTTCAGCTAA GTTACAGACT TCGGGAGAGC CCAGGGAGTA TGGGGTAGAA
5401 TCTTTACAAG CAGAAGTAGA AGAGAAGGTG GATGATTACA ATAAGCTGTT
5451 ATTAGAAAAG GAACAAAAAC ATCAAGAAAT TGCAGCTCGT GATAAAGAGA
5501 TTGAAAAACT GGTGGCACAA GTACAAGAAC TGGAGCACAG CAGTACTGAA
5551 GTCTCAAAGA CTGTAAACTA CTTGCAACAA CAACTTCAAA AAATGAAGAA
5601 AGTAGAAACT GAATTAAAAC AGGATAAAGA AGCATTGCAA CAGCAGCAGT
5651 ACAACAATTT GATCCAGATC TCTGCCCTGC AATCTAAATT GGATGAAGTG
5701 AGGCATGGAG TACCTGTGGA AGGCACTTCT GACCAAGAGC TGAAGGAACA
5751 GTTACAGGCA GAACAGGAAT CACTTGAGAG GAAAGAAGGA GAGATTGCAA
```

```
5801 GCTTGTTAGA CCACCTAGAA CAACATAAAG ATATATTGAC CAGTAAAAAT
5851 GAGGAGATAT TACAGCTGAA ATTGCAGCTA GAGGTGCAAA AAAATCTTAG
5901 CACTTCCACC ATCAACCAGC TTCAGATAGA GAATGCACAA TTGAAGGATC
5951 TAGCAAAACT TCATGTAAAG CAAAATCGGG ACTCGGATGT AGGTGATTCC
6001 TCAGCTCTGT CCTTCCCACA AGCACTACTT GAAGAAAAGA ATCAAGAAAT
6051 AGATCACCTG AATGAACAGC TGAGAAGACT CAAGTATGAT CAAGTGAATA
6101 CCCTTGAGAA TAAAGTTGTG GAAGACCAAA AATCTGAAAT TGAAGAACTC
6151 AGGTCTGTTA TTGAGTACCT TCGTGGTGAC CAGGAACGGC TGTGTAAGGA
6201 CAAAGATGAA GAGGTAGAGC AACTTCACGA AGTAATTGAG AAGCTCCAAA
6251 AAGAGTTGGC ACAAATTGGA CCAGTATGTC ATGAAGTTAG TGACAACCAA
6301 GGTGACATTT TTCAATTTGG ATTGGAAAAG TCAGTGGAAA ACCTGCAGAA
6351 GGAGTTGAAA AAGGGATTGA TAGATTGTCA GGGTGATACT GATCTAGATG
6401 GAAGAAATGC ATTGCTACTC TGCAAGGTGA GGGAACTTGA AGAAGATCTA
6451 GAGTTTGCCT CAGCTGCTAA AAAAGATCTG CAGCAGCAGT TGGAAGAGAA
6501 AGAATCACAG TTCAAAATGG AAGTGGAAAT TTTAGAGAAA AAATGCCAAA
6551 ATTTACAGGA ATCATCAAGG CAGCACTTTG CAGAGCTAAA CACTCTGAGA
6601 TTACAGTACC ATGCACTTCA GGAAGAGTAC AGCCTTCTCC AAACACATAT
6651 TTCTCAGAGA GAATTGGAAG CAAGGATTGC TTCTTCTTGT GTTCAGGAAC
6701 TCAAAGATAG TATGAAAGAG AGGGAAGTGA GTATTCTTGG AAAAGATAGC
6751 CAGATACAGG CAATGGCACA TCAAAGAGAA GCTGATGAAG GTGAATTGCG
6801 GTACTTAACA GAACAGGCAT CAGATCTTGA AACTGAGTTG AAAAAGAGAG
6851 ATGCAAGTCA GGCTCAAGAT GTTCATAGTC CTGAGTTAGA AGTTTCTAGA
6901 CTTGATTTGC ATGTGCAAGC AATGAATCAG AAAGAAGTAT CTAAGCAGAG
6951 AGAAATTGAT GAATTGCAAG GTAGCACAAC AAAATTGAAA GATCAAATCA
7001 AGATATACAC AAAAGAGCTT GAAGCCTTAC ATTTGGAAAG AGATGAACTT
7051 ATTTCACAGT TGGAATTGTA CAAGCCAAAG GAGCAGTGTG ATAAAGAGAA
7101 TGCTAACTGT CTTGAGCTGT TCTGCTGGGG ACAAAGACAA GGCGAGGTCC
7151 TTAAGGAGGG AATGGAGGAG TTGGAATCAC TGGAAACACA TGTTGATCAG
7201 TCATTTGCTT CCCCAGCTGA TAATCTGGAA AAGGTTGCTT TGTTTGACTT
7251 CACTGCTCAT GATATAAGTA AACAATCTCA GGTTAAGCAA TCAGAAGAAA
7301 ATATCTCAAT TCAGAAATTG GACATGATCA ACAGCTCTGA AGAACAGCAA
7351 ACTTTGAAAA AGCATCACCA TCAAACTCTC GATTCTCCAA AAATCATTGT
7401 GAATGCAGGC TGTACTGAAG GTACTCTTAA AAACTTCCAG GATTTCATTG
7451 TAGATGTGAC TTCATGGGAT TCGCCTGAGA TTATGAGAAA ACAAGATATA
7501 AGTATGGAAC TTCCACCAGC GCTTAATCTG ACACCCTTTT CAGAAGCTGA
7551 AAGTACAGGT CTTGAAATGG CGCACAGTAG GTCATCCCTG CAGGGTGATA
7601 ATTCTGTTTT GTTGGGATTT TCTCACCTTT ATGAAAATGG CAGTGAGGAA
7651 GCAGCAGGCA GAGCAGATGT AAAATCTCCA GTTTCCTCTG AAAGTATCTA
7701 CTCTGGTGCT GATCGTGACC AAGATCTGAA GAAGACGACT TTGATGAGCG
7751 GAACAGATAA TCTAACTCCA TCAGATTTGC AAGATGATGT AAGATCGGGA
7801 GCATCTGCCA TAGATGTGAT GAGCAATGGA TGTGACAGCA GTACCAGATC
7851 AAATTTGGAG GCTAAACTGA AGGAGCAGTT ACAAACATCA GACCACTCGG
7901 ATGCTAATTT CATGGCTTAT CTGCAGTACT GTGGCATGTT TCCAGATATT
7951 ATGGAATCAG TGAGAGAAAA GGAAATACTT TCACCACAAC TAAAGACTGT
```

```
 8001 GCTGAAGTTG GTGTATGAAG AGAGCCACAA GATATTGGCT TTGTCAGAAC
 8051 ATTCCTTTGG TTTTAGGGAG CTGAAAAATG TTCATCAGAC CAAAGCACTG
 8101 ATGGAGGGAT GGCAAAAAGA GGGCTTAGCC TTGCTGAATG CTATACAGTC
 8151 ACTGAAAGAT TATCTTAGCA AGGTGGCAGA TAGAGGAGAT AAGGAGGAAC
 8201 AGAGGCAGAT GGTTGTGGAG CACCTTTTCT CTTCGGACCG GAACAGCTTG
 8251 CTCTCTGAGA TACAGGAGCT TCGAGCTCAA CTACGCATGA CACATCTTCA
 8301 GAACCAGGAG AAGCTACAAC AGTTGCAGGA AACTCTTACT AGTGTAGAAG
 8351 ATCATGGGAG CAAACAAGAA CACCAGCTTC GAAGGAAAGT TGAATTATTA
 8401 GAATATAAGC TTCAGCAGGA AAAATGCATT GTAAGTGACC TGCATAGCAC
 8451 GCTGTCTGAG GAGCAGAAGA GAGCCTCTGA AACACGTGAA CTCTTGAGTC
 8501 AAGAAAAAGC AGCAGTTTCA ACCCTGAAGT CAGATCTATA TGAACGTAAG
 8551 CAAGAGAATG AAAGGCTGAA AAAATCCCTA GAAGAGCATC AGAGAGAAAT
 8601 AAACAAGCTC TGTTTTGAAT TGGAAAGTAA AGAGAAGGAT TTGACAGCTA
 8651 CTCTGCAAGA GTTGGAGGCT GAACGTCTTA CAGAAACAGA GCTGCGAGTT
 8701 TTGCTTGAGG AACAACAGCT TCAGCATAAG AAAGCAGAAG ATGAAAAGAA
 8751 AAAGGCCTTG GAGGATTTAC AGGCTGCCTT GGATTTGCAG ACTGCGCAGA
 8801 ATAGGAAGCT GTCTGTATCC TTAGAGCATG AACAAATTAT AAATGATAAT
 8851 CTCCGCAAGG AACTTCGGAT AGAATATTCT CGCTGTGAAG CATTATTGTC
 8901 CCAAGAACAT GACAAAGTGT TGGAGCTACA GAAAAACTTG GATGCTGAGA
 8951 GAAATCGTTC TTTGGAGCTC TTGAATTCCT TGAATCATGA ACGTATTTTG
 9001 ACAGAACAGT TGAGCGTGCA AGCTAAGGAG GATGCTTCTT GTCAGCGCAG
 9051 GGAGTTGTTG CTGGAACAGG CCTTTATCCG AGAGCTCCAA GCCCAGCTGG
 9101 AGGAAGAGAG ATCCCAAAAG ACGGAGCTGG CTGTAATTAC TGAGAAAACA
 9151 CACCAGAGAG CCATTCGTTC CAAGAGGCAG CTAGAGGCTG AAGTACAGAT
 9201 GTGTTGTGAA GAAACACAGA AGGAGAAAGA GATCACTAAC AAACTCCGAG
 9251 TGATGCTGGA CTCTCTTCAG AGTCAAAAGC AAGAGCAAAA CTTGGAACTG
 9301 CAACACCAGA GGGATGAACA AAGAATTAAA GAGATGCAGG AAATCGTGGC
 9351 AATCTTAGGA GAAACAGAAA GAAGTCCTCC ATCTCCCAGC AGTCAACAAG
 9401 GACTGTTGTG TACTTCAGAC AAAGATCAAA ATGCCAAAGA GCCCATGACA
 9451 ATAGAAATTG GAAAATTCAA CTTGCAGCAG CAGCAGAAGC AACAGCTGGA
 9501 GAAGATAAGA CAACAGTTGC TTTTCGTAGC TGCACATCTC ATTGAGTTAA
 9551 TGTGTAAAAC TGTAGATAAA ACAGTTAACG ACTGGTATGT ATCAAATGAT
 9601 GAAGCTGTAG CATCTTTACT GCAGACATTA AAGGAACTAA AATCAGATTT
 9651 ATTGTCTCCT GCATCTCAGA TCAGATCTAC AGATGATTCC AACCCTGTTC
 9701 AAGAACTGGA AAGAGCTGCT TGGCAGCAAG AAAGAAACAT TCTGCAGAAT
 9751 GCACTGAAAC AGGCAGAATC CAAACTGGCT AAAGCAACTG CTGAAACTGA
 9801 AAACAAACCA GCCATGGAAG CATTCAATCC TAAGTTACAG AGATTATATA
 9851 GGAAGTACCT AAGAGCGGAG AGCTTTAGAA AGGCTCTGGT TTATCAGAAG
 9901 AAATACCTCT TGCTGCTTCT TGGTGGATTT CAAGACTGCG AACAAGCAAC
 9951 TCTCTCTCTA ATAGCACGCA TGGGAATCTA CCCCTCGCCT GCAGACCTGC
10001 AGCTTTCTGC CTCCCGCTCC CGCCCTTTTA CCAAGTTCAG ATGCGCAGTC
10051 AGAGCAGTCA TTGCTGTATC AAGGTTGAAG TTTTTGGTGA AAAAGTGGAA
10101 CAAACTTAAC AGAAAAAATG CCCAGGCTGA AACAGTTTCC CAAAACACAG
10151 GAAGTAATAC TGCCTCTGGT GCCAGAACAG AAACTCTGAA ACAGCAGCAG
```

```
10201 CTCACAGCTG TTCATGTAAG CTCTCCCCCA ACCTGGGACA CTGGCCTGTG
10251 CCACAGAACC AGCTCTGCAA GATCTGTGAG CTGCTCCTCC AAATCCTCTC
10301 ACCGGTCACA CAGCAGATTG CCTCCATCCA CTTCAGAAAA GTCACCTGTG
10351 CCTACTCAGG ATCCTGAACG ATCACTTACA GAATATATCC ACCGCTTGGA
10401 GATTATCCAG CAAAGACTAG GAGGGATGCA GCCAGGACAA GTTCCGGGCC
10451 CGCCTTGCCA AAGAAACATG AAAAAGTGA
```

Appendix 3. Full length chicken *Eb1* cDNA

```
  1 ATGGCAGTGA ATGTGTACTC CACGTCGGTG ACGAGCGACA ACCTGAGCCG
 51 GCACGACATG CTGGCGTGGA TCAACGAATC CCTGCAGCTG ACGCTGACCA
101 AGATCGAGCA GCTGTGCTCA GGTGCTGCTT ACTGCCAGTT CATGGACATG
151 CTCTTCCCAG GTTCGGTAGC TCTCAAGAAA GTGAAGTTTC AAGCAAAATT
201 GGAACACGAG TACATACAGA ACTTCAAGGT TCTACAAGCA GGTTTCAAAC
251 GAATGGGCGT TGACAAAATA ATCCCTGTGG ACAAACTTGT GAAAGGAAAA
301 TTTCAGGATA ACTTTGAATT TGTTCAGTGG TTCAAAAAAT TTTTTGATGC
351 AAACTACGAT GGGAAGGAAT ACGACCCCGT GGCTGCCCGG CAAGGCCAGG
401 AGACAGTGGC ACCAAACCTC GTTGCTCCGG TGGTGAACAA ACCCAAGAAA
451 CCTCTCGGTA CTGGCAGTGC AGCCCCACAG AGGCCCATTG TTGCACAGAG
501 GACCCCAGCA ACTCCCAAAG GCAGCACTGG GATGGTCAAA AAGGCTGCAG
551 GAGATGATGA ATCAGCAGGA TTGATTGAGC AGATCAACGT GTTGAAGCTC
601 ACTGTTGAAG ACCTGGAGAA GGAGAGGGAC TTCTACTTTG GCAAACTGCG
651 GAACATTGAG CTGATCTGCC AGGAGAACGA AGGGGAGAAC GACCCGGTGC
701 TGCAGAGGAT TGTGGAAATC CTTTACGCCA CAGATGAAGG CTTTGTGATA
751 CCCGACGAAG GAGCGCCGCA GGAGGAGCAA GAAGAGTATT AA
```

Appendix 4. Scientific communications

Manuscripts

Wang Y, Dantas, TJ**,** Lalor P, Dockery P, Morrison CG. Pericentrin controls nuclear Chk1 activation. (Manuscript in preparation for Oncogene)

Dantas TJ, **Wang Y**, Lalor P, Dockery P, Morrison CG (2011). Defective nucleotide excision repair with normal centrosome structures and functions in the absence of all vertebrate centrins. *J Cell Biol* 193**:** 307-18.

Posters presented

Irish Association for Cancer Research annual meeting, Galway, Ireland, March 3-5, 2010: **Wang Y**, Dantas TJ, Morrison CG. *"Reverse genetic analysis of pericentrin"* (and) Dantas TJ, **Wang Y**, Liptrot C, Dockery P, Morrison CG. *"Dissecting the roles of centrin isoforms in a vertebrate cell line"*;

American Society for Cell Biology 49th annual meeting, San Diego, USA, December 5-9, 2009: **Wang Y**, Dantas TJ, Morrison CG. *"Reverse genetic analysis of pericentrin"* (and) Dantas TJ, **Wang Y**, Liptrot C, Dockery P, Morrison CG. *"Dissecting the roles of centrin isoforms in a vertebrate cell line"*.